2007

Initial Studies on a Novel Target-Promoted DNA Alkylation System

Ting Xu
Virginia Commonwealth University

INITIAL STUDIES ON A NOVEL TARGET-PROMOTED DNA ALKYLATION SYSTEM

A thesis submitted in partial fulfillment of the requirements for the degree of Master of Science at Virginia Commonwealth University.

by

TING XU
Bachelor of Pharmaceutical Science, Shenyang Pharmaceutical University, China, 1999

Director: QIBING ZHOU, Ph.D.
ASSISTANT PROFESSOR, DEPARTMENT OF CHEMISTRY

Virginia Commonwealth University
Richmond, Virginia
May 2007

Acknowledgement

I would like to express my deep and sincere gratitude to my supervisor, Dr. Qibing Zhou, for his help and direction throughout this work.

I wish to extend my warmest thanks to all those who have taught and helped me during my graduate school.

I am also grateful to Department of Chemistry for providing me with teaching assistantship to support my living and study in the past three years.

Finally, I must dedicate this thesis to my husband Chaoxuan Li and my parents for their love, support and encouragement.

Table of Contents

Page

List of Tables

Page

List of Figures

Page

List of Schemes

Page

List of Abbreviations

DNA	Deoxyribonucleic acid
QM	Quinone methide
EVE	Ethyl vinyl ether
Tf_2O	Trifluoromethanesulfonic anhydride
DIPEA	N,N-Diisopropylethylamine
THF	Tetrahydrofuran
TFA	Trifluoroacetic acid
TFAA	Trifluoroacetic anhydride
DIAD	Diisopropyl azodicarboxylate
EDCI	1-(3-Dimethylaminopropyl)-3-ethylcarbodiimide hydrochloride
HOBt	1-Hydroxybenzotriazole
4Å MS	4Å Molecular sieve
HBTU	O-Benzotriazole-N,N,N',N'-tetramethyl-uronium-hexafluoro-phosphate
DMAP	Dimethylaminopyridine
DMF	N,N-Dimethylformamide
TBDMSCl	*tert*-Butyldimethylsilyl chloride
TBAF	Tetrabutylammonium fluoride
HSAB	Hard-soft-acid-base concept
DMSO	Dimethyl sulfoxide

COSY	Correlation Spectroscopy
HMQC	Heteronuclear Multiple Quantum Correlation
HMBC	Heteronuclear Multiple Bond Correlation
Mops	3-(N-morpholino) propane sulfonic acid

Abstract

INITIAL STUDIES ON A NOVEL TARGET-PROMOTED DNA ALKYLATION SYSTEM

By Ting Xu, M.S.

A thesis submitted in partial fulfillment of the requirements for the degree of Master of Science at Virginia Commonwealth University.

Virginia Commonwealth University, 2007

Major Director: Dr. Qibing Zhou
Assistant Professor, Department of Chemistry

A novel target-promoted DNA alkylation system was designed, which consists of a DNA intercalating/alkylating quinone methide (QM) precursor, a removable amine linker, and a sequence-specific delivery. The QM in this system was regenerated by eliminating the amino linker promoted by the hydrophobic interaction between the target DNA and the intercalating QM precursor. Three alkylation model systems (methoxyl polycyclic system, intramolecular hydrogen bonding system and biaryl system) were proposed and synthesized. The potential DNA QM alkylation was investigated by deoxyadenosine (dA)

and deoxyguanosine (dG) alkylation with the biaryl system. Only one deoxynucleoside adduct was observed when dA or dG reacted with quinoline or naphthalene QM precursor, in which both dA adducts degraded with time, while dG adducts remained unchanged after 72 h at room temperature. The quinoline dG adduct was fully characterized as quinoline dG N1 adduct by NMR techniques. Naphthalene dG was found as a 1:1 mixture of diastereomers.

This document was created in Microsoft Word 2002 SP3.

CHAPTER 1 DNA Alkylation with Quinone Methides

1.1 Introduction of deoxyribonucleic acid (DNA)

DNA plays a crucial role in cellular biological processes. The genetic information encoded in DNA determines function and development of living organisms. DNA is a double helix which contains two antiparallel polynucleotide strands being held together by repetitive phosphate-sugar-phosphate backbone (Figure 1.1). In the backbone of DNA, hydrogen bonds are formed between two nucleobase pairs of DNA. Adenine forms two hydrogen bonds with thymine, while guanine is paired with cytosine with three hydrogen bonds. Along the duplex structure of DNA, there are two kinds of grooves: the major groove which is wide and shallow and the minor groove which is narrow and deep.

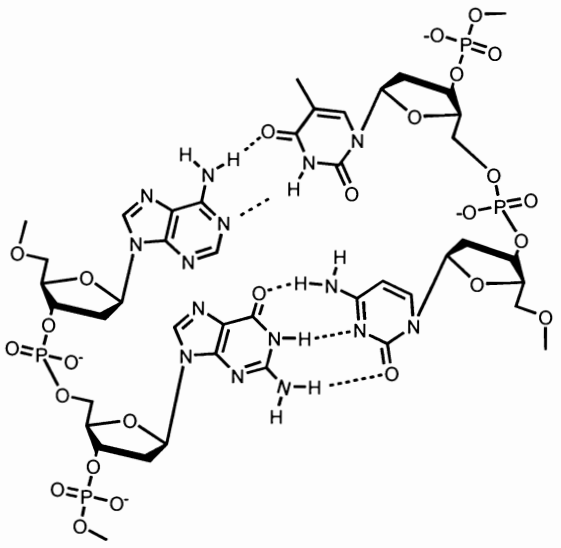

Figure 1.1: Chemical structure of DNA

Given its importance, DNA constitutes a primary target for a variety of bioactive chemicals such as carcinogens and anticancer agents to interfere with gene expression, protein synthesis, and DNA replication. Compared to DNA-binding proteins, small organic DNA-binding molecules can be conveniently synthesized and modified as a highly diversified scaffold, which leads to the understanding of DNA characteristics and the development of cancer chemotherapy agents. The major interactions between DNA and small molecules include: (a) strand cleavage; (b) intercalation; (c) groove bindings and (d) alkylation (Figure 1.2).[1]

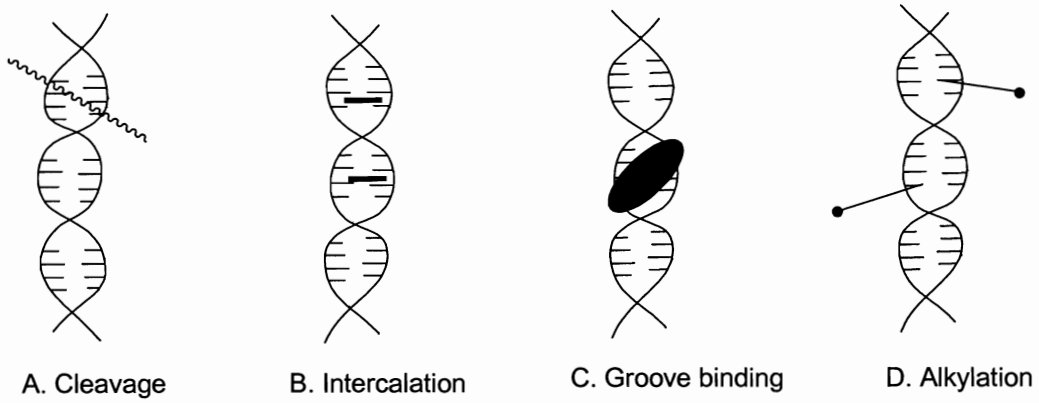

Figure 1.2: Interactions between DNA and small molecules

A. Strand cleavage. As a result of DNA cleavage, the backbones of nucleic acids are broken into short strands by the actions of organic molecules such as the enediyne class of antitumor antibiotics, including esperamicin, dynemicin, and calicheamicin. This class of molecules is structurally featured by a nine or ten membered ring containing two triple bonds separated by one double bond, and goes through a Bergman cycloaromatization,

which generates a DNA-damaging radical, 1,4-benzeniod diradical to break the single and double strand.[2,3]

B. Intercalation. Most intercalating drugs, such as anthracycline, are able to reversibly wedge between adjacent DNA bases because they have planar aromatic rings. They interact with the DNA structure nonconvalently, such as unwinding of the double helix, and eventually affect the DNA functions including transcripition.[1,4] DNA intercalating agents have been widely used for cancer chemotherapy.[5]

C. Groove binding. Some drugs bind to the exterior of the major or minor groove of DNA double helix by hydrogen bonding, hydrophobic contacts, salt bridges and Van Der Waals interactions.[1] The typical groove binding drug is a flat crescent moon shaped molecule which results in a close match of the architectural shape of the DNA grooves, such as netropsin, a specific AT minor groove binder.[6,7,8]

D. Alkylation. A number of potent anticancer drugs form covalent bonds with DNA bases. Anthramycin, a member of the pyrrolo[1,4]benzodiazepine family of antibiotics, bonds sequence-selectively to DNA resulting in the base-pairing mismatch and the inhibition of DNA replication.[9] Alkylation agents can contain bifunctional reaction sites to cross-link DNA duplex structure. (Figure 1.3).[10] For example, cisplatin used to treat a wide range of cancers contains two chlorine leaving groups and readily forms a cross link between complementary DNA strands to prevent the separation during the replication process.[11]

Quinone methides (QMs) are a group of reactive alkylating agents and have been used as antibiotics, xenobiotics and antitumor drugs.[12,13] They are the key molecules for

our proposed target promoted DNA alkylation and the review on the recent development and application is presented as following.

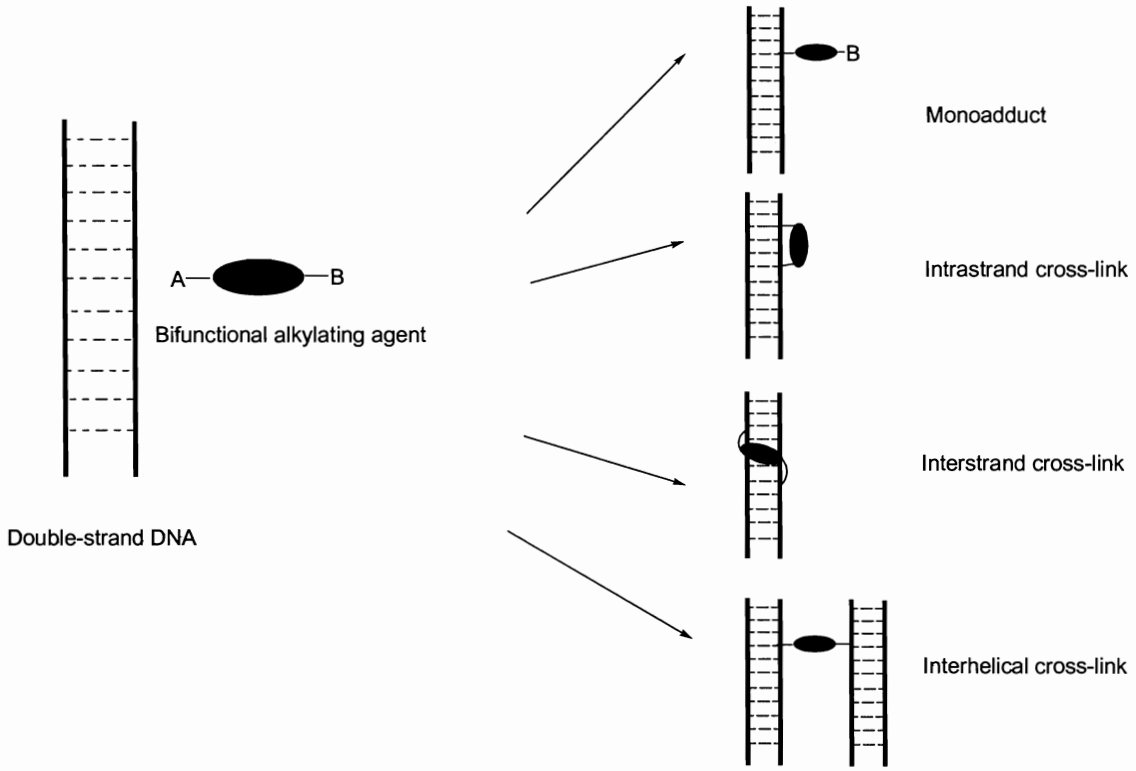

Figure 1.3: DNA alkylations

1.2 Introduction of quinone methides

QMs as methylene cyclohexadienones are structurally similar to quinones except that one of the carbonyl oxygens is replaced by a methylene group (Figure 1.4). QMs have three types of isomers: *ortho*-QM, *meta*-QM and *para*-QM. *o*- and *p*-QM are highly reactive due to their resonance structures, while *m*-QMs are diradicals and examples of non-Kekulé molecules.[14,15] QMs are Michael acceptors for nucleophiles at electrophilic

methylenes to form phenol adducts. This electrophilicity is the basis of QMs in various biological applications such as modification of peptides, proteins and nucleic acid. For example, prostatic acid phosphatase was inhibited by 4-(fluoromethyl)phenyl phosphate through active site modification by *p*-QMs (Scheme 1.1).[16,17] In the absence of nucleophiles, QMs are readily polymerized and the rate of polymerization is dependent on steric factors of QMs.[18]

In the following, the formation of QMs, DNA nucleobases alkylation, phosphate alkylation, and the sequence-specific DNA alkylation will be reviewed. Finally, a target-promoted DNA alkylation system and our new improved target-promoted system will be discussed.

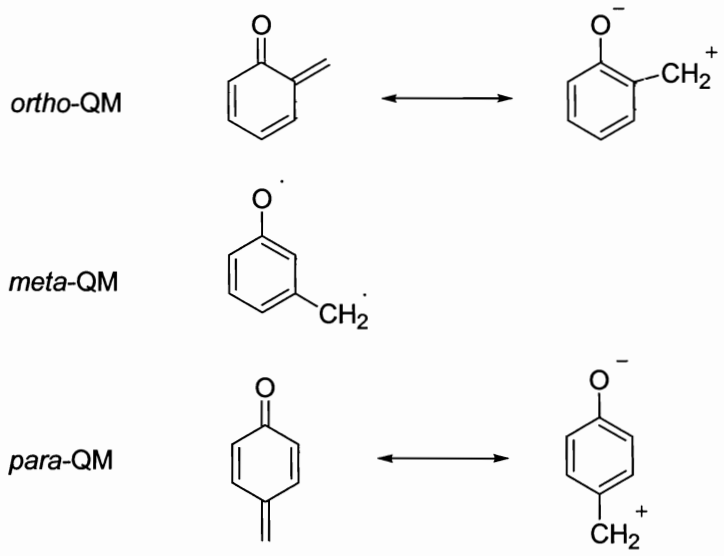

Figure 1.4: Structures and isomers of quinone methides

Scheme 1.1: QMs as suicidal enzyme inhibitors

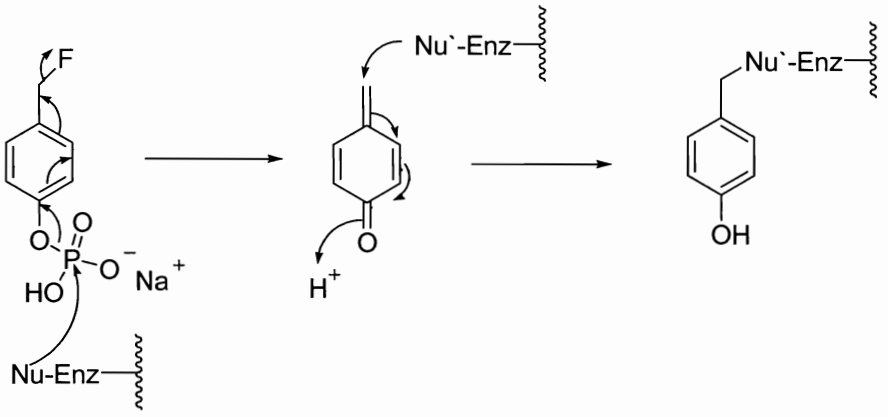

1.3 Formation of QMs

QMs can be generated by various methods including oxidation, reduction, tautomerization, fluoride initiation, photolysis, and thermal initiation.

A. Oxidation. Antioxidant 2, 6-di-*tert*-butyl-4-methy phenol (BHT) and food addictive 4-allyl-2-methoxyphenol (Eugenol) are oxidized to QM metabolites by cytochrome *P*-450 (Scheme 1.2). The former QM induces hepatotoxicity, pulmonary toxicity, and tumors, while the latter QM alkylates cellular proteins and thiols leading to cytotoxicity.[19-21]

B. Reduction. Reduction is another method to generate QMs, which can be exemplified by the antitumor effects of mitomycin C. The mechanism of mitomycin C activation includes the reduction of quinones to hydroquinone by oxidoreductases, such as cytochrome *P*-450 reductase and xanthine oxidase. This reduction is followed by elimination of methanol to give rise to an unstable imine. The imine then tautomerizes to an indole and the subsequent opening of the aziridine ring leads to a QM intermediate

which alkylates DNA bases. Further elimination generates a second electrophile to form the cross-linked DNA adduct (Scheme 1.3).[19,22]

Scheme 1.2: Oxidation of BHT and eugenol to QMs by cytochrome *P*-450

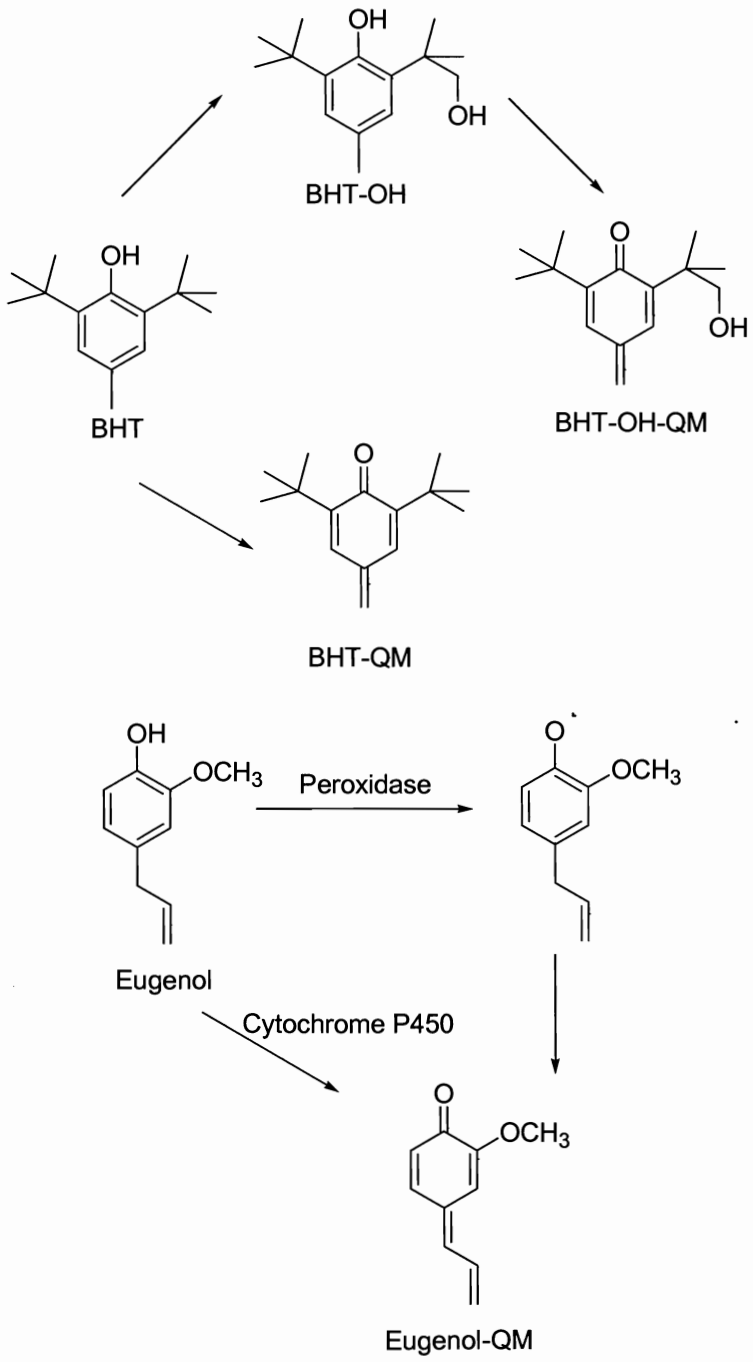

Scheme 1.3: Mechanism of mitomycin C-DNA alkylation

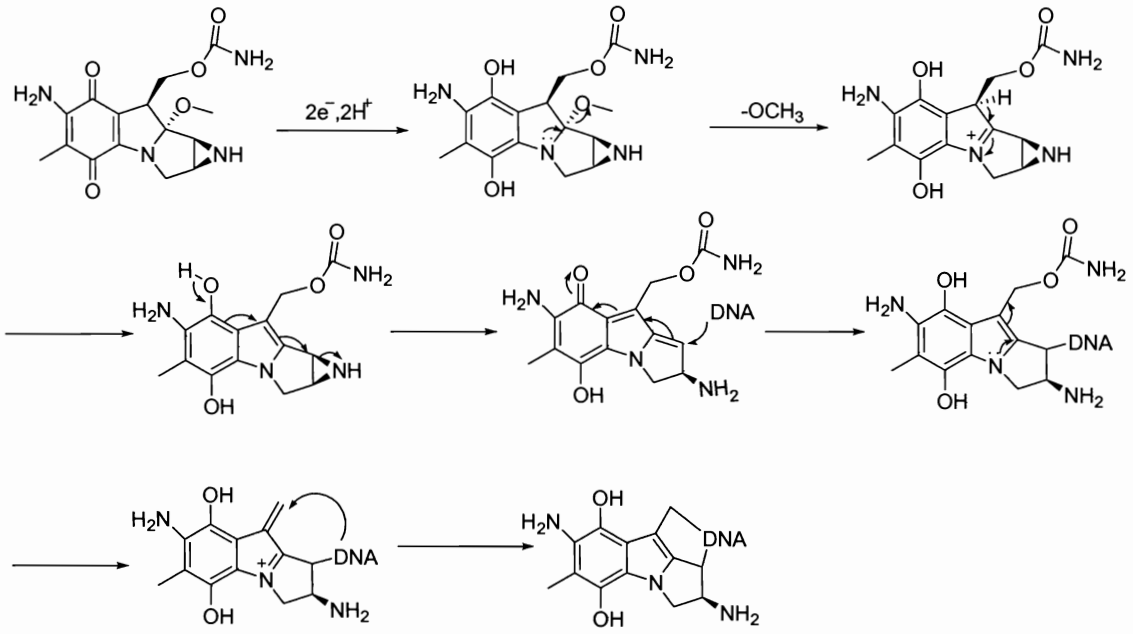

C. Tautomerization. An *o*-QM can be generated by tautomerization of an α–substituted *p*-quinone with an allylic proton adjacent to the quinone ring such as the tautomerization of vitamine K_1 under biological conditions. (Scheme 1.4).[23]

Scheme 1.4: Tautomerization of vitamin K1

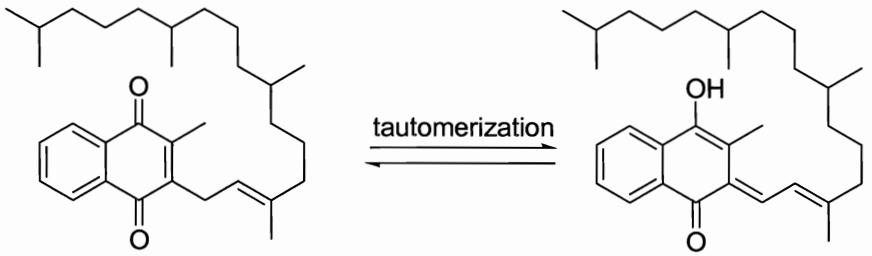

Vitamin K_1

D. Fluoride initiation. As shown in Scheme 1.5, fluoride can remove the silyl ether to generate a phenol. The subsequent elimination of leaving groups X^- or AcO^- could form QMs. Fluroride initiation was first reported by Rokita's group.[24-33]

Scheme 1.5: Fluoride initiation of QMs

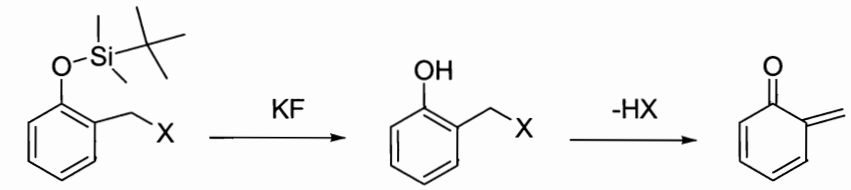

X=OAc or Br

E. Photolysis. Photolysis is an important method to generate QMs. Wan's group did a lot work on photolysis of QMs such as the generation of *o*-QM and *m*-QM by light.[34,35] QM intermediates can also be photogenerated through elimination of Mannich bases or their ammonium salts on phenols (Scheme 1.6).[36,37]

Scheme 1.6: Photo-generation and reactivity of Binol-QMs

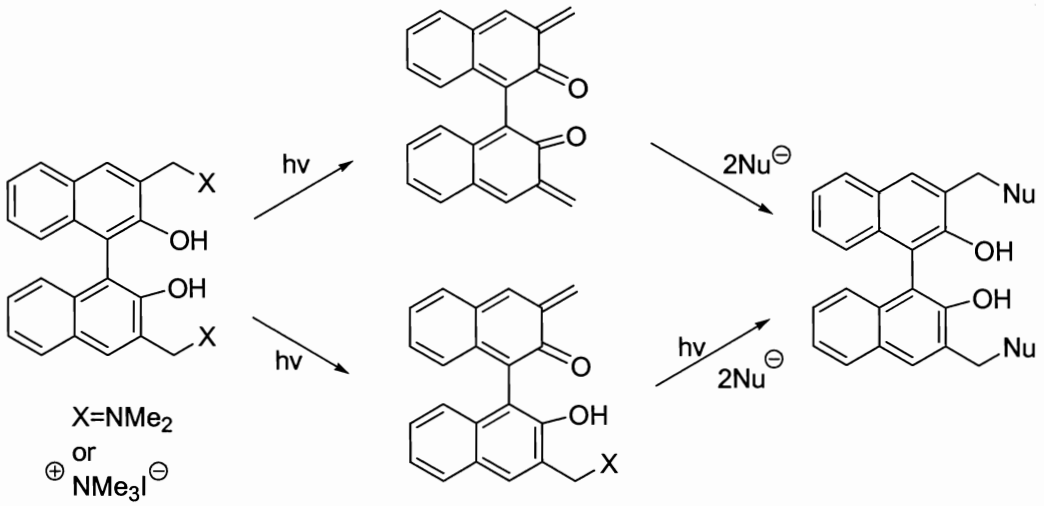

F. Thermal generation. Thermolysis is a synthetic method to produce QMs, such as dehydration of *o*-hydroxybenzyl alcohol at high temperature, flash vacuum pyrolysis of 4,6-dimethyl-2-(hydroxymethyl) phenol and pyrolysis of 4*H*-1,2-benzoxazine (Scheme 1.7).[38-40] However, this method can not be applied to thermally unstable QM precursors.

Scheme 1.7: Thermal initiation of QMs

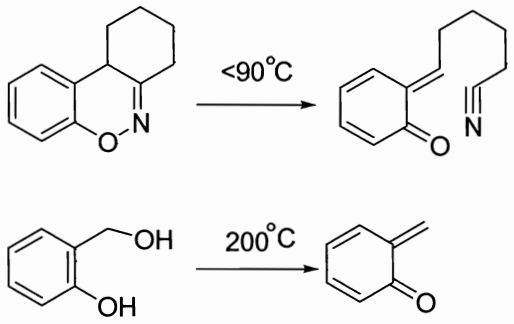

1.4 Selective alkylation of DNA nucleobases by QMs

The intrinsic reactivity of DNA nucleobases has been extensively studied using QM precursors.[36] Rokita's group have demonstrated the possible alkylation sites in pyrimidine and purine bases, and almost every nitrogen and oxygen could be alkylated under certain situation (Figure 1.5).[26,36] They first characterized the major products generated by deoxynucleosides with QMs. *o*-QMs tended to alkylate exo-amino groups of both 2'-deoxyguanosine (dG) and 2'-deoxyadenosine (dA) to form dG N^2 adducts and dA N^6 adducts, respectively. In contrast, 2'-deoxycytidine (dC) reacted at its cyclic N3 position to generate dC N3 adduct, and 2'-deoxythymidine (dT) remained inert under all conditions tested. It was also observed that reactivity of pyrimidines and purines was

suppressed with single-stranded deoxyoligonucleotide and duplex DNA. This was due to steric hindrance, differences in electrostatic effects and changes in solvation of polymers vs. monomer. Interestingly, the efficiency of modification of cytosine was affected most. Guanine, instead of cytosine, became the predominant target in duplex DNA. This was ascribed to the diminished accessibility of dC N3 due to its central position within three hydrogen bonds formed between cytosine and guanine. Both dG N^2 and dA N^6 maintained some exposure to the minor and major grooves, respectively. The hydrophobic nature of the minor groove might also increase the local concentration of QM precursor in the vicinity of dG N^2.[26,41] This selectivity is in accord with the selectivity observed in most natural QM precursors.[42-45]

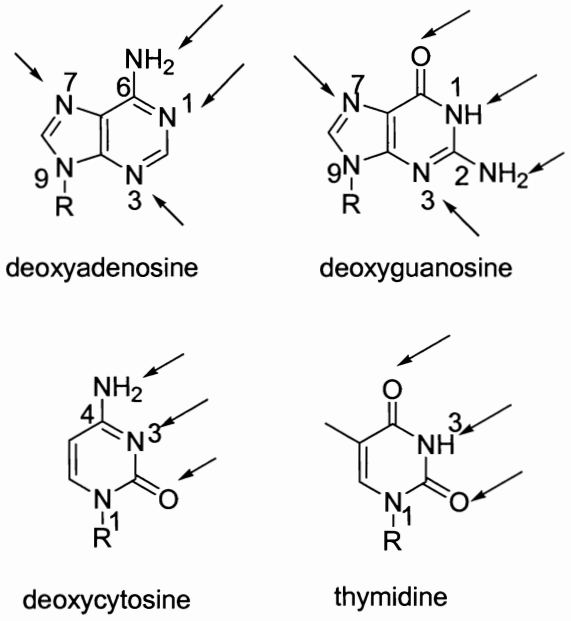

Figure 1.5: Possible alkylation sites on purine and pyrimidine nucleobases

Scheme 1.8: Adducts of dA alkylated by *o*-QM

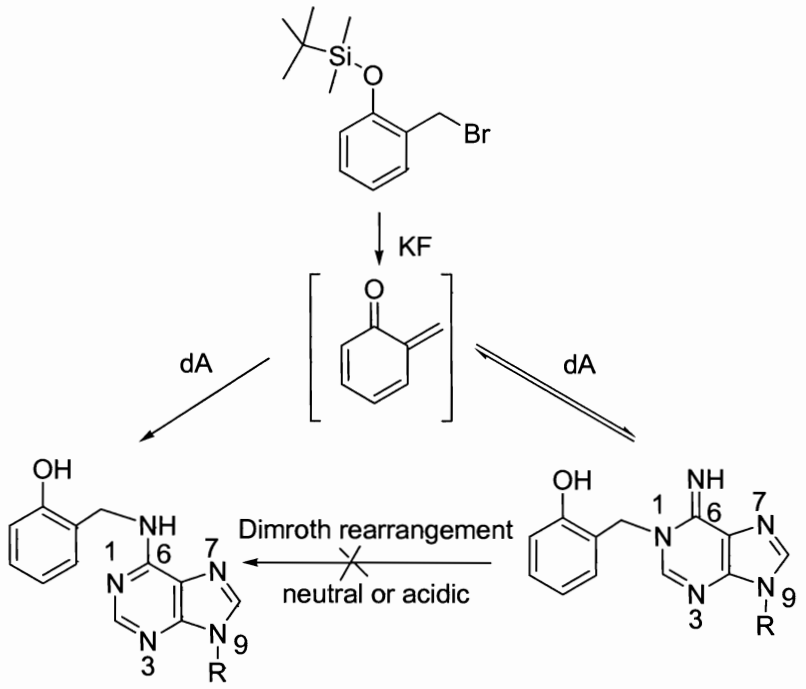

Rokita's group later identified the complete range of QM adducts formed by dG and guanine residues in duplex DNA using reverse-phase chromatography and NMR techniques.[28] The dG N1 adduct formed more readily than dG N^2 in unbuffered 85% aqueous DMF on account of deprotonation of N1 ($pK_a = 9.2$). Under neutral condition, the N^2 adduct was the major product of conjugation. The N7 adduct of guanine was resulted from spontaneous deglycosylation of the corresponding dG N7 adduct.[28] The data from dA adducts indicated that the most nucleophilic site, dA N1 was preferentially, but reversibly coupled to a QM. A Dimroth rearrangement failed to explain the potential conversion of the dA N1 adduct to its dA N^6 derivative under neutral or acidic condition.

Rokita and coworkers hypothesized that the kinetic product, dA N1 adduct would collapse to regenerate QM which was subsequently trapped by the N^6 position to give rise to the thermodynamically stable dA N^6 (Scheme 1.8).[27]

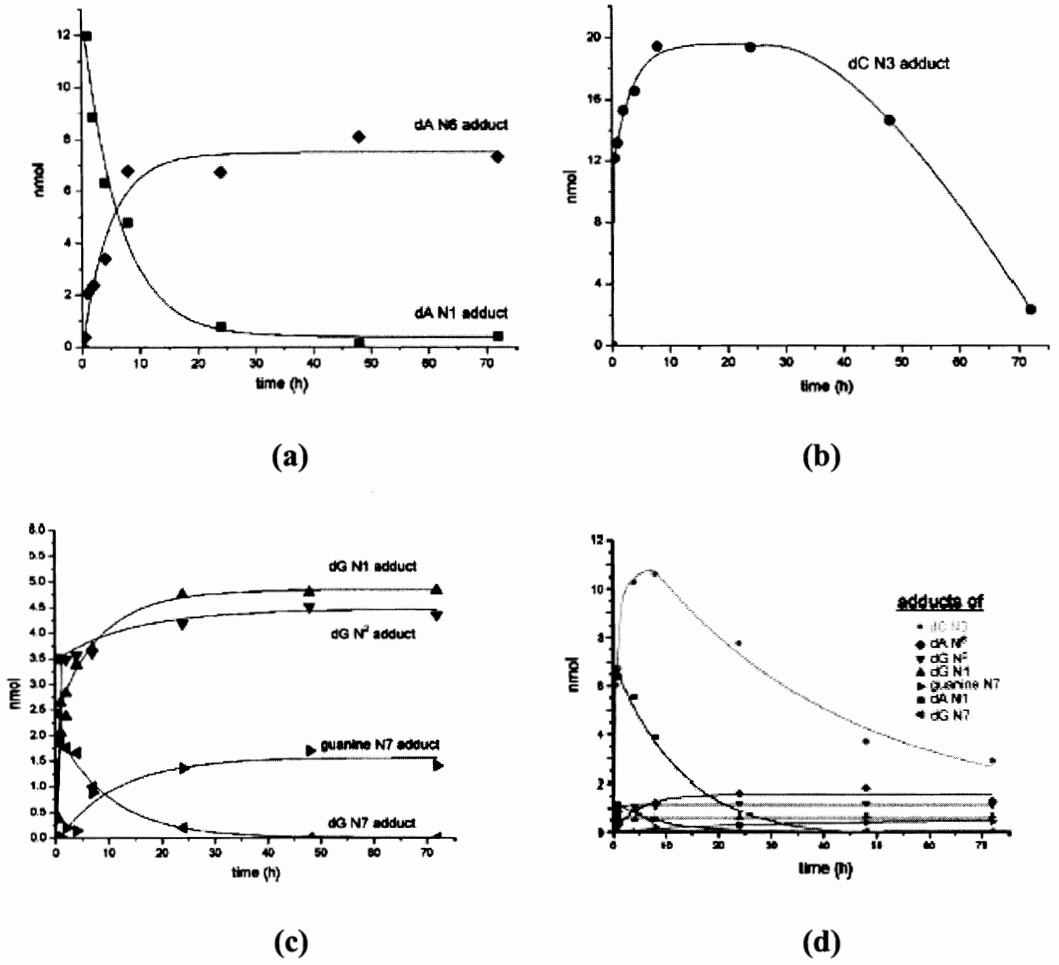

Figure 1.6: Time-dependent profiles of deoxynucleoside alkylation by *o*-QMs: (a) dA alkylation profile, (b) dC alkylation profile, (c) dG alkylation profile, and (d) a mixture of equimolar dC, dG, dA, and T.[33]

Rokita's group also published time-dependent interconversion profiles of deoxynucleoside QM conducts.[33] These observations could be explained by the reversibility of kinetic adducts and the shift from kinetic to thermodynamic adducts. Strong nucleophiles such as the N1 of dA, the N7 of dG and the N3 of dC formed kinetic adducts initially, but these unstable adducts dissipated over time to release QMs. Thermodynamic adducts such as dA N^6 adduct, dG N1 adduct, and dG N^2 adduct accumulated due to irreversible reaction between regenerated QMs and these weak nucleophiles (Figure 1.6). They explained the contradiction between nucleophilicity and leaving group ability by pK_a values of the nucleophiles or its conjugate acid. For nucleophiles with conjugate acids of pK_a value less than 4, kinetic adducts rapidly formed and then were decomposed to regenerate QMs. When pK_a values of the conjugate acids range from 4 to 9, QMs were released slowly. With the pK_a values of nucleophiles greater than 9, irreversibly thermodynamically favored adducts were produced (Figure 1.7).[33]

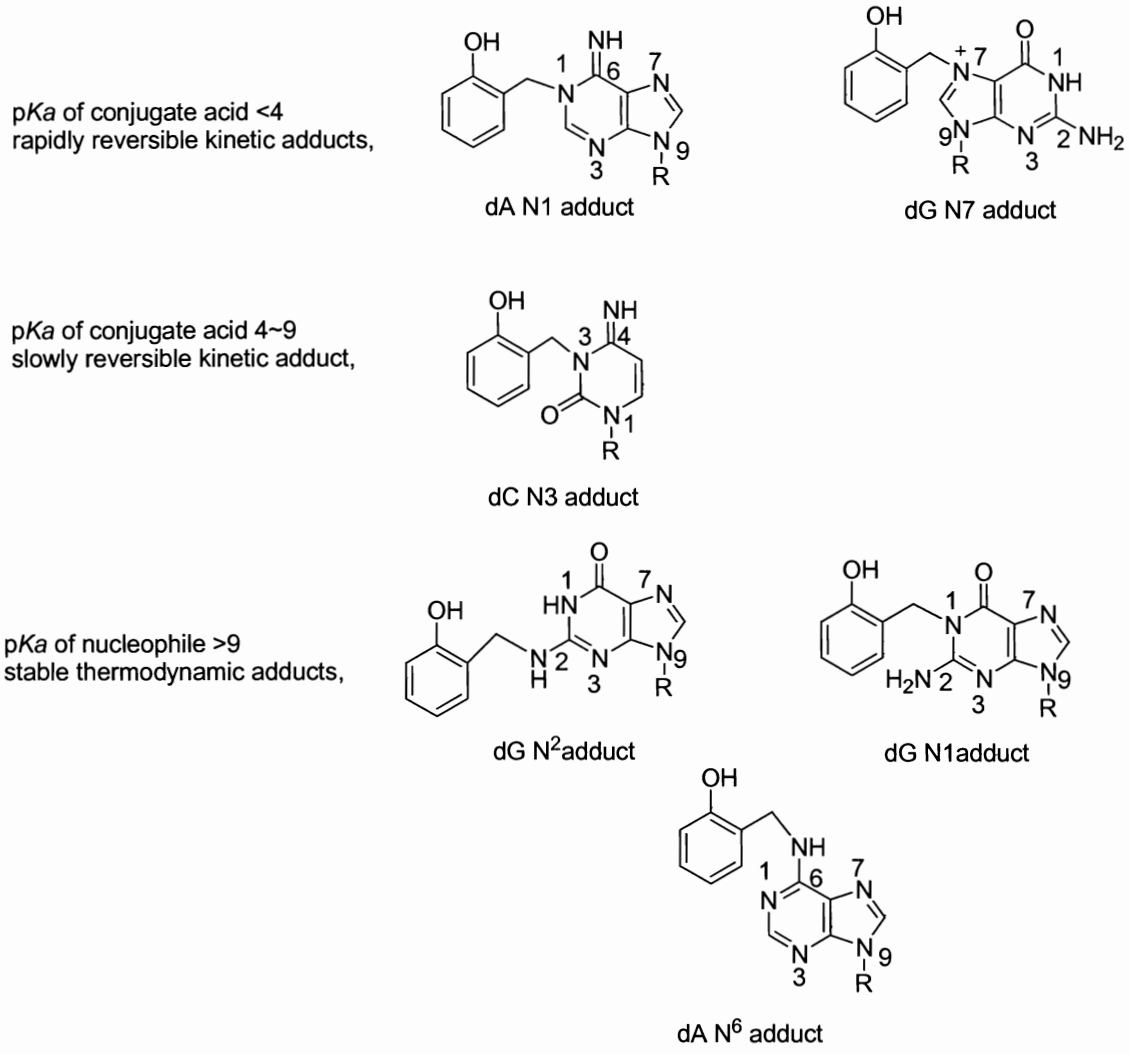

Figure 1.7: Relationship between QM adducts and pK_a of nucleophiles or conjugate acids

Recently, Rokita's group found that electron-donating groups in QM precursors could facilitate initial formation of QM and its regeneration from the reversible deoxynucleoside-QM adducts, while electron-withdrawing substitutions destabilized QM intermediates and suppressed initial generation and subsequent regeneration of QM.[46]

These characteristics were consistent with the electron-deficient nature of QMs and allowed for the prediction of stability and reactivity of various QM drugs in the future.[46]

Freccero's computational data also displayed that the alkylation at the adenine N1, the guanine O^6 and N7 in water were kinetically controlled processes and that the adducts of the *exo*-amino groups of guanine N^2 and adenine N^6 were thermodynamically favored products.[47] Freccero also reported that QM amino acid alkylation adducts such as glycine ($pK_a = 9.78$), serine ($pK_a = 9.15$), and lysine ($pK_a = 8.95$) adducts regenerated *o*-QM under heat or irridation.[48] This results was different from Rokita's hypothesis about reversibility of the nucleobase alkylation adducts related to the pK_a values of the nucleophiles on DNA nucleobases.[33] However, both studies suggested a new perspective for the application of reversible adducts as *o*-QM carriers.

1.5 Alkylation of the phosphate backbone by QMs

As the most abundant nucleophilic functional group of DNA, phosphodiesters can be alkylated by QMs; however, no studies were reported due to the relative weak nucleophilicity of phosphodiesters. The alkylation of phosphodiesters with a *p*-QM has been studied by Turnbull's group. They found that a phosphodiester was alkylated with a *p*-QM when promoted by a BrØnsted acid under anhydrous situations, while the alkylation of a phosphodiester with a *p*-QM under aqueous conditions was an acid-catalyzed, second-order process.[49,50] Phosphodiester-QM adducts could be trapped and stabilized through *in situ* lactonization.[51] The rate and efficacy of trialkyl phosphate formation and trapping was enhanced by a phenol derived *p*-quinone methide (Scheme 1.9).[52]

Scheme 1.9: Alkylation of phosphodiesters with a *p*-QM

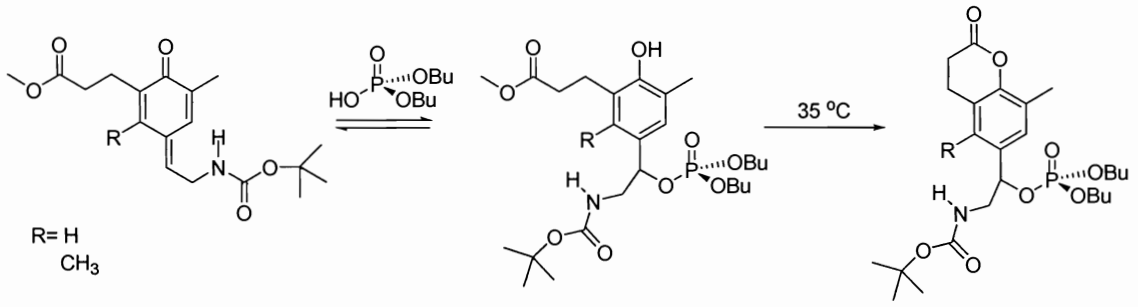

1.6 Sequence-specific DNA alkylation

One major focus of further anti-cancer drug development is the target specificity. Many commercially available anticancer drugs including *N*-mustards chlorambucil and cyclophosphamide are extremely toxic and cause severe side effects due to non-specificity.[53-55] DNA sequence specific agents have recently been designed and synthesized by conjugating the DNA alkylating units with sequence-specific binders. Sequence binders deliver alkylating agents only on the target DNA in the major groove such as triple helix forming, or in the minor groove such as hairpin polyamides. Thus, alkylation occurs specifically in the region of DNA targeted sequence.[56-60] Rokita's group first reported a sequence-specific DNA alkylation by a photo-induced or enzymatic reduction-induced naphthoquinone alkylating agent attached to an oligonucleotide (Scheme 1.10).[55] A photo-induced dimethylanthraquinone-oligodeoxynucleotide conjugate system was found to provide higher yields of target modification compared to the original naphthoquinone appendage (Scheme 1.11).[61]

Scheme 1.10: Sequence-specific DNA alkylation by a naphthoquinone

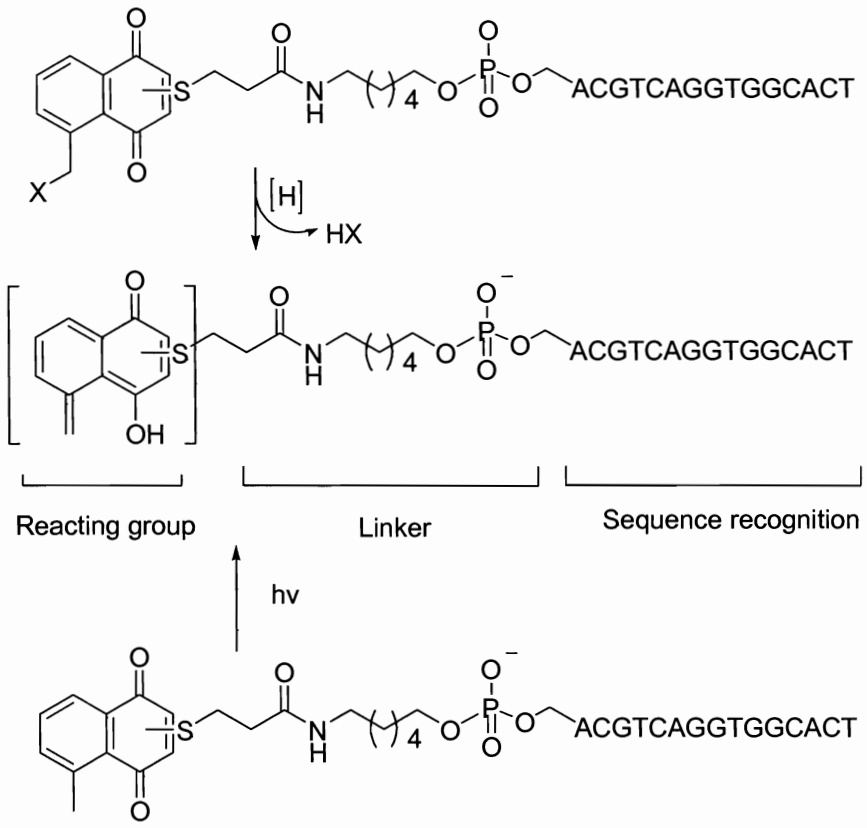

A silyl-protected quinine methide precursor was later chosen as alkylating unit based on its great stability at physiological pH and easy activation by addition of fluoride.[62,63] They once conjugated a silyl-protected phenol to oligodeoxynucleotide and then delivered it to the major groove of DNA through triplex recognition. The precursor triggered by fluoride induced reactive QM intermediates that subsequently alkylated each oligonucleotide in the target duplex. However, the theoretically possible cross-linking to both oligonucleotides was not observed. One possibility was the restricted orientation of

the intermediate or the short length of the linker between the phenol derivative and the recognition site (Scheme 1.12).[29]

Scheme 1.11: Sequence-specific DNA alkylation by a dimethylanthraquinone

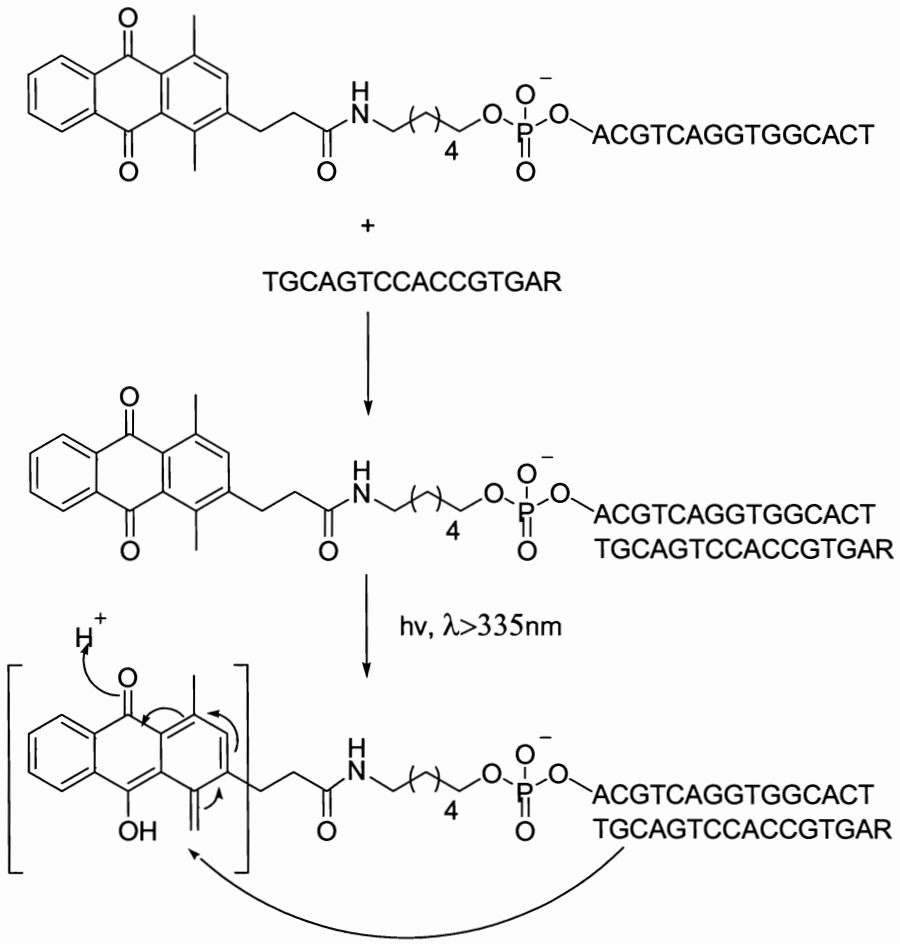

Scheme 1.12: Triplex recognition and selective alkylation

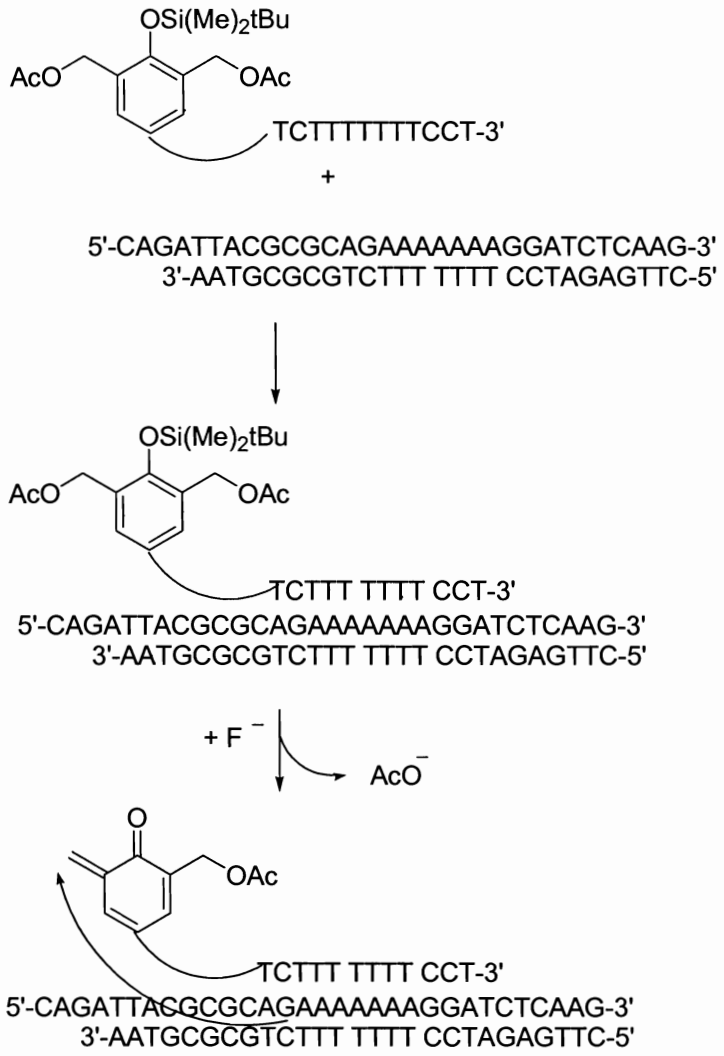

1.7 Target-promoted DNA alkylation systems

Target-promoted alkylation has been observed in natural products such as CC-1065 (Scheme 1.13). The CC-1065 selectively and covalently binds to the N3 position of adenine within the A-T rich minor groove of DNA. Researchers have proposed that this

sequence-selectivity originates from a noncovalent binding selectivity (shape-selective recognition) and a DNA binding-induced conformational change (shape-selective catalysis). The maximum noncovalent binding was achieved in the narrower, deeper AT-rich minor groove. As a result, this preferential AT-rich noncovalent binding not only selectively delivered CC-1065 to the AT-rich minor groove possessing sterically accessible adenine N3 bonding sites, but also induced conformational changes that twisted the linked amide, disrupted the vinylogous amide conjugation, and activated the cyclopropane for nucleophilic attack. This binding-induced conformational change, which was dependent on the shape of the minor groove and was greatest within the narrower, deeper AT-rich noncovalent bonding sites, accelerated the alkylation reaction more than 1000-fold.[2,64] However, target-promoted alkylation of natural products has low sequence selectivity due to the limited recognition. Modification of natural products to improve selectivity is a challenge because the rich variety of functional groups that are characteristic of natural products makes synthetic processes usually quite difficult and laborious.[65]

Scheme 1.13: CC-1065 sequence-specific alkylation

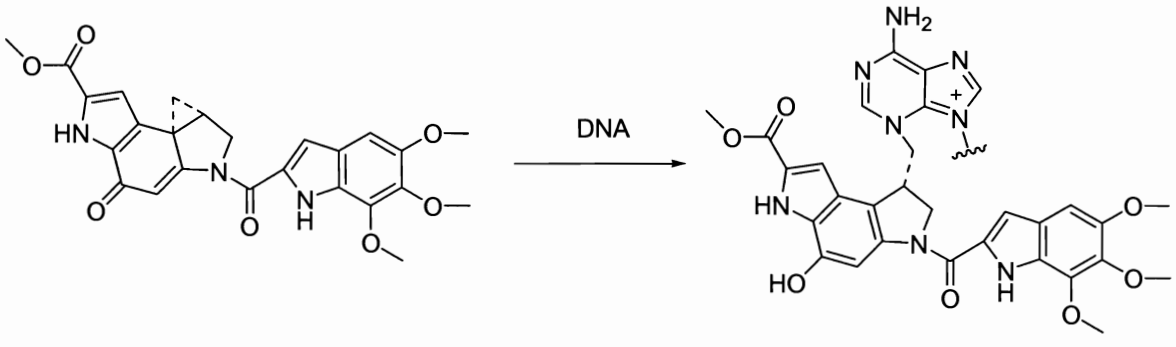

Most recently, Zhou and Rokita reported a simple target-promoted DNA alkylation system based on reversible intramolecular trapping of a reactive QM by an oligonucleotide-QM adduct (Scheme 1.14).[31] The sequence delivery oligonucleotide only alkylated its complementary DNA strand. The driving force was hypothesized through the complementary base pairing to break the self adduct and to regenerate the reactive QM to remove the conformational restriction. Thus, QM formation was favored in the presence of target DNA and the nascent QM was subsequently pseudo-intramolecularly transferred to the target DNA. A unique advantage of this system was that alkylating ability of the self-adduct was controlled by its complementary sequence of DNA. In the absence of the target DNA, the self-adduct and the transient reactive QM were unreactive with water, noncomplementary strands, even at 450-fold excess of a strong nucleophile, 2-mercaptoethanol.[31]

However, this system has several disadvantages. First, self-adducts formed between delivery sequence and nascent QMs may not be reversible, which could be a detrimental factor for this system. For example, the conjugate of a hairpin pyrrole-imidazole polyamide to a QM precursor enhanced the target selectivity; however, no target promoted alkylation was observed.[32] Second, the application of this target-promoted alkylating agent to a duplex target is also challenging because biological application of triplex-formation oligonucleotides are compromised by biophysical limitations. Triplex formation not only involves overcoming charge-charge repulsion effects, but also requires conformational changes on the DNA target recognition ligand and some distortion of the underlying duplex strands. Most triplex formations are less stable than the underlying duplex.[66]

Scheme 1.14: Target- promoted alkylation system

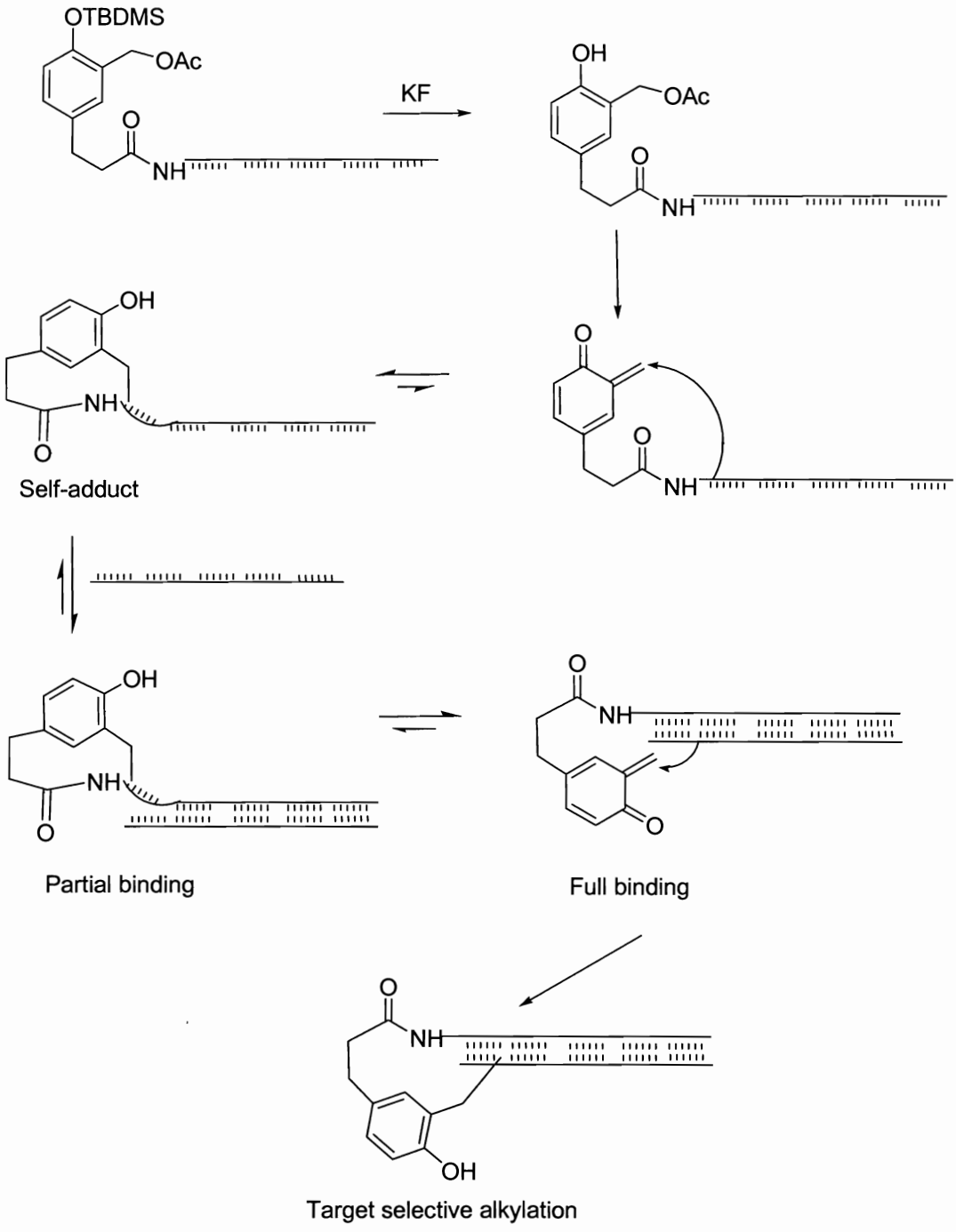

To maintain high specificity and resolve the disadvantages of the original system, our novel target-promoted alkylation system was designed on the basis of these literature results. Figure 1.8 illustrates the mechanism of this improved target-DNA alkylation system, which is composed of three components: a reversible intercalating QM precursor as the latent DNA alkylation agent, an amine linker, and a sequence delivery. Under physiological conditions, an amine linker is protonated and can be eliminated as an ammonium to release QM intermediate. However, alkylating conjugate 1 remains as a stable precursor in the absence of target DNA because the intramolecular trapping of QM is favored. On the other hand, when the sequence delivery recognizes and binds to the sequence-specific target DNA, the QM precursor partially intercalates into DNA. The increased hydrophobic interaction between DNA nucleobase stacking and the intercalator facilitates the elimination of the amino linker and the regeneration of a reactive QM, which can fully intercalate into the DNA bases. Finally, the trapped QM covalently modifies either strand of DNA. In this system, the formation of the intermolecular QM-DNA adduct is driven thermodynamically during the transfer of QM from the delivery sequence to the target DNA. At the same time, the delivery sequence can be released from the target with minimized disturbance on DNA structure.

This novel target promoted alkylation system improves upon the previous system in several respects. First, this novel QM alkylation system transfers QM to targets and releases the sequence specific binder, and minimizes the disturbance in DNA structures. Second, this system can be used for studies on the mutagenic effects of nucleobase QM adducts because it delivers QMs sequence specifically without the interference on the

sequence specific binders. Third, it can be used to covalently modify both single strand and duplex DNA. Fourth, the reversibility of self-adducts is determined by the elimination of amine linkers. Therefore, the change of delivery sequence will not affect the mechanism of this new target-promoted process and the alkylation efficiency of QM intermediates. Finally, the novel activation of the QM intermediate avoids the use of fluoride and makes it more applicable in biological systems.

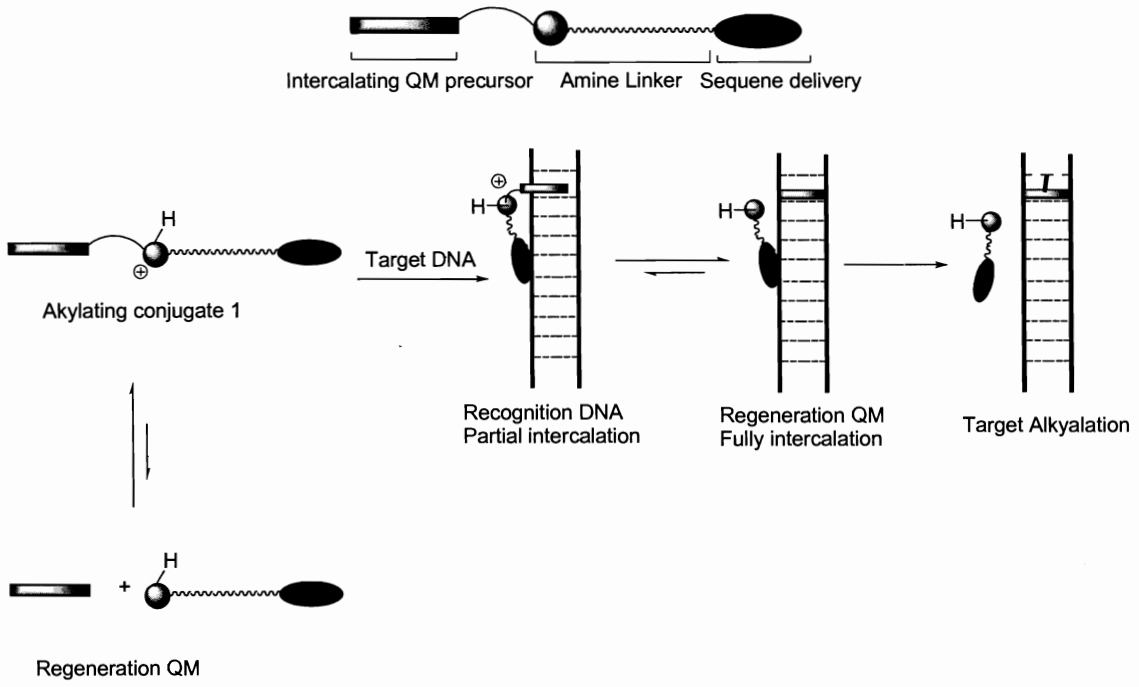

Figure 1.8: A novel target-promoted system

In the following study, three alkylation model systems were designed and synthesized. Nucleobase alkylation by the third system was investigated and the major QM deoxyguanosine adduct was fully characterized by 1D and 2D NMR techniques. The

goal of this study is to provide a fundamental understanding as the basis for the development of this novel target-promoted DNA alkylation strategy.

CHAPTER 2 Synthesis and Investigation of Fused Polycyclic Alkylation Systems

2.1 Introduction

Recently, Zhou and Rokita found that an oligonucleotide-QM adduct could form a stable intramolecularly trapped *o*-QM intermediate, which was released only when target DNA was recognized.[31] Although this target-promoted DNA alkylation system can selectively alkylate a chosen sequence of DNA, it requires an activation of QM with fluoride and a reversible trapping of nascent QM by a sequence delivery. We are trying to develop a novel target-promoted DNA alkylation system for application of QMs to drug design and drug delivery.

Our target-promoted DNA alkylation system contains an intercalating/alkylating QM precursor, an eliminable amine linker, and a DNA sequence delivery illustrated in Figure 1.8. Our first QM precursor has an intercalating fused three-ring structure. A similiar QMs has been reported by Fischer and his colleagues through the photosolvolysis of 1-hydroxy-9-fluorenol in aqueous solution, and this *o*-QM was confirmed by a [4+2] cycloaddition with ethyl vinyl ether (Scheme 2.1).[67] However, this QM formation required a hydroxylated QM precursor to lose one molecule of water in the laser flash photolysis. To our knowledge, a mild generation of this type of QM has not been reported to datee. In this chapter, the fused polycyclic alkylation system was presented, and two model systems

including methoxyl polycyclic and intramolecular hydrogen bonding systems were synthesized and investigated.

Scheme. 2.1: Photosolvolysis of 1-hydroxy-9-fluorenol

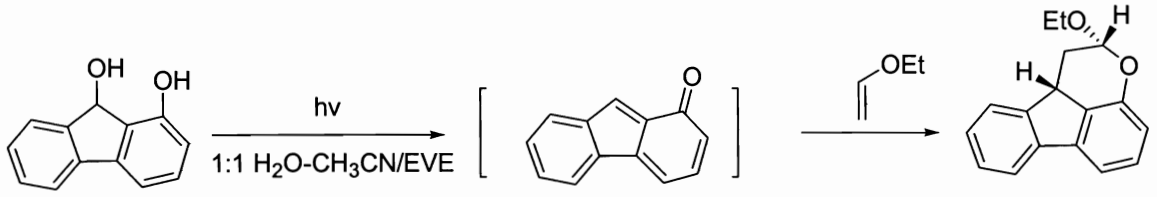

2.2 Methoxyl polycyclic system

Methoxyl polycyclic system consists of three components: a reversible QM precursor in a planar three-ring intercalating system, an amine linker, and a sequence-specific binder (R`) as presented in Figure 2.1. The amine is protonated at neutral pH and can be eliminated as a leaving group in the formation of QMs. As an electron-donating group, methoxyl group may facilitate the formation of electron-deficient QMs. In the absence of DNA target, the regenerated QMs are trapped by the amine as a favored process in the equilibrium. Once target DNA is recognized by a sequence-specific binder, DNA complex A is formed and only partial intercalation can be achieved due to the steric hindrance between the agent and DNA. The increased hydrophobic interaction between DNA nucleobase stacking and the three-ring system is the driving force to promote the formation of QM and result in a fully intercalated DNA complex B. Finally, the trapped QM can covalently modify DNA nucleobases to form DNA adduct. Therefore, target

DNA alkylation is achieved through initial sequence recognition, DNA intercalation and final alkylation. The efficacy of DNA-QM interaction will be enhanced significantly by cooperative intercalation and alkylation.

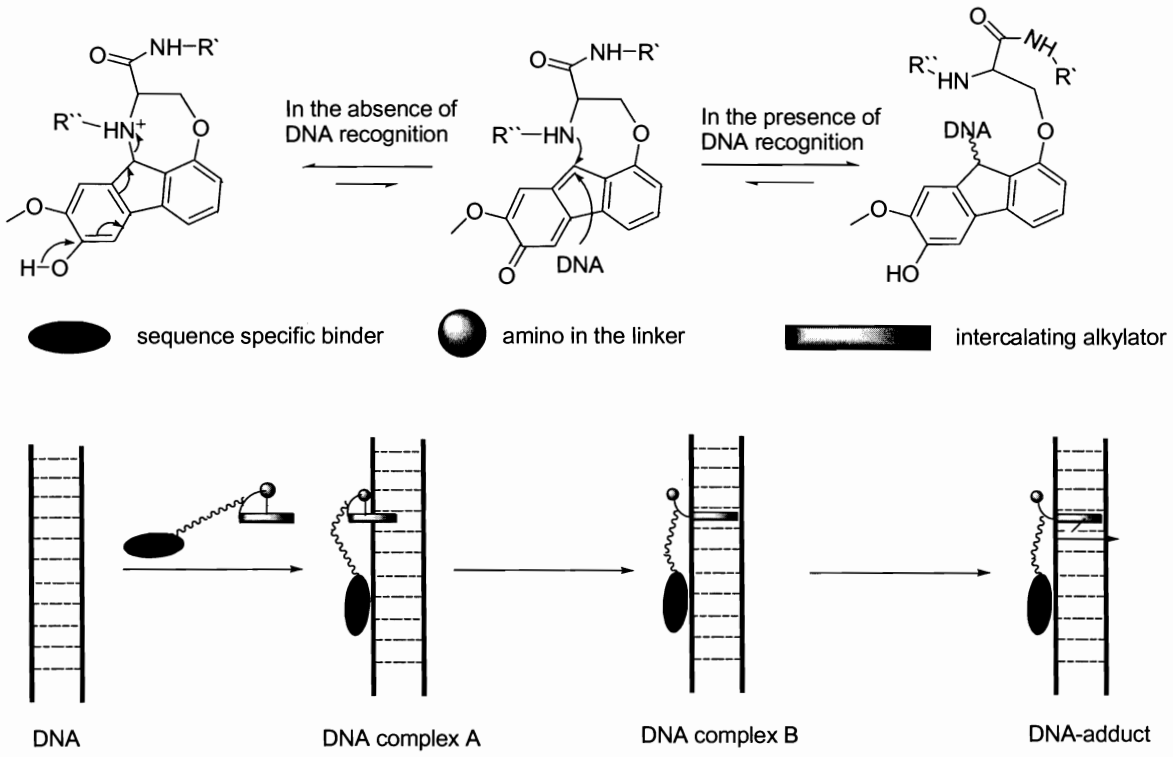

Figure 2.1. Methoxyl polycyclic target-promoted DNA alkylation system

This system was initially conjugated with a 9-aminoacridine derivative instead of a sequence-specific DNA binder due to the synthetic simplicity, the intercalating ability of acridine, and its capability to direct reagents to the major groove.[30,68-72] It was reported that acridine conjugates enhanced the binding of *N*-mustards to DNA and localized them in the major groove near their preferred site of reaction, guanosine N7.[30,71,72] In our system,

acridine and QM precursor can insert between two stacked bases in DNA to produce DNA bis-intercalation which may result in enhanced bending and unwinding of the DNA duplex.[73] 9-Aminoacridine has a pK_a of 9.9 and is positively charged under physiological conditions. The association to the negatively charged phosphate groups of DNA plays a very important role in formation of QM precursor/DNA complexes as the first step in the target recognition.[74]

2.2a Synthesis and DNA alkylation

The acridine conjugate **18** was synthesized from commercially available 2,6-dihydroxy-benzoic acid **1** (Scheme 2.2). Benzoic acid **1** was first converted to lactonized ether **2**, and the phenol group was triflated to triflate **3** with Tf_2O and DIPEA.[75,76] Baeyer-Villiger oxidation of commercially available 5-bromo-2-methoxybenzaldehyde **4** afforded 5-bromo-2-methoxyphenol **5** followed by protection of the free phenol group with benzyl bromide.[77,78] Bromide **6** was converted to boronic acid **7** and then coupled with **3** via Suzuki coupling to afford the biphenyl **8** in 73% yield.[79,80] Biaryl **8** was hydrolyzed with NaOH and cyclized to fluorenone **10** with TFA and TFAA.[81] Mitsunobu coupling of fluorenone **10** and serine derivative **13** obtained by amide synthesis from **11** and **12** afforded adduct **14** in 45% yield under sonication.[82,83] Deprotection of the Boc group followed by reductive amination resulted in aminofluorene **15**.[84,85] Formic acid was used to remove two benzyl groups in the presence of Pd/C to afford free acid **16,** which was condensed with acridine **17** to afford desired acridine conjugate **18**.[86-88] This final product

was purified by reverse-phase HPLC and confirmed by ESI-MS analysis as 604.6 m/z ($M+H^+$) as compared to the calculated mass 604.3 ($M+H^+$).

Conjugate **18** was investigated by Dr. Zhou on a short duplex DNA with radiolabeled P-32. Acridine conjugates were mixed with the duplex DNA at a concentration ratio of 4:1 and incubated overnight at ambient temperature because each acridine conjugate needed at least two intercalating sites and there were 24 possible intercalating sites on this duplex DNA. The reaction mixture was finally treated with hot piperidine, a common method used to induce strand scission at guanine N7, adenine N3 and adenine N7 alkylation, and cleaved nucleotides were separated by electrophoresis and analyzed with phosphorimaging.[30,89-91] Unfortunately, no nucleobase alkylation was observed and variation of pH didn't improve the extent of nucleobase modification.

Scheme 2.2: Synthesis of methoxyl polycyclic system

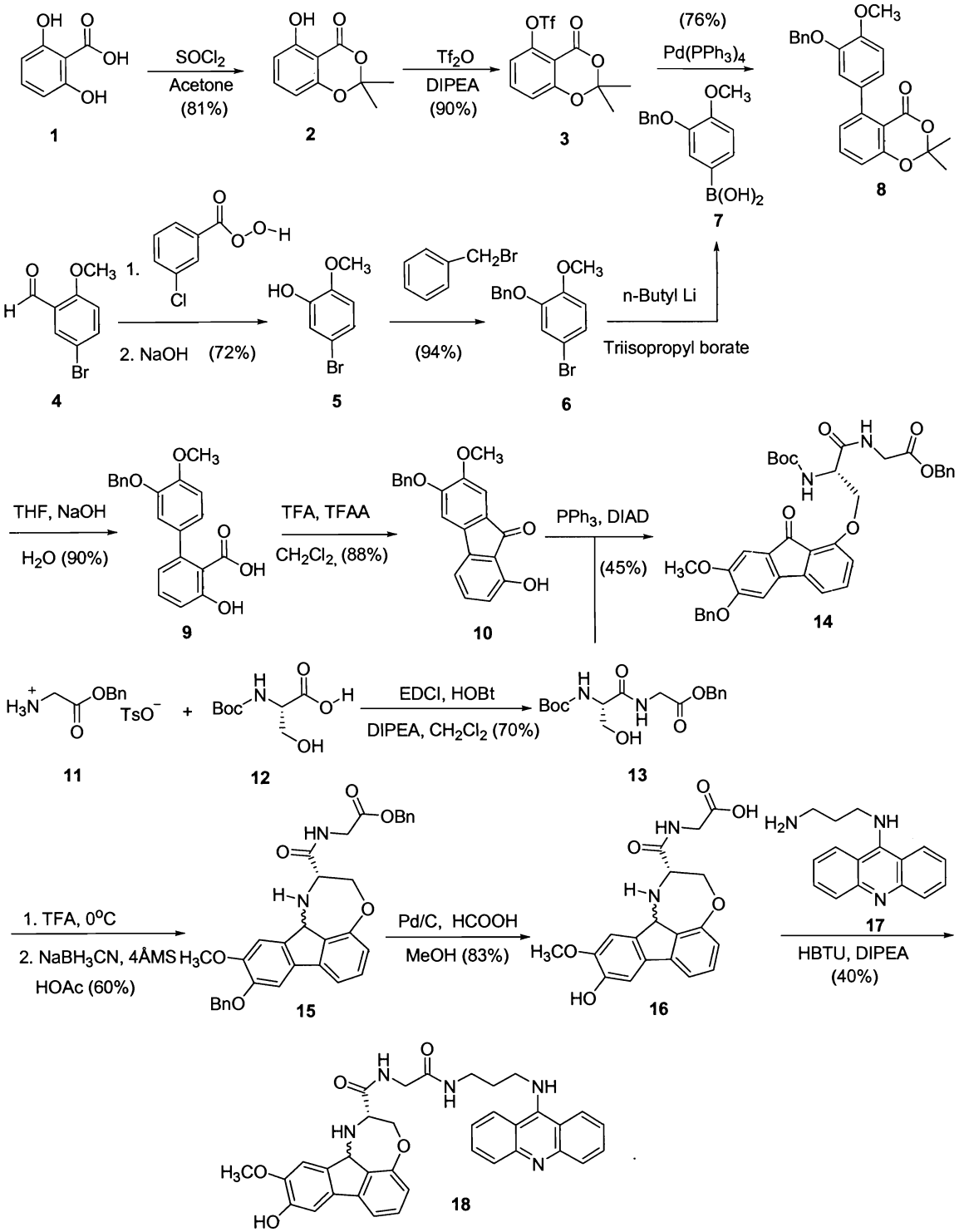

2.2b Modification

The lack of nucleobase alkylation was possibly due to the poor leaving group. The previously synthesized tertiary amine **19** did not show any DNA alkylation either (Figure 2.2), though this tertiary amine has a higher electron density and was expected to be more easily protonated and eliminated than the secondary amine **18**. The reason may be that the steric inhibition of solvation on tertiary amines offsets the effect of electron donation. An amino group can be converted to a very good leaving group, a quaternary ammonium salt **20** by exhaustive methylation.[92] Unfortunately, this quaternized conjugate could not be obtained possibly due to steric factors in the structure.

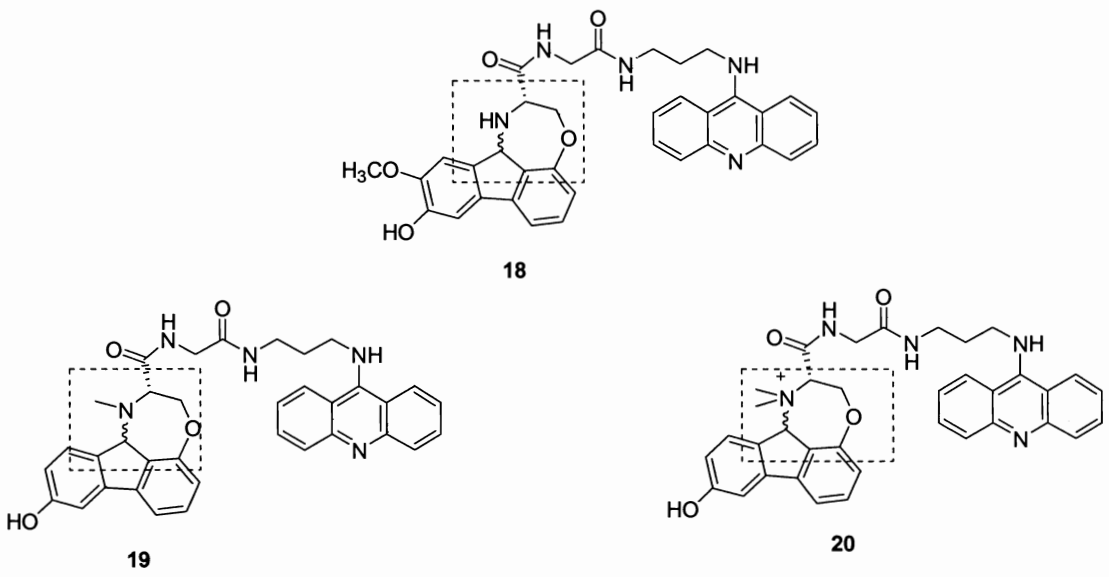

Figure 2.2: DNA alkylators

Another key factor could be the presence of the seven-membered cycloamine ring (Figure 2.2), which disfavors the QM generation through elimination. Generally, five-membered and six-membered rings are kinetically and thermodynamically favored,

respectively. The strain energy of cycloheptane is close to that of cylcopentane and is much smaller than unstable cycloalkanes.[93] In addition, rate of ring closure is a function of ring size and the order 5 > 6 > 3 >7 > 4 > 8-10 is a general trend.[93] Since an aromatic ring was a part of the 7-membered cylcoamine ring structure, it was highly possible that intramolecular trapping was a favored process which prevented the target-promoted alkylation process. Based on this assumption, we believed that the increased size of cycloamine might promote the reversibility of QM regeneration and favor the transfer of QM upon DNA intercalation.

Our first attempt was to increase this seven-membered cyclo amine to a twelve-membered ring **26** by extending the serine linker (Scheme 2.3). For the longer linker, 4-Boc protected aminobutyric acid **23** was condensed with serine **21** to form dipeptide **24,** which was confirmed by ESI-MS as 460 m/z ($M+Na^+$). Dipeptide **24** was then coupled with fluorenone **10** under Mitsunobu condition. However, analysis of the reaction products only showed the triphenylphosphine oxide and a DIAD complex. No desired product **25** was observed despite our early successful coupling between fluorenone and a simple serine. One possibility was that an ester bond was formed by carboxylic acid **23** with a hydroxyl group in **21** instead of an amine group. However, ^1H NMR spectra was consistent with the amide formation in addition to no detection of primary amines by ninhydrin test.

Scheme 2.3: First attempt to modify methoxyl polycyclic system

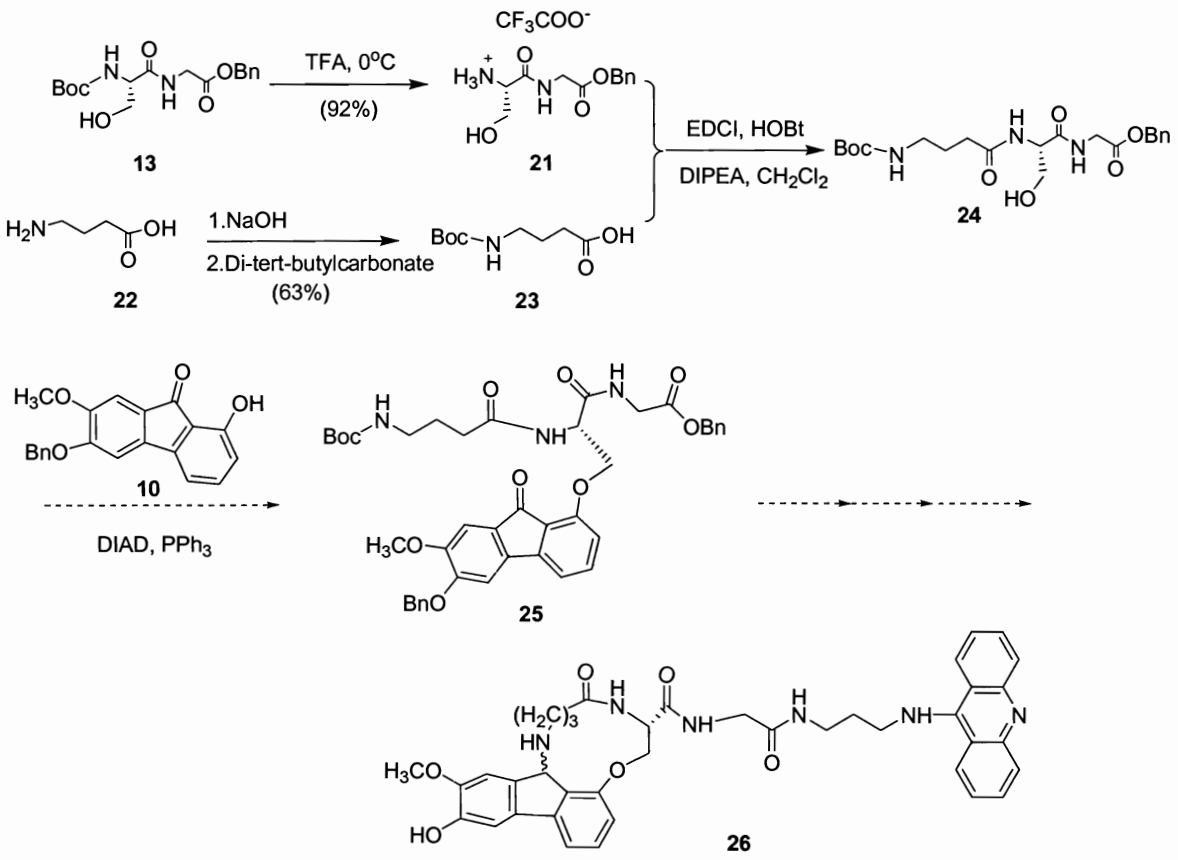

We tried to overcome this barrier by extending the linker in **27** with compound **23** prior to the reductive amination step (Scheme 2.4). However, no desired product **25** was observed even with an activated butyric succinimide ester **28**. A possibility was that the free amine of **27** formed an imide intermediate intramolecularly with the ketone and was not available for amide formation.

Scheme 2.4: Second attempt to modify methoxyl polycyclic system

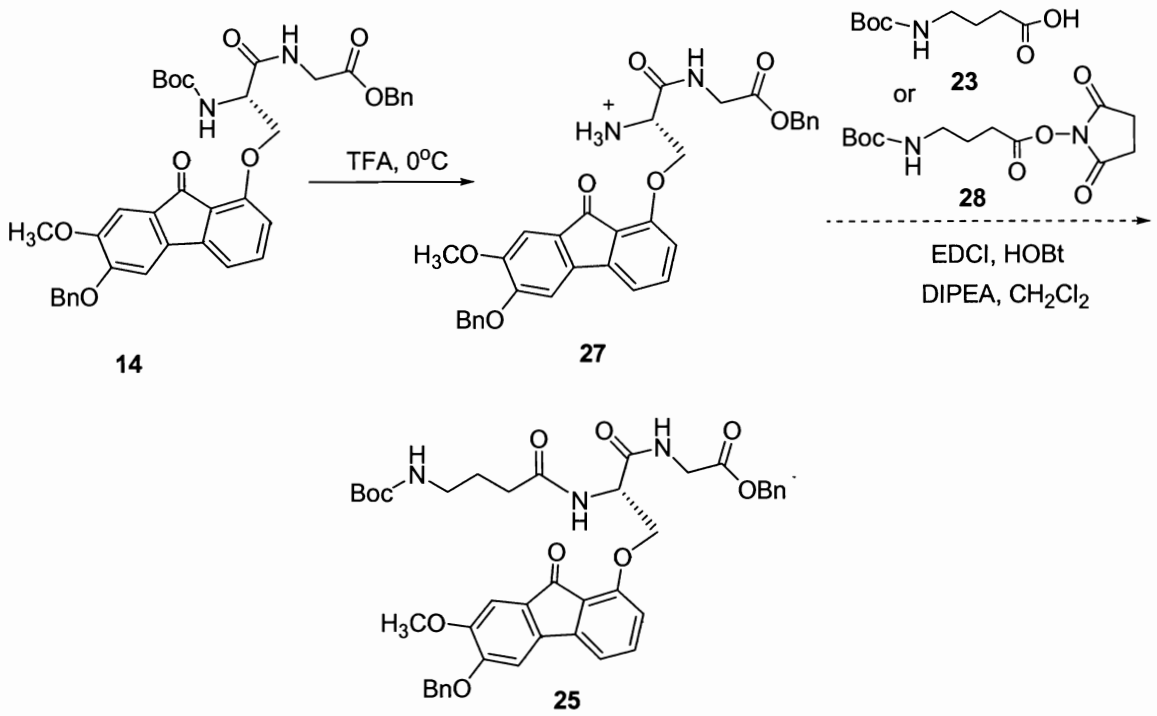

A third alternative was to replace the serine with L-lysine as an 11-membered cyclic amine **34** via an ester bond (Scheme 2.5). To achieve this, the terminal amine of L-lysine was selectively protected by benzaldehyde to allow selective protection of β–amino group with benzyl chloroformate. The terminal amine was then released and protected by a Boc group to lysine **32**.[94] Ester **33** formed readily in the presence of EDCI and DMAP. After the Boc group of ester **33** was removed by trifluoroacetic acid at 0 °C degree, the reaction solution was freeze-dried. The resulting residue was subject to reductive amination in the presence of $NaBH_3CN$. Unfortunately, no desired compound **34** was observed and only **10** and a 7-membered cyclic amide **35** were isolated. This was

attributed to favored intramolecular amide formation (7-membered versus 11-membered) under refluxing condition.

Scheme 2.5: Third attempt to modify methoxyl polycyclic system

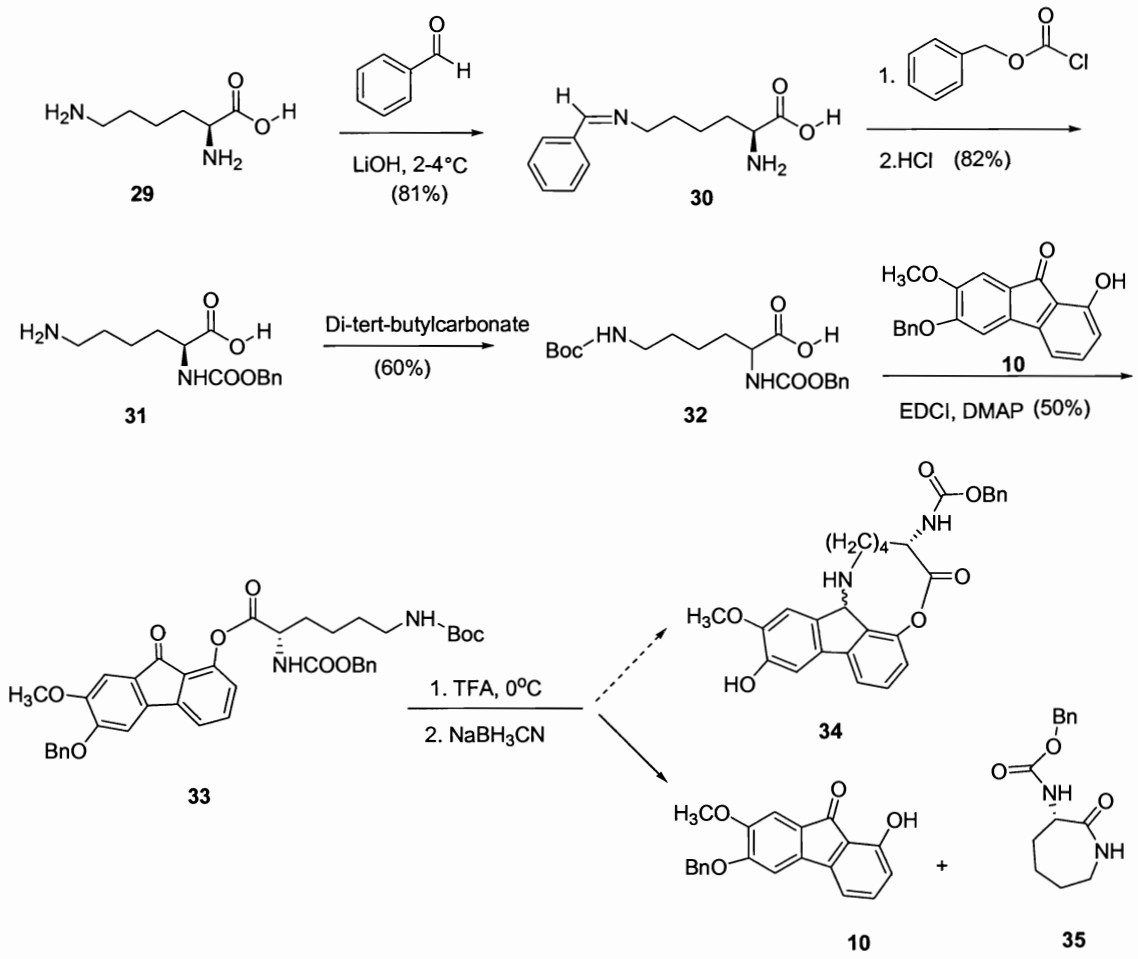

2.3 Intramolecular hydrogen bonding system

On the basis of the preliminary results of the polycyclic system, the target-promoted DNA alkylation system was modified as an intramolecular hydrogen bonding system (Figure 2.3). In this system, the cyclic amine linker was removed and replaced

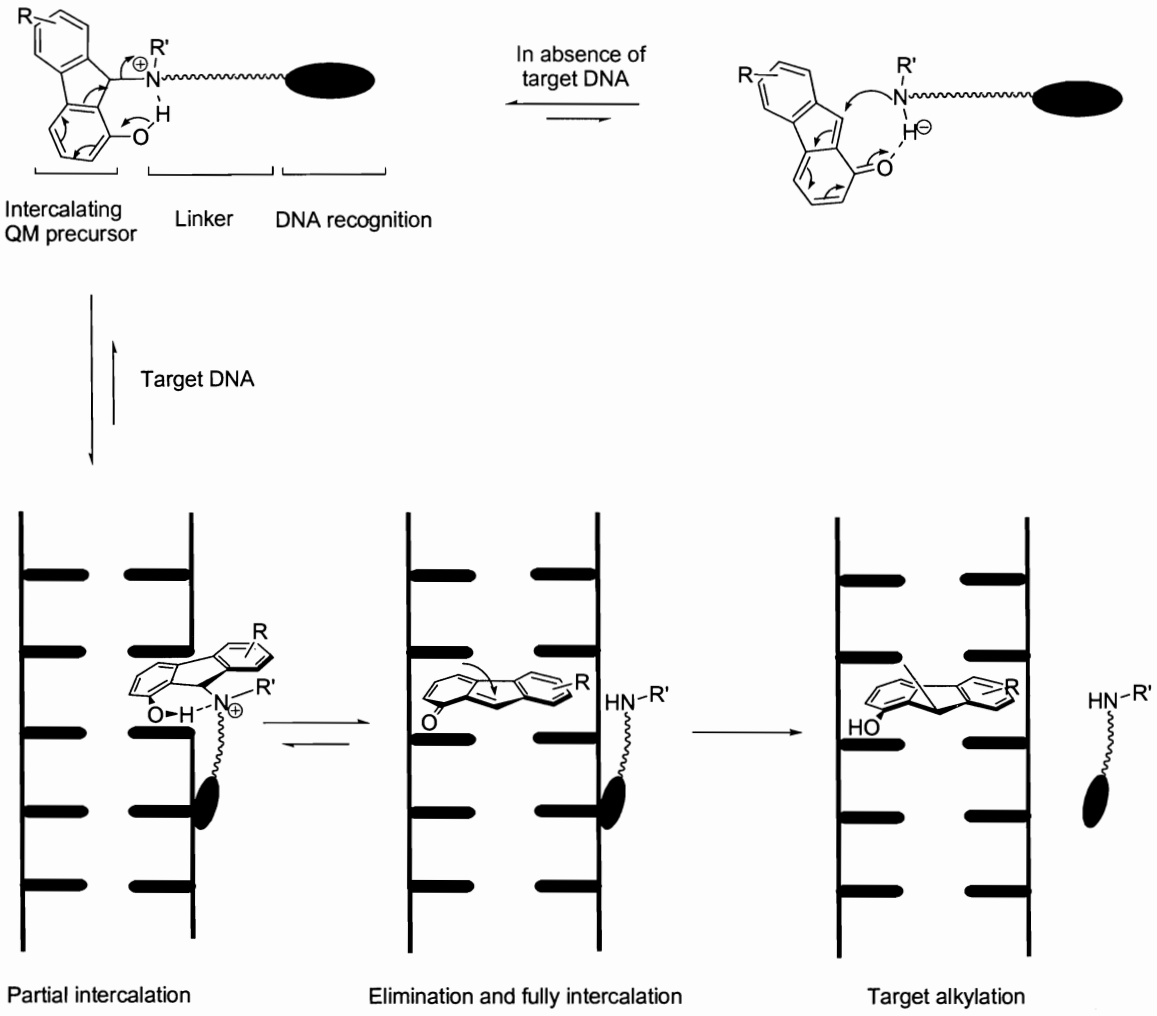

Figure 2.3: Intramolecular hydrogen bonding target-promoted DNA alkylation system

with a linear amine linker, which links the intercalating three-ring planar QM precursor with a DNA sequence delivery. A key feature of this model is that the amine can easily form an intramolecular hydrogen bond with the hydrogen of the phenol group due to a free pair of electrons. In the absence of target DNA, the regeneration of QM will be achieved by elimination of ammonium; however, the H-bonded amine can trap the QM as a favored

pseudo-intramolecular process. In the presence of the target DNA, the QM precursor partially intercalated into DNA duplex via increasing hydrophobic interaction between DNA and QM precursor. Upon the generation of QM, nascent planar QM fully fitted between adjacent base pairs within the DNA structure overcoming the pseudo-intramolecular trapping process. The alkylation of nucleobase would be achieved by subsequent addition of the QM. The sequence recognition was simultaneously released from the alkylating agent.

In order to increase the hydrophobic interaction between stacked nucleobases and QM precursor, naphthalene derivative **45** was designed and synthesized from commercially available naphthalene bromide **36** (Scheme 2.6). Naphthalene bromide **36** was converted to boronic acid **37** through halogen-metal exchange and then coupled with the previously synthesized triflate **3** through Suzuki coupling. Suzuki product **38** was hydrolyzed and then cyclized to an inseparable mixture of **40** and its regioisomer. After reacted with *tert*-butyldimethylsilyl chloride (TBDMSCl) in the presence of imidazole, phenol **40** was converted into silyl ether **41** which has different polarity compared to its isomer and was separated by the silica gel flash column. The structure of silyl ether **41** was further confirmed by 2D-NMR Correlation Spectroscopy (COSY).

When silyl ether **41** was reduced by $NaBH_4$ in THF solution, no reduction was observed until the addition of MeOH. Apparently, methanol reacts with $NaBH_4$ to form methoxyborohydride species, which acts as a stronger reductive agent than $NaBH_4$ in THF due to electron donation from oxygen ligands.[95] On the other hand, silyl ether **41** did not

fully dissolve in 100% MeOH and thus a mixture of THF:MeOH (4:1) was found to produce alcohol **42** in 90% yield.

Scheme 2.6: Synthesis of naphthalene derivative

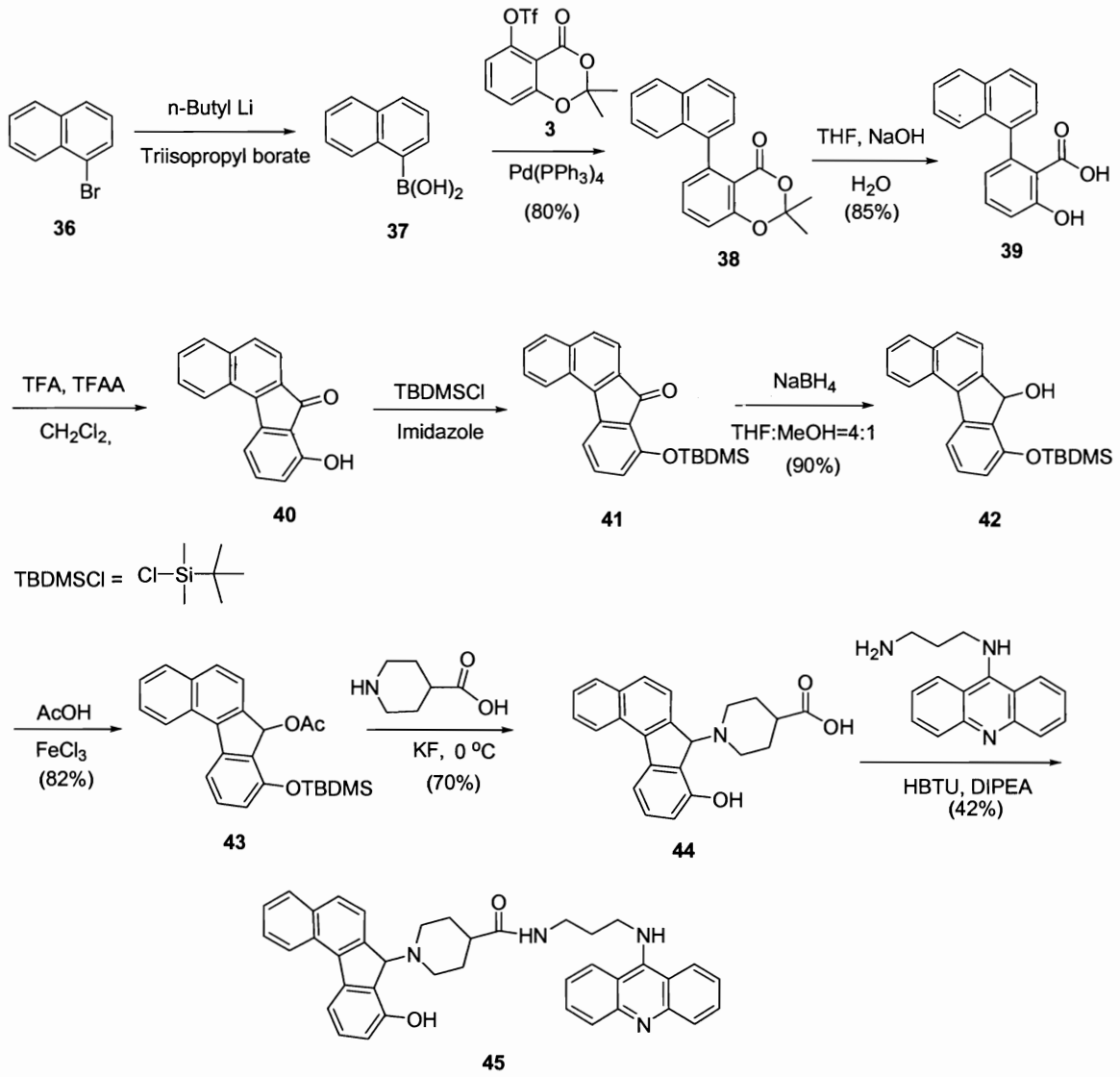

Acylation of alcohol **42** was initially conducted in pure acetyl chloride on rotary bath which removed HCl generated in the reaction.[96] However, this reaction was not consistent and produced a mixture in low yield. Replacement of acetyl chloride with acetic anhydride and $FeCl_3$ was not successful.[97] After investigation of various organic solvents and amounts of $FeCl_3$ under different reaction temperatures, acylation was found to work well with acetic acid (AcOH) in the presence of one equivalent of $FeCl_3$ and the yield was 82%.

The next reactions were QM generation and nucleophilic addition. Naphthalene QM was formed by desilylation with fluoride and then elimination of acetate group, and generated QM was *in situ* attacked by the amine group of piperidine carboxylic acid to produce compound **44** (Scheme 2.7). Due to its insolubility in DMF, piperidine carboxylic acid was dissolved in water; however, considering the high reactivity of QM and nucleophilicity of H_2O, the amount of H_2O was kept in the minimum level in this reaction. Initial reactions were not successful at ambient temperature, and the reaction failed after adding fluoride. Reaction conditions were modified and finally, this problem was solved by carrying out the alkylation at 0 °C. We also examined the QM generation with tetrabutylammonium fluoride (TBAF) which is a phase transfer catalyst for organic-insoluble ionic fluoride. TBAF only produced compound **44** in 36% yield, while KF produced 70% yield under the same condition. Therefore, KF was chosen as a desilylation agent. Compound **44** was subsequently condensed with acridine **17** using our previously discussed methods to afford desired acridine conjugate **45,** which was confirmed by ESI-MS analysis.

Scheme 2.7: Quinone methide generation and nucleophilic addition

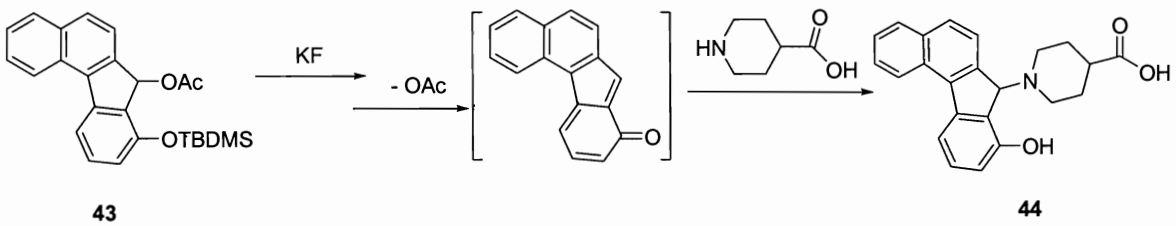

43 **44**

In an addition to compound **45**, a second model compound **50** was synthesized to compare the efficiency of generation of QM with electron-donation groups (Scheme 2.8). Since QMs are electron deficient, electron-donating groups can facilitate the formation of QM. The previously synthesized **10** was protected by silyl group and then the ketone group was reduced by $NaBH_4$ to produce alcohol **47**. Acetate **48** was initially produced in 20% yield with AcOH and $FeCl_3$ due to hydrolysis of the acid fragile methoxyl and benzyloxy groups on starting material **47**. The reaction condition was investigated by varying temperature and decreasing concentration of AcOH with CH_2Cl_2. We found that the yield was increased at 0 °C; however, the reaction solution froze when the concentration of AcOH was more than 80%. The optimal yield was achieved with one equivalent of $FeCl_3$ in a mixture solution of AcOH: CH_2Cl_2 (65:35) at 0 °C (Table 2.1). The acetate **48** was desilylated by KF and reacted with piperidine carboxylic acid *in situ* to give rise to product **49** which was subsequently coupled with acridine to produce acridine conjugate **50.**

Scheme 2.8: Synthesis of methoxyl derivative

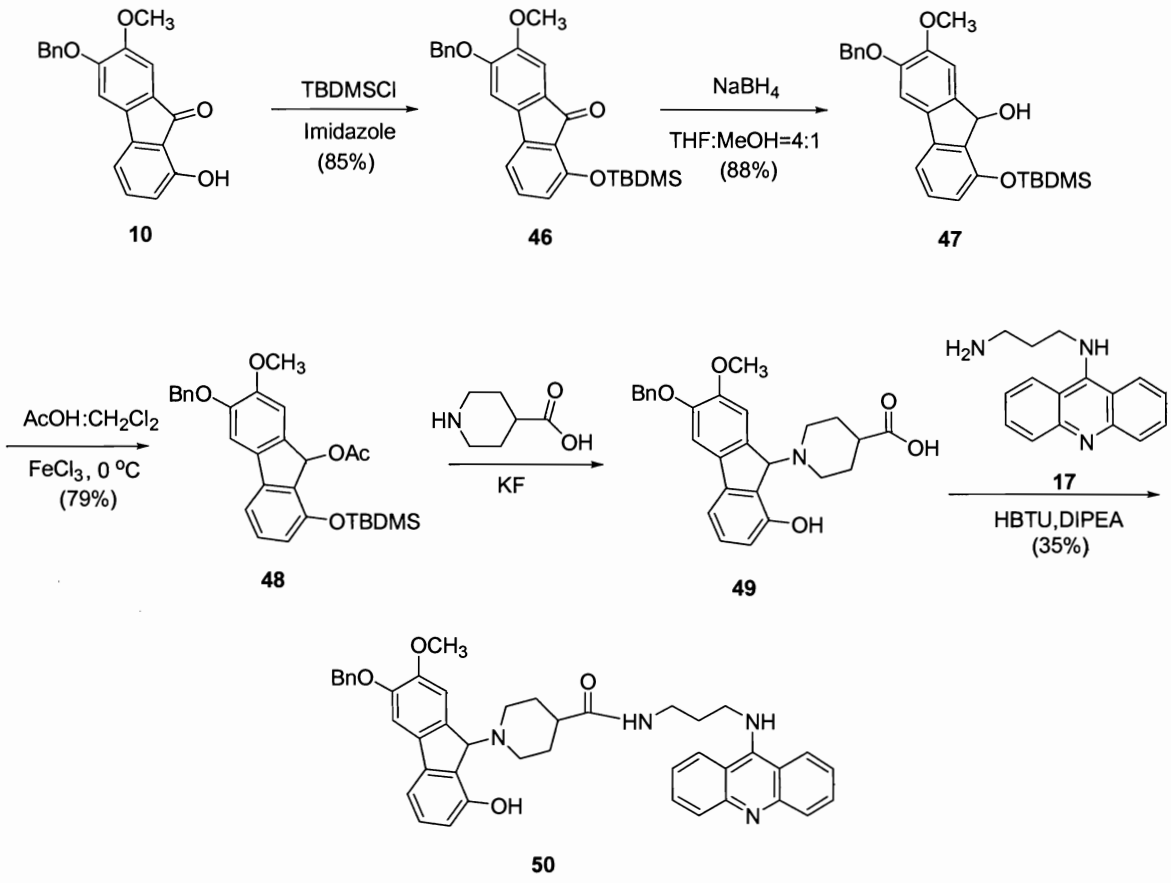

Table 2.1. Investigation of acylation condition

Solvent		Temperature	Yield
AcOH	CH_2Cl_2		
100%		ambient	20%
80%	20%	0 °C	63%
75%	25%	0 °C	51%
70%	30%	0 °C	69%
65%	35%	0 °C	79%

DNA alkylation with acridine conjugates **45** and **50** were investigated on a target DNA by Dr. Zhou using the method described above. However, nucleobase alkylation was not observed. One possibility was that QM was not be regenerated from the QM-amine adduct in the process, although numerous examples have been reported and discussed in Chapter 1. It was unclear if the QM of this three-ring system could be formed due to the lack of literature precedences, even though we were able to form the acetate to the amine such as **43** to **44** and **48** to **49**, respectively. We were not sure if compounds **44** and **49** were formed from the generated QM or directly from SN1 reaction after desilylation. Therefore, a third model system biaryl QM system was designed and synthesized, which was presented in the following chapters.

2.4 Conclusion

For an improved target-promoted DNA alkylation system, a fused polycyclic alkylation system was designed, which contains an intercalating quinone methide precursor that can be converted into a thermodynamically favored quinone methide driven by hydrophobic interaction between DNA nucleobases and QM precursor. This system included two proposed models. The first model system, methoxyl polycylic system was synthesized through a Mitsunobu coupling of a fluorenone and a *L*-serine derivative, followed by reductive amination and coupling with an acridine derivative. However, this QM precursor didn't show alkylation on DNA, which was ascribed to high stability and fast cyclization rate of the 7-membered cyclic amine preventing the regeneration and transfer of QMs.

The first model system was modified to a 12-membered or an 11-membered cyclic amine ring. The syntheses were undertaken by coupling fluorenone **10** with a long chain serine **24** and a *L*-lysine derivative **32**, respectively. However, Mitsunobu coupling of **10** and **24** did not produce the desired product while the reductive amination of compound **33** favored an unexpected 7-membered ring formation and regeneration of the earlier precursor **10**.

In the second intramolecular hydrogen bonding system, a linear amine linker replaced the cyclic amine linker, and two model compounds (naphthalene derivative **45** and benzene derivative **50**) were synthesized. Both model compounds **45** and **50** were investigated on double strand DNA; however, no DNA damage was observed.

It was reported that an *o*-QM was generated through photosolvolysis of 1-hydroxy-9-fluorenol. However, further investigation would be required to confirm the formation of QM under mild conditions. Studies in this chapter have provided the synthetic routes and initial analysis of the preliminary system, which has potentially benefited the development and optimization of this target-promoted DNA alkylation strategy presented in the following chapters.

CHAPTER 3 Biaryl Alkylation System and Its Alkylation of Nucleobases

3.1 Introduction

Based on preliminary data of previously studied systems, a biaryl system was designed and two new QM precursors, naphthalene derivative and quinoline derivative, were synthesized in this chapter (Scheme 3.1). Compared to the systems described in the previous chapter, the conformational restriction in the biaryl system is removed, while the potential hydrophobic interaction with DNA remains. In addition, the intercalating moieties, naphthalene and quinoline rings, can potentially facilitate the target-promoted DNA alkylation through enhanced hydrophobic intercalations with DNA. Figure 3.1 shows the molecular modeling of quinoline/DNA alkylation product generated from Spartan software using AM1 calculation. In this model, deoxyguanosine N7 is alkylated by a QM and the perpendicular quinoline ring adopts a conformation which is intercalating into DNA. The distance between the intercalating moiety and the base pair is 3.3-3.8 Å, which is close to 3.4 Å, the average distance between stacked base pairs of DNA, suggesting that enhanced hydrophobic interaction will be achieved in this system.

Scheme 3.1: Naphthalene and quinoline QM precursors

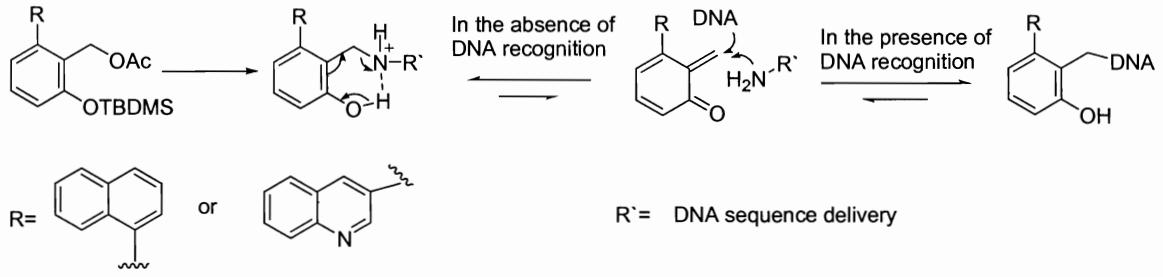

In this chapter, syntheses of QM precursors were first presented and the potential for DNA QM alkylation was investigated by nucleobase alkylation including dA and dG with our QM precursors.

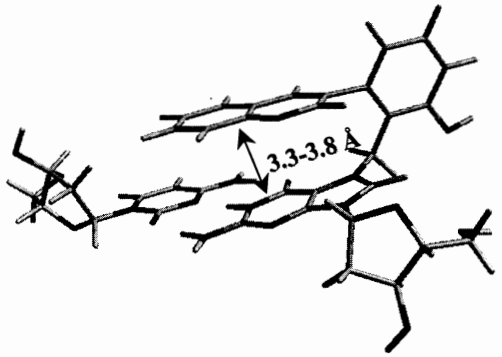

Figure 3.1: Molecular modeling of quinoline derivative

3.2 Synthesis of biaryl QM precursors

For naphthalene compound, the synthetic route of naphthalene QM precursor was summarized in Scheme 3.2. Previously synthesized compound **38** was reduced by lithium aluminum hydride in dry THF solution to give phenol **51** in 80% yield. The two hydroxyl groups in phenol **51** were subsequently converted into silyl ethers based on the procedure

described in Chapter 2. The next step was the selective transformation of one silyl group to an acetate group. A detailed solvent study with varied temperatures and ratios of $FeCl_3$ led us to find that the optimal condition of the acetyl-conversion was to use a mixed solution of acetic acid and acetic anhydride in a 1:1 ratio with one equivalent of $FeCl_3$, which produced the desired product **53** in 79% yield.

Scheme 3.2: Synthetic route of naphthalene QM precursor.

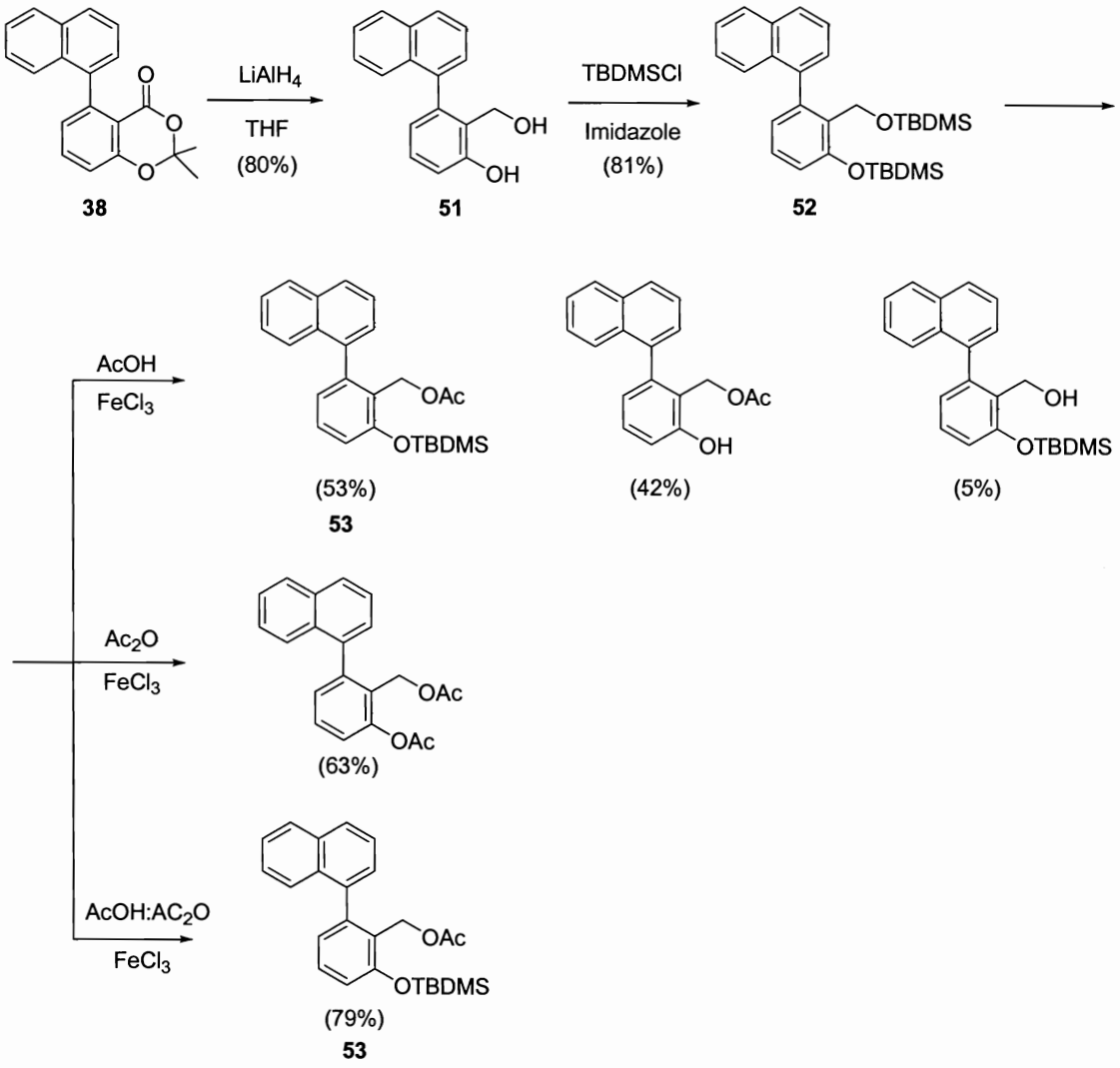

For the quinoline compound **59**, the synthetic route was summarized in Scheme 3.3. Boronic acid **55** was prepared according to the published methods of which n-butyl lithium was added dropwise into a dry THF solvent of 3-bromoquinoline and triisopropyl borate.[98] Boronic acid **55** was then coupled with triflate **3** to give rise to product **56** in 73% yield which was subsequently reduced by $LiAlH_4$ in 88% yield. Disilyl ether **58** was produced in 87% yield using the previously described method in Chapter 2. The following acylation reaction in acetic anhydride with 1.5 equivalents of $FeCl_3$ afforded desired compound **59** in 30 minutes in 74% yield.

Scheme 3.3: Synthetic route of quinoline QM precursor.

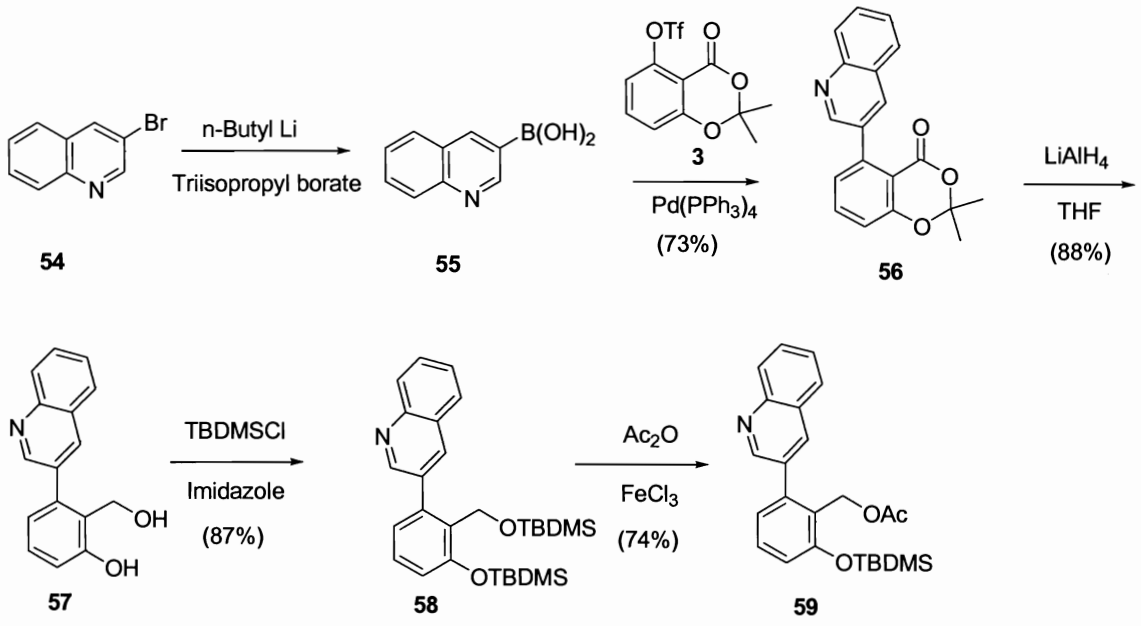

3.3 Alkylation studies of deoxynucleoside adducts

The potential for DNA alkylation was investigated by QM nucleobase alkylation. Structural characterization of QM nucleobase adducts could help us to understand the intrinsic reactivity of DNA nucleobases and the mechanisms of our potential target-promoted DNA alkylating agent. DNA nucleobase alkylation with QMs has been extensively studied by Rokita's group, and they reported that major products generated by deoxynucleosides with QMs were dG N^2 adduct, dA N^6 adduct, and dC N3 adduct.[26,41] It is possible that the intrinsic reactivity of QM towards the nucleobases will lead to specific modification of nucleobases. Our QM precursors are structurally similar to their QM model, yet have additional intercalating aromatic moieties. The difference in structures may lead to different reactivity and adduct distribution with deoxynucleosides.

Quinoline dG alkylation was first assessed over 72 h with the quinoline QM precursor **59**, dG, and KF in aqueous DMF (90% DMF). The final concentrations were 3.6 mM QM precursor, 5.4 mM dG, and 18 mM KF. The reaction solution was stirred at room temperature, and 50 μL of reaction solution was mixed with 50 μL of water prior to injection to minimize the impact of DMF on the retention time in the HPLC separation. The HPLC analysis was carried out using a gradient condition of 10%-70% CH_3CN in triethylammonium acetate (50 mM, pH 6.0) over 40 min (1 mL/min). The major signal was observed at 19 min and was identified by ESI-MS as a quinoline dG adduct, 500.9 m/z (M^+) and 385.1 m/z (dG de-sugar adduct + H^+) consistent with the calculated mass 500.2 (M^+) and 385.1 (dG de-sugar adduct + H^+). Over 72 h, the quinoline dG adduct remained unchanged (Figure 3.2).

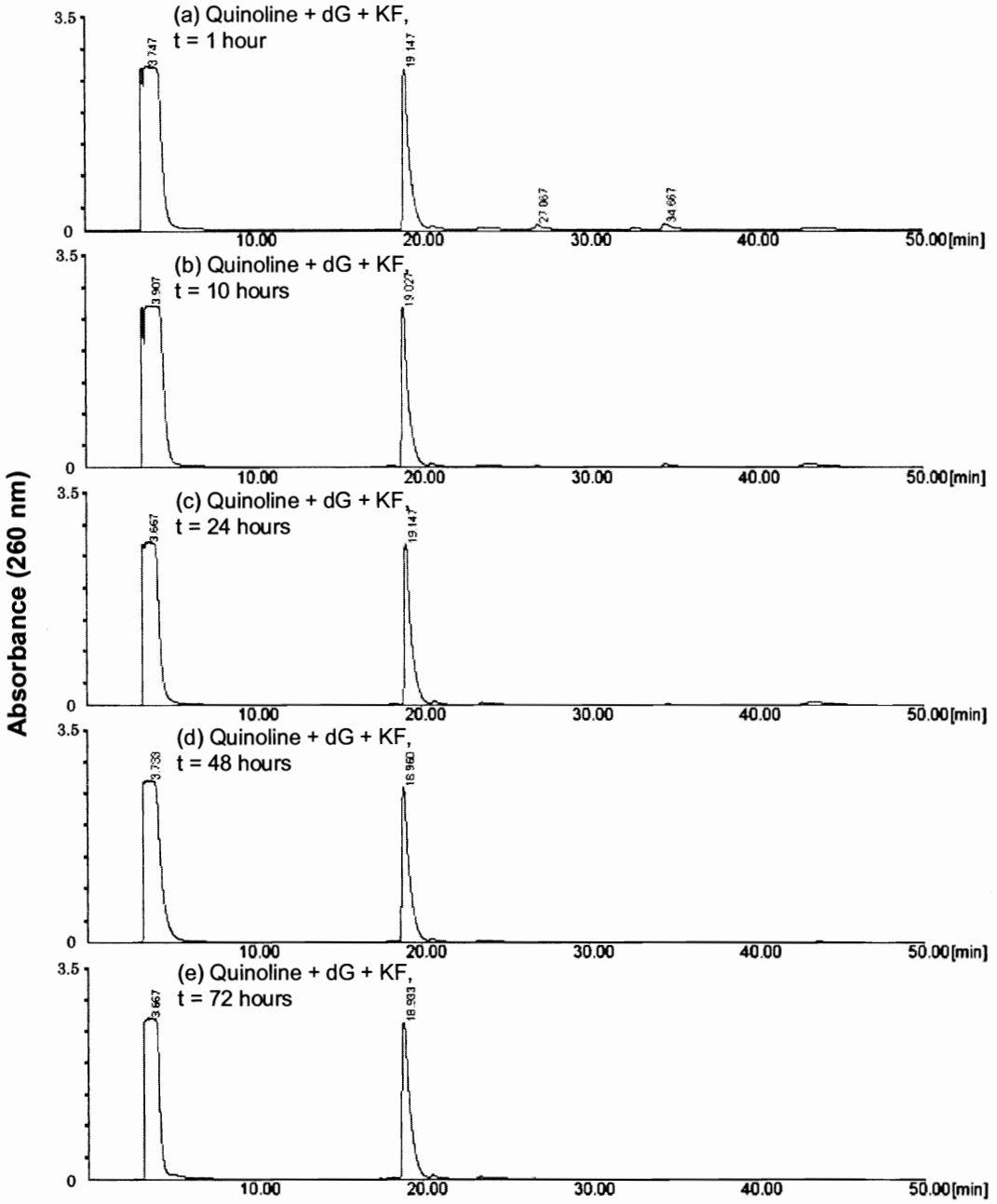

Figure 3.2: Time course of quinoline dG alkylation by HPLC analysis at room temperature over 72 h. The reaction solution contained 3.6 mM quinoline QM precursor, 5.4 mM dG, and 18 mM KF in aqueous DMF (90% DMF).

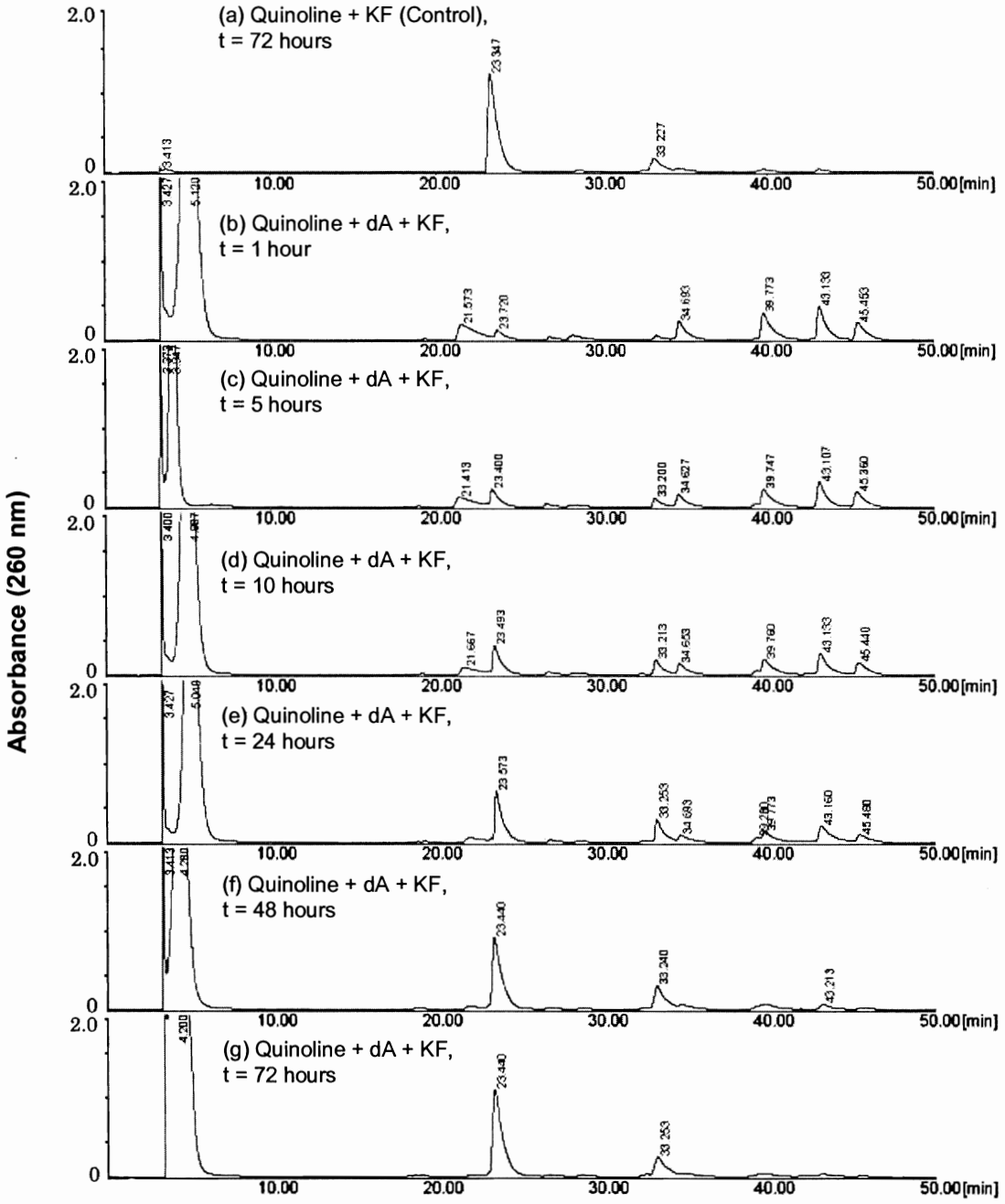

Figure 3.3: Time course of quinoline dA alkylation by HPLC analysis at room temperature over 72 h. The reaction solution contained 3.6 mM quinoline QM precursor and 18 mM KF without/with 5.4 mM dA in aqueous DMF (90% DMF).

The time-dependent analysis of quinoline dA alkylation was investigated using the same method described above. A control, QM precursor **59** and KF without deoxynucleoside, was presented in Figure 3.3 (a). Profiles (b)-(g) were the time course study of the quinoline dA alkylation. In contrast to dG adduct, multiple peaks were observed, and only the signal at 21 min was quinoline dA adduct as a MS signal at 485.4 m/z (M^+) in ESI-MS. This signal decreased with time, which indicated quinoline dA adduct was labile. On the other hand, the signal at 23 min increased with time and became the major peak after 24 h. After 72 h, quinoline dA reaction solution produced the same HPLC chromatogram as the quinoline control, which indicated that both signals at 23 min and 33 min were related to the hydrolysis of quinoline QM. Indeed, direct ESI-MS analysis of the HPLC fractions confirmed that signal at 23 min was the hydrolyzed product compound **57** with a MS signal at 251 m/z (M^+).

Naphthalene dG alkylation was also investigated by using the same method as mentioned above. The major peak at 22 min was analyzed by ESI-MS and identified as a naphthalene dG adduct, 500.3 m/z ($M + H^+$) and 383.5 m/z (dG de-sugar adduct $^+$) consistent with the calculated mass 500.2 ($M + H^+$) and 383.1 (dG de-sugar adduct $^+$). Similar to quinoline dG adduct, this adduct was stable and had no degradation over 3 days at ambient temperature (Figure 3.4).

The time course of dA alkylation by naphthalene was also investigated (Figure 3.5). Direct ESI-MS analysis of the HPLC fractions identified that the signals at 24 min and 30 min were a naphthalene dA adduct as 483.9 m/z (M^+) and 367.9 m/z (dA de-sugar

adduct $^{+}$), and the hydrolyzed naphthalene QM product **51** as 249 m/z ($M\text{-}H^{-}$), respectively.

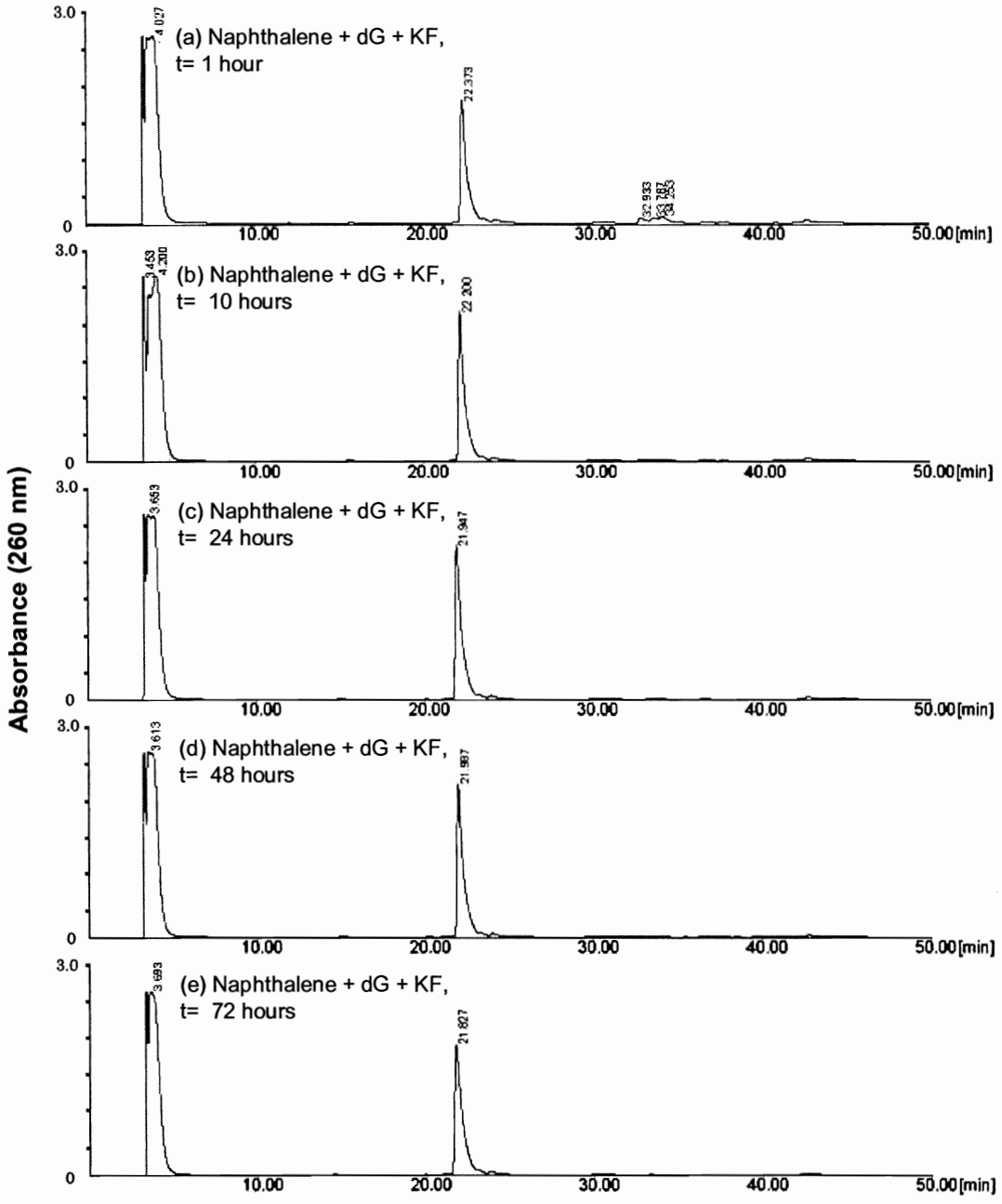

Figure 3.4: Time course of naphthalene dG alkylation by HPLC analysis at room temperature over 72 h. The reaction solution contained 3.6 mM naphthalene QM precursor, 5.4 mM dG, and 18 mM KF in aqueous DMF (90% DMF).

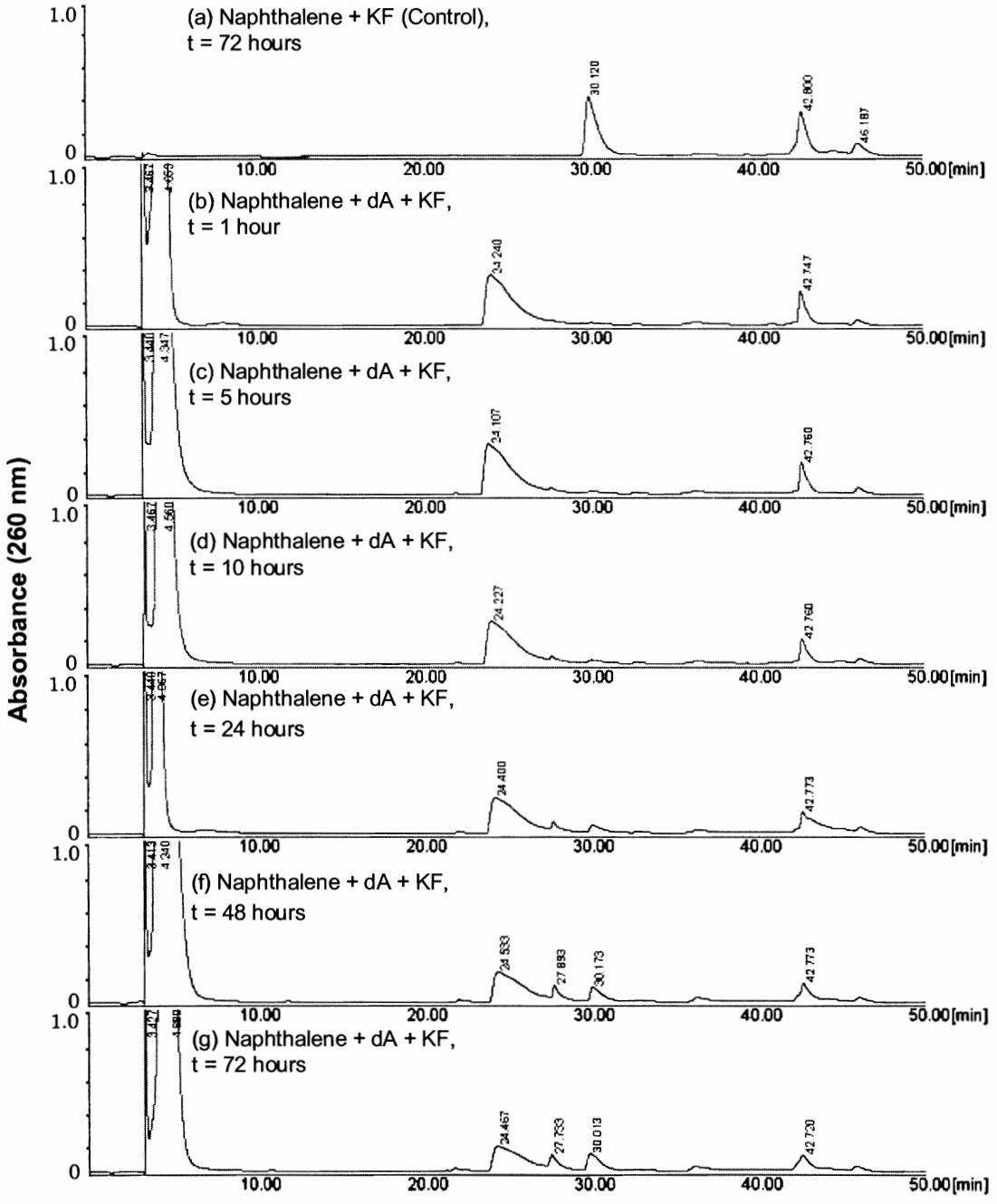

Figure 3.5: Time course of naphthalene dA alkylation by HPLC analysis at room temperature over 72 h. The reaction solution contained 3.6 mM naphthalene QM precursor and 18 mM KF without/with 5.4 mM dA in aqueous DMF (90% DMF).

The naphthalene dA adduct was observed to decrease gradually, while the hydrolyzed product **51** slowly increased and unreacted naphthalene QM precursor **53** remained after 72 h.

Time course studies showed that QM dG adducts formed more readily than QM dA adducts under the same condition, and QM dA addition was competed by QM hydrolysis. Moreover, dG adducts were stable, while dA adducts degraded over time. Because the time course study of deoxynucleobases alkylated by unsubstituted QM has been reported, our interest is to reveal the structures of stable substituted QM dG adducts in contrast with unsubstituted QM dG adduct.[33] In the next section of this chapter, the structural characterization of QM dG adducts were presented.

3.4 Structural characterization of quinoline dG adduct

Deoxyguanosine has five nitrogens and one oxygen, and almost every nitrogen and oxygen can react with QMs under certain situation to produce the possible dG alkylation adducts: dG N1 adduct, dG N^2 adduct, dG N3 adduct, dG O^6 adduct, dG N7 adduct and guanine N7 adduct (Figure 3.6).[26,36] However, each adduct is distinguishable. The dG N7 adduct is not stable and tends to lose the deoxyribose to generate the G N7 adduct. Based on the previous time course study, dG N7 and G N7 adducts were ruled out since no degradation of the quinoline dG adduct was observed and the quinoline dG adduct was confirmed by ESI-MS as 500.8 m/z (M^+), 385.1 m/z (dG de-sugar adduct + H^+). The formation of the QM dG O^6 adduct has not been reported, which could be explained by the hard-soft-acid-base concept (HSAB). This concept proposes that hard nucleophiles prefer

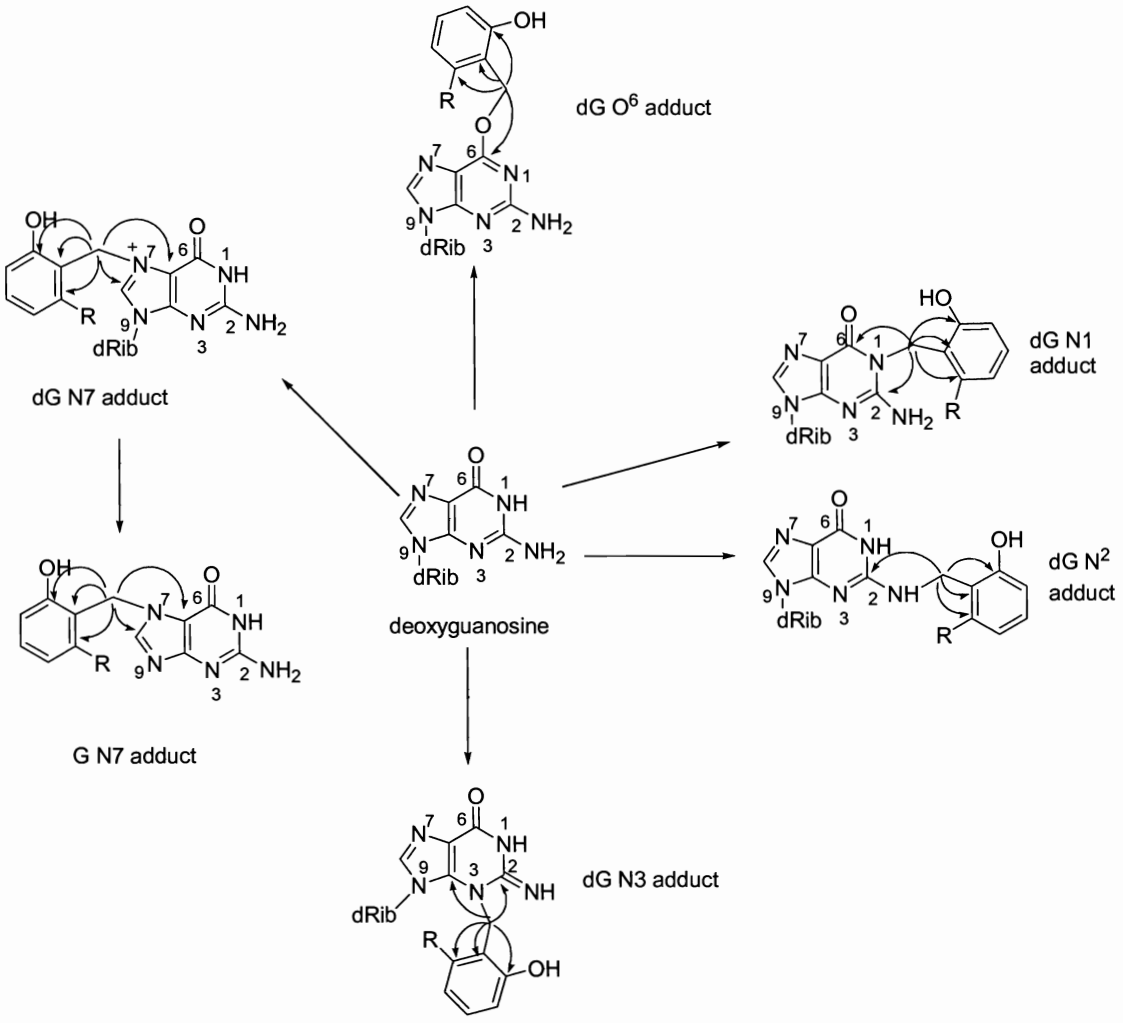

Figure 3.6: Possible dG alkylation adducts

hard electrophiles, while soft nucleophiles prefer soft electrophiles. For example, hard electrophiles generated by *N*-alkyl-*N*-nitrosourea react preferentially at dC O^2 and dG O^6 and soft electrophiles such as methyl iodide primarily modify nitrogen nucleophiles.[26] The soft electrophilic methylenes in QMs unlikely react with the hard nucleophile dG O^6. Actually, dG adducts could be distinguished by NMR techniques because the benzylic proton on each adduct has a unique connectivity with purine carbons. For example, the

benzylic proton correlates with C2 and C6 in dG N1adducts, interacts with C2 in dG N^2 adducts, and coupled with C4 and C2 in dG N3 adducts in long-distance couplings. In order to elucidate the structure, ^1H, ^{13}C and some 2D-NMR techniques were used and the results were presented as shown in the following in details.

First, ^1H spectrum of quinoline dG adduct in deuterated DMSO was obtained, and the chemical shifts and the splitting patterns were summarized in Figure 3.7. On the basis of the chemical structure, we predicted that quinone dG adduct has 19 protons, of which there are 10 aromatic protons, 2 benzylic protons and 7 deoxyribose protons. In the aromatic region, 3 singlets, 4 doublets, 3 triplets were predicted (Figure 3.8). Our observation in the ^1H spectrum was 2 singlets, 4 doublets, 2 triplets, and 1 multiplet. The integration of each singlet, doublet, and triplet was 1, while the multiplet was integrated as 2 protons, which found to be a triplet overlapped with a singlet after expansion. Thus, the total number and the splitting patterns of aromatic protons were consistent with our prediction. In the nonaromatic region, the ^1H signals only accounted for 7 protons. The missing 2 protons could be explained as being overlapped at the shoulder of water signal, which was independently confirmed by using a deuterated methanol solvent.

As a second step to elucidate structure, the correlations between the splitting protons were analyzed by the ^1H-^1H NMR Correlation Spectroscopy (COSY) experiment. COSY is a two-dimensional NMR experiment, and the cross peaks off diagonal axis in COSY spectra arise from geminal or vicinal protons (2- or 3- bond) coupling. The COSY spectrum of aromatic region was shown in Figure 3.9. In the left corner of COSY spectrum, pseudo-singlets at 8.71 ppm and 8.04 ppm in ^1H spectrum were actually two

doublets, which were revealed by the symmetric cross peaks in COSY. Since these two doublets only coupled with each other, and the other doublets (H5``, H8``, H14`` and H16``) interacted with triplets, these two doublets were assigned to H2`` and H4`` which split each other through a long rang 4-bond coupling. In the center of this COSY spectrum, the correlation was evident that a doublet correlated with a triplet which was coupled to the other triplet which was further correlated with the other doublet. These correlations were consistent with the predicted splitting pattern of H5``, H6``, H7``, and H8`` in the quinoline ring. However, further information was needed to assign each proton accurately. The only singlet 7.68 ppm was assigned to H8 on dG because it was isolated and didn't couple with any other proton. In the top right corner, a triplet 7.15 ppm was coupled to both doublets at 6.84 ppm and 6.61 ppm, respectively. These three peaks corresponded to the protons as H14``, H15``, and H16``, among which the triplet at 7.15 ppm was assigned as the H15``.

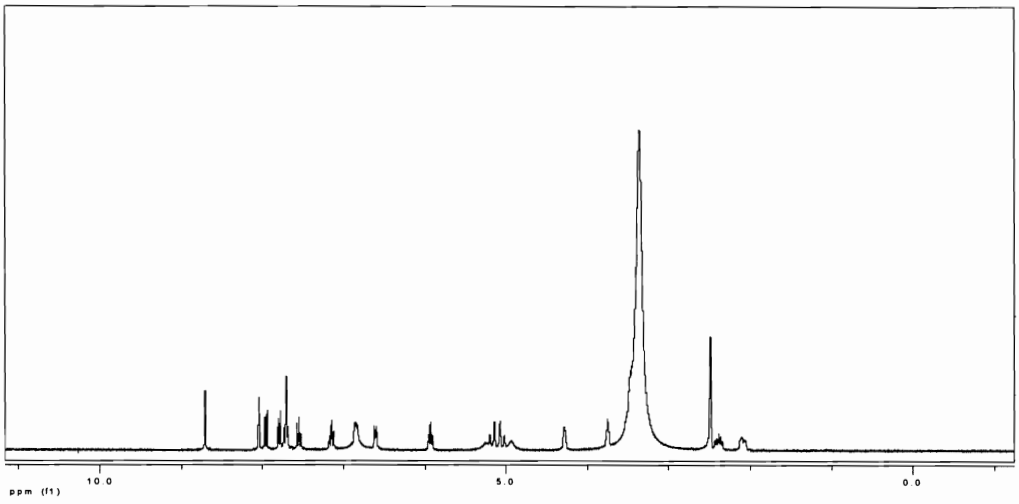

Proton (ppm)	Splitting patterns	Integration
8.71	s	1
8.04	s	1
7.96	d	1
7.79	d	1
7.74-7.68	m	2
7.55	t	1
7.15	t	1
6.84	d	1
6.61	d	1
5.93	dd	1
5.17	d	1
5.04	d	1
4.28	m	1
3.75	m	1
2.43-2.33	m	1
2.12-2.06	m	1

Figure 3.7: ^{1}H spectrum of quinoline dG adduct

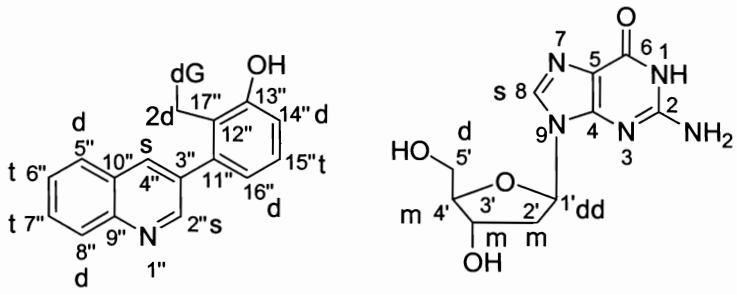

Figure 3.8: Predicted splitting patterns of quinoline dG adduct

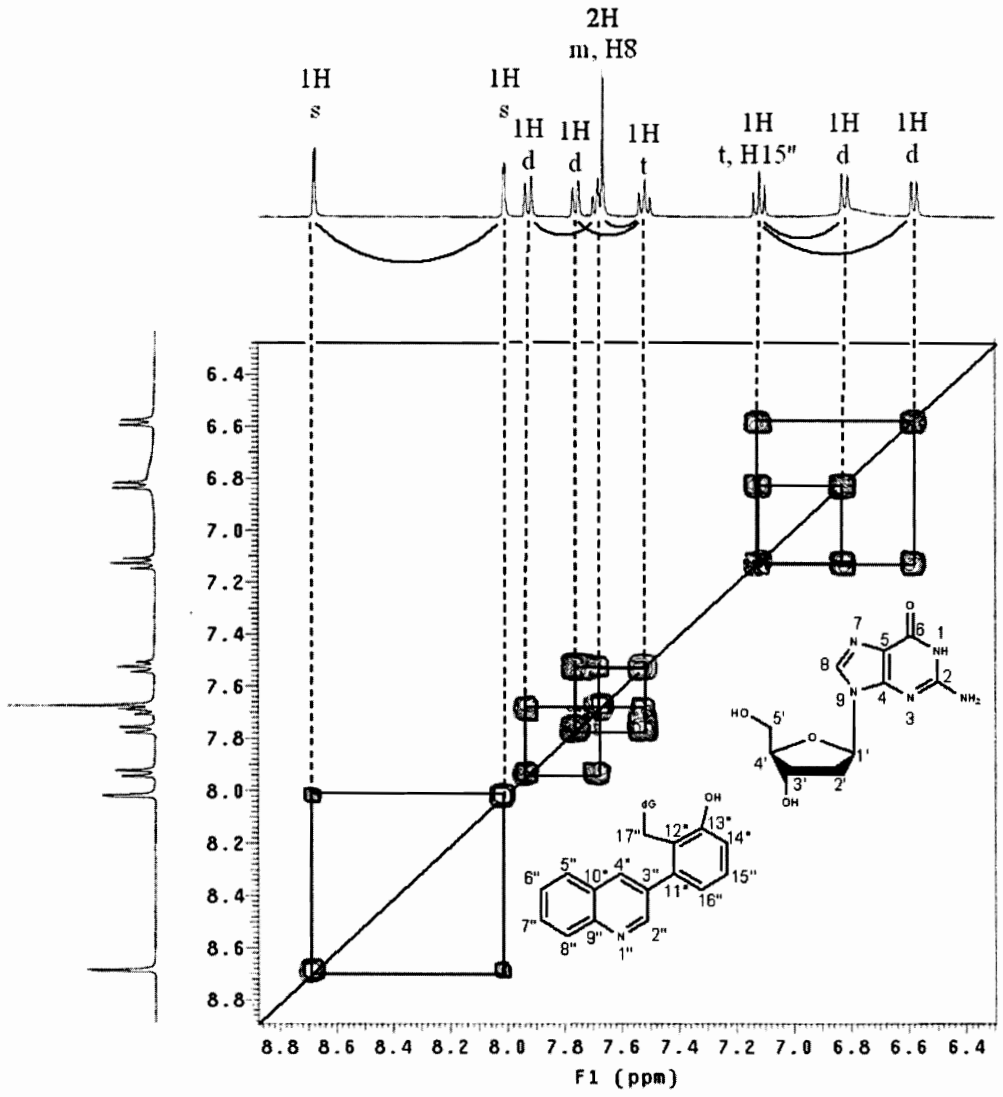

Proton (ppm)	Splitting patterns	Integration	Coupled protons (ppm)
8.71	d	1	8.04
8.04	d	1	8.71
7.96	d	1	7.69
7.79	d	1	7.55
7.69	t	1	7.96; 7.55
7.68	s	1	None
7.55	t	1	7.79; 7.69
7.15	t	1	6.84; 6.61
6.84	d	1	7.15
6.61	d	1	7.15

Figure 3.9: Aromatic region in COSY spectrum of quinoline dG adduct

For the sugar/benzylic region in the COSY spectrum, correlations were showed in Figure 3.10. Two doublets at 5.17 ppm and 5.04 ppm only coupled with each other and corresponded to two benzylic protons at benzylic 17`` position, which were generated by the geminal coupling between two diastereotopic benzylic protons. The other signals were coupled with one other, and these correlations were consistent with the interactions of deoxyribose protons. Thus, ^{1}H signals of deoxyribose were assigned based on these correlations. That is, the doublet doublet peak at 5.93 ppm was assigned as H1` which coupled with two protons at H2` position appearing as two multiplets at 2.43-2.33 ppm and 2.12–2.06 ppm. Both multiplets geminally coupled with each other and also coupled with H3` proton at 4.28 ppm that further interacted with H4` at 3.75 ppm which coupled with two H5` protons at 3.40 ppm which was overlapped by the shoulder of the water signal in the ^{1}H-NMR.

In order to clearly assign the ^{1}H signals and ^{13}C signals of the quinoline dG adduct, ^{13}C chemical shifts of dG adduct were first achieved by ^{13}C NMR. Based on the structure, the quinoline dG adduct have 26 carbons: 1 carbonyl carbon, 19 aromatic carbons, and 6 sugar/benzylic carbons. In the ^{13}C NMR spectrum, 20 carbons between 180-110 ppm and 4 carbons in nonaromatic region were observed, and 2 missing nonaromatic carbons were buried by deuterated DMSO solvent signal, which was later confirmed using 2D HMQC spectral analysis.

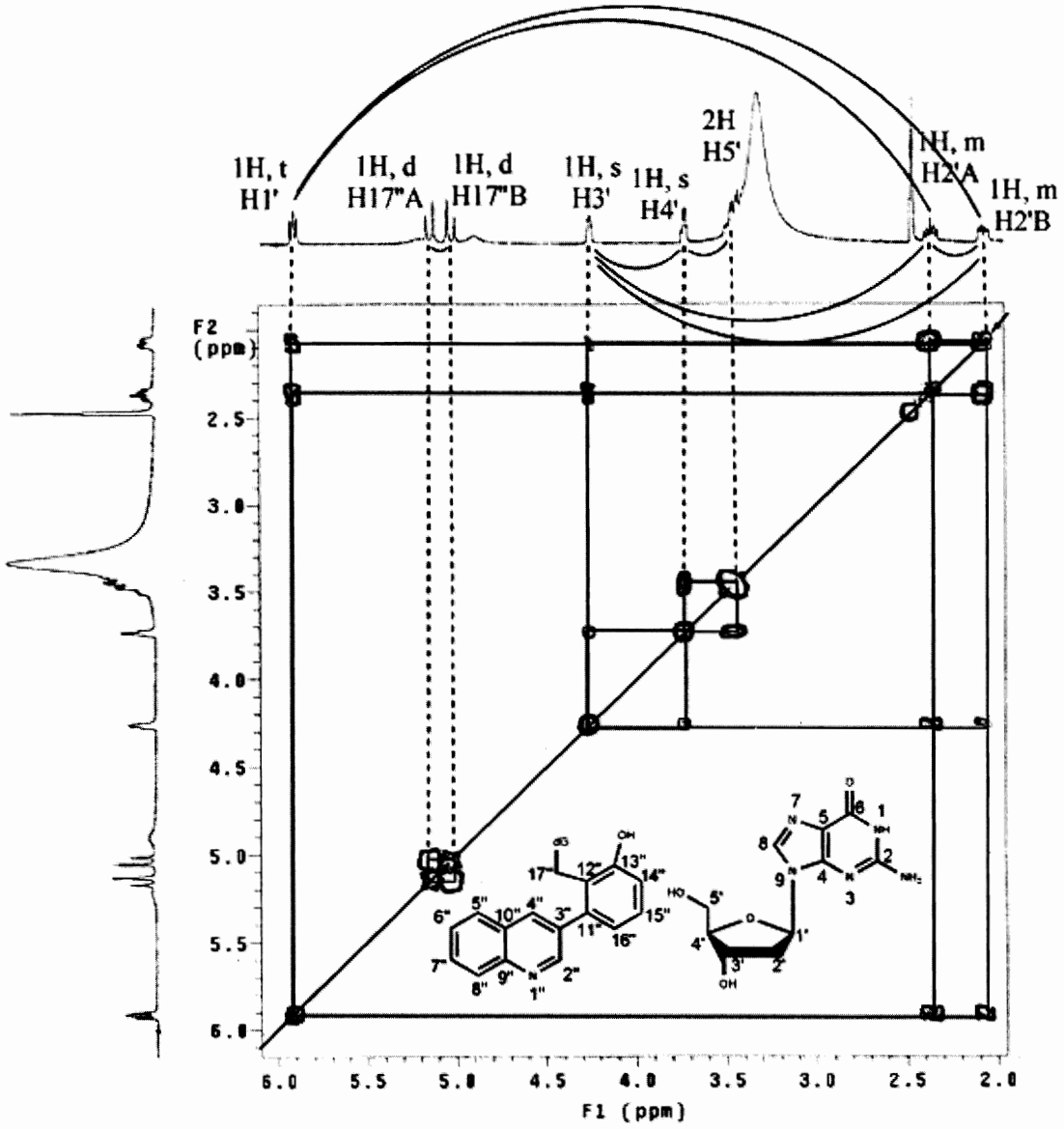

Proton (ppm)	Splitting patterns	Integration	Coupled protons (ppm)
5.93	dd	1	2.43-2.33; 2.12-2.06
5.17	d	1	5.04
5.04	d	1	5.17
4.28	m	1	3.75; 2.43-2.33; 2.12-2.06
3.75	m	1	4.28; 3.40
2.43-2.33	m	1	5.93; 4.28; 2.12-2.06
2.12-2.06	m	1	5.93; 4.28; 2.43-2.33

Figure 3.10: Nonaromatic region in COSY spectrum of quinoline dG adduct

For the structural elucidation, the correlation between carbons and the attached protons needed to be revealed, which was achieved by Heteronuclear Multiple Quantum Correlation (HMQC). HMQC is a 2D-NMR technique to detect ^{13}C-^{1}H correlations which are shown as cross peaks resulted from direct proton attachment on carbon nuclei. Thus, quaternary or carbonyl carbons don't produce any signal in the HMQC spectrum, and there are 10 carbons without protons deduced form the HMQC result, which was in accordance with the structure of the quinoline dG adduct. Figure 3.11 and Figure 3.12 shows the aromatic region and nonaromatic region in HMQC spectrum, respectively. The corresponding carbon of each proton can be detected by drawing a line from each ^{1}H signal directly to the right to intersect the cross peaks and then tracing up from each cross peak to meet ^{13}C signal. Thus, the carbons associated with the known protons were easily assigned. For example, H15`` at 7.15 ppm was correlated to C15`` at 128.4 ppm, and H8 at 7.68 ppm was related to C8 at 135.6 ppm. The ^{13}C signals of the deoxyribose were also fully identified. The assigned and unassigned ^{1}H and ^{13}C signals were summarized in Table 3.1.

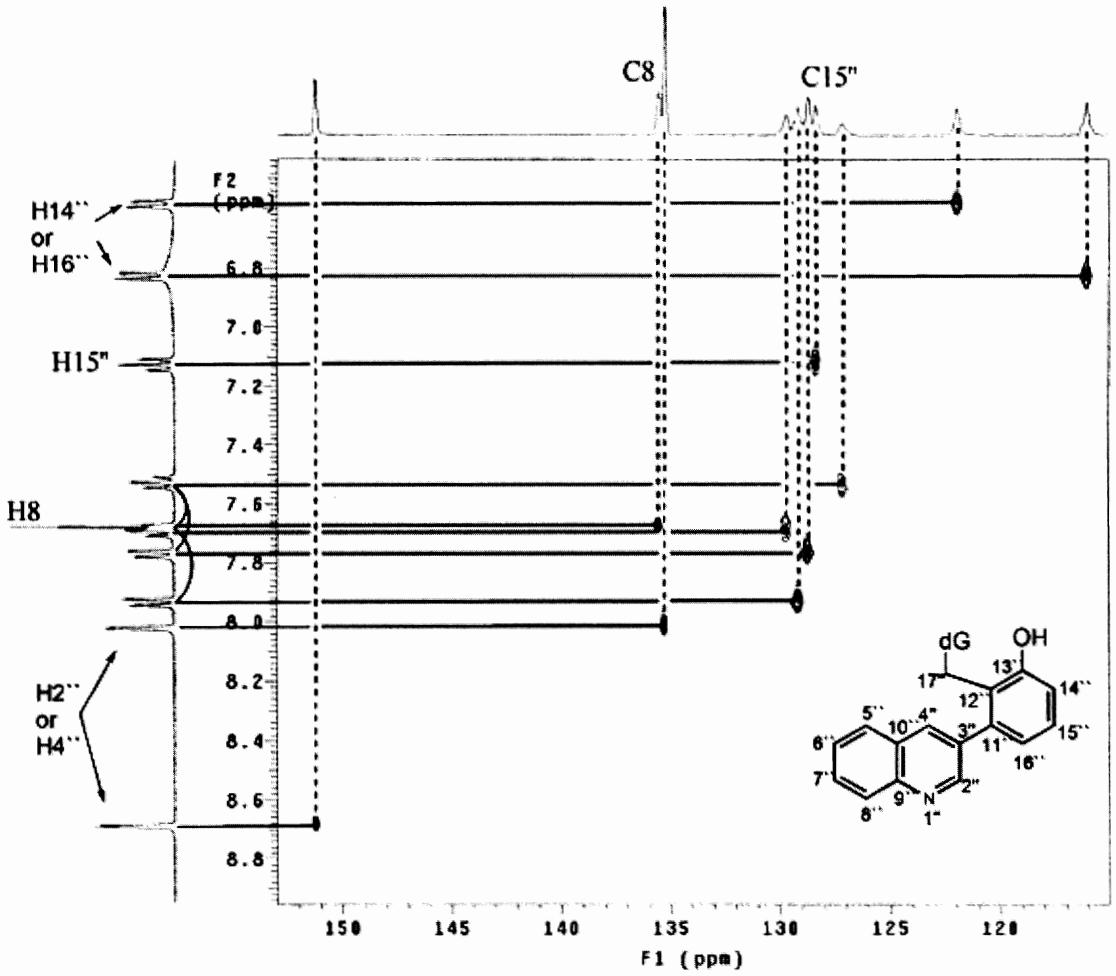

Proton (ppm)	Splitting patterns	Integration	Coupled carbon (ppm)
8.71	d	1	151.3
8.04	d	1	135.3
7.96	d	1	129.2
7.79	d	1	128.8
7.69	t	1	129.8
7.68	s	1	135.6
7.55	t	1	127.2
7.15	t	1	128.4
6.84	d	1	116.1
6.61	d	1	122.0

Figure 3.11: Aromatic region in HMQC spectrum of quinoline dG adduct

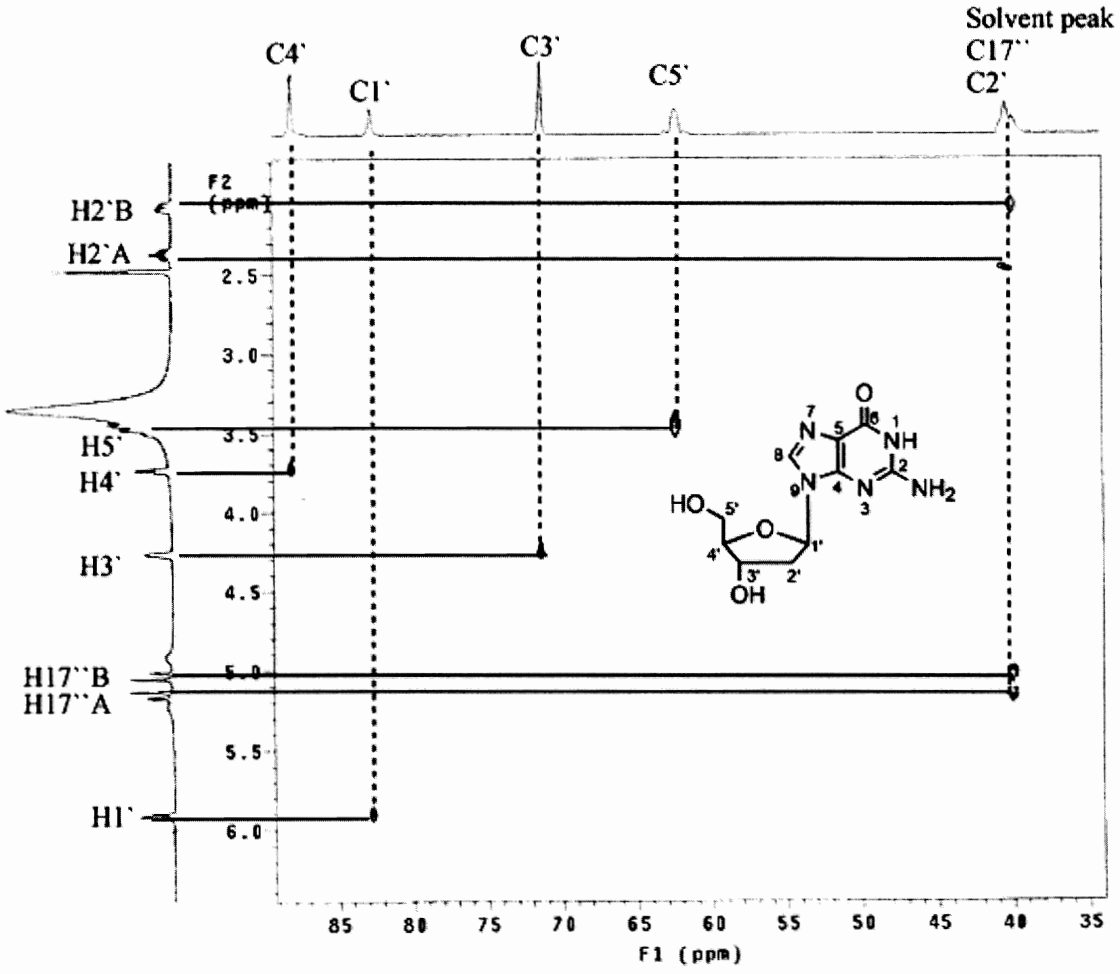

Proton (ppm)	Splitting patterns	Integration	Coupled carbon (ppm)	Assigned position
5.93	dd	1	82.7	1`
5.17	d	1	40.0	17``
5.04	d	1	40.0	17``
4.28	m	1	71.4	3`
3.75	m	1	88.1	4`
2.43-2.33	m	1	40.0	2`
2.12-2.06	m	1	40.0	2`
3.40	overlapped by water signal		62.4	5`

Figure 3.12: Nonaromatic region in HMQC spectrum of quinoline dG adduct

Table 3.1. Assignment of ^{1}H and ^{13}C signals

Proton (ppm)	Coupled carbons (ppm)	Assigned position
8.71	151.3	2`` or 4``
8.04	135.3	2`` or 4``
7.96	129.2	5`` or 8``
7.79	128.8	5`` or 8``
7.69	129.8	6`` or 7``
7.68	135.6	8
7.55	127.2	6`` or 7``
7.15	128.4	15``
6.84	116.1	14`` or 16``
6.61	122.0	14`` or 16``
5.93	82.7	1`
5.17;5.04	40.0	17``
4.28	71.4	3`
3.75	88.1	4`
2.43-2.33	40.0	2`
2.12-2.06	40.0	2`
3.40	62.4	5`

Last, the unambiguous assignments were accomplished through Heteronuclear Multiple Bond Correlation (HMBC). HMBC experiment provides information of long range couplings including two- or three-bond ^{1}H - ^{13}C couplings and in some cases some four-bond ^{1}H - ^{13}C couplings. On the other hand, one-bond ^{1}H - ^{13}C couplings are not observed. Because benzylic proton H17`` would exhibit a unique connectivity with carbons on dG, the cross peaks of quinoline dG adduct on HMBC were verified first. Five crosspeaks of H17`` were observed at 157.4 ppm, 156.9 ppm, 154.9 ppm, 140.5 ppm, and 121.3 ppm (Figure 3.13). In order to identify the dG adduct, these five cross peaks of H17`` needed to be assigned. Scheme 3.4 showed the strategy for structural characterization of the dG adduct. The ^{1}H and ^{13}C signals on deoxyribose had been first assigned by ^{1}H-NMR, COSY and HMQC. In the second step, the long range couplings

such as interactions along H1` on the deoxyribose and C8, C4 on the purine and interactions along H8, C4 and C5 were used to distinguish the ^{1}H and ^{13}C signals on the purine. Third, the cross peaks of H17`` were identified and the possible dG adduct was predicted. Finally, every ^{1}H and ^{13}C signals on quinoline were assigned to confirm the predicted structure of the quinoline dG adduct.

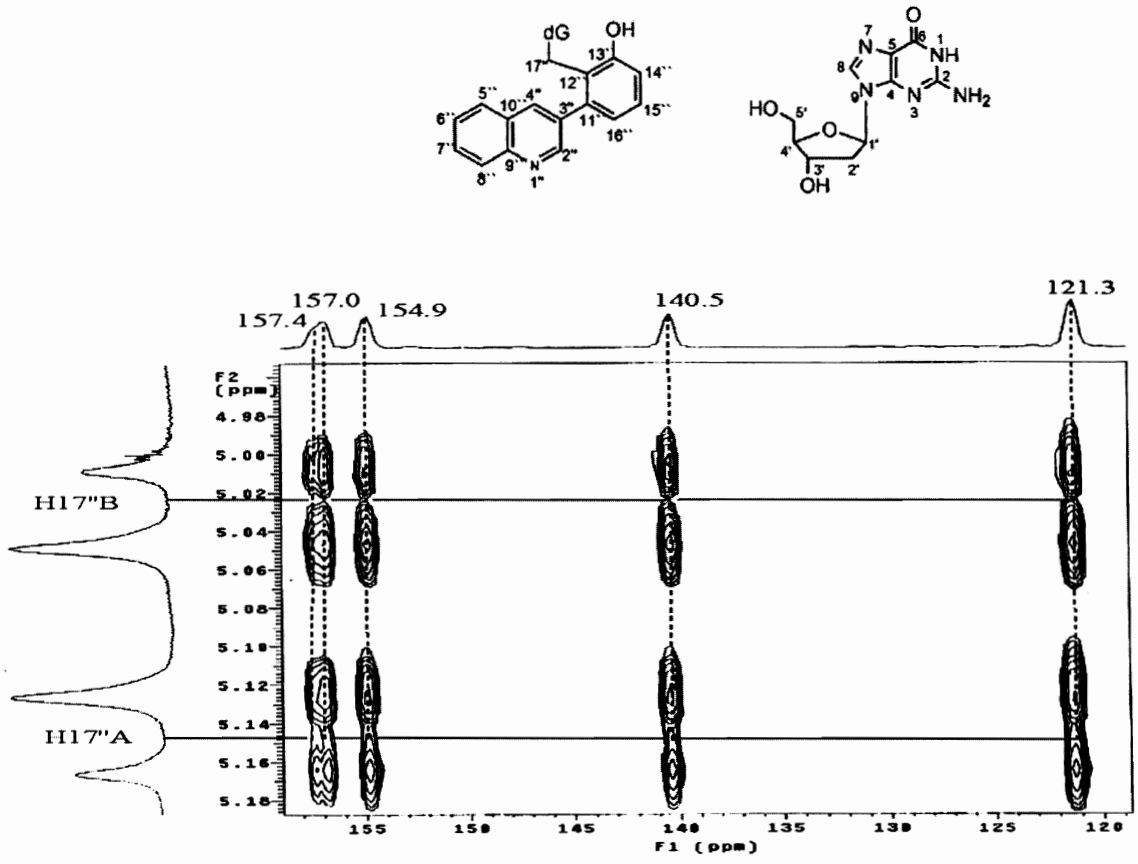

Figure 3.13: HMBC spectrum of benzylic protons in quinoline dG adduct

Since H1` on the deoxyribose correlated with C8 and C4, H1` was first studied. In Figure 3.14, the H1` was observed to produce two cross peaks with carbon at 149.2 ppm and 135.6 ppm (C8) which had been assigned previously. Thus, C4 was assigned as 149.2 ppm. Tracing from H8 to the right, one weak peak at 156.9 ppm and two intense cross peaks at 149.2 ppm (C4) and 116.5 pm were observed. H8-C4 and H8-C5 were the three-bond interactions, while H8-C6 was the four-bond coupling. The intense cross peak at 116.5 ppm was assigned as C5 and the weak cross peak at 156.9 ppm was assigned as carbonyl C6. Thus, one of the cross peaks of benzylic proton H17`` was carbonyl C6. Therefore, it is highly unlikely that dG N3 adduct was formed due to the missing cross peak between H17`` and C4.

Scheme. 3.4: Strategy for structural characterization of the quinoline dG adduct

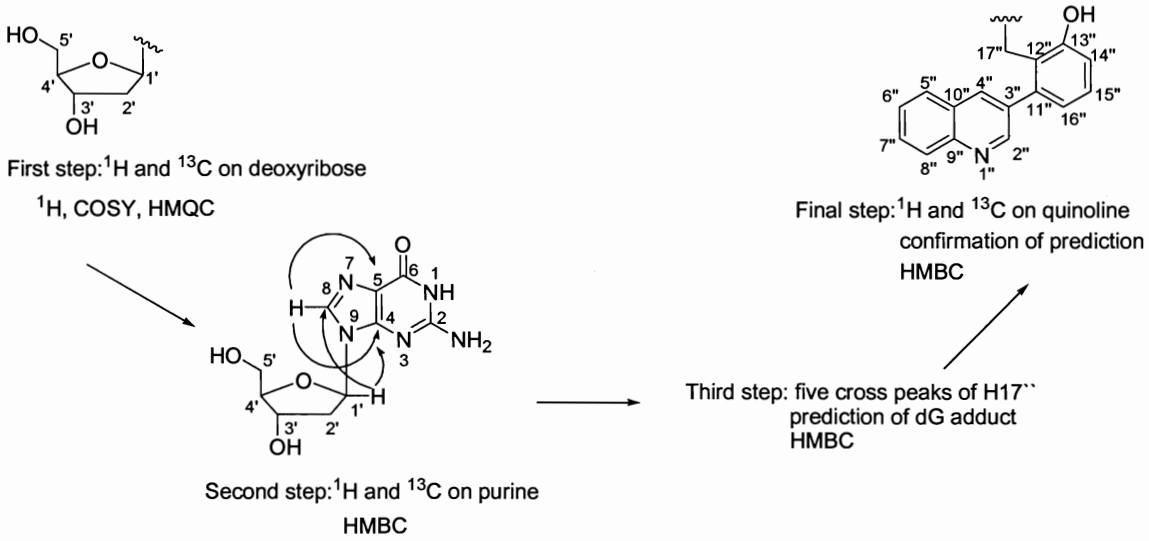

The remaining cross peaks of H17`` were corresponding to quaternary carbons based on HMQC, of which the carbon at 154.9 ppm had no interaction with other protons except H17``. Thus, C2 was assigned at 154.9 ppm because it is isolated in the structure unlike other quaternary carbons which also couple with 2- or 3- bond away protons.

The other cross peaks of H17`` at 157.4 ppm, 140.5 ppm, and 121.3 ppm were also observed in H15``, and those cross peaks were believed to be produced by C11``, C12`` and C13`` because H17`` and H15`` could produce the same cross peaks with these three carbons in any possible dG adduct. The H15``-C11`` and H15``-C13`` interactions were 3-bond correlations, while the H15``-C12`` was 4-bond coupling. Thus, two intense cross peaks at 157.4 ppm and 140.5 ppm were assigned as C11`` and C13``, and the weak cross peak at 121.3 ppm was assigned as C12``. Since C11``also coupled with H4`` and H2``, the cross peaks of H2`` and H4`` should be observed when tracing C11`` directly down. Thus, C11`` was easily assigned as the peak at 140.5 ppm and then C13`` was assigned at 157.4 ppm.

After assignment of each cross peak of H17``, the possible dG adducts were analyzed in Scheme 3.5. In dG $O^6$ and dG N2 adducts, the interaction H17``-C2 and H17``-C6 were 5-bond couplings, which is unreasonable in HMBC. The cross peaks of dG N1 adduct were produced by 2- or 3- bond couplings. Moreover, the cross peaks of H17`` are intense. Thus, the quinoline dG adduct was assigned as dG N1 adduct.

Scheme 3.5: Analysis of dG adducts

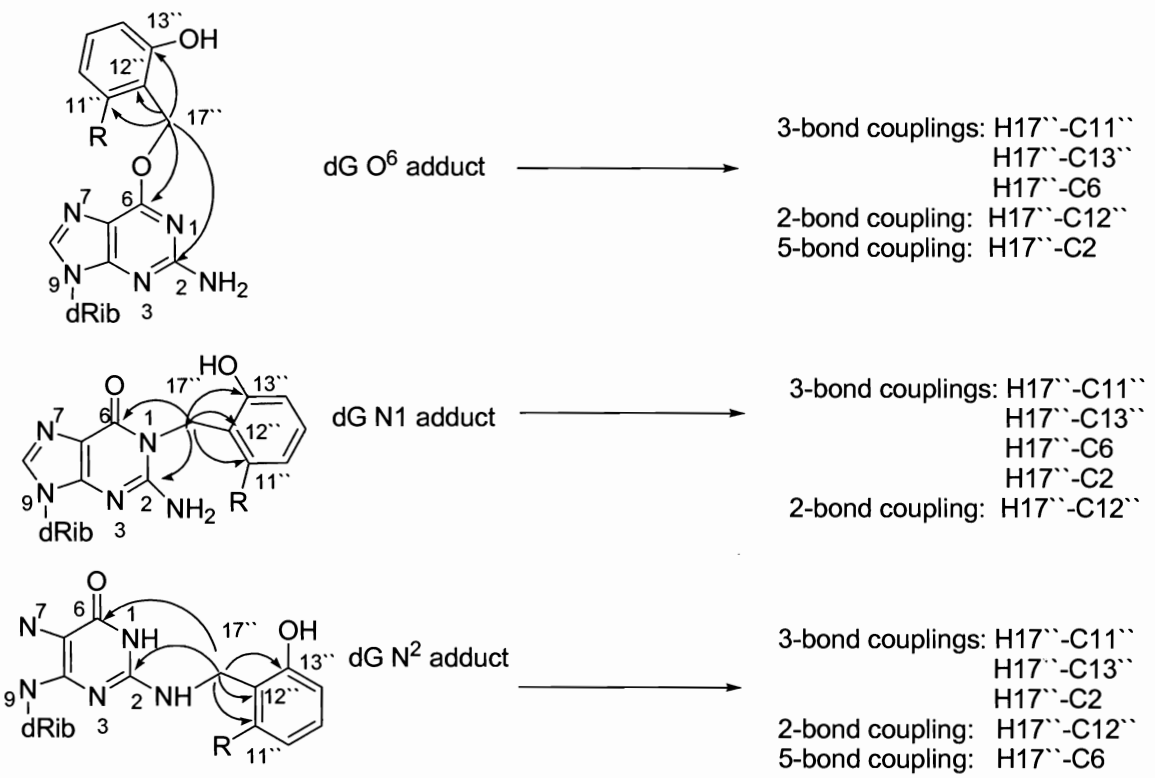

After the assignment of deoxyribose and purine, we further assigned carbons and protons on the quinoline aromatic ring to determine if the prediction of dG adduct was reasonable. In aromatic rings, the most common correlations seen in HMBC spectra are 3-bond correlations because $^{2}J_{CH}$ is 1Hz and $^{3}J_{CH}$ is typically 7.6 Hz, which is the value for which the experiment is optimized. Table 3.2 helped us to assign the remaining carbons and hydrogens.

Table 3.2. HMBC correlations for the aromatic region.

H \ C	2"	3"	4"	5"	6"	7"	8"	9"	10"	11"	12"	13"	14"	15"	16"
2" s			3					3		3					
4" s	3			3				3		3					
5" d			3			3		3							
6" t							3		3						
7" t				3				3							
8" d					3				3						
14" d											3				3
15" t										3		3			
16" d		3									3		3		

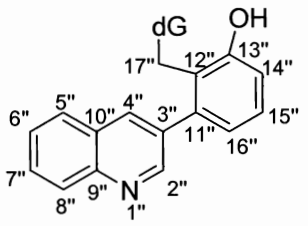

Doublets at 6.84 ppm and 6.61 ppm were roughly known as H14`` and H16``. The doublet at 6.84 had two intense cross peaks, and the other at 6.61 had three intense cross peaks in Figure 3.14. Based on the numbers of crosspeaks of H14`` and H16`` on Table 3.2, doublet at 6.61 ppm was assigned as H16`` and doublet at 6.84 ppm was as H14``. Based on the HMQC results in Figure 3.11, C14`` was found at 116.1 ppm and C16`` was at 122.0 ppm. Since H16`` coupled with C3``, C12`` (121.3 ppm) and C14`` (116.1 ppm), C3`` was at 134.5 ppm. The same strategy could be used to distinguish H4`` and H2``. H4`` correlated with C2``, C5``, C9``, and C11`` to produce 4 cross peaks, while H2`` coupled with C4``, C9``, and C11`` to produce 3 cross peaks on Table 3.2.

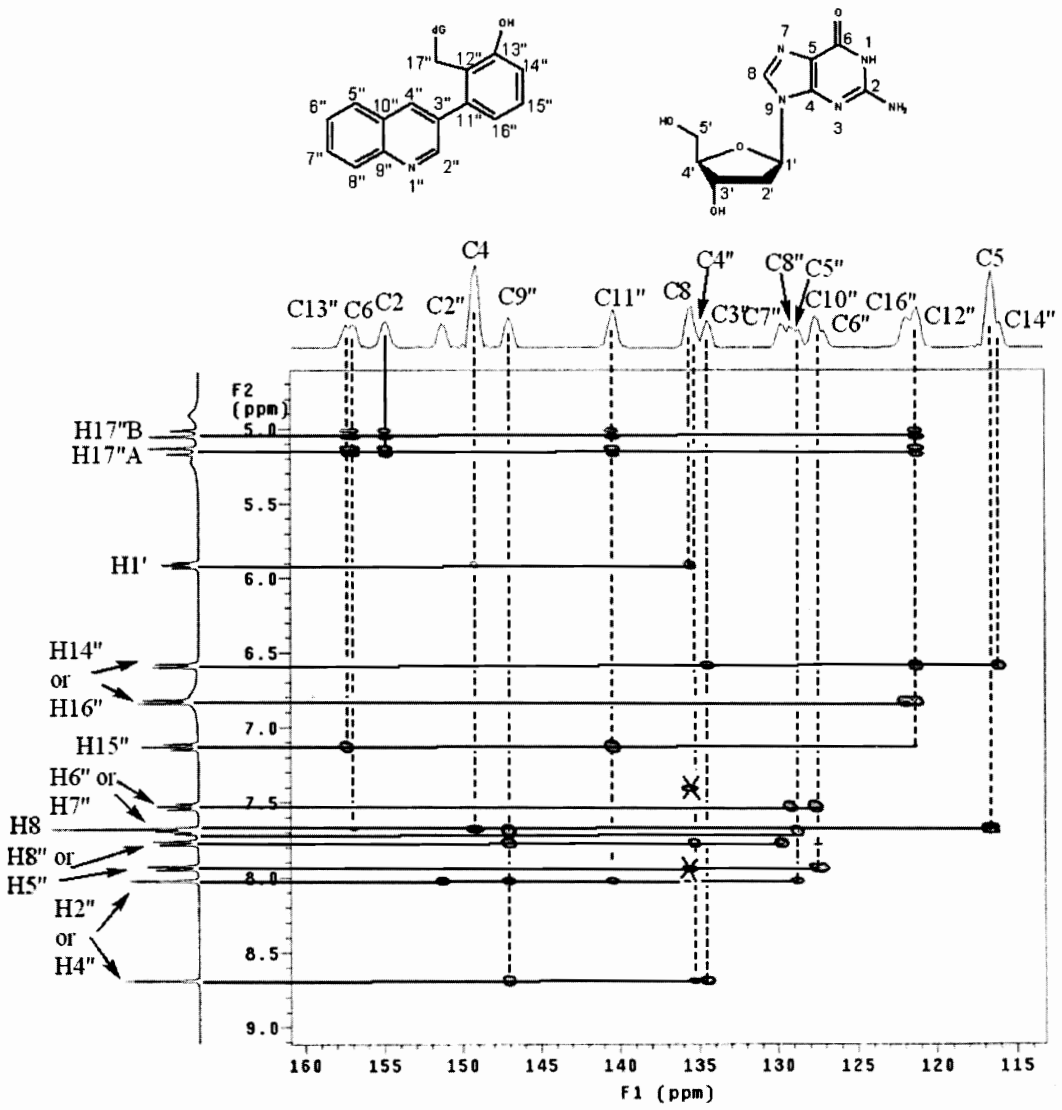

Proton (ppm)	Assigned position	HMBC correlation with carbons (ppm)
8.71	2`` or 4``	147.0;135.3;134.5
8.04	2`` or 4``	151.3;147.0;140.5;128.8
7.96	5`` or 8``	127.7;127.2
7.79	5`` or 8``	147.0;135.3;129.8
7.69	6`` or 7``	147.0;128.8
7.68	8	156.9;149.2;116.6
7.55	6`` or 7``	129.2; 127.7
7.15	15``	157.4; 140.5;121.3
6.84	14`` or 16``	122.0;121.3
6.61	14`` or 16``	134.5;121.3;116.1
5.93	1`	149.2;135.6
5.17;5.04	17``	157.4;156.9;154.9;140.5;121.3

Figure 3.14: Long distance couplings in aromatic/benzylic regions of HMBC

Therefore, H4`` was 8.04 ppm and C4`` was 135.3 ppm, and H2`` was 8.71 ppm and C2`` was 151.3 ppm through HMQC in Figure 3.11. Since both of H4`` and H2`` correlated with C9`` and C11`` (140.5 ppm), C9`` was assigned at 147.0 ppm. Tracing H4`` met C2`` (151.3 ppm), C9`` (147.0 ppm), C11`` (140.5 ppm) and 128.8 ppm, which was assigned to C5``. Thus, H5`` was obtained at 7.79 ppm from HMQC (Figure 3.11). Consequently, H8`` was at 7.96 ppm and C8`` was at 129.2 ppm. Since H5`` correlated with C9`` (147.0 ppm), C4`` (135.3 ppm), and C7``, C7`` was 129.8 ppm and H7`` was at 7.69 ppm derived from HMQC (Figure 3.11). As a result, H6`` was assigned at 7.55 ppm and C6`` was 127.2 ppm. Because C10`` coupled with both H6`` and H8`` and produced two cross peaks, the carbon at 127.7 ppm was assigned as C10``.

Complete ^{1}H and ^{13}C chemical shifts matched the predicted structure of the quinoline dG N1 adduct, and the chemical shifts were summarized in Figure 3.15.

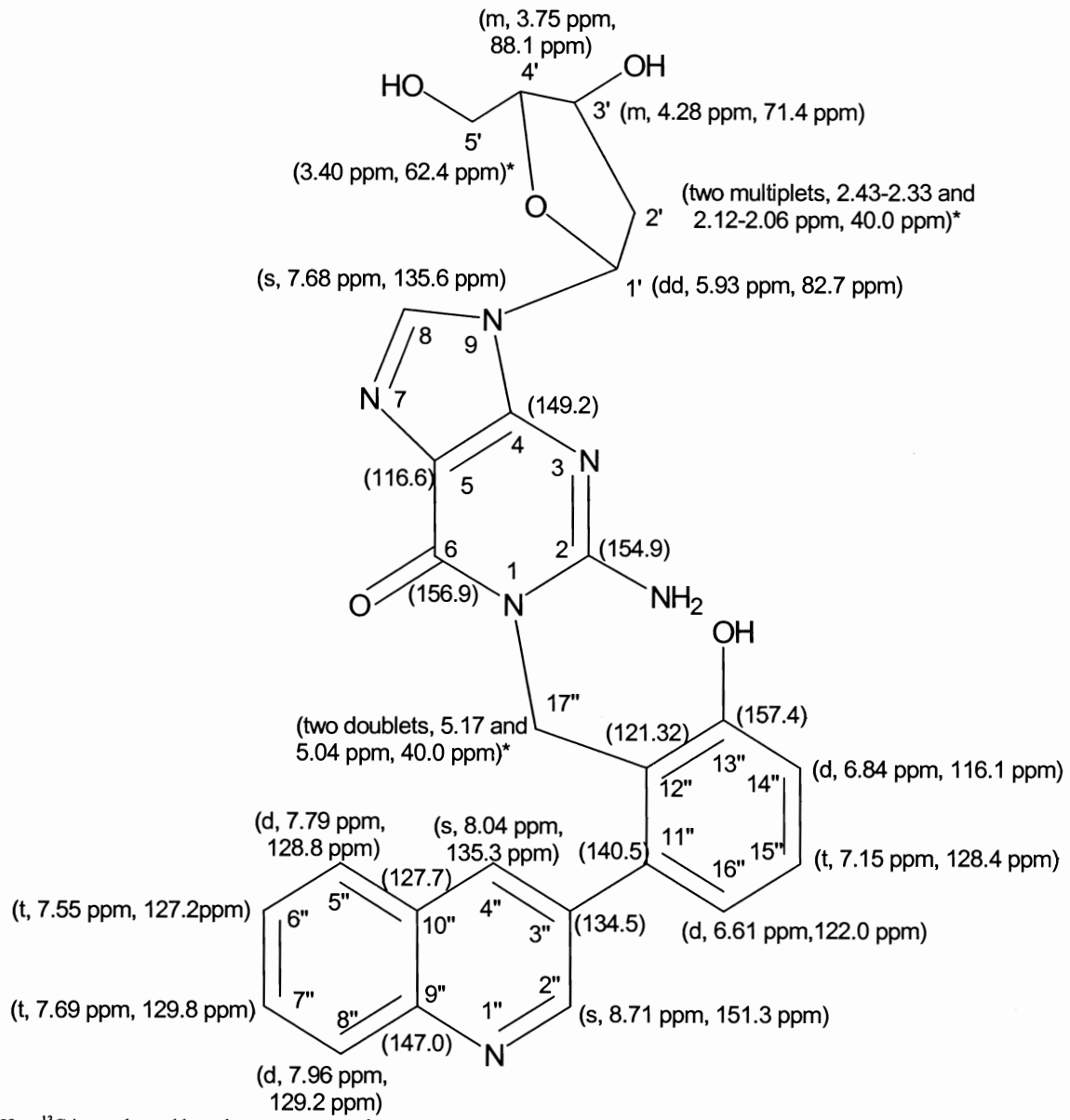

[1]H or [13]C is overlapped by solvent or water peaks.

Figure 3.15: Quinoline dG N1 adduct

3.5 Structural characterization of naphthalene dG adduct

Similarly, naphthalene dG adduct was also isolated and analyzed for structural elucidation. However, benzylic protons were observed as 4 doublets and the integration

for each is 0.5 proton relative to the other signals in the ^{1}H NMR spectrum. Further COSY experiment revealed the correlations along these four doublets. Figure 3.16 showed that the doublet at 4.56 ppm was coupled to the doublet at 5.25 ppm and the doublet at 4.62 ppm correlated with the doublet at 5.10 ppm, which suggested that this naphthalene adduct was a 1:1 mixture of diastereomers.

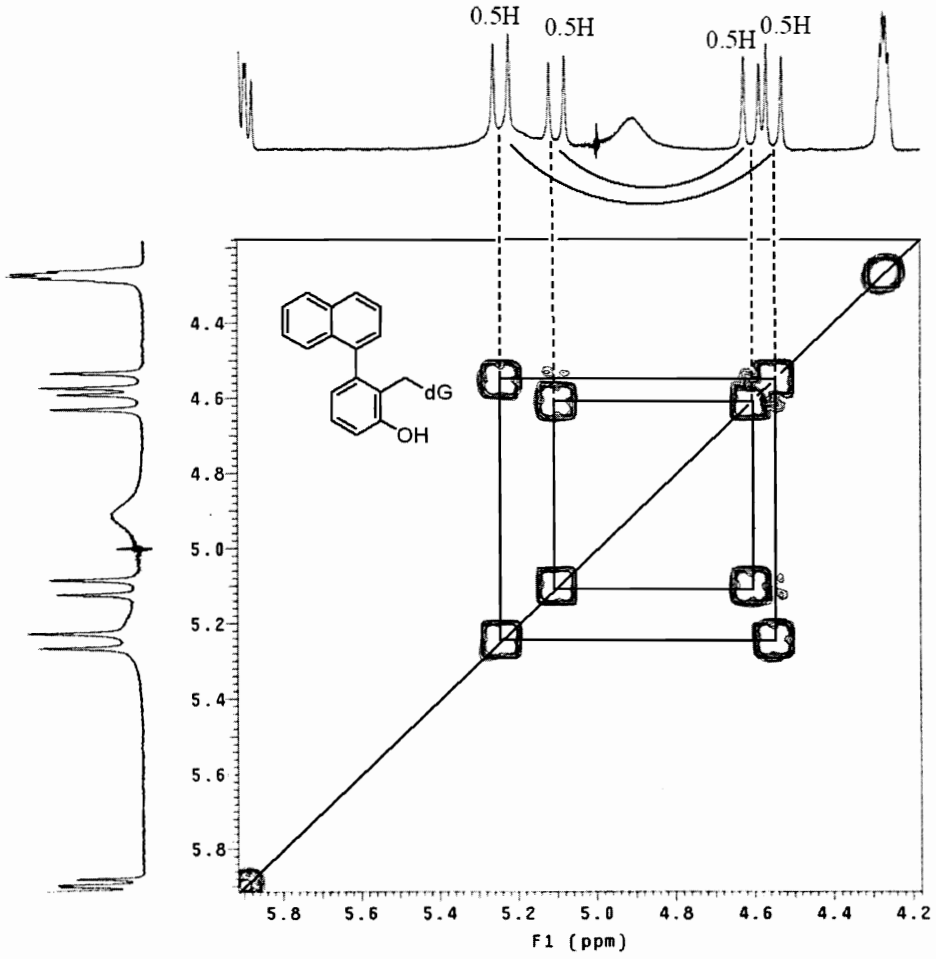

Figure 3.16: Partial COSY spectrum of naphthalene dG adduct

The ^{13}C NMR spectrum of naphthalene dG confirmed this assumption because most carbons were observed as a set of two close signals and the difference between two signals are less than 0.2 ppm. This diastereoisomeric phenomenon is produced by the steric interaction between the proton 8 on the naphthalene ring and large benzylic substituents. Large substituents are so steric that the rotation of single bond is "frozen" and the conformationally locked adduct can exist only in one of the two staggered conformations. When subsititutions are achiral, two adducts are enantiomers. Two benzylic protons are not chemical-shift equivalent and split each other to produce two doublets on NMR spectra. However, enantiomers can't be distinguished by NMR. This is the reason why benzylic protons on naphthalene QM precursors **52, 53** are observed as two doublets. For example, ^{1}H NMR spectrum of naphthalene silyl ether **52** shows that two benzylic protons couple with each other and even impact the "remote" two methyl groups of the TBDMS groups as individual signals (Figure 3.17). However, dG is chiral and consequently naphthalene dG adducts are diastereomers, which explained that benzylic protons are shown as four doublets in NMR spectra. Since HPLC could not separate naphthalene dG diastereomers, the structural characterization of naphthalene dG adducts was not further investigated due to complication of signals.

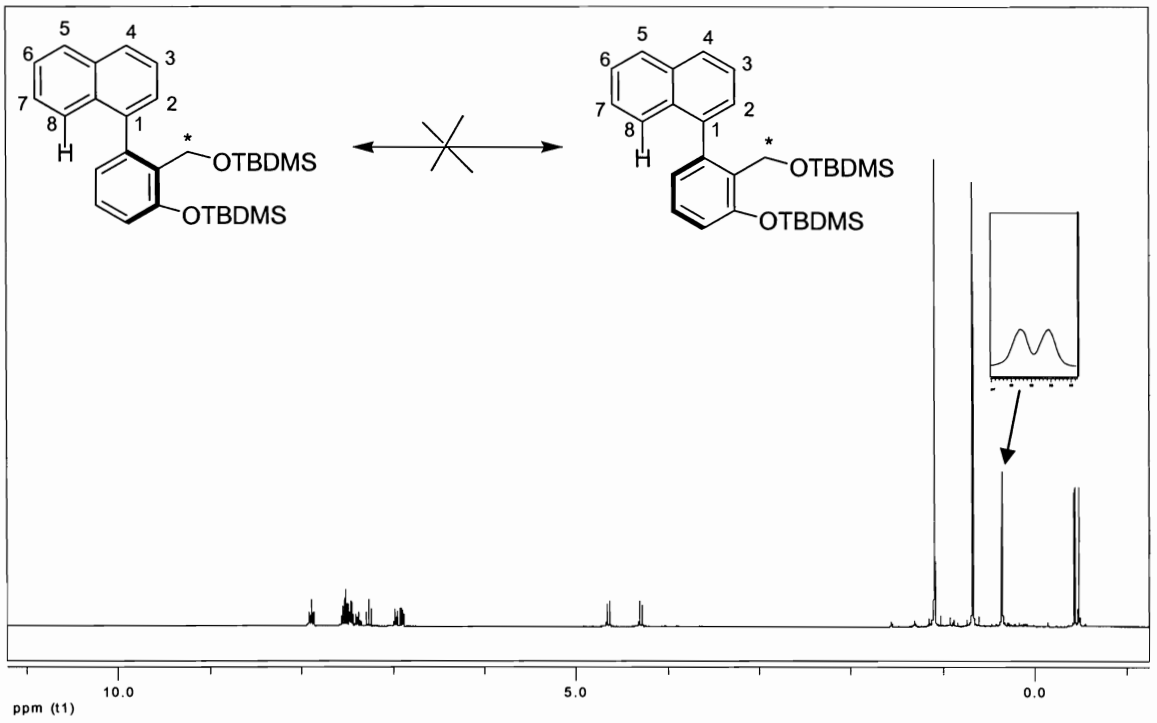

Figure 3.17. ^{1}H NMR spectrum of naphthalene silyl ether **52**.

3.6 Conclusion

In this study, we have successfully synthesized model compounds of the biaryl system: quinoline and naphthalene derivatives. The potential DNA QM alkylation was investigated by QM alkylation with deoxyadenosine and deoxyguanosine. With dA, each QM derivative generated one adduct, and time course study showed that both dA adducts degraded over time possibly through hydrolysis. Quinoline dA adduct degraded faster and almost disappeared after 24 h while naphthalene dA adduct degraded at a slower rate and there was approximate one third of naphthalene dA adduct remaining after 72 h.

On the other hand, dG formed stable adducts with both naphthalene and quinoline derivatives, which remained unchanged after 72 h at room temperature. Naphthalene dG

was separated by HPLC and was found as a 1:1 mixture of diastereomers due to the blocked rotation between diaryl groups.

For quinoline, the dG adduct was characterized by NMR analysis as quinoline dG N1 adduct. Interestingly, Rokita's group reported that both dG N1 and dG N^2 were the major dG adducts with their QM model. They first found that dG N^2 adduct was the major adduct in unbuffered 83% aqueous DMF.[26] Later, the dG N1 adduct was reported to form more readily than dG N^2 in unbuffered 85% aqueous DMF. They ascribed this to the deprotonation of dG N1 ($pK_a = 9.2$), and they suggested that the N^2 adduct was the major product under neutral condition.[28] However, they later found that both dG N1 and dG N^2 adduct were major adducts under neutral buffered condition, and dG N1 adduct was slightly more than dG N^2adduct.[33] We only observed dG N1 adduct in quinoline QM alkylation. The structural difference between our substituted QM model and Rokita's unsubstituted QM model may favor one adduct over the other.

CHAPTER 4 Future Studies on Biaryl Alkylation System

4.1 Introduction

As discussed in chapter 3, two biaryl QM precursors, naphthalene derivative and quinoline derivative, have been successfully synthesized, and the potential of DNA alkylation has been proved by nucleobase alkylation by both QM precursors under KF induced conditions. Thus, this biaryl alkylation system was further modified to investigate the potentials of target-promoted DNA alkylation, and the mechanism involved was illustrated in Figure 4.1.

This biaryl alkylation system is composed of a QM precursor, a linear amine linker, and a single strand DNA working as the DNA sequence delivery. The amine is easily protonated under physiological condition and forms an intramolecular hydrogen bond with the hydrogen of the phenol group. QM will be regenerated through the elimination of the positively charged nitrogen. In the absence of DNA target, this process is reversible and the formation of QM adduct 1 is favored, because the amine is ready to pseudo-intramolecularly attack QM to regenerate QM adduct 1. On the other hand, upon target recognition naphthalene or quinoline ring can intercalate into DNA duplex by hydrophobic interaction and the generated QM can be transferred to nearby nucleobases, which leads to DNA specific alkylation. The regeneration of *o*-QM has been reported with amino acid alkylation adducts under heat or irradiation by Freccero's group.[48] In this chapter, initial

studies on this biaryl system were presented and the potential future study will be discussed.

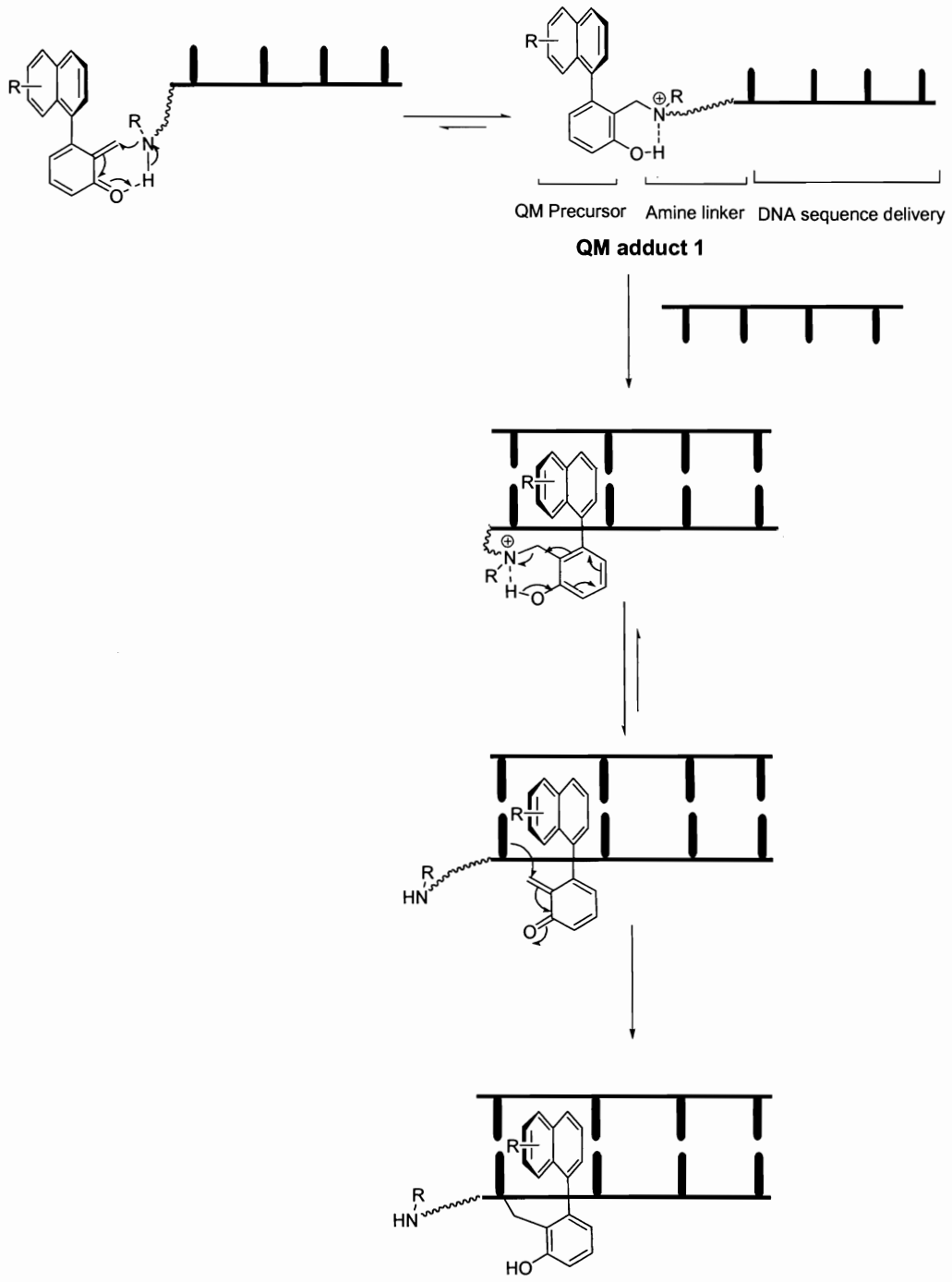

Figure 4.1: Biaryl target-promoted DNA alkylation system

4.2 Initial studies and future efforts

Scheme 4.1 shows the synthetic strategy of naphthalene DNA conjugate **64** and quinoline DNA conjugate **65**. The previously synthesized acetate **53** or **59** was converted into piperidine carboxylic acid **60** or **61** through QM formation. The carboxylic acid in compound **60** or **61** was activated into succinimide ester in the presence of 1-(3-dimethylaminopropyl)-3-ethylcarbodiimide hydrochloride (EDCI) which then coupled with a single strand DNA, 5-Amine B15 in Mops buffer (250 mM, pH 7.5) to produce DNA adducts **64** or **65**. However, the synthesis of DNA adduct **64** and **65** was challenging and only a small amount of succinimide esters coupled with DNA in a very low yield. This was attributed to several factors: (a) the excess EDCI from the synthesis of succinimide esters might couple with DNA to generate the side product; (b) the ratio of DMF and Mops buffer was crucial, which could affect the solubility of DNA and QM precursors and possibly precipitate them in the mixed solution; (c) the pH of Mops buffer also affected the coupling. The acid condition prevented the deprotonation of the phenol and thus blocked the generation of QM, while the basic solution induced a competitive nucleophile, hydroxide ion; (d) succinimide esters are highly instable and subject to degradation during reaction. The optimization of reactions is currently in progress in our group.

Our target-promoted alkylation system requires eliminable amine linkers. Based on Rokita's previous study, the reversibility of QM/DNA nucleobase adducts depended on the pK_a values of the nucleophiles on DNA nucleobases.[33] The nucleophiles with conjugate acids of pK_a value less than 4 formed unstable kinetical adducts which rapidly decomposed

and regenerated QMs. If pK_a values of the conjugate acids were from 4 to 9, QMs were released slowly. With the pK_a values of nucleophiles greater than 9, irreversibly thermodynamic adducts were produced (Figure 1.7).[33] However, Freccero reported thermal and photochemical regeneration of *o*-QM in the amino acid alkylation adducts such as QM glycine, QM serine, and QM lysine adducts.[48] Except that lysine has a pK_a value of 8.95, the pK_a values of the amino groups of other amino acids are greater than 9. Thus, the relationship between pK_a and reversibility need to be further studied.

Scheme 4.1: Synthetic route of naphthalene and quinoline derivatives.

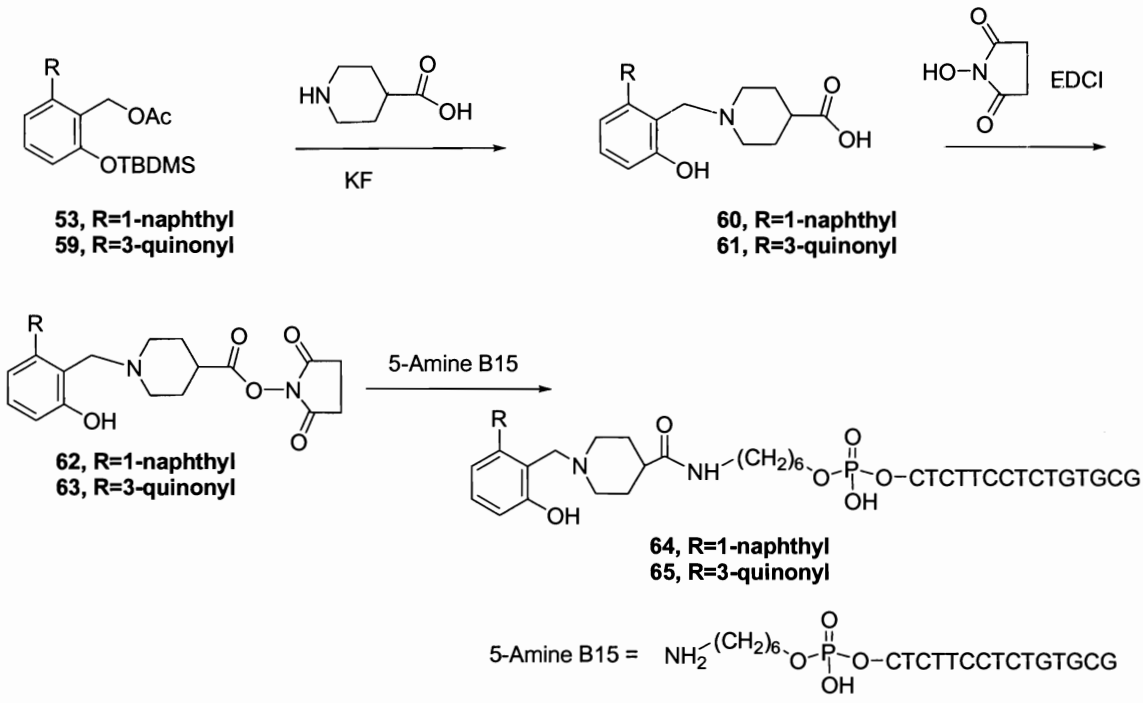

CHAPTER 5 Experimental Procedures

General methods. All solvents and chemicals were purchased from Fisher Scientific (Pittsburgh, PA) or Sigma-Aldrich (Milwaukee, WI) and used without further purification. The flash column chromatographic separations were performed with silica gel 60 (230-400 mesh). All ^{1}H NMR and ^{13}C NMR spectra were recorded on Varian 300 and 400 NMR spectrometers. All NMR chemical shifts (δ) were reported in parts per million (ppm) and were determined relative to the standard values for deuterated solvents. Electrospray ionization mass spectroscopy (ESI-MS) analysis was carried out using Q-TOF2 from Micromass (Manchester, U.K.). Some compounds were separated and quantified analytically by a Varian reversed-phase C18 column using a Jasco HPLC system. Compounds 2, 3, 13 and 17 were previously synthesized and reported by Dr. Dai and Dr. Zhou.[99] Compounds 30, 31, 32 were obtained as published previously.[94]

5-Bromo-2-methoxyphenol (5). To a solution of 5-bromo-2-methoxybenzaldehyde (2.15 g, 10 mmol) in dry CH_2Cl_2 (50 mL) was added 3-chloroperoxybenzoic acid (3.70 g, 21.5 mmol). The reaction mixture was stirred for 2 h at room temperature. Crushed sodium hydroxide pellets (1 g, 25 mmol) and a mixture of MeOH/H_2O solution (4:1, 50 mL) was added into the reaction flask. After 1 h, the pH of the reaction solution was adjusted to pH 4~5 with 1 M HCl and then extracted with diethyl ether (150 mL × 3). The organic layer was collected, washed with saturated $NaHCO_3$

solution, dried with $MgSO_4$, and evaporated. A white solid **5** (1.47 g) was produced in 72% yield. ^{1}H NMR ($CDCl_3$, 300MHz): δ 7.07 (s, 1H), 6.96 (d, J = 8.6 Hz, 1H), 6.70 (d, J = 8.6 Hz, 1H), 5.72 (br, 1H, *OH*), 3.86 (s, 3H). ^{13}C NMR ($CDCl_3$, 75MHz): δ 146.7, 146.1, 123.0, 118.1, 113.5, 112.1, 56.3.

2-Benzyloxy-4-bromo-1-methoxybenzene (6). To a solution of benzylbromide (1.36 g, 7.95 mmol) in dry DMF (20 mL) was added phenol **5** (1.47 g, 7.24 mmol) and potassium carbonate (1.20 g, 8.70 mmol). The reaction was stirred under N_2 for 7 h at room temperature. The reaction solution was then quenched with 1 M NaOH (150 mL) and extracted with diethyl ether (150 mL × 3). The organic layer was collected, washed with water twice and then with brine, dried with $MgSO_4$, and concentrated. Flash chromatographic separation (25% EtOAc in hexanes) afforded pure **6** as a white solid (2.00 g) in 94% yield. ^{1}H NMR ($CDCl_3$, 300MHz): δ 7.24-7.06 (m, 5H), 6.86-6.83 (m, 2H), 6.56 (d, J = 8.2 Hz, 1H), 4.91 (s, 2H), 3.66 (s, 3H). ^{13}C NMR ($CDCl_3$, 75MHz): δ 149.2, 149.2, 136.6, 128.9, 128.3, 127.6, 124.2, 117.4, 113.2, 112.8, 71.4, 56.4.

3-Benzyloxy-4-methoxyphenyboronic acid (7). To a solution of **6** (1.04 g, 3.55 mmol) in dry THF (10 mL) was added *n*-butyllithium (2.3 mL of 1.6 M in hexane, 3.73 mmol) dropwise under N_2 at -78 °C. The mixture was stirred for 50 min at this temperature and then triisopropylborate (1.23 mL, 1.00 g, 5.32 mmol) was added. The dry ice bath was removed and stirring was continued for 12 h at room temperature. The reaction mixture was hydrolyzed with H_2O (10 mL) and rapidly extracted with diethyl ether (70 mL × 3). The combined organic layer was dried with $MgSO_4$ and evaporated on a rotary evaporator.

The residue was dried under high vacuum for 8h to afford crude product as an oil which was directly used for the following reaction.

5-(3-Benzyloxy-4-methoxy-phenyl)-2,2-dimethyl-benzo[1,3]dioxin-4-one (8). To triflate **3** (228 mg, 0.70 mmol), boronic acid **7** (217 mg, 0.84 mmol), $Pd(PPh_3)_4$ (40 mg, 0.035 mmol), KBr (83 mg, 0.70 mmol), and Cs_2CO_3 (341 mg, 1.05 mmol) was added dry THF (20 mL). The mixture was stirred for 15 min and then 150 μL water was added. The reaction mixture was further stirred and refluxed for overnight. The reaction solution was diluted with diethyl ether (150 mL), washed with brine, dried with $MgSO_4$, and concentrated. Flash chromatographic separation (10%-25% EtOAc in hexanes) afforded **8** as a white solid (207 mg) in 76% yield. ^{1}H NMR ($CDCl_3$, 300MHz): 7.49-7.29 (m, 6H), 6.94-6.89 (m, 5H), 5.15 (s, 2H), 3.92 (s, 3H), 1.77 (s, 6H). ^{13}C NMR ($CDCl_3$, 75MHz): δ 159.7, 157.4, 149.8, 147.9, 145.9, 137.5, 135.2, 132.8, 128.8, 128.0, 127.6, 126.0, 122.0, 116.3, 115.5, 112.1, 111.5, 105.4, 71.6, 56.2, 25.9.

6-Benzyloxy-1-hydroxy-7-methoxy-fluoren-9-one (10). To a solution of **8** (200 mg, 0.51 mmol) in THF (20 mL) was added NaOH (100 mg, 2.5 mmol) and water (2 mL). The reaction was refluxed and monitored by TLC. The resulting reaction solution was poured into water (100 mL) and washed with diethyl ether (70 mL). The aqueous layer was collected, acidified with 2.5 M HCl to pH 4~5, and then extracted with diethyl ether (100 mL × 2). The organic layer was collected, washed with brine, dried with $MgSO_4$, evaporated to afford a viscous oil **9** (161 mg) in 90% yield.

To a solution of **9** (161 mg) in dry CH_2Cl_2 (5 mL) was added trifluoroacetic acid (2 mL) and trifluoroacetic anhydride (1 mL) at 0 °C and the resulting reaction solution was

stirred under N_2 at this temperature for 1 h. The reaction solution was adjusted to pH 5 with 10 M NaOH and then was extracted with CH_2Cl_2 (50 mL × 3). The organic layer was collected, washed with brine, dried with $MgSO_4$, and concentrated. Flash chromatographic separation (10% EtOAc in hexanes) afforded a yellow solid **10** (134 mg) in 88% yield. ^{1}H NMR ($CDCl_3$, 300MHz): δ 8.33 (s, 1H, *OH*), 7.48 – 7.27 (m, 6H), 7.18 (s, 1H), 7.01 (s, 1H), 6.81 (d, J= 8.47 Hz, 1H), 6.67 (d, J = 8.47 Hz, 1H), 5.26 (s, 2H), 3.92 (s, 3H). ^{13}C NMR ($CDCl_3$, 75MHz): δ 195.9, 157.0, 153.9, 150.5, 143.7, 139.2, 137.2, 136.3, 129.0, 128.5, 127.5, 127.3, 118.0, 117.8, 112.2, 107.5, 106.5, 71.4, 56.7.

[3-(6-Benzyloxy-7-methoxy-9-oxo-9H-fluoren-1-yloxy)-2-*tert*-butoxycarbonylamino-propionylamino]-acetic acid benzyl ester (14). To a round bottomed flask was added **10** (60 mg, 0.18 mmol), serine **13** (76 mg, 0.22 mmol), PPh_3 (71 mg, 0.27 mmol), and dry THF (60 μL). The mixture was sonicated for 15 min to give a clear and highly viscous solution, and diisopropyl azodicarboxylate (42 μL, 44 mg, 0.22 mmol) was added dropwise to the reaction mixture. The reaction mixture was sonicated for additional 40 min and then diluted in CH_2Cl_2 (100 mL). The organic layer was washed with brine, dried with $MgSO_4$, and concentrated. The mixture was purified by a flash column (10%-40% EtOAc in hexanes) to afford **14** as an orange oil (54 mg) in 45% yield. The recovered unreacted **10** was further converted into **14** under the same condition. The combined yield of these two repeats was 81%. ^{1}H NMR ($CDCl_3$, 300MHz): δ 8.38 (br, 1H, *NH*), 7.48-7.24 (m, 11H), 7.10 (s, 1H), 6.99 (s, 1H), 6.91 (d, J = 6.70 Hz, 1H), 6.67 (d, J = 8.47 Hz, 1H), 5.89 (br, 1H, *NH*), 5.26 (s, 2H), 5.10 (d, J = 6.70 Hz, 1H), 5.04 (d, J = 6.70 Hz, 1H), 4.60 (br, 2H), 4.25 (dd, J_1 = 17.57 Hz, J_2 = 6.08 Hz, 1H), 4.10 (dd, J_1 = 17.57 Hz,

J_2 = 6.08 Hz, 1H), 3.90 (s, 3H), 3.79 (t, J = 10.56 Hz, 1H), 1.47 (s, 9H). ^{13}C NMR ($CDCl_3$, 75MHz): δ 192.2, 170.3, 169.6, 155.8, 155.6, 153.6, 150.7, 146.0, 138.1, 137.0, 136.3, 135.6, 129.0, 128.9, 128.7, 128.5, 128.5, 128.4, 127.6, 127.5, 113.8, 113.2, 107.5, 106.1, 80.3, 71.4, 67.5, 67.1, 56.5, 52.7, 42.0, 28.6.

[(10-Benzyloxy-9-methoxy-5,6,7,7a-tetrahydro-4-oxa-7-aza-cyclohepta[jk]fluorene-6-carbonyl)-amino]-acetic acid benzyl ester (15). To a solution of **14** (95 mg, 0.14 mmol) in dry CH_2Cl_2 (2 mL) was added CF_3COOH (1 mL) at 0 °C. After stirring for 3 h under N_2 at this temperature, the reaction solution was frozen by liquid N_2, and the solvent was removed under high vacuum for 8 h. The residue was redissolved in dry CH_2Cl_2 (1 mL) and dry CH_3CN (3 mL), and refluxed for 4 h under N_2. Dried molecular sieve (4 Å, 30 mg) was added and the reaction was further refluxed for 2 h. $NaBH_3CN$ (96 mg, 1.5 mmol) was added into the cooled reaction solution which was stirred for 1.5 h under N_2 at room temperature. The reaction was quenched with concentrated acetic acid (300 μL) and was stirred for 2 h. The reaction solution was diluted with CH_2Cl_2 (100 mL) and was washed with saturated $NaHCO_3$ solution, dried with $MgSO_4$, and concentrated. Flash chromatographic separation (20%-40% EtOAc in hexanes) afforded **15** as a yellow solid (47 mg) in 60% yield. ^{1}H NMR ($CDCl_3$, 300MHz): δ 7.87 (br, 1H), 7.49 – 7.20 (m, 14H), 6.87 (d, J = 7.17 Hz, 1H), 5.28-5.17 (m, 5H), 4.77 (br, 1H), 4.17-4.05 (m, 4H), 3.97 (s, 3H), 3.63 (br, 1H). ^{13}C NMR ($CDCl_3$, 75MHz): δ 169.8, 157.1, 150.4, 149.5, 142.1, 137.1, 135.3, 133.3, 131.0, 130.3, 128.9, 128.9, 128.9, 128.8, 128.7, 128.6, 128.2, 127.6, 117.8, 114.3, 109.2, 106.3, 77.5, 71.6, 67.9, 67.5, 56.7, 54.4, 41.5. MS (ESI/MS): *m/z* 551.4 ($M + H^+$). Calcd for $C_{33}H_{30}N_2O_6$ ($M + H^+$): 551.60.

[(10-Hydroxy-9-methoxy-5,6,7,7a-tetrahydro-4-oxa-7-aza-cyclohepta[*jk*]fluorene-6-carbonyl)-amino]-acetic acid (16). To a solution of **15** (25 mg, 0.045 mmol) in 4% HCOOH in MeOH (10 mL) was added 10% palladium on activated carbon (40 mg). The reaction was stirred for 20 min under N_2 and filtered through a micro filter. After adding CF_3COOH (0.5 mL), the solvent was evaporated to afford **16** as a yellow solid (18 mg) in 83% yield. MS (ESI/MS): *m/z* 371.3 ($M + H^+$). Calcd for $C_{19}H_{18}N_2O_6$ ($M + H^+$): 371.4.

General experimental procedure of de-Boc reaction (21, 27). To a solution of a Boc-protected amine (0.15 mmol) in dry CH_2Cl_2 (2 mL) was added CF_3COOH (1 mL) at 0 °C. After stirring for 3 h under N_2 at 0 °C, the reaction solution was lyophilized for 8 h to afford a non-Boc amine.

4-*tert*-Butoxycarbonylamino-butyric acid (23). To a solution of 4-aminobutyric acid (1.0 g, 9.70 mmol) in 1 M NaOH (50 mL) was added a solution of di-*tert*-butyldicarbonate (2.33 g, 10.7 mmol) in dioxane (25 mL). After the reaction solution was stirred for 1 h, it was diluted with H_2O (50 mL) and washed with diethyl ether (100 mL). The aqueous phase was collected, adjusted to pH 4~5 with 20% H_2SO_4, and extracted by CH_2Cl_2 (100 mL × 3). The combined organic layer was dried with $MgSO_4$, and evaporated to give an oil **23** (1.24 g) in 63% yield. ^1H NMR ($CDCl_3$, 300MHz): δ 3.25-3.08 (m, 2H), 2.37 (t, J = 7.23 Hz, 2H), 1.80 (p, J = 7.06 Hz, 2H), 1.42 (s, 9H).

***N*-Succinimidyl 4-*tert*-butoxycarbonylaminobutanoate (28).** To the solution of **23** (82 mg, 0.40 mmol) and *N*-hydroxysuccinimide (51 mg, 0.44 mmol) in dry CH_2Cl_2 (15 mL) was added N-(3-dimethylaminopropyl)-N'-ethylcarbodiimide hydrochloride (EDCI,

85 mg, 0.44 mmol). After the reaction was stirred for 12 h under N_2 at room temperature, the reaction mixture was diluted with CH_2Cl_2 (100 mL). The organic layer was washed with 1 M HCl twice and with saturated $NaHCO_3$ twice, dried with $MgSO_4$, and evaporated to give a white solid of **28** (107 mg) in 88% yield. ^{1}H NMR ($CDCl_3$, 300MHz): δ 3.23-3.17 (m, 2H), 2.81 (s, 4H), 2.63 (t, J = 7.39 Hz, 2H), 1.91 (p, J = 7.07 Hz, 2H), 1.41 (s, 9H).

2-Benzyloxycarbonylamino-6-tert-butoxycarbonylamino-hexanoic acid 6-benzyloxy-7-methoxy-9-oxo-9H-fluoren-1-yl ester (33). A mixture of **10** (67 mg, 0.20 mmol), L-lysine derivative **32** (89 mg, 0.23 mmol), EDCI (41 mg, 0.21 mmol) and DMAP (25 mg, 0.20 mmol) was dissolved in dry CH_2Cl_2 (25 mL) and stirred for 12 h under N_2 at room temperature. The reaction mixture was diluted with CH_2Cl_2 (100 mL), washed with saturated $NaHCO_3$ twice and then with 1 M HCl twice, dried with $MgSO_4$, and concentrated. The organic mixture was separated by flash column chromatography (10%-30% EtOAc in hexanes) afforded **33** as a yellow solid (70 mg) in 50% yield. ^{1}H NMR ($CDCl_3$, 400MHz): δ 7.46-7.25 (m, 11H), 7.13-7.12 (m, 2H), 6.98 (s, 1H), 6.80 (d, J = 7.93 Hz, 1H), 5.59 (br, 1H), 5.23 (s, 2H), 5.14 (s, 2H), 4.72-4.64 (m, 2H), 3.88 (s, 3H), 3.15 (br, 2H), 2.20 (br, 1H), 1.98 (br, 1H), 1.58-1.57 (m, 4H), 1.41 (s, 9H).

Naphthalene-1-boronic acid (37). To a solution of **36** (1.00 g, 4.83 mmol) in dry THF (10 mL) was added *n*-butyllithium (3.32 mL of 1.6 M in hexane, 5.31 mmol) dropwise under N_2 at -78 $^\circ$C. The mixture was stirred for 50 min at this temperature and then triisopropylborate (1.68 mL, 1.362 g, 7.25 mmol) was added. The dry ice bath was removed and stirring was continued for 12 h at room temperature. The reaction mixture

was hydrolyzed with H_2O (10 mL) and rapidly extracted with diethyl ether (70 mL × 3). The combined organic layer was dried with $MgSO_4$ and evaporated on a rotary evaporator. The residue was dried under high vacuum for 8h to afford crude product as an oil which was directly used for the following reaction.

2,2-Dimethyl-5-naphthalen-1-yl-benzo[1,3]dioxin-4-one (38). Triflate **3** (522 mg, 1.60 mmol), boronic acid **37** (330 mg, 1.92 mmol), $Pd(PPh_3)_4$ (92 mg, 0.08 mmol), KBr (190 mg, 1.60 mmol), and Cs_2CO_3 (780 mg, 2.40 mmol) were mixed and dissolved in dry THF (30 mL). The mixture was stirred for 15 min and then 150 μL water was added. The reaction mixture was further stirred and refluxed for overnight. The reaction solution was diluted with diethyl ether (250 mL), washed with brine, dried with $MgSO_4$, and concentrated. Flash chromatographic separation (5%-15% EtOAc in hexanes) afforded **38** as a brown solid (389 mg) in 80% yield. ^{1}H NMR ($CDCl_3$, 300MHz): δ 7.91-7.87 (m, 2H), 7.63-7.31 (m, 6H), 7.10 – 7.05 (m, 2H), 1.81 (s, 3H), 1.78 (s, 3H). ^{13}C NMR ($CDCl_3$, 75MHz): δ 159.0, 157.1, 144.3, 138.7, 135.3, 133.6, 132.0, 128.6, 128.2, 126.7, 126.2, 125.9, 125.8, 125.4, 125.3, 117.1, 113.8, 105.6, 26.2, 25.9. MS (ESI/MS): *m/z* 327.1 (M + Na^+). Calcd for $C_{20}H_{16}NaO_3$ (M + Na^+): 327.3.

8-Hydroxy-benzo[c]fluoren-7-one (40). To a solution of **38** (375 mg, 1.23 mmol) in THF (20 mL) was added NaOH (100 mg, 2.5 mmol) and water (2 mL). The reaction was refluxed and monitored by TLC until the starting material disappeared. The resulting reaction solution was poured into water (100 mL) and washed with diethyl ether (70 mL). The aqueous layer was collected, acidified with 2.5 M HCl to pH 4, and then extracted

with diethyl ether (100 mL × 2). The organic layer was combined, washed with brine, dried with $MgSO_4$, evaporated to afford a viscous oil **39** (277 mg) in 85% yield.

To a solution of **39** (277 mg, 1.05 mmol) in dry CH_2Cl_2 (5 mL) was added trifluoroacetic acid (2 mL) and trifluoroacetic anhydride (1 mL) at 0 °C and the resulting reaction solution was stirred under N_2 at this temperature for 1 h. The reaction solution was adjusted to pH 4 by adding 10 M NaOH and then was extracted with CH_2Cl_2 (50 mL × 3). The organic layer was collected, washed with brine, dried with $MgSO_4$, and concentrated. Flash chromatographic separation (0%-3% EtOAc in hexanes) afforded an inseparatable orange mixture of **40** and side product (184 mg).

8-(*tert*-Butyldimethylsilanyloxy)-benzo[c]fluoren-7-one (41). To a solution of a mixture of **40** and its isomer (184 mg) in dry DMF (25 mL) was added TBDMSCl (366 mg, 2.43 mmol) and imidazole (165 mg, 2.43 mmol). The reaction solution was stirred overnight under N_2 and diluted with diethyl ether (150 mL). The collected ether layer was washed with 1 M HCl (50 mL), water (100 mL × 2), brine (100 mL × 2), dried with $MgSO_4$ and concentrated. Flash chromatographic separation (0%-5% EtOAc in hexanes) afforded **41** as a yellow solid (167 mg). ^{1}H NMR ($CDCl_3$, 300MHz): δ 8.50 (d, J = 7.76 Hz, 1H), 7.88 (d, J = 7.76 Hz, 1H), 7.81 – 7.52 (m, 5H), 7.38 (t, J = 8.41 Hz, 1H), 6.75 (d, J = 8.41 Hz, 1H), 1.10 (s, 9H), 0.31(s, 6H). ^{13}C NMR ($CDCl_3$, 75MHz): δ 192.6, 154.5, 147.2, 141.4, 137.9, 136.0, 132.7, 130.2, 129.9. 129.0 128.0, 127.9, 125.0, 123.1, 123.0, 119.9, 117.3, 26.1, 25.9, 18.7, -4.0.

8-(*tert*-Butyldimethylsilanyloxy)-7*H*-benzo[c]fluoren-7-ol (42). To a solution of **41** (167 mg, 0.46 mmol) in THF:MeOH solution (4:1, 20 mL) was added $NaBH_4$ (175 mg,

4.63 mmol). The reaction solution was stirred for 30 min and diluted with diethyl ether (120 mL). The collected ether layer was washed with 1 M HCl (50 mL), brine (100 mL), dried with $MgSO_4$ and concentrated. Flash chromatographic separation (0%-5% EtOAc in hexanes) afforded yellow solid **42** (150 mg) in 90% yield. ^{1}H NMR ($CDCl_3$, 300MHz): δ 8.64 (d, J = 8.25 Hz, 1H), 7.94 (d, J = 8.11 Hz, 1H), 7.90 – 7.78 (m, 3H), 7.62 (t, J = 8.11 Hz, 1H), 7.53 (t, J = 7.16 Hz, 1H), 7.37 (t, J = 7.90 Hz, 1H), 6.81 (d, J = 8.20 Hz, 1H), 5.81 (d, J = 3.91 Hz, 1H), 2.70 (d, J = 3.91 Hz, 1H, OH), 1.10 (s, 9H), 0.37 (s, 3H), 0.34 (s, 3H). ^{13}C NMR ($CDCl_3$, 75MHz): δ 153.1, 144.1, 143.5, 135.6, 135.3, 134.8, 130.8, 129.6, 129.5, 129.1, 127.0, 125.9, 124.2, 122.8, 117.9, 116.9, 74.0, 26.0, 18.4, -3.6, -3.9.

Acetic acid 8-(*tert*-butyldimethylsilanyloxy)-7*H*-benzo[c]fluoren-7-yl ester (43). $FeCl_3.6H_2O$ (108 mg, 0.40 mmol) was added to a stirred solution of **42** (145 mg, 0.40 mmol) in AcOH (20 mL). After 10 min, the reaction mixture was diluted with diethyl ether (120 mL). The collected ether layer was washed with 1 M NaOH (100 mL × 2), brine (100 mL), dried with $MgSO_4$ and concentrated. Flash chromatographic separation (0%-5% EtOAc in hexanes) afforded yellow solid **43** (132 mg) in 82% yield. ^{1}H NMR ($CDCl_3$, 300MHz): δ 8.64 (d, J = 7.99 Hz, 1H), 7.94-7.87 (m, 2H), 7.80 (d, J = 8.40 Hz, 1H), 7.71 (d, J = 8.40 Hz, 1H), 7.62 (t, J = 7.55 Hz, 1H), 7.53 (t, J = 7.38 Hz, 1H), 7.39 (t, J = 7.95 Hz, 1H), 7.06 (s, 1H), 6.81 (d, J = 8.23 Hz, 1H), 2.17 (s, 3H), 1.03 (s, 9H), 0.32 (s, 3H), 0.30 (s, 3H). ^{13}C NMR ($CDCl_3$, 75MHz): δ 171.8, 153.4, 144.7, 141.6, 136.4, 135.0, 131.4, 131.4, 129.5, 129.4, 129.2, 127.1, 126.1, 124.2, 123.4, 118.4, 116.8, 73.7, 25.9, 21.6, 18.4, -3.6, -3.7.

1-(8-Hydroxy-*7H*-benzo[c]fluoren-7-yl)-piperidine-4-carboxylic acid (44). To a solution of **43** (57 mg, 0.14 mmol) in DMF (10 mL) was added piperidine-4-carboxylic acid (91mg, 0.70 mmol) in water (600 μL) at 0 °C. The reaction solution was stirred for 10 min and added KF (82 mg, 1.41 mmol) in water (50 μL). Stirring was continued for 12 h at 0 °C and diluted with diethyl ether (120 mL). The collected ether layer was washed with water (50 mL), brine (100 mL), dried with $MgSO_4$ and concentrated. The wet reaction mixture was loaded onto a silica gel flash column and separated with 0%-7% MeOH in CH_2Cl_2 to afford white solid **44** (35 mg) in 70% yield. ^{1}H NMR ($CDCl_3$: CD_3OD, 300MHz): δ 8.64 (d, J = 8.45 Hz, 1H), 7.94-7.80 (m, 4H), 7.62 (t, J = 6.95 Hz, 1H), 7.53 (t, J = 6.95 Hz, 1H), 7.39 (t, J = 7.86 Hz, 1H), 6.83 (d, J = 8.21 Hz, 1H), 5.27 (s, 1H), 3.43-3.34 (m, 1H), 3.18 (t, J = 10.42 Hz, 1H), 2.86 (br, 1H), 2.62 (br, 1H), 2.40 (br, 1H), 2.21-2.08 (m, 1H), 1.97-1.82 (m, 3H). ^{13}C NMR ($CDCl_3$: CD_3OD, 75MHz): δ 177.2, 155.1, 142.5, 140.3, 137.3, 134.5, 131.0, 129.8, 129.2, 128.2, 127.1, 126.7, 126.1, 124.2, 123.6, 115.5, 114.5, 69.8, 51.6, 46.7, 40.5, 29.1, 28.2.

6-Benzyloxy-1-(*tert*-butyl-dimethyl-silanyloxy)-7-methoxy-fluoren-9-one (46). To a solution of **10** (250 mg, 0.75 mmol) in dry DMF (25 mL) was added TBDMSCl (369 mg, 2.45 mmol) and imidazole (167 mg, 2.45 mmol). The reaction solution was stirred overnight under N_2 and diluted with diethyl ether (150 mL). The collected ether layer was washed with 1 M HCl (50 mL), water (100 mL × 2), brine (100 mL × 2), dried with $MgSO_4$ and concentrated. Flash chromatographic separation (0%-10% EtOAc in hexanes) afforded **46** as a yellow solid (285 mg) in yield of 85%. ^{1}H NMR ($CDCl_3$, 300MHz): δ 7.48-7.18 (m, 7H), 7.00 (s, 1H), 6.90 (d, J = 7.20 Hz, 1H), 6.60 (d, J = 8.34 Hz, 1H), 5.25

(s, 2H), 3.90 (s, 3H), 1.07 (s, 9H). ^{13}C NMR ($CDCl_3$, 75MHz): δ 191.5, 154.3, 153.4, 150.7, 146.0, 138.0, 136.5, 135.8, 129.0, 128.4, 127.9, 127.5, 123.3, 122.4, 112.9, 107.2, 105.8, 71.4, 56.5, 25.9, 18.6, -4.1.

6-Benzyloxy-1-(*tert*-butyl-dimethyl-silanyloxy)-7-methoxy-9*H*-fluoren-9-ol (47). To a solution of **46** (186 mg, 0.42 mmol) in THF/MeOH solution (4:1, 20 mL) was added $NaBH_4$ (158 mg, 4.16 mmol). The reaction solution was stirred for 30 min and diluted with diethyl ether (120 mL). The collected ether layer was washed with 1 M HCl (50 mL), brine (100 mL), dried with $MgSO_4$ and concentrated. Flash chromatographic separation (0%-10% EtOAc in hexanes) afforded white solid **47** (164 mg) in 88% yield. ^{1}H NMR ($CDCl_3$, 300MHz): δ 7.50-7.19 (m, 7H), 7.15 (s, 1H), 7.09 (d, J = 7.44 Hz, 1H), 6.66 (d, J = 8.07 Hz, 1H), 5.67 (s, 1H), 5.22 (s, 2H), 3.95 (s, 3H), 1.07 (s, 9H), 0.32 (s, 3H), 0.29(s, 3H). ^{13}C NMR ($CDCl_3$, 75MHz): δ 153.1, 150.4, 149.3, 142.8, 138.4, 137.3, 134.7, 133.0, 130.7, 128.8, 128.1, 127.6, 117.5, 112.8, 109.0, 106.6, 73.9, 71.6, 56.5, 26.0, 18.4, -3.70, -4.0.

Acetic acid 6-benzyloxy-1-(*tert*-butyl-dimethyl-silanyloxy)-7-methoxy-9*H*-fluoren-9-yl ester (48). $FeCl_3.6H_2O$ (76 mg, 0.28 mmol) was added to a stirred solution of **47** (124 mg, 0.28 mmol) in AcOH: CH_2Cl_2 (65:35, 75 mL) at 0 °C. After 20 min, the reaction mixture was diluted with diethyl ether (100 mL). The collected ether layer was washed with 1 M NaOH (75 mL × 2), brine (75 mL), dried with $MgSO_4$ and concentrated. Flash chromatographic separation (0%-15% EtOAc in hexanes) afforded brown oil **48** (108 mg) in 79% yield. ^{1}H NMR ($CDCl_3$, 300MHz): δ 7.50-7.21 (m, 6H), 7.17 (s, 1H), 7.13 (s, 1H), 7.08 (d, J = 7.43 Hz, 1H), 6.08 (s, 1H), 6.67 (d, J = 8.13 Hz, 1H), 5.22 (s, 2H), 3.91

(s, 3H), 2.14 (s, 3H), 1.00 (s, 9H), 0.28(s, 3H), 0.25(s, 3H). ^{13}C NMR ($CDCl_3$, 75MHz): δ 172.0, 153.3, 150.3, 149.8, 143.9, 137.2, 135.8, 134.1, 131.3, 130.5, 128.8, 128.2, 127.6, 118.0, 112.5, 110.4, 106.3, 73.9, 71.6, 56.6, 25.9, 21.6, 18.3, -3.7, -3.9.

1-(6-Benzyloxy-1-hydroxy-7-methoxy-9*H*-fluoren-9-yl)-piperidine-4-carboxylic acid (49). To a solution of **48** (77 mg, 0.16 mmol) in DMF (10 mL) was added piperidine-4-carboxylic acid (101mg, 0.78 mmol) in water (680 μL). The reaction solution was stirred for 10 min and added KF (91 mg, 1.57 mmol) in water (50 μL). Stirring was continued for 12 h and diluted with diethyl ether (100 mL). The collected ether layer was washed with water (50 mL), brine (100 mL), dried with $MgSO_4$ and concentrated. The wet reaction mixture was loaded onto a silica gel flash column and separated with 0%-10% MeOH in CH_2Cl_2 to afford a white solid **49** (50 mg) in 72% yield. ^{1}H NMR ($CDCl_3$: CD_3OD, 300 MHz): δ 7.57-7.53 (m, 3H), 7.46-7.31 (m, 4H), 7.26-7.17 (m, 2H), 6.64 (d, *J* = 7.75 Hz, 1H), 5.21 (s, 2H), 5.11 (s, 1H), 3.91 (s, 3H), 3.48-3.39 (m, 1H), 3.19 (t, *J* = 11.01 Hz, 1H), 2.57-2.21 (m, 3H), 1.90-1.81 (m, 2H), 1.73-1.57 (m, 2H). ^{13}C NMR (CD_3COD_3, 75MHz): δ 175.2, 155.5, 149.7, 149.6, 142.0, 137.9, 134.9, 130.9, 130.4, 128.6, 128.0, 128.0, 114.4, 113.7, 111.2, 110.9, 106.7, 70.9, 69.6, 56.0, 51.4, 45.9, 40.4. MS (ESI/MS): *m/z* 445.89 (M^+). Calcd for $C_{27}H_{27}NO_5$ (M^+): 445.51.

General experimental procedure of acridine coupling (18, 45, 50). To a solution of **16**, or **44**, or **49** (0.011 mmol), acridine salt **17** (6 mg, 0.022mmol), and HBTU (9 mg, 0.022 mmol) in dry *N,N*- dimethylformamide (DMF, 1 mL) was added diisopropylethylamine in dry DMF (41.2 mM, 545 μL, 0.022 mmol). The reaction was stirred at room temperature under N_2. After 2 h, the reaction mixture was separated by a

reversed-phase HPLC system with a gradient of 10%-70% CH_3CN in triethylammonium acetate (50 mM, pH 6.0) over 30 min (1 mL/min). The acridine adduct was collected and solution was lyophilized to afford product as a yellow solid which was confirmed by ESI-MS.

2-Hydroxymethyl-3-naphthalen-1-yl-phenol (51). To a solution of **38** (500 mg, 1.6 mmol) in dry THF (30 mL) was added lithium aluminum hydride (374 mg, 9.8 mmol) at 0 °C. The ice bath was then removed, and the reaction mixture was stirred under N_2 for 1 h at room temperature. The reaction was quenched with ammonium chloride solution (50 mg/mL) dropwise at 0 °C until no bubble was generated. The reaction solution was diluted with water (50 mL), adjusted to pH 5 with 1 M HCl and then extracted with diethyl ether (80 mL × 2). The organic layer was collected, washed with brine (100 mL), dried with $MgSO_4$, and concentrated. Flash chromatographic separation (10%-20% EtOAc in hexanes) afforded pure **51** as a brown solid (329 mg) in 80% yield. ^{1}H NMR ($CDCl_3$, 300 MHz): δ 7.92-7.86 (m, 3H), 7.53-7.26 (m, 5H), 7.00 (d, J = 8.14 Hz, 1H), 6.84 (d, J = 7.55 Hz, 1H), 4.53 (s, 2H). ^{13}C NMR ($CDCl_3$, 75 MHz): δ 157.0, 139.8, 138.2, 133.6, 132.5, 129.1, 128.5, 128.1, 127.0, 126.6, 126.2, 126.0, 125.5, 123.5, 122.7, 116.4, 62.2. MS (ESI/MS): *m/z* 249.1 (M - H^+). Calcd for $C_{17}H_{13}O_2$ (M - H^+): 249.3.

1-[3-(*tert*-Butyldimethylsilanyloxy)-2-(*tert*-butyldimethylsilanyloxymethyl)-phenyl]-naphthalene (52). To a solution of **51** (300 mg, 1.2 mmol) in dry DMF (25 mL) were added TBDMSCl (903 mg, 6.0 mmol) and imidazole (408 mg, 6.0 mmol). The reaction solution was stirred overnight under N_2 and then diluted with diethyl ether (120 mL). The organic layer was washed with 1 M HCl (50 mL), water (100 mL × 2), brine

(100 mL × 2), dried with $MgSO_4$ and concentrated. Flash chromatographic separation (0%-5% EtOAc in hexanes) afforded **52** as a brown oil (464 mg) in 81% yield. ^{1}H NMR ($CDCl_3$, 300 MHz): δ 7.92-7.86 (m, 2H), 7.55-7.35 (m, 5H), 7.26 (t, J = 7.85 Hz, 1H), 6.97 (d, J = 8.16 Hz, 1H), 6.90 (d, J = 7.52 Hz, 1H), 4.65 (d, J = 9.93 Hz, 1H), 4.29 (d, J = 9.93 Hz, 1H), 1.09 (s, 9H), 0.68 (s, 9H), 0.36 (s, 3H), 0.36 (s, 3H), -0.48 (s, 3H), -0.43 (s, 3H). ^{13}C NMR ($CDCl_3$, 75 MHz): δ 154.7, 143.3, 139.2, 133.7, 132.8, 130.3, 128.2, 128.2, 127.6, 127.5, 126.9, 126.1, 125.8, 125.3, 124.1, 118.4, 57.6, 26.2, 26.1, 18.7, 18.4, -3.7, -3.8, -5.8, -5.9. MS (ESI/MS): *m/z* 496.4 ($M + NH_4^+$). Calcd for $C_{29}H_{46}NO_2Si_2$ ($M + NH_4^+$): 496.9.

Acetic acid 2-(*tert*-butyldimethylsilanyloxy)-6-naphthalen-1-yl-benzyl ester (53). $FeCl_3.6H_2O$ (70 mg, 0.26 mmol) was added to a stirred solution of **52** (125 mg, 0.26 mmol) in AcOH: Ac_2O (1:1, 10 mL). After 15 min, the reaction mixture was diluted with diethyl ether (100 mL). The ether layer was washed with 1 M NaOH (75 mL × 2), brine (75 mL), dried with $MgSO_4$ and concentrated. Flash chromatographic separation (0%-10% EtOAc in hexanes) afforded a brown oil **53** (84 mg) in 79% yield. ^{1}H NMR ($CDCl_3$, 300 MHz): δ 7.92-7.86 (m, 2H), 7.55-7.35 (m, 5H), 7.26 (t, J = 7.85Hz, 1H), 6.97 (d, J = 8.16Hz, 1H), 6.90 (d, J = 7.52Hz, 1H), 4.65 (d, J = 9.93Hz, 1H), 4.29 (d, J = 9.93Hz, 1H), 1.09 (s, 9H), 0.68 (s, 9H), 0.48 (s, 3H), 0.43 (s, 3H), 0.36 (s, 3H). ^{1}H NMR ($CDCl_3$, 300 MHz): δ 7.89-7.84 (m, 2H), 7.51-7.26 (m, 6H), 6.98-6.92 (m, 2H), 4.91 (d, J = 11.18 Hz, 1H), 4.68 (d, J = 11.18 Hz, 1H), 1.71(s, 3H), 1.01 (s, 9H), 0.33 (s, 3H), 0.32 (s, 3H). ^{13}C NMR ($CDCl_3$, 75 MHz): δ 170.8, 155.4, 143.8, 138.2, 133.7, 132.6, 129.4, 128.3, 128.1,

127.0, 126.6, 126.0, 126.0, 125.4, 125.2, 123.9, 118.1, 60.1, 25.9, 20.8, 18.5, -3.8, -4.0. MS (ESI/MS): *m/z* 429.4 ($M + Na^+$). Calcd for $C_{25}H_{30}NaO_3Si$ ($M + Na^+$): 429.6.

Quinoline-3-boronic Acid (55). To a solution of triisopropyl borate (2.8 mL, 12 mmol) and 3-bromoquinoline **54** (2.08 g, 10 mmol) in dry THF (20 mL) was added *n*-butyllithium (7.5 mL of 1.6 M in hexane, 12 mmol) dropwise via a syringe pump over 1 h under N_2 at -78 °C. After 2 h, the acetone/dry ice bath was removed and the reaction solution was allowed to warm up. The reaction solution was then quenched with 2 M HCl solution (10 mL) at 0 °C. The aqueous layers were neutralized to pH 7 with a 5 M NaOH solution and then extracted with diethyl ether (100 mL × 3). The combined ether layer was dried with $MgSO_4$ and evaporated. The residue was dried under high vacuum for 8h to afford crude product **55** as an oil which was directly used for the following reaction.

2,2-Dimethyl-5-quinolin-3-yl-benzo[1,3]dioxin-4-one (56). To triflate **3** (456 mg, 1.40 mmol), boronic acid **55** (290 mg, 1.68 mmol), $Pd(PPh_3)_4$ (81 mg, 0.07 mmol), KBr (167 mg, 1.40 mmol), and Cs_2CO_3 (682 mg, 2.10 mmol) was added dry THF (30 mL). The resulting mixture was stirred for 15 min and then 150 μL water was added. The reaction mixture was refluxed for 18 h. The reaction solution was diluted with diethyl ether (150 mL), and the organic layer was washed with brine, dried with $MgSO_4$, and concentrated. Flash chromatographic separation (30%-45% EtOAc in hexanes) afforded **56** as a brown solid (312 mg) in 73% yield. ^1H NMR ($CDCl_3$, 300 MHz): δ 8.85 (s, 1H), 8.17-8.12 (m, 2H), 7.85 (d, J= 8.12 Hz, 1H), 7.73 (t, J= 8.43 Hz, 1H), 7.63-7.54 (m, 2H), 7.09-7.05 (m, 2H), 1.82 (s, 6H). ^{13}C NMR ($CDCl_3$, 75 MHz): δ 159.8, 157.6, 150.9, 147.2,

142.4, 135.8, 134.9, 133.6, 129.9, 129.4, 128.3, 127.9, 127.1, 126.5, 117.8, 112.2, 105.9, 25.9. MS (ESI/MS): *m/z* 306.1 ($M + H^+$). Calcd for $C_{19}H_{16}NO_3$ ($M + H^+$): 306.3.

2-Hydroxymethyl-3-quinolin-3-yl-phenol (57). To a solution of **56** (312 mg, 1.02 mmol) in dry THF (20 mL) was added lithium aluminum hydride (232 mg, 6.12 mmol) at 0 °C. The ice bath was then removed, and the reaction mixture was stirred under N_2 for 1 h at room temperature. The reaction was quenched with ammonium chloride solution (50 mg/mL) dropwise at 0 °C until no bubble was generated. The reaction solution was diluted with water (50 mL), adjusted to pH 5 with 1 M HCl and then extracted with diethyl ether (60 mL × 2). The organic layer was collected, washed with brine (100 mL), dried with $MgSO_4$, and concentrated. Flash chromatographic separation (10% MeOH in CH_2Cl_2) afforded pure **57** as a brown oil (225 mg) in 88% yield. ^{1}H NMR (CD_3OD, 300 MHz): δ 8.94 (s, 1H), 8.41(s, 1H), 8.08 (d, J = 8.30 Hz, 1H), 7.99 (d, J = 8.17 Hz, 1H), 7.80 (t, J = 8.44 Hz, 1H), 7.65 (t, J = 8.09 Hz, 1H), 7.27 (t, J = 7.84 Hz, 1H), 6.94 (d, J = 8.15 Hz, 1H), 6.89 (d, J = 7.59 Hz, 1H), 4.58 (s, 2H). ^{13}C NMR (CD_3OD, 75 MHz): δ 157.2, 151.0, 146.4, 139.8, 136.6, 134.6, 129.9, 129.0, 128.3, 128.1, 127.7, 127.3, 124.9, 121.4, 115.3, 56.8. MS (ESI/MS): *m/z* 252.1 ($M + H^+$). Calcd for $C_{16}H_{14}NO_2$ ($M + H^+$): 252.3.

3-[3-(*tert*-butyldimethylsilanyloxy)-2-(*tert*-butyldimethylsilanyloxymethyl)-phenyl]-quinoline (58). To a solution of **57** (200 mg, 0.80 mmol) in dry DMF (20 mL) were added TBDMSCl (720 mg, 4.78 mmol) and imidazole (325 mg, 4.78 mmol). The reaction solution was stirred for 16 h under N_2 and then diluted with diethyl ether (120 mL). The organic layer was washed with 1 M HCl (50 mL), water (100 mL × 2), brine (100 mL × 2), dried with $MgSO_4$ and concentrated. Flash chromatographic separation

(10%-15% EtOAc in hexanes) afforded **58** as a white solid (332 mg) in 87% yield. ^{1}H NMR ($CDCl_3$, 300 MHz): δ 8.95 (s, 1H), 8.26(s, 1H), 8.16 (d, J = 8.52 Hz, 1H), 7.83 (d, J = 8.43 Hz, 1H), 7.73 (t, J = 8.45 Hz, 1H), 7.58 (t, J = 8.07 Hz, 1H), 7.26 (t, J = 7.89 Hz, 1H), 6.92 (d, J = 7.90 Hz, 2H), 4.62 (s, 2H), 1.05 (s, 9H), 0.77 (s, 9H), 0.31 (s, 6H), -0.19 (s, 6H). ^{13}C NMR ($CDCl_3$, 75 MHz): δ 154.7, 151.6, 147.2, 141.6, 135.9, 134.8, 129.6, 129.5, 129.4, 128.7, 128.1, 127.8, 127.0, 123.7, 118.9, 57.3, 26.2, 26.1, 18.7, 18.4, -3.7, -5.4. MS (ESI/MS): *m/z* 480.3 ($M + H^+$). Calcd for $C_{28}H_{42}NO_2Si_2$ ($M + H^+$): 480.8.

Acetic acid 2-(*tert*-butyldimethylsilanyloxy)-6-quinolin-3-yl-benzyl ester (59). $FeCl_3.6H_2O$ (204 mg, 0.76 mmol) was added to a stirred solution of **58** (242 mg, 0.50 mmol) in Ac_2O (5 mL). After 15 min, the reaction mixture was diluted with diethyl ether (100 mL). The ether layer was washed with 1 M NaOH (75 mL × 2), brine (75 mL), dried with $MgSO_4$ and concentrated. Flash chromatographic separation (5%-20% EtOAc in hexanes) afforded a yellow oil **59** (153 mg) in 74% yield. ^{1}H NMR ($CDCl_3$, 300 MHz): δ 8.94 (s, 1H), 8.19-8.14 (m, 2H), 7.83 (d, J = 8.10Hz, 1H), 7.76 (t, J = 8.42 Hz, 1H), 7.60 (t, J = 8.42 Hz, 1H), 7.36 (t, J = 8.10 Hz, 1H), 7.01-6.95 (m, 2H), 4.99 (s, 2H), 2.04 (s, 3H), 1.01 (s, 9H), 0.32 (s, 6H). ^{13}C NMR ($CDCl_3$, 75 MHz): δ 170.9, 155.9, 151.0, 147.1, 142.0, 136.0, 133.8, 130.1, 130.1, 129.3, 128.2, 127.7, 127.5, 124.4, 123.4, 118.6, 60.1, 25.8, 21.2, 18.5, -3.9. MS (ESI/MS): *m/z* 408.2 ($M + H^+$). Calcd for $C_{24}H_{30}NO_3Si$ ($M + H^+$): 408.6.

N1 adduct of quinoline dG. To a solution of **59** (15 mg, 0.037 mmol) and dG (15 mg, 0.054 mmol) in DMF (10 mL) were added KF (11mg, 0.18 mmol) and 100 μL water. After stirred for 12 h at room temperature, the reaction solution was diluted with 3

equivalent amount of water and filtered to remove suspended solids. The reaction mixture was isolated by a reversed-phase HPLC system with a gradient of 10%-70% CH_3CN in triethylammonium acetate (50 mM, pH 6.0) over 40 min (1 mL/min). The signal with a retention time of 19 min was collected and lyophilized to provide white solid in 56% yield as the quinoline dG N1 adduct. ^1H NMR (DMSO, 300MHz): δ 8.71 (d, J = 2.00 Hz, 1H), 8.04 (d, J = 2.00 Hz, 1H), 7.96 (d, J = 8.44 Hz, 1H), 7.79 (d, J = 8.09 Hz, 1H), 7.69 (t, J = 8.42 Hz, 1H), 7.68 (s, 1H), 7.55 (t, J = 7.37Hz, 1H), 7.15 (t, J = 7.93 Hz, 1H), 6.84 (d, J = 8.69 Hz, 1H), 6.61 (d, J = 8.43 Hz, 1H), 5.93 (dd, J = 7.09 Hz, 1H), 5.17 (d, J = 16.34 Hz, 1H), 5.04 (d, J = 16.34 Hz, 1H), 4.28 (m, 1H), 3.75 (m, 1H), 2.43-2.33 (m, 1H), 2.12-2.06 (m, 1H). ^{13}C NMR (DMSO, 75 MHz): δ 157.4, 157.0, 154.9, 151.3, 149.2, 147.0, 140.5, 135.6, 135.3, 134.5, 129.8, 129.2, 128.8, 128.4, 127.7, 127.2, 122.0, 121.3, 116.6, 116.1, 88.1, 82.7, 71.4, 62.4.

Time course study for deoxyguanosine or deoxyadenosine alkylation by naphthalene 53 or quinoline 59 individually. To QM precursor **53** or **59** and deoxynucleoside (dG or dA) in aqueous DMF (90% DMF) were added KF to yield a final concentration of 3.6 mM QM precursor, 5.4 mM deoxynucleoside, and 18 mM KF. The reaction was stirred at room temperature, and 50 μL of reaction solution was diluted with 50 μL of water at the indicated time. Each resulting aliquot was analyzed by a reverse-phase HPLC with a gradient of 10%-70% CH_3CN in triethylammonium acetate (50 mM, pH 6.0) over 40 min (1 mL/min).

1-(2-Hydroxy-6-naphthalen-1-yl-benzyl)-piperidine-4-carboxylic acid (60). To a solution of **53** (61 mg, 0.15 mmol) in DMF (10 mL) was added piperidine-4-carboxylic

acid (97 mg, 0.75 mmol) in water (650 μL). The reaction solution was stirred for 10 min and added KF (87 mg, 1.50 mmol) in water (50 μL). Stirring was continued for 12 h and then diluted with diethyl ether (100 mL). The collected ether layer was washed with water (50 mL), brine (100 mL), dried with $MgSO_4$ and concentrated. The wet reaction mixture was loaded onto a silica gel flash column and separated with 0%-10% MeOH in CH_2Cl_2 to afford a brown solid **60** (45 mg) in 83% yield. ^{1}H NMR ($CDCl_3$: CD_3OD, 300 MHz): δ 7.91-7.86 (m, 2H), 7.53-7.45 (m, 2H), 7.38-7.37 (m, 2H), 7.30-7.25 (m, 2H), 6.93 (d, J = 8.09 Hz, 1H), 6.78 (d, J = 7.51 Hz, 1H), 3.61 (d, J = 14.00 Hz, 1H), 3.46 (d, J = 14.00 Hz, 1H), 2.91 (br, 2H), 2.17 (br, 3H), 1.93-1.77 (m, 2H), 1.77-1.59 (m, 2H). ^{13}C NMR ($CDCl_3$: CD_3COD_3, 75MHz): δ 178.5, 157.8, 141.2, 138.4, 133.6, 132.3. 129.0, 128.5, 128.1, 126.8. 126.5, 126.2, 125.9, 125.4, 122.2, 119.0, 115.7, 57.3, 51.9, 29.8, 27.3.

1-(2-Hydroxy-6-quinolin-3-yl-benzyl)-piperidine-4-carboxylic acid (61). To a solution of **59** (42 mg, 0.10 mmol) in DMF (10 mL) was added piperidine-4-carboxylic acid (66 mg, 0.51 mmol) in water (600 μL). The reaction solution was stirred for 10 min and added KF (60 mg, 1.03 mmol). Stirring was continued for 12 h and diluted with diethyl ether (100 mL). The collected ether layer was washed with water (50 mL), brine (100 mL), dried with $MgSO_4$ and concentrated. The wet reaction mixture was loaded onto a silica gel flash column and separated with 0%-10% MeOH in CH_2Cl_2 to afford a white solid **61** (26 mg) in 70% yield. ^{1}H NMR ($CDCl_3$, 300 MHz): δ 8.85 (s, 1H), 8.19 (d, J = 8.38 Hz, 1H), 8.06 (s, 1H), 7.87 (d, J = 7.88 Hz, 1H), 7.77 (t, J = 7.57 Hz, 1H), 7.62 (t, J = 7.49 Hz, 1H), 7.27 (t, J = 7.70 Hz, 1H), 6.96 (d, J = 7.89 Hz, 1H), 6.79 (d, J = 7.61 Hz, 1H), 3.74 (s, 2H), 3.08-2.74 (br, 2H), 2.52-2.09 (m, 3H), 2.04-1.80 (br, 4H). ^{13}C NMR

($CDCl_3$, 75MHz): δ 178.2, 159.0, 150.9, 146.6, 138.8, 136.3, 134.3, 130.2, 129.2, 128.8, 128.2, 128.0, 127.6, 121.9, 118.9, 117.1, 58.0, 52.1, 29.9, 27.7.

General experimental procedure of the synthsis of succinimide esters (62, 63). To a solution of **60**, or **61** (0.01 mmol), *N*-hydroxysuccinimide (0.1 mmol) in dry DMF (1 mL) was added EDCI (0.02 mmol). The reaction was stirred at room temperature under N_2 for 12 h. The reaction mixture was diluted with diethyl ether (10 mL). The collected ether layer was washed with water (10 mL) and dried with $MgSO_4$ and evaporated. The residue was dried under high vacuum for 8h to afford crude succinimide ester **62** or **63** which was directly used for the following reaction.

General experimental procedure of DNA coupling (64, 65). Succinimide ester **62** or **63** in DMF was combined with a single strand DNA, 5-Amine B15 in Mops buffer (250 mM, pH 7.5). After the reaction solution was incubated for 24 h at ambient temperature, the DNA conjugate was purified by HPLC, dialyzed against water and lyophilized to afford DNA conjugate **64** or **65**.

List of References

References

1. Mountzouris, J. A.; Hurley, L. H. In *Bioorganic Chemistry: Nucleic Acids*; Hecht, S. M., Ed.; Oxford University Press: New York, **1996**, pp 288-323.

2. Wolkenberg, S. E.; Boger, D. L. "Mechanisms of in situ activation for DNA-targeting antitumor agents," *Chem. Rev.* **2002**, *102*, 2477-2495.

3. Shen, B.; Liu, W.; Nonaka, K. "Enediyne natural products: biosynthesis and prospect towards engineering novel antitumor agents," *Curr. Med. Chem.* **2003**, *10*, 2317-2325.

4. Hortobagyi, G. N. "Anthracyclines in the treatment of cancer. An overview," *Drugs* **1997**, *54 Suppl 4*, 1-7.

5. Denny, W. A. "DNA-intercalating ligands as anti-cancer drugs: prospects for future design," *Anticancer Drug Des.* **1989**, *4*, 241-263.

6. Coll, M.; Aymami, J.; van der Marel, G. A.; van Boom, J. H.; Rich, A.; Wang, A. H. "Molecular structure of the netropsin-d(CGCGATATCGCG) complex: DNA conformation in an alternating AT segment," *Biochemistry* **1989**, *28*, 310-320.

7. Kopka, M. L.; Yoon, C.; Goodsell, D.; Pjura, P.; Dickerson, R. E. "Binding of an antitumor drug to DNA, Netropsin and C-G-C-G-A-A-T-T-BrC-G-C-G," *J. Mol. Biol.* **1985**, *183*, 553-563.

8. Kopka, M. L.; Yoon, C.; Goodsell, D.; Pjura, P.; Dickerson, R. E. "The molecular origin of DNA-drug specificity in netropsin and distamycin," *Proc. Natl. Acad. Sci. U S A* **1985**, *82*, 1376-1380.

9. Hurley, L. H.; Reck, T.; Thurston, D. E.; Langley, D. R.; Holden, K. G.; Hertzberg, R. P.; Hoover, J. R.; Gallagher, G., Jr.; Faucette, L. F.; Mong, S. M.; et al. "Pyrrolo[1,4]benzodiazepine antitumor antibiotics: relationship of DNA alkylation and sequence specificity to the biological activity of natural and synthetic compounds," *Chem. Res. Toxicol.* **1988**, *1*, 258-268.

10. Rajski, S. R.; Williams, R. M. "DNA Cross-Linking Agents as Antitumor Drugs," *Chem. Rev.* **1998**, *98*, 2723-2796.

11. Ho, Y. P.; Au-Yeung, S. C.; To, K. K. "Platinum-based anticancer agents: innovative design strategies and biological perspectives," *Med. Res. Rev.* **2003**, *23*, 633-655.

12. Peter, M. G. "Chemical modifications of biopolymers by quinones and quinone methides," *Angew. Chem. Int. Ed. Engl.* **1989**, *28*, 555-570.

13. Wan, P.; Barker, B.; Diao, L.; Fischer, M.; Shi, Y.; Yang, C. "Quinone methides: relevant intermediates in organic chemistry.," *Can. J. Chem.* **1996**, *74*, 465-475.

14. Amouri, H.; Le Bras, J. "Taming Reactive Phenol Tautomers and *o*-Quinone Methides with Transition Metals: A Structure-Reactivity Relationship," *Acc. Chem. Res.* **2002**, *35*, 501-510.

15. Freccero, M. "Quinone methides as alkylating and cross-linking agents," *Mini-Rev. Org. Chem.* **2004**, *1*, 403-415.

16. Myers, J.; Widlanski, T. "Mechanism-based inactivation of prostatic acid phosphatase," *Science* **1993**, *262*, 1451-1453.

17. Myers, J. K.; Cohen, J. D.; Widlanski, T. S. "Substituent Effects on the Mechanism-Based Inactivation of Prostatic Acid Phosphatase," *J. Am. Chem. Soc.* **1995**, *117*, 11049-11054.

18. Turner, A. B. "Quinone methides," *Q. Rev. Chem. Soc. Lond.* **1964**, *18*, 347-360.

19. Thompson, D. C.; Thompson, J. A.; Sugumaran, M.; Moldeus, P. "Biological and toxicological consequences of quinone methide formation," *Chem. Biol. Interact.* **1992**, *86*, 129-162.

20. Lanigan, R. S.; Yamarik, T. A. "Final report on the safety assessment of BHT(1)," *Int. J. Toxicol.* **2002**, *21 Suppl 2*, 19-94.

21. Fujisawa, S.; Atsumi, T.; Kadoma, Y.; Sakagami, H. "Antioxidant and prooxidant action of eugenol-related compounds and their cytotoxicity," *Toxicology* **2002**, *177*, 39-54.

22. Peterson, D. M.; Fisher, J. "Autocatalytic quinone methide formation from mitomycin c," *Biochemistry* **1986**, *25*, 4077-4084.

23. Water, R. W. V. D.; Pettus, T. R. R. "*o*-Quinone methides: intermediates underdeveloped and underutilized in organic synthesis," *Tetrahedron* **2002**, *58*, 5367-5405.

24. Li, T.; Zeng, Q.; Rokita, S. E. "Target-Promoted Alkylation of DNA," *Bioconjugate Chem.* **1994**, *5*, 497-500.

25. Zeng, Q.; Rokita, S. E. "Tandem Quinone Methide Generation for Cross-Linking DNA," *J. Org. Chem.* **1996**, *61*, 9080-9081.

26. Pande, P.; Shearer, J.; Yang, J.; Greenberg, W. A.; Rokita, S. E. "Alkylation of Nucleic Acids by a Model Quinone Methide," *J. Am. Chem. Soc.* **1999**, *121*, 6773-6779.

27. Veldhuyzen, W. F.; Shallop, A. J.; Jones, R. A.; Rokita, S. E. "Thermodynamic versus kinetic products of DNA alkylation as modeled by reaction of deoxyadenosine," *J. Am. Chem. Soc.* **2001**, *123*, 11126-11132.

28. Veldhuyzen, W. F.; Lam, Y. F.; Rokita, S. E. "2'-Deoxyguanosine reacts with a model quinone methide at multiple sites," *Chem. Res. Toxicol.* **2001**, *14*, 1345-1351.

29. Zhou, Q.; Pande, P.; Johnson, A. E.; Rokita, S. E. "Sequence-specific delivery of a quinone methide intermediate to the major groove of DNA," *Bioorg. Med. Chem.* **2001**, *9*, 2347-2354.

30. Veldhuyzen, W. F.; Pande, P.; Rokita, S. E. "A transient product of DNA alkylation can be stabilized by binding localization," *J. Am. Chem. Soc.* **2003**, *125*, 14005-14013.

31. Zhou, Q.; Rokita, S. E. "A general strategy for target-promoted alkylation in biological systems," *Proc. Natl. Acad. Sci. U S A* **2003**, *100*, 15452-15457.

32. Kumar, D.; Veldhuyzen, W. F.; Zhou, Q.; Rokita, S. E. "Conjugation of a Hairpin Pyrrole-Imidazole Polyamide to a Quinone Methide for Control of DNA Cross-Linking," *Bioconjugate Chem.* **2004**, *15*, 915-922.

33. Weinert, E. E.; Frankenfield, K. N.; Rokita, S. E. "Time-dependent evolution of adducts formed between deoxynucleosides and a model quinone methide," *Chem. Res. Toxicol.* **2005**, *18*, 1364-1370.

34. Fischer, M.; Wan, P. "Nonlinear Solvent Water Effects in the Excited-State (Formal) Intramolecular Proton Transfer (ESIPT) in m-Hydroxy-1,1-diaryl

Alkenes: Efficient Formation of m-Quinone Methides," *J. Am. Chem. Soc.* **1999**, *121*, 4555-4562.

35. Foster, K. L.; Baker, S.; Brousmiche, D. W.; Wan, P. "*o*-Quinone Methide Formation from Excited State Intramolecular Proton Transfer (ESIPT) in an o-Hydroxystyrene," *J. Photochem. Photobiol., A,* **1999**, *129*, 157-163.

36. Wang, P.; Song, Y.; Zhang, L.; He, H.; Zhou, X. "Quinone methide derivatives: important intermediates to DNA alkylating and DNA cross-linking actions," *Curr. Med. Chem.* **2005**, *12*, 2893-2913.

37. Richter, S. N.; Maggi, S.; Mels, S. C.; Palumbo, M.; Freccero, M. "Binol Quinone Methides as Bisalkylating and DNA Cross-Linking Agents," *J. Am. Chem. Soc.* **2004**, *126*, 13973-13979.

38. Dorrestijn, E.; Kranenburg, M.; Ciriano, M. V.; Mulder, P. "The Reactivity of o-Hydroxybenzyl Alcohol and Derivatives in Solution at Elevated Temperatures," *J. Org. Chem.* **1999**, *64*, 3012-3018.

39. Qiao, G. G.; Lenghaus, K.; Solomon, D. H.; Reisinger, A.; Bytheway, I.; Wentrup, C. "4,6-Dimethyl-o-quinone Methide and 4,6-Dimethylbenzoxete," *J. Org. Chem.* **1998**, *63*, 9806-9811.

40. Yato, M.; Ohwada, T.; Shudo, K. "4H-1,2-Benzoxazines as novel precursors of o-benzoquinone methide," *J. Am. Chem. Soc.* **1990**, *112*, 5341-5342.

41. Rokita, S. E.; Yang, J.; Pande, P.; Greenberg, W. A. "Quinone Methide Alkylation of Deoxycytidine," *J. Org. Chem.* **1997**, *62*, 3010-3012.

42. Egholm, M.; Koch, T. H. "Coupling of the anthracycline antitumor drug menogaril to 2'-deoxyguanosine through reductive activation," *J. Am. Chem. Soc.* **1989**, *111*, 8291-8293.

43. Woo, J.; Sigurdsson, S. T.; Hopkins, P. B. "DNA interstrand cross-linking reactions of pyrrole-derived, bifunctional electrophiles: evidence for a common target site in DNA," *J. Am. Chem. Soc.* **1993**, *115*, 3407-3415.

44. Williams, R. M.; Herberich, B. "DNA Interstrand Cross-Link Formation Induced by Bioxalomycin alpha-2," *J. Am. Chem. Soc.* **1998**, *120*, 10272-10273.

45. Shibutani, S.; Ravindernath, A.; Suzuki, N.; Terashima, I.; Sugarman, S. M.; Grollman, A. P.; Pearl, M. L. "Identification of tamoxifen-DNA adducts in the

endometrium of women treated with tamoxifen," *Carcinogenesis* **2000**, *21*, 1461-1467.

46. Weinert, E. E.; Dondi, R.; Colloredo-Melz, S.; Frankenfield, K. N.; Mitchell, C. H.; Freccero, M.; Rokita, S. E. "Substituents on quinone methides strongly modulate formation and stability of their nucleophilic adducts," *J. Am. Chem. Soc.* **2006**, *128*, 11940-11947.

47. Freccero, M.; Gandolfi, R.; Sarzi-Amade, M. "Selectivity of Purine Alkylation by a Quinone Methide. Kinetic or Thermodynamic Control?," *J. Org. Chem.* **2003**, *68*, 6411-6423.

48. Modica, E.; Zanaletti, R.; Freccero, M.; Mella, M. "Alkylation of Amino Acids and Glutathione in Water by o-Quinone Methide. Reactivity and Selectivity," *J. Org. Chem.* **2001**, *66*, 41-52.

49. Zhou, Q.; Turnbull, K. D. "Phosphodiester Alkylation with a Quinone Methide," *J. Org. Chem.* **1999**, *64*, 2847-2851.

50. Zhou, Q.; Turnbull, K. D. "Quinone Methide Phosphodiester Alkylations under Aqueous Conditions," *J. Org. Chem.* **2001**, *66*, 7072-7077.

51. Zhou, Q.; Turnbull, K. D. "Trapping Phosphodiester-Quinone Methide Adducts through in Situ Lactonization," *J. Org. Chem.* **2000**, *65*, 2022-2029.

52. Bakke, B. A.; McIntosh, M. C.; Turnbull, K. D. "Improved alkylation and product stability in phosphotriester formation through quinone methide reactions with dialkyl phosphates," *J. Org. Chem.* **2005**, *70*, 4338-4345.

53. Chabner, B. A.; Ryan, D. P.; Paz-Ares, L.; Garcia-Carbonero, R.; Calabresi, P. In *Goodman & Gilman's The Pharmacological Basis of Therapeutics*; 10th ed.; Gilman, A. G., Ed.; McGraw–Hill, New York, **2001**, p 1389–1459.

54. Eckhardt, S. "Recent progress in the development of anticancer agents," *Curr. Med. Chem. Anticancer Agents* **2002**, *2*, 419-439.

55. Chatterjee, M.; Rokita, S. E. "The Role of a Quinone Methide in the Sequence Specific Alkylation of DNA," *J. Am. Chem. Soc.* **1994**, *116*, 1690-1697.

56. Beal, P.; Dervan, P. "Second structural motif for recognition of DNA by oligonucleotide-directed triple-helix formation," *Science* **1991**, *251*, 1360-1363.

57. Mokhir, A. A.; Kraemer, R. "Conjugates of PNA with Naphthalene Diimide Derivatives Having a Broad Range of DNA Affinities," *Bioconjugate Chem.* **2003**, *14*, 877-883.

58. Lukhtanov, E.; Mills, A.; Kutyavin, I.; Gorn, V.; Reed, M.; Meyer, R. "Minor groove DNA alkylation directed by major groove triplex forming oligodeoxyribonucleotides," *Nucl. Acids Res.* **1997**, *25*, 5077-5084.

59. Takasugi, M.; Guendouz, A.; Chassignol, M.; Decout, J.; Lhomme, J.; Thuong, N.; Helene, C. "Sequence-Specific Photo-Induced Cross-Linking of the Two Strands of Double- Helical DNA by a Psoralen Covalently Linked to a Triple Helix-Forming Oligonucleotide," *PNAS* **1991**, *88*, 5602-5606.

60. Wang, Y.-D.; Dziegielewski, J.; Wurtz, N. R.; Dziegielewska, B.; Dervan, P. B.; Beerman, T. A. "DNA crosslinking and biological activity of a hairpin polyamide-chlorambucil conjugate," *Nucl. Acids Res.* **2003**, *31*, 1208-1215.

61. Kang, H.; Rokita, S. E. "Site-specific and photo-induced alkylation of DNA by a dimethylanthraquinone-oligodeoxynucleotide conjugate," *Nucleic Acids Res.* **1996**, *24*, 3896-3902.

62. Shirai, N.; Moriya, K.; Kawazoe, Y. "PH dependence of hydrolytic removal of silyl group from trialkylsilyl ethers," *Tetrahedron* **1986**, *42*, 2211-2214.

63. Marino, J. P.; Dax, S. L. "An efficient desilylation method for the generation of o-quinone methides: application to the synthesis of (+)- and (-)-hexahydrocannabinol," *J. Org. Chem.* **1984**, *49*, 3671-3672.

64. Boger, D. L.; Garbaccio, R. M. "Shape-Dependent Catalysis: Insights into the Source of Catalysis for the CC-1065 and Duocarmycin DNA Alkylation Reaction," *Acc. Chem. Res.* **1999**, *32*, 1043-1052.

65. Shen, B. "Accessing natural products by combinatorial biosynthesis," *Sci. STKE.* **2004**, *2004*, pe14.

66. Seidman, M. M.; Glazer, P. M. "The potential for gene repair via triple helix formation," *J. Clin. Invest.* **2003**, *112*, 487-494.

67. Fischer, M.; Shi, Y.; Zhao, B.; Snieckus, V.; Wan, P. "Contrasting behaviour in the photosolvolysis of 1- and 2-hydroxy-9-fluorenols in aqueous solution," *Can. J. Chem.* **1999**, *77*, 868-874.

68. Bentin, T.; Nielsen, P. E. "Superior Duplex DNA Strand Invasion by Acridine Conjugated Peptide Nucleic Acids," *J. Am. Chem. Soc.* **2003**, *125*, 6378-6379.

69. Delcros, J.-G.; Tomasi, S.; Carrington, S.; Martin, B.; Renault, J.; Blagbrough, I. S.; Uriac, P. "Effect of spermine conjugation on the cytotoxicity and cellular transport of acridine," *J. Med. Chem.* **2002**, *45*, 5098-5111.

70. Kuzuya, A.; Machida, K.; Mizoguchi, R.; Komiyama, M. "Conjugation of Various Acridines to DNA for Site-Selective RNA Scission by Lanthanide Ion," *Bioconjugate Chem.* **2002**, *13*, 365-369.

71. Prakash, A. S.; Denny, W. A.; Gourdie, T. A.; Valu, K. K.; Woodgate, P. D.; Wakelin, L. P. G. "DNA-directed alkylating ligands as potential antitumor agents: sequence specificity of alkylation by intercalating aniline mustards," *Biochemistry* **1990**, *29*, 9799-9807.

72. Kohn, K. W.; Orr, A.; O'Connor, P. M.; Guziec, L. J.; Guziec, F. S. "Synthesis and DNA-sequence selectivity of a series of mono- and difunctional 9-aminoacridine nitrogen mustards," *J. Med. Chem.* **1994**, *37*, 67-72.

73. Markovits, J.; Pommier, Y.; Mattern, M. R.; Esnault, C.; Roques, B. P.; Le Pecq, J. B.; Kohn, K. W. "Effects of the bifunctional antitumor intercalator ditercalinium on DNA in mouse leukemia L1210 cells and DNA topoisomerase II," *Cancer Res.* **1986**, *46*, 5821-5826.

74. Murza, A.; Alvarez-Mendez, S.; Sanchez-Cortes, S.; Garcia-Ramos, J. V. "Interaction of antitumoral 9-aminoacridine drug with DNA and dextran sulfate studied by fluorescence and surface-enhanced Raman spectroscopy," *Biopolymers* **2003**, *72*, 174-184.

75. Hadfield, A.; Schweitzer, H.; Trova, M. P.; Green, K. "Practical, large scale synthesis of 2,2-dimethyl-5-hydroxy-4-oxo-benzo-1,4-dioxin," *Synth. Commun.* **1994**, *24*, 1025-1028.

76. Takahashi, S.; Kamisukib, S.; Mizushinac, Y.; Sakaguchib, K.; Sugawarab, F.; Nakataa, T. "Total synthesis of dehydroaltenusin," *Tetrahedron Letters* **2003**, *44*, 1875-1877.

77. Schreiner, P. R.; Fokina, N. A.; Tkachenko, B. A.; Hausmann, H.; Serafin, M.; Dahl, J. E.; Liu, S.; Carlson, R. M.; Fokin, A. A. "Functionalized nanodiamonds: triamantane and [121]tetramantane," *J. Org. Chem.* **2006**, *71*, 6709-6720.

78. Li, X.; Abell, C.; Congreve, M. S.; Warrington, B. H.; Ladlow, M. "A novel phase-switching protecting group for multi-step parallel solution phase synthesis," *Org. Biomol. Chem.* **2004**, *2*, 989-998.

79. Koch, K.; Podlech, J.; Pfeiffer, E.; Metzler, M. "Total synthesis of alternariol," *J. Org. Chem.* **2005**, *70*, 3275-3276.

80. Oh-e, T.; Miyaura, N.; Suzuki, A. "Palladium-catalyzed cross-coupling reaction of organoboron compounds with organic triflates," *J. Org. Chem.* **1993**, *58*, 2201-2208.

81. Coelho, P. J.; Carvalho, L. M.; Rodrigues, S.; Oliveira-Campos, A. M. F.; Dubest, R.; Aubard, J.; Samat, A.; Guglielmetti, R. "Synthesis and photochromic behaviour of novel 2*H*-chromenes derived from fluorenone," *Tetrahedron* **2002**, *58*, 925-931.

82. Wang, W.; McMurray, J. S. "A selective method for the preparation of primary amides: synthesis of Fmoc--4-carboxamidophenylalanine and other compounds," *Tetrahedron Lett.* **1999**, *40*, 2501-2504.

83. Lepore, S. D.; He, Y. "Use of Sonication for the Coupling of Sterically Hindered Substrates in the Phenolic Mitsunobu Reaction," *J. Org. Chem.* **2003**, *68*, 8261-8263.

84. Brinkman, H. R.; Landi, J. J., Jr.; Paterson, J. B., Jr.; Stone, P. J. "The use of p-toluenesulfonic acid for removal of the *N-tert*-butoxycarbonyl protecting group in solid phase peptide synthesis," *Synth. Commun.* **1991**, *21*, 459-465.

85. Bacos, D.; Célérier, J. P.; Marx, E.; Saliou, C.; Lhommet, G. "Reduction of 2,5-dialkylpyrrolines. A key step in a synthesis of natural insecticides," *Tetrahedron Lett.* **1989**, *30*, 1081-1082.

86. Ashley, E. R.; Cruz, E. G.; Stoltz, B. M. "The Total Synthesis of (-)-Lemonomycin," *J. Am. Chem. Soc.* **2003**, *125*, 15000-15001.

87. Dent, A.; Aslam, M. In *Bioconjugation: protein coupling techniques for the biomedical sciences*; Dent, A., Ed.; Macmillan Reference Ltd.: London, **1998**, pp 364-482.

88. Buchi, G.; Weinreb, S. M. "Total syntheses of aflatoxins M1 and G1 and an improved synthesis of aflatoxin B1," *J. Am. Chem. Soc.* **1971**, *93*, 746-752.

89. Burrows, C. J.; Muller, J. G. "Oxidative Nucleobase Modifications Leading to Strand Scission," *Chem. Rev.* **1998**, *98*, 1109-1152.

90. Andrus, A.; Kuimelis, R. G. In *Current Protocols in Nucleic Acid Chemistry*; Jones, R. A., Ed.; John Wiley and Sons: New York, **1999**, Section 10.14.

91. Rokita, S. E. In *Current protocols in Nucleic Acid Chemistry*; Jones, R. A., Ed.; John Wiley and Sons: New York, **2001**, Section 6.6.

92. Wade, L. G. *Organic chemistry*; 5th ed.; Pearson Education, Inc.: Upper Saddle River, NJ, **2003**; Chapter 19.

93. Carey, F. A.; Sundberg , R. J. *Advanced Organic Chemistry Part A: Structure and Mechanisms*; 3 ed.; Springer, **1990**.

94. Scott, J. W.; Parker, D.; Parrish, D. R. "Improved syntheses of N^{ϵ}-tert-butyloxycarbonyl -L-lysine and N^{a}-benzyloxycarbonyl -N^{ϵ}-tert-butyloxycarbonyl-L-lysine," *Synth. Commun.* **1981**, *11*, 303–314.

95. Soai, K.; Oyamada, H.; Takase, M.; Ookawa, A. "Practical procedure for the chemoselective reduction of esters by sodium borohydride. Effect of the slow addition of methanol," *Bull. Chem. Soc. Jpn.* **1984**, *57*, 1948-1953.

96. Tamaddon, F.; Amrollahi, M. A.; Sharafat, L. "A green protocol for chemoselective *O*-acylation in the presence of zinc oxide as a heterogeneous, reusable and eco-friendly catalyst," *Tetrahedron Lett.* **2005**, *46*, 7841-7844.

97. Danishefsky, S. J.; Mantlo, N. "Total Synthesis of (±)-Heptelidic Acid," *J. Am. Chem. Soc.* **1988**, *110*, 8129-8133.

98. Li, W.; Nelson, D. P.; Jensen, M. S.; Hoerrner, R. S.; Cai, D.; Larsen, R. D.; Reider, P. J. "An Improved Protocol for the Preparation of 3-Pyridyl- and Some Arylboronic Acids," *J. Org. Chem.* **2002**, *67*, 5394-5397.

99. Dai, J.; Zhou, Q. "A Convenient Synthesis of an N-(1-Alkoxyl-9-fluorenyl)serine Acridine Conjugate," *Synth. Comm.* **2007**, *37*, 129-135.

APPENDIX

^{1}H and ^{13}C NMR spectra.

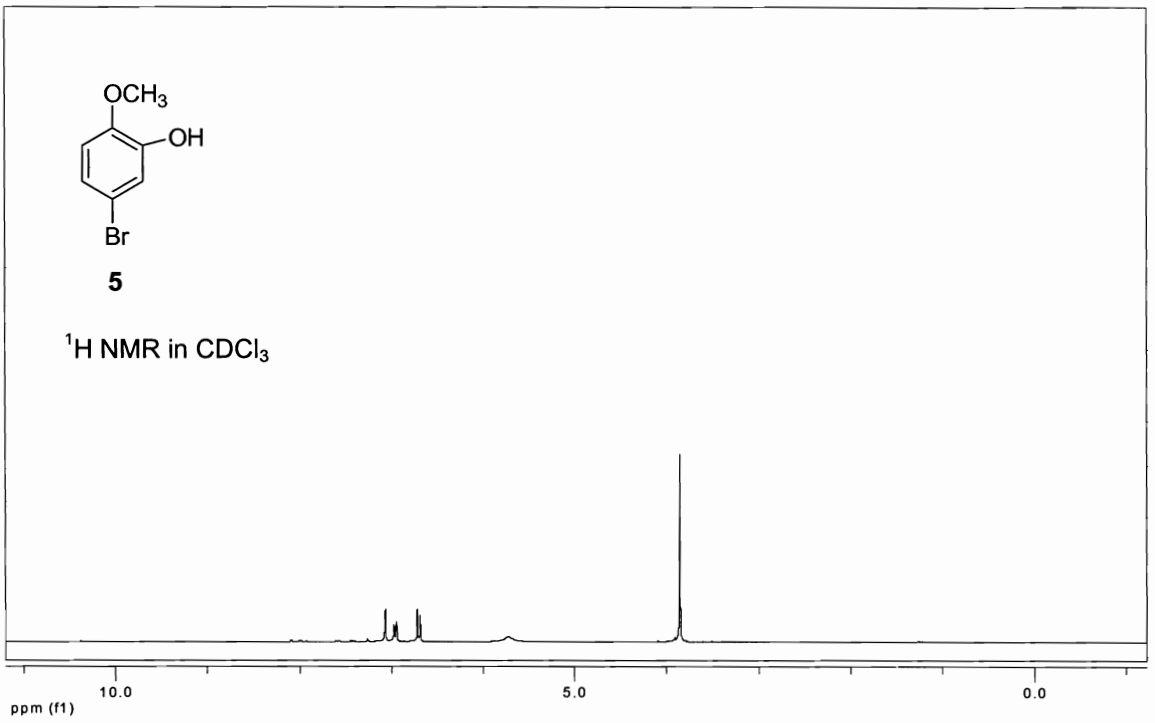
OCH3
OH
Br
5
1H NMR in CDCl3
10.0
5.0
0.0
ppm (f1)

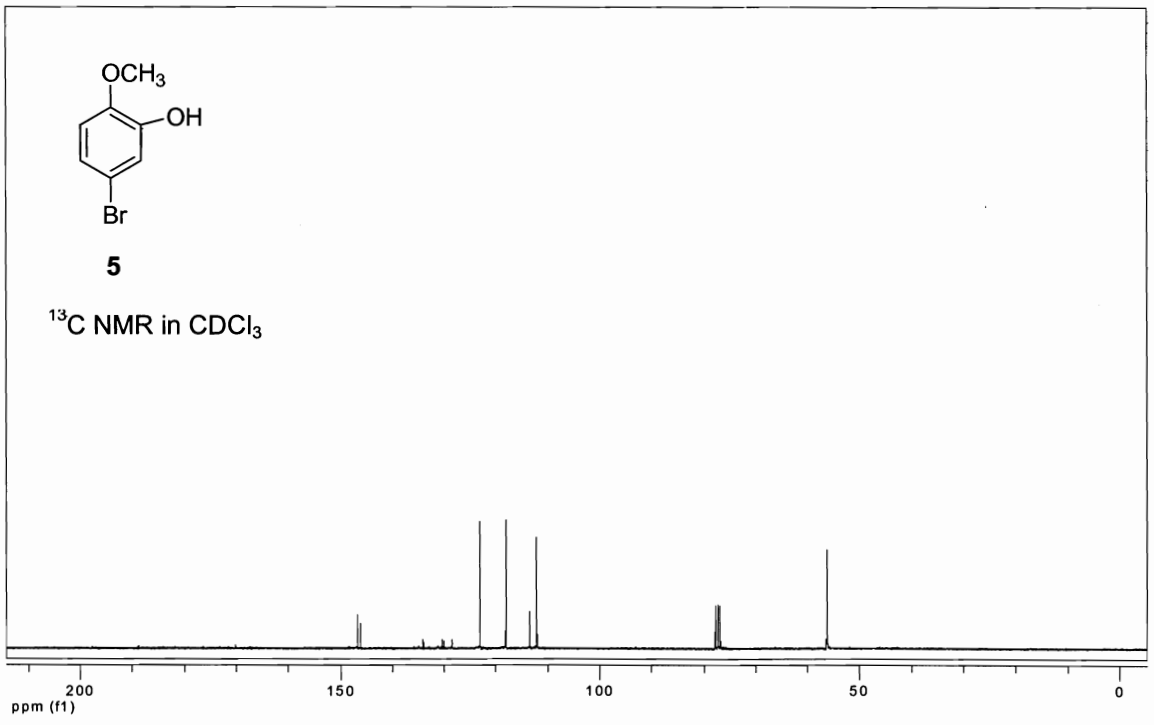
OCH3
OH
Br
5
13C NMR in CDCl3
200
150
100
50
0
ppm (f1)

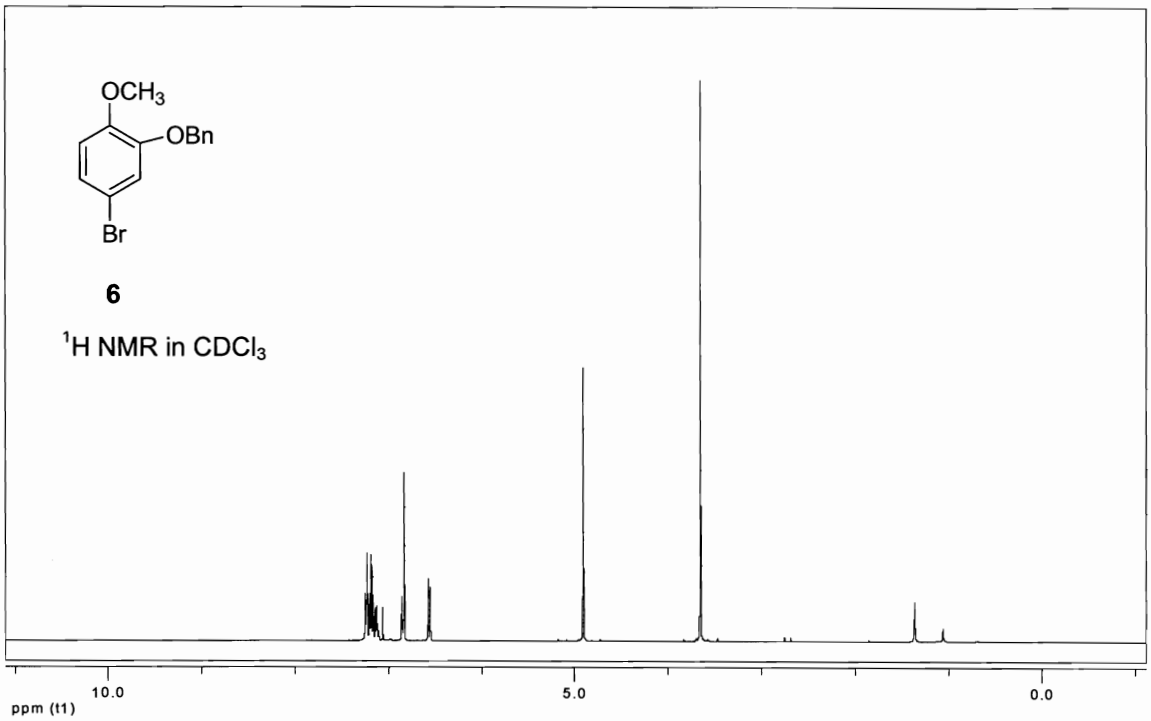
OCH3
OBn
Br
6
1H NMR in CDCl3
10.0
5.0
0.0
ppm (t1)

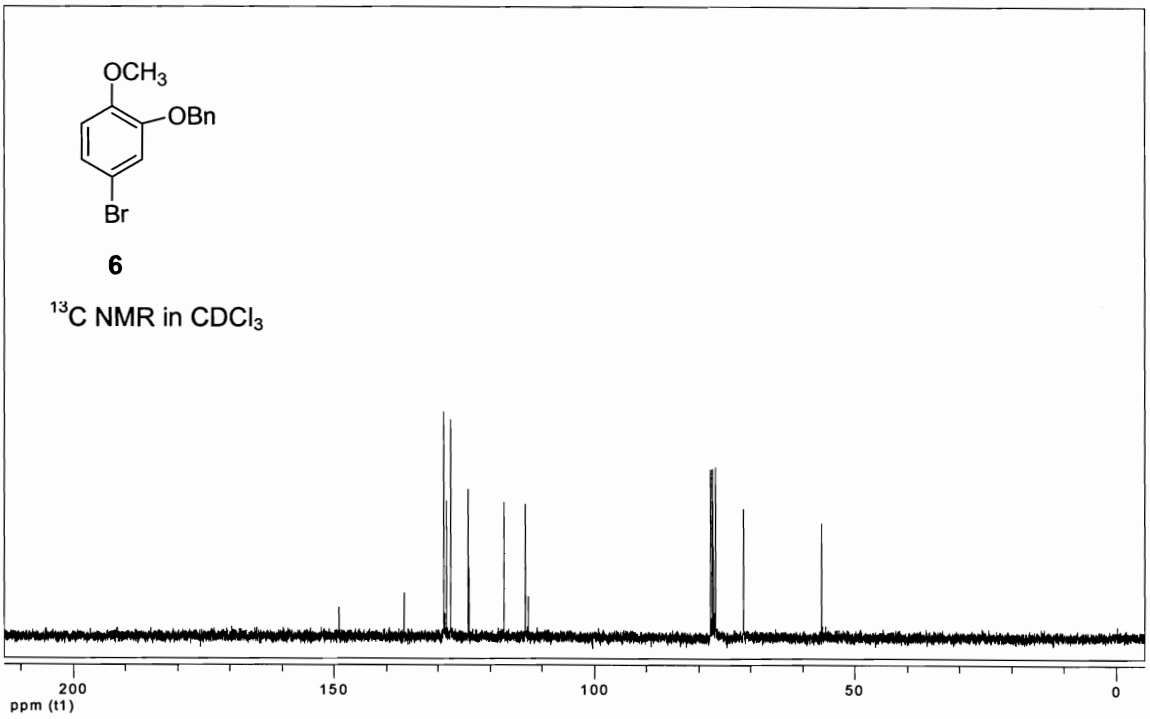
OCH3
OBn
Br
6
13C NMR in CDCl3
200
150
100
50
0
ppm (t1)

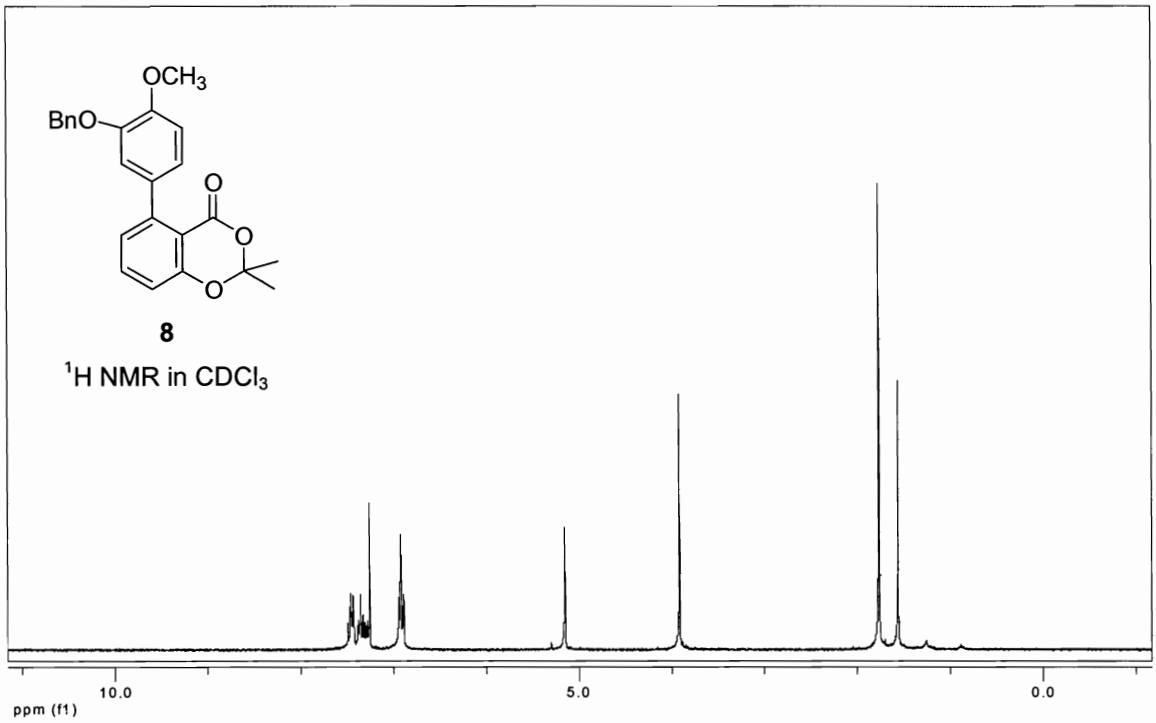

8

^{1}H NMR in $CDCl_3$

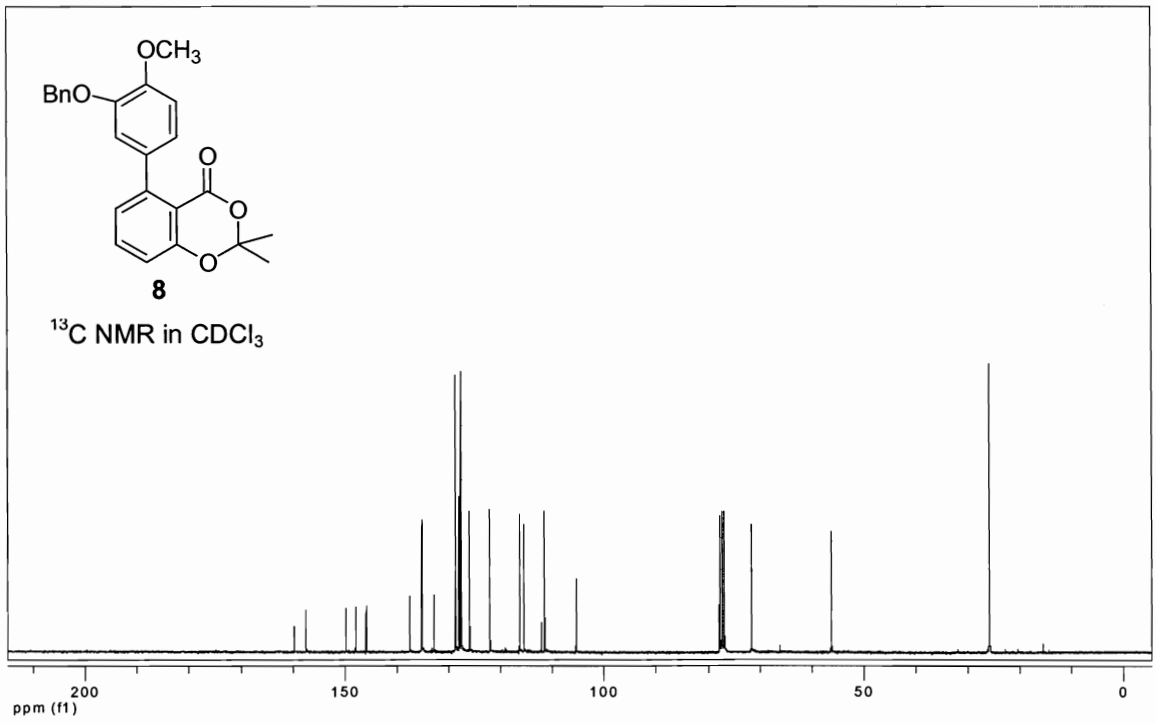

8

^{13}C NMR in $CDCl_3$

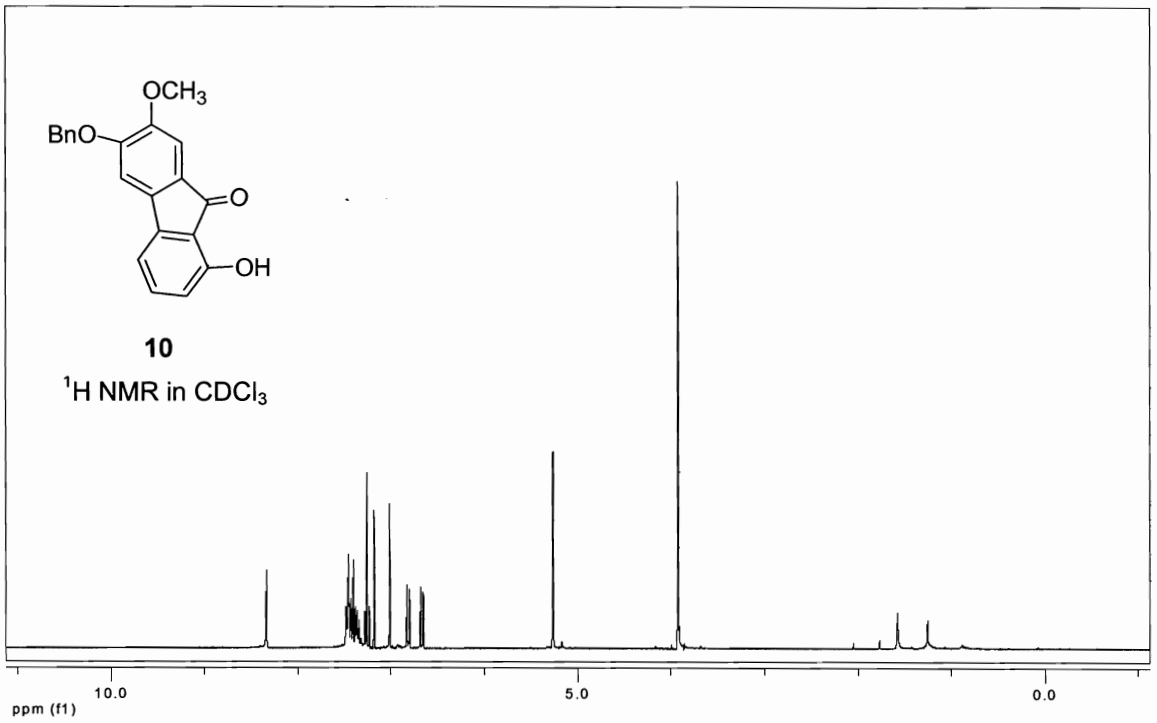
OCH3
BnO
O
OH
10
1H NMR in CDCl3
10.0
5.0
0.0
ppm (f1)

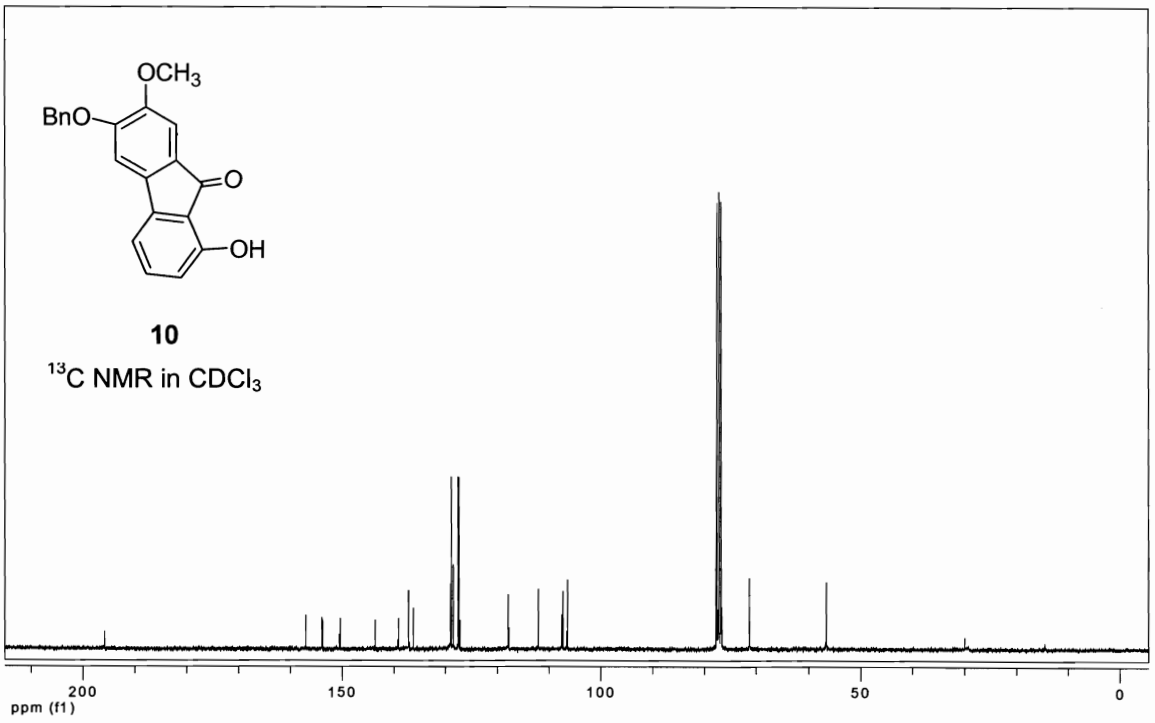
OCH3
BnO
O
OH
10
13C NMR in CDCl3
200
150
100
50
0
ppm (f1)

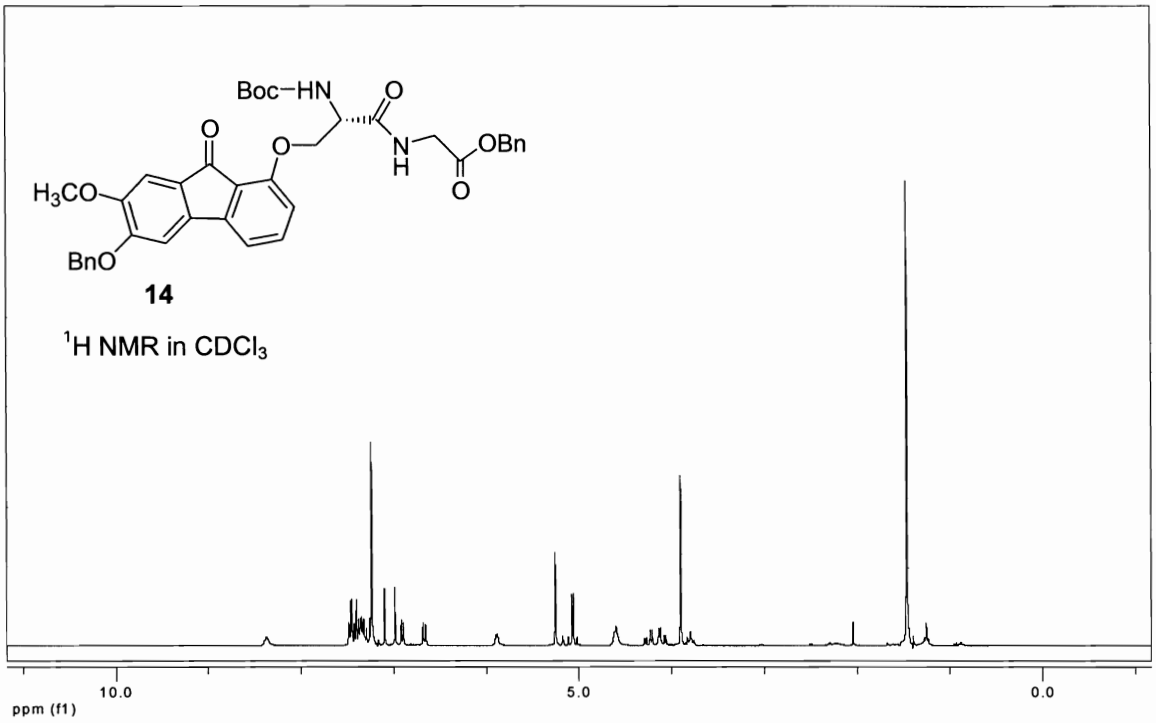
Boc–HN
O
O
O
N
H
OBn
O
H3CO
BnO
14
1H NMR in CDCl3
10.0
5.0
0.0
ppm (f1)

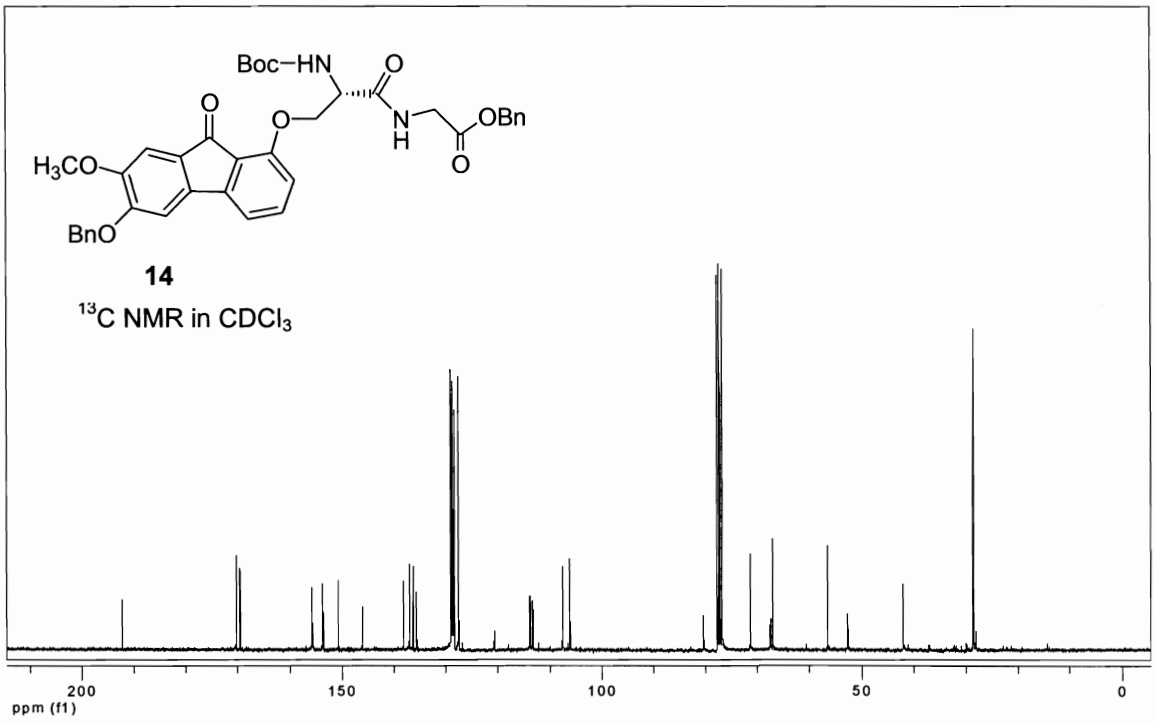
Boc–HN
O
O
O
N
H
OBn
O
H3CO
BnO
14
13C NMR in CDCl3
200
150
100
50
0
ppm (f1)

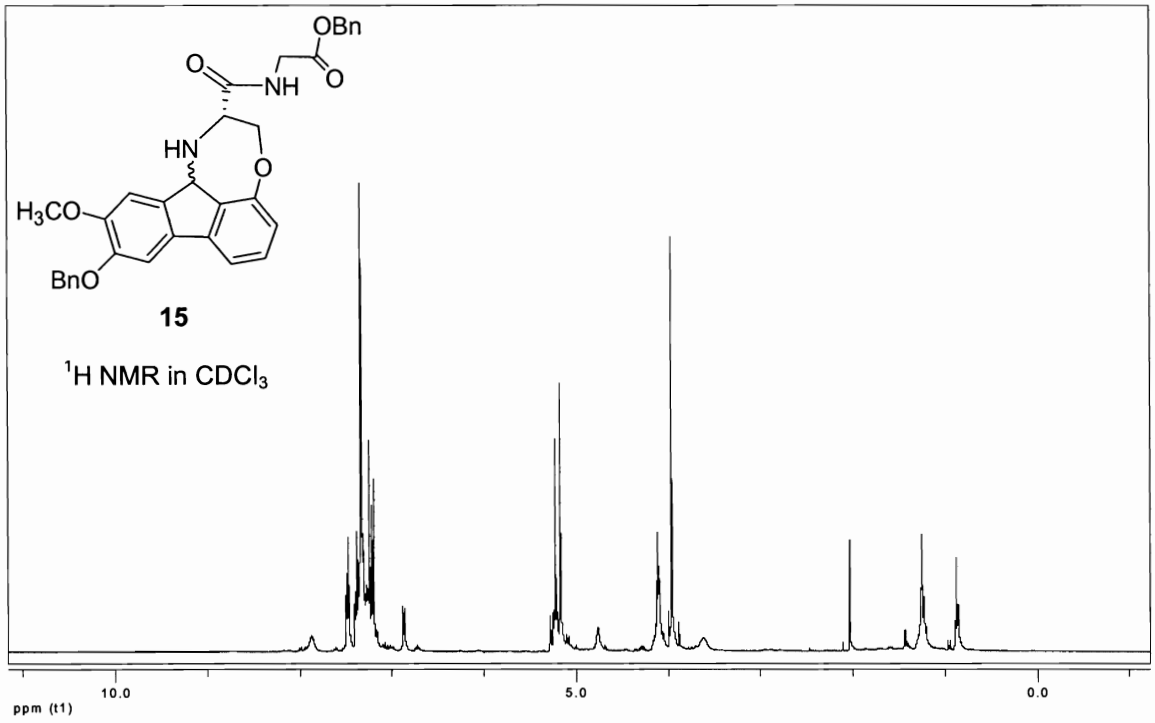

15

^{1}H NMR in $CDCl_3$

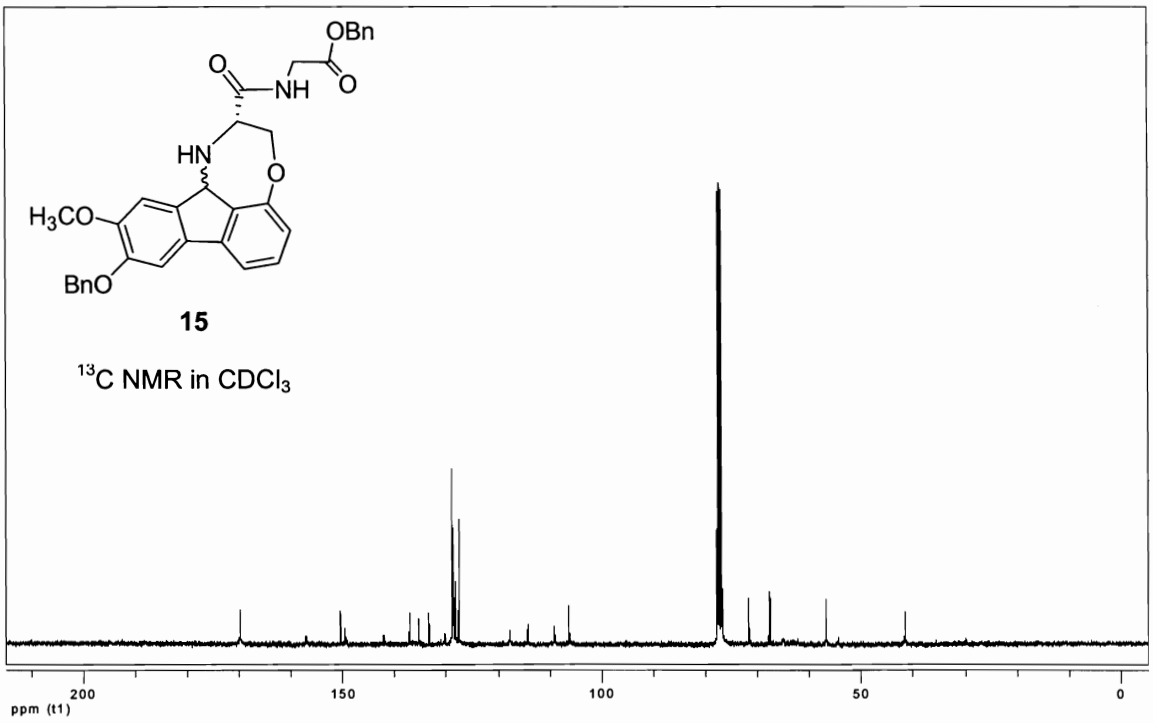

15

^{13}C NMR in $CDCl_3$

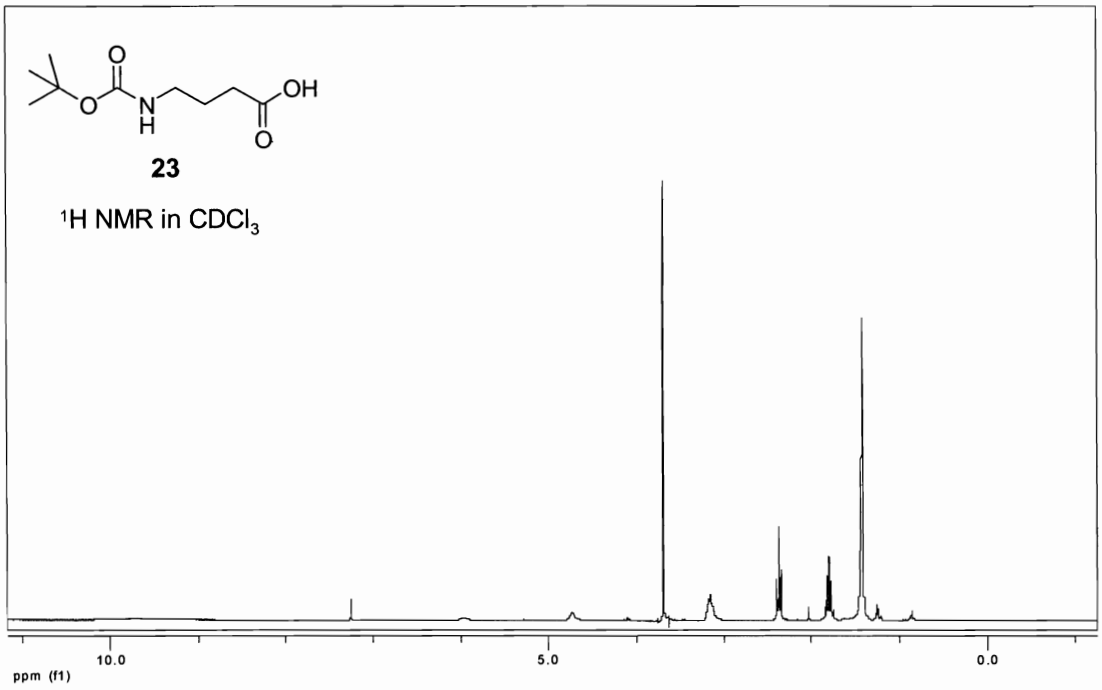

23

^{1}H NMR in $CDCl_3$

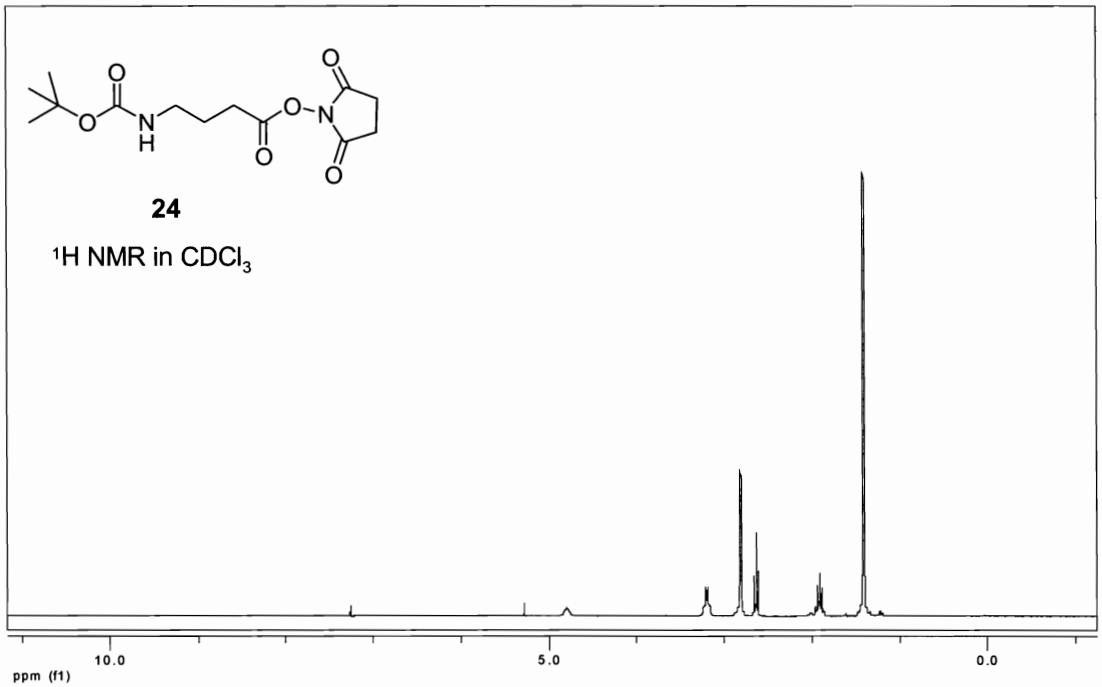

24

^{1}H NMR in $CDCl_3$

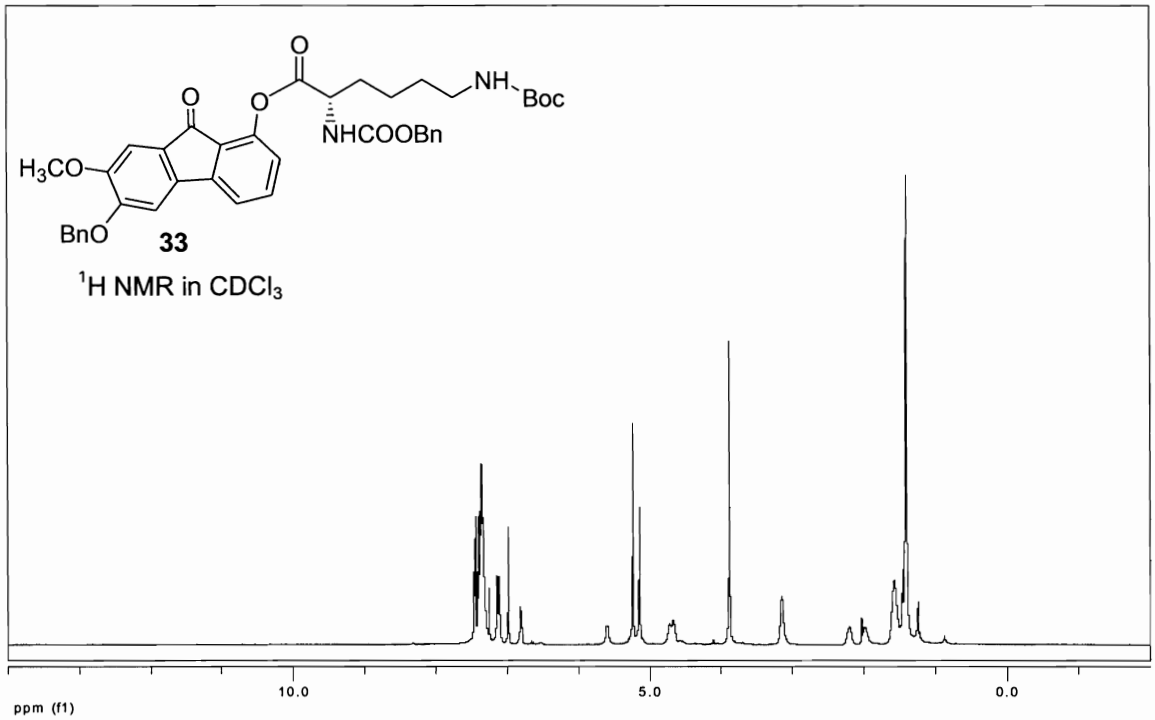
O
O
O
NH
Boc
NHCOOBn
H3CO
BnO
33
1H NMR in CDCl3
10.0
5.0
0.0
ppm (f1)

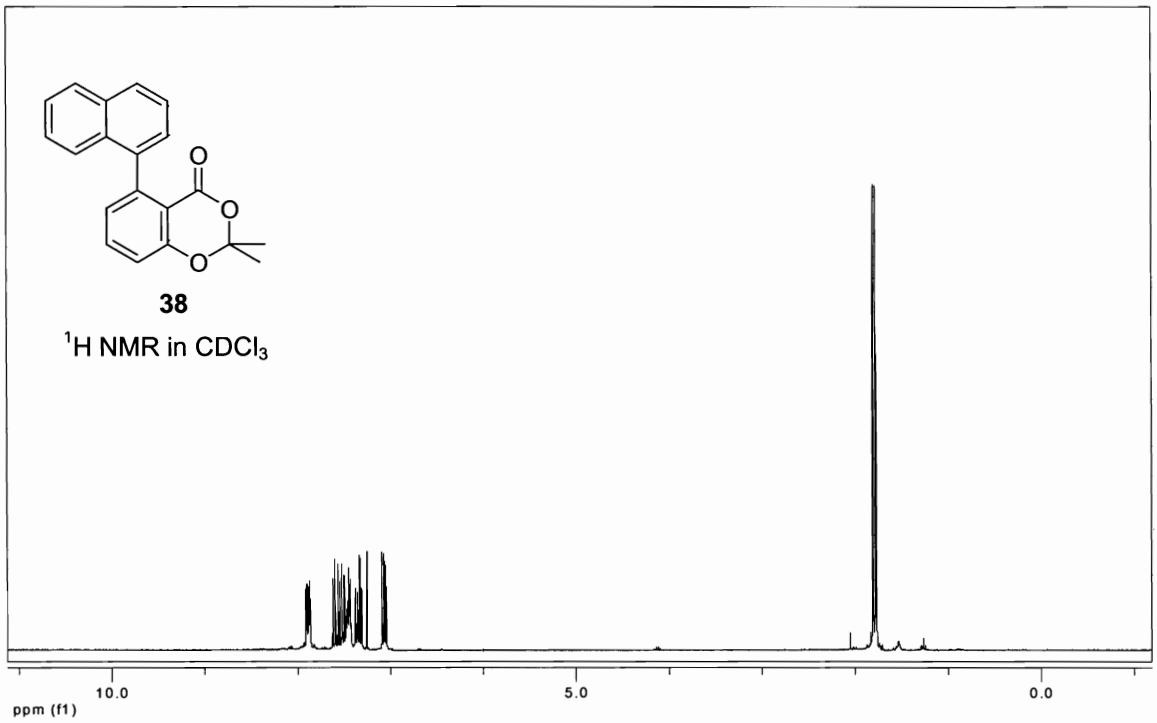

38

^{1}H NMR in $CDCl_3$

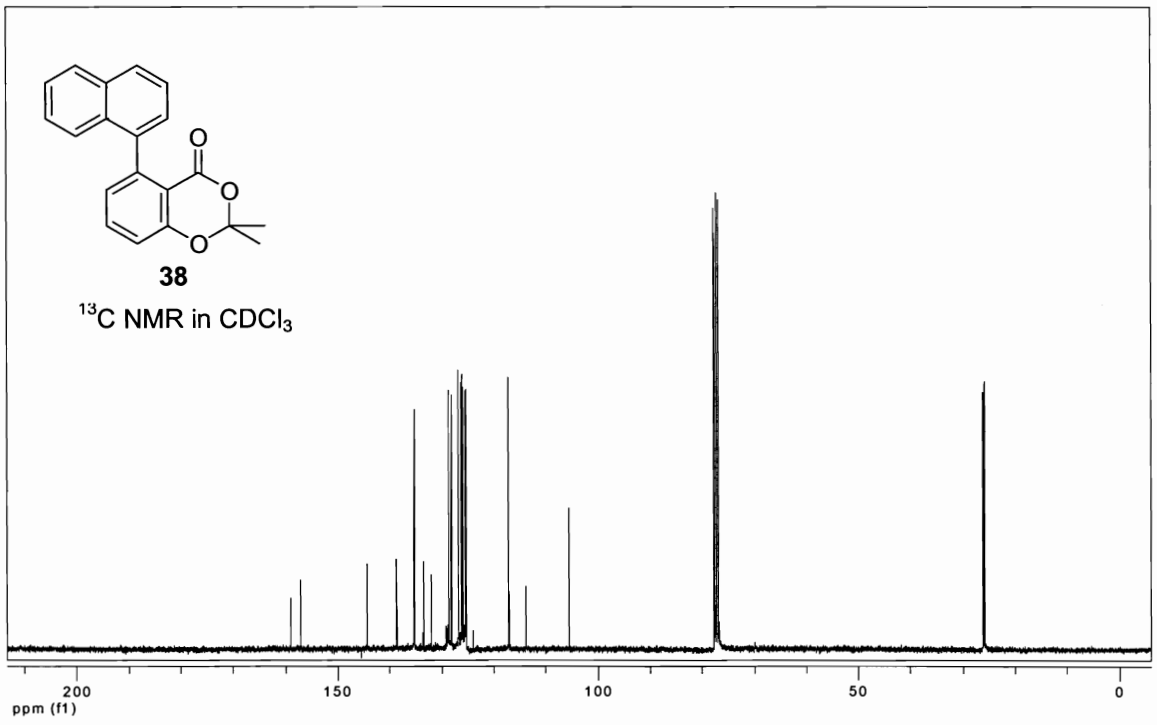

38

^{13}C NMR in $CDCl_3$

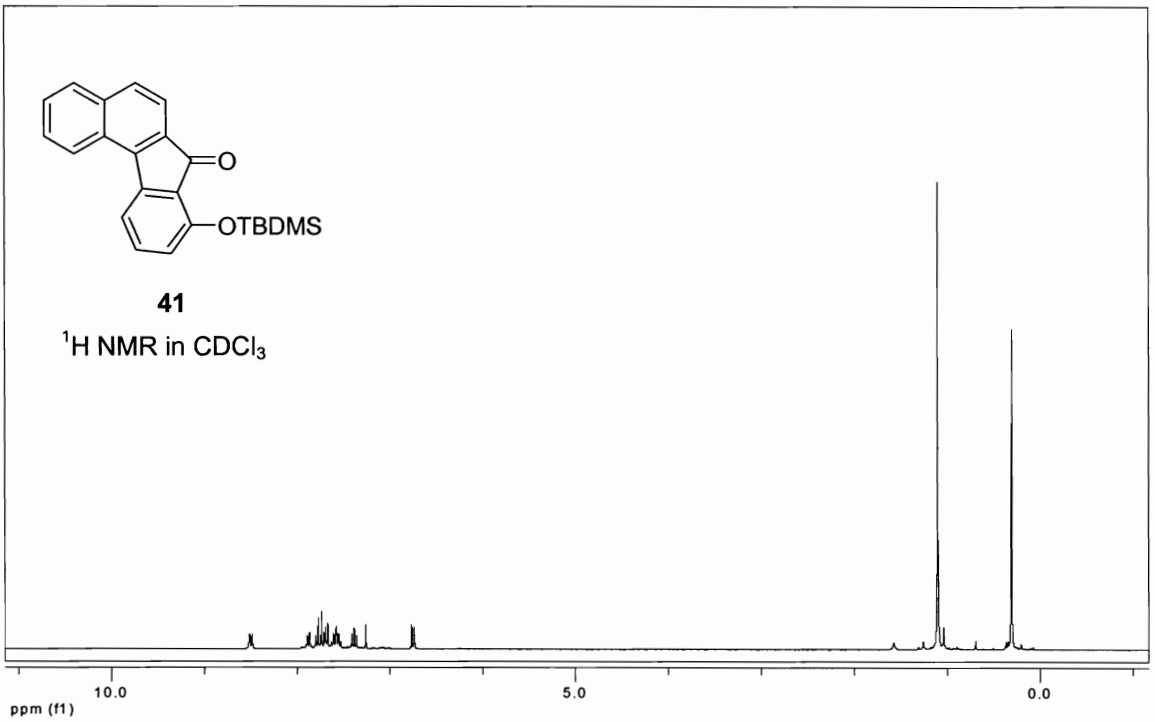

41

^{1}H NMR in $CDCl_3$

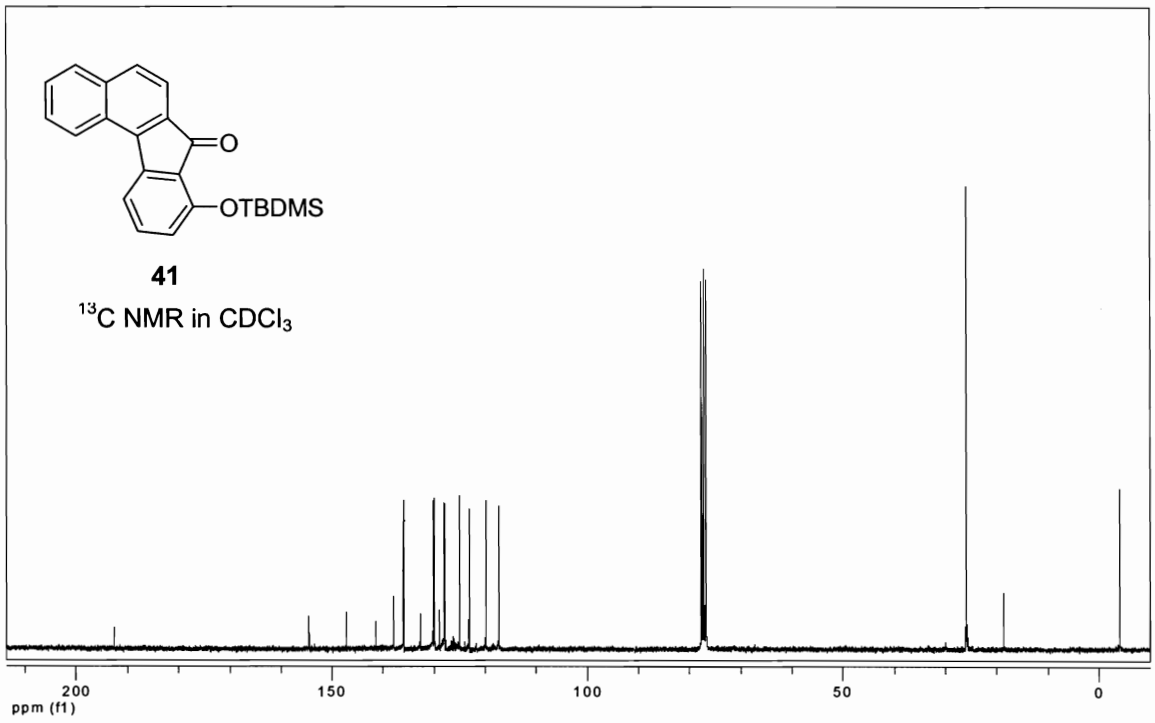

41

^{13}C NMR in $CDCl_3$

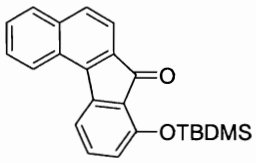

41

COSY in $CDCl_3$

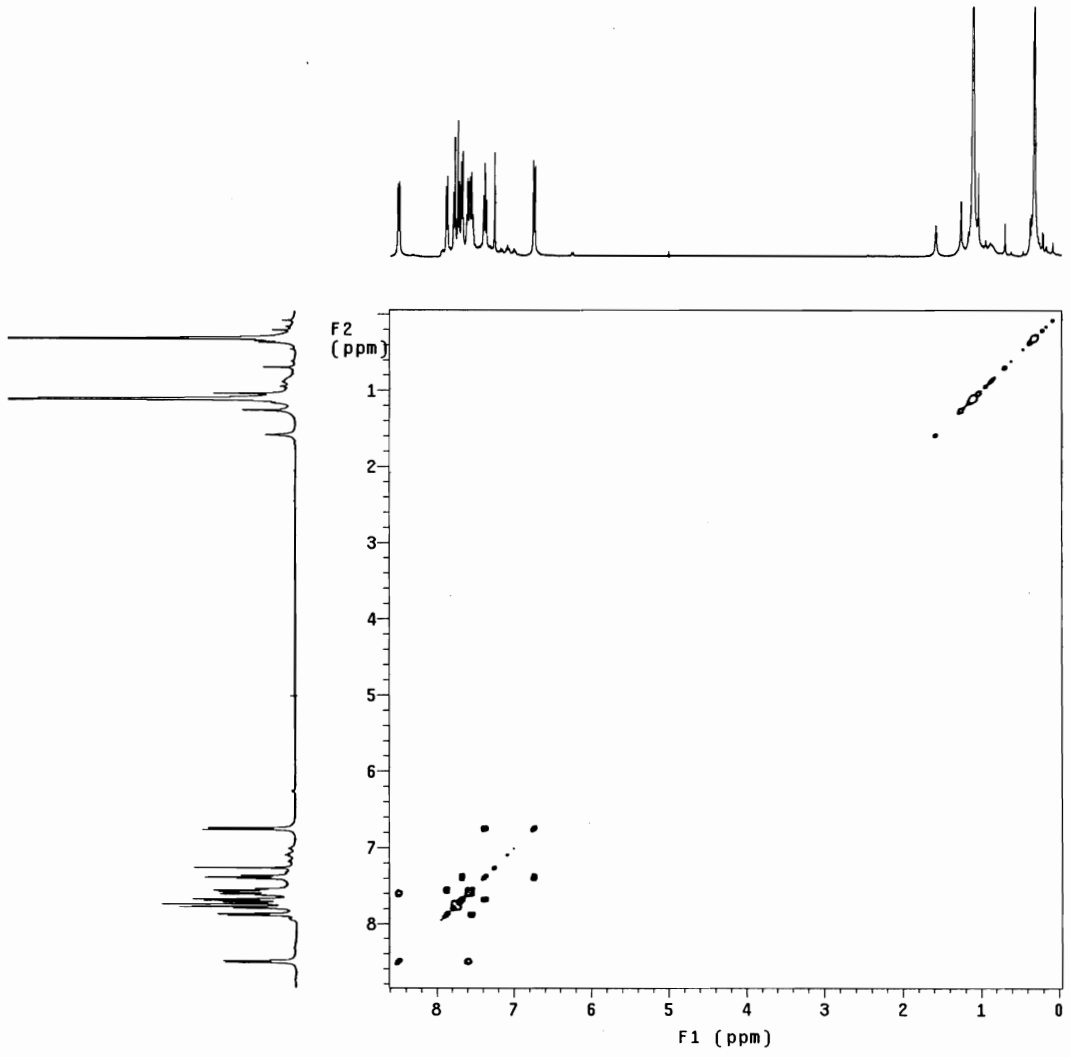

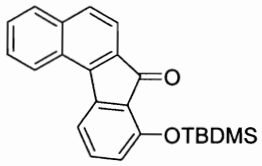

41

COSY in $CDCl_3$ (expanded)

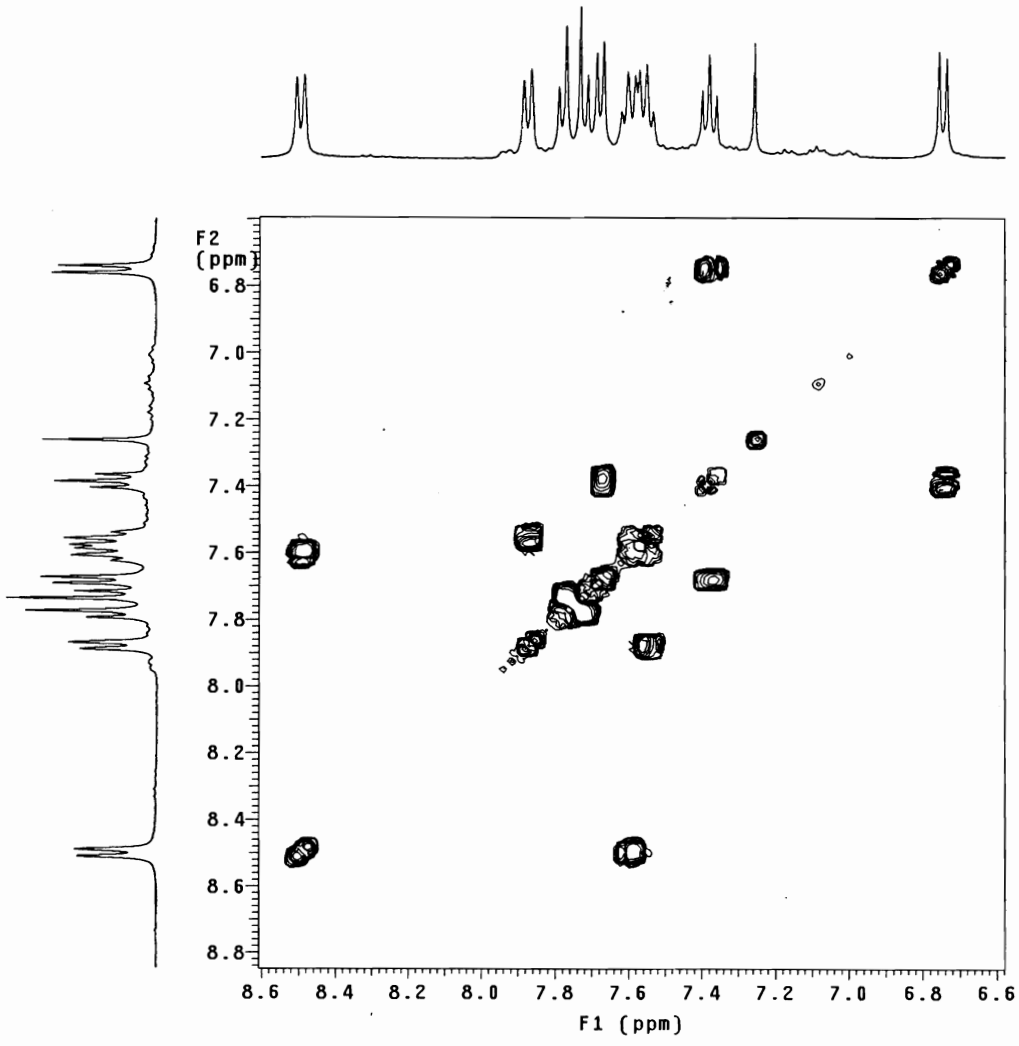

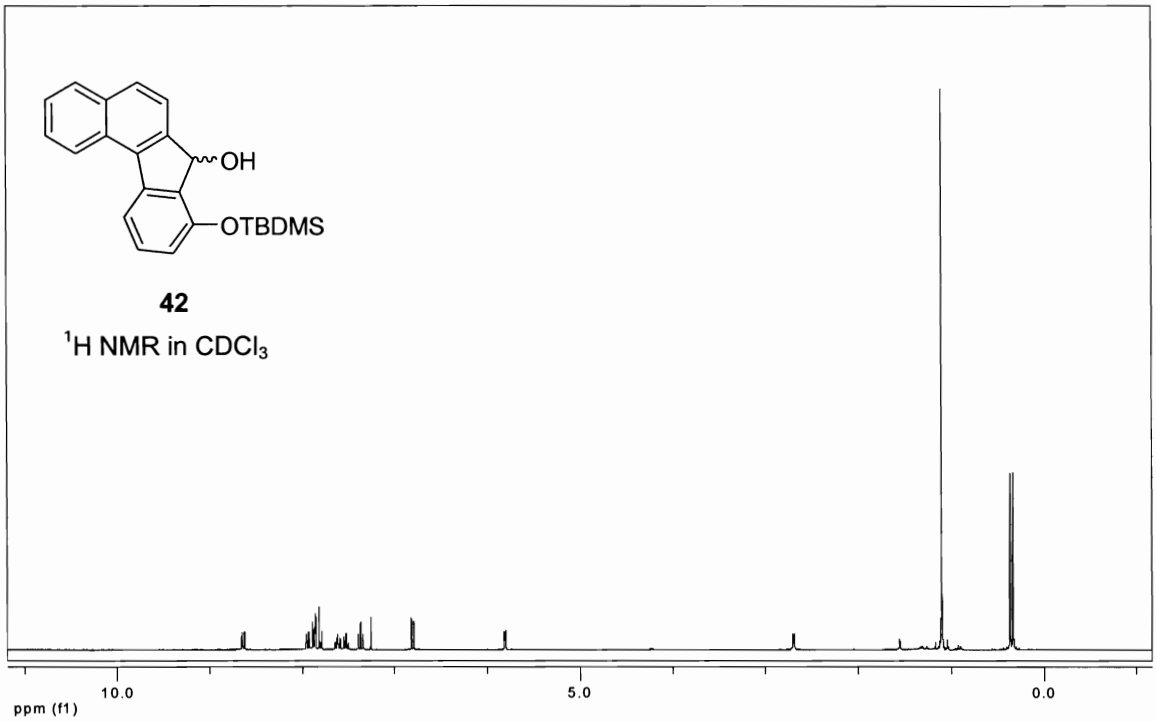
OH
OTBDMS
42
^{1}H NMR in $CDCl_3$
10.0
5.0
0.0
ppm (f1)

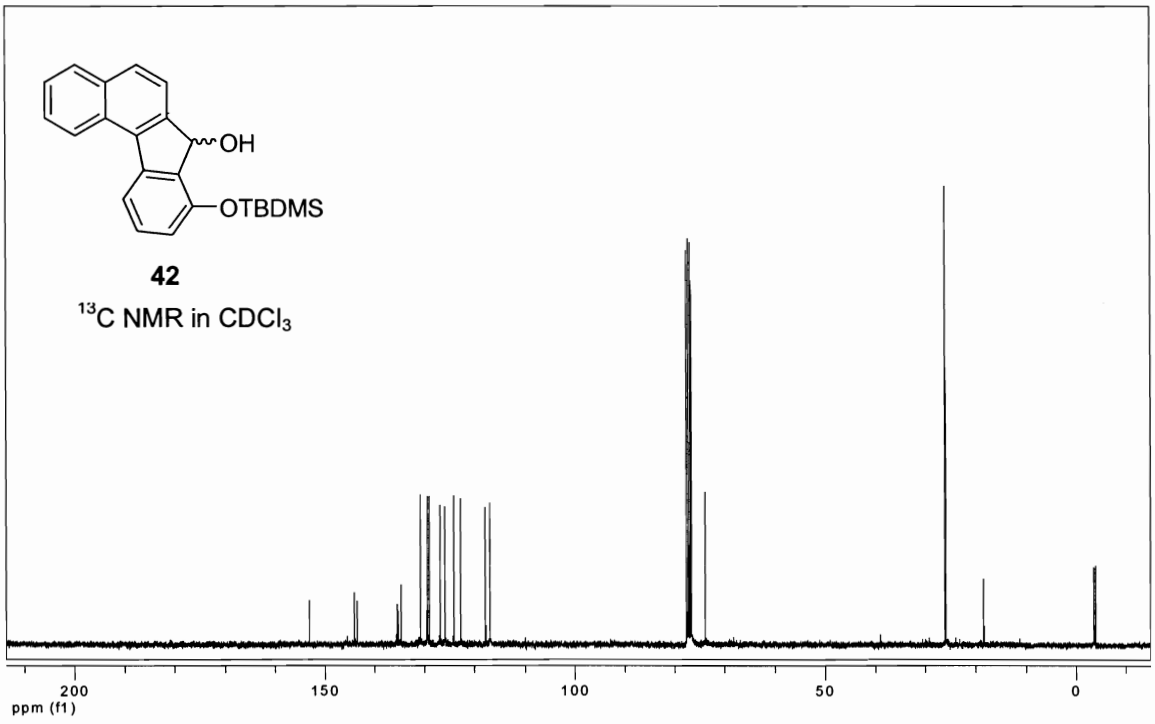
OH
OTBDMS
42
^{13}C NMR in $CDCl_3$
200
150
100
50
0
ppm (f1)

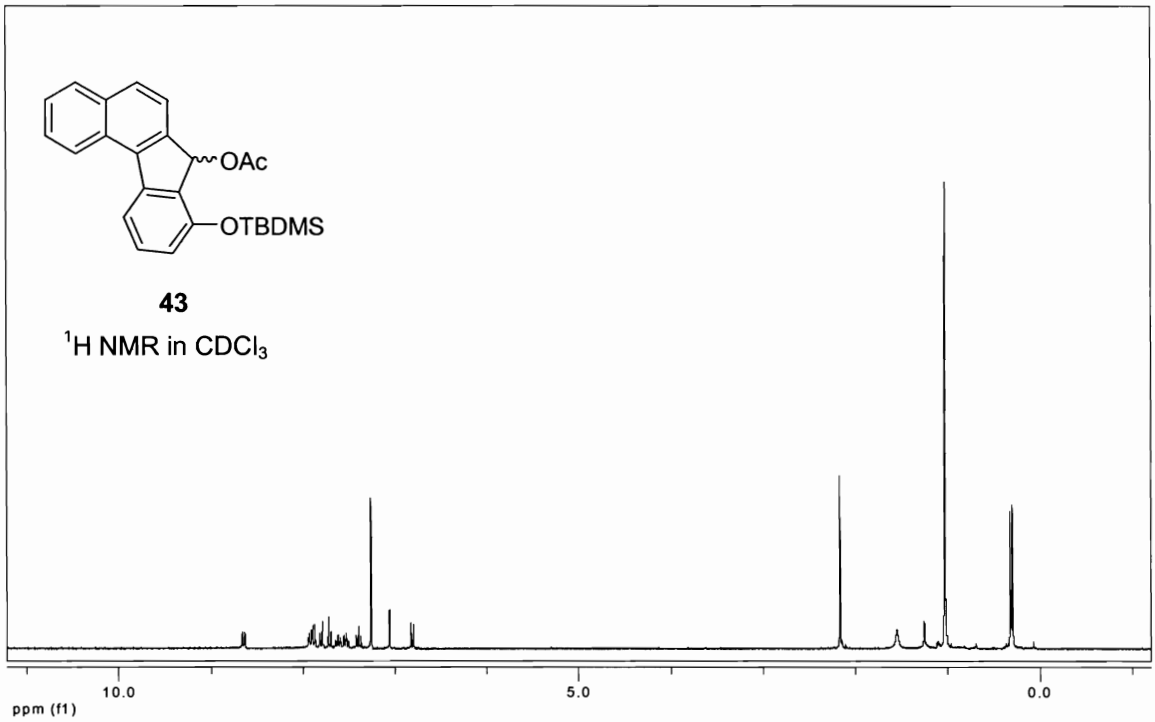

43

^{1}H NMR in $CDCl_3$

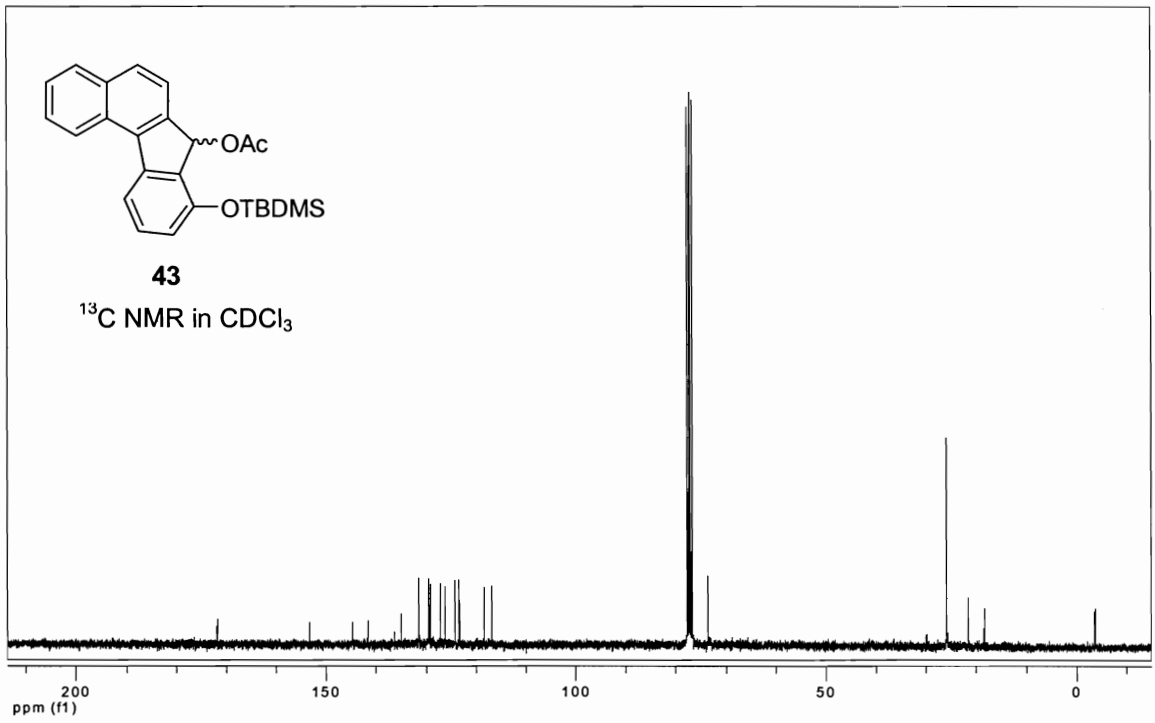

43

^{13}C NMR in $CDCl_3$

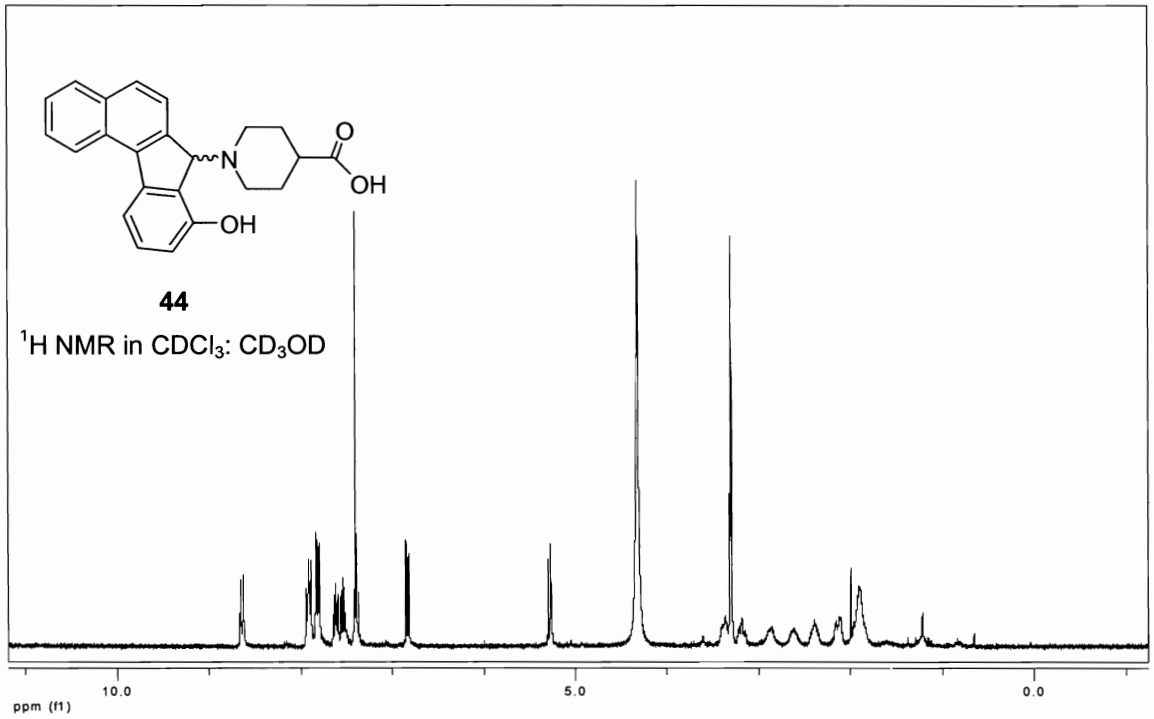

44

^{1}H NMR in $CDCl_3$: CD_3OD

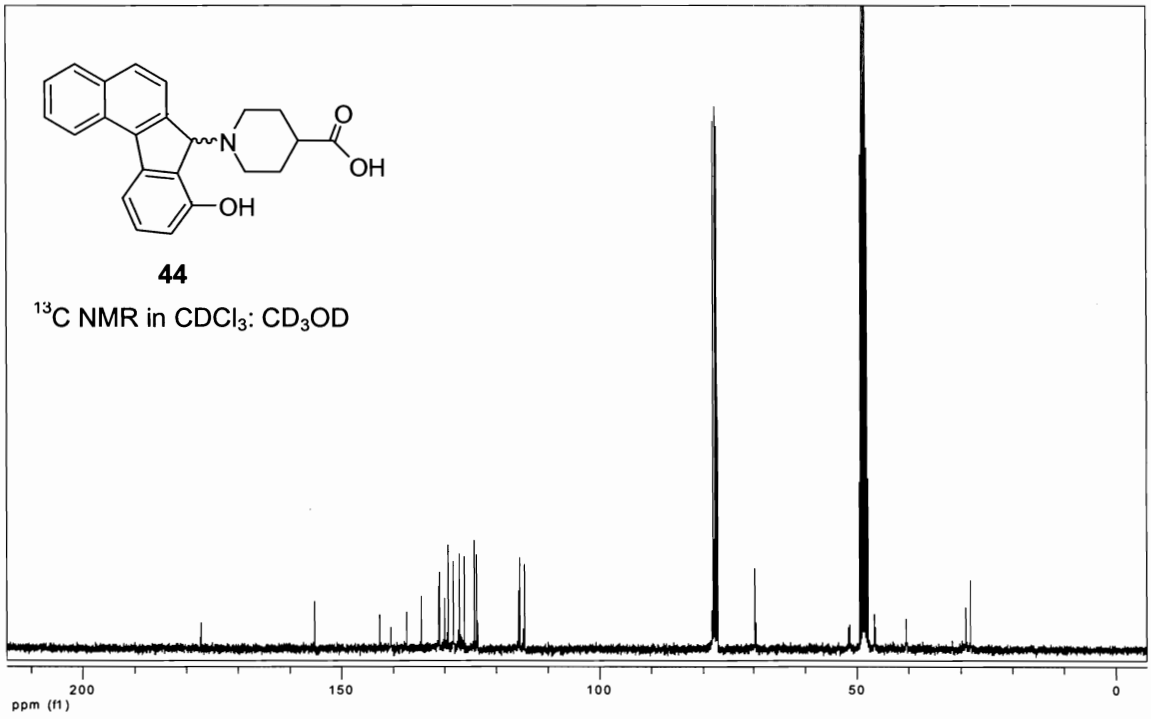

44

^{13}C NMR in $CDCl_3$: CD_3OD

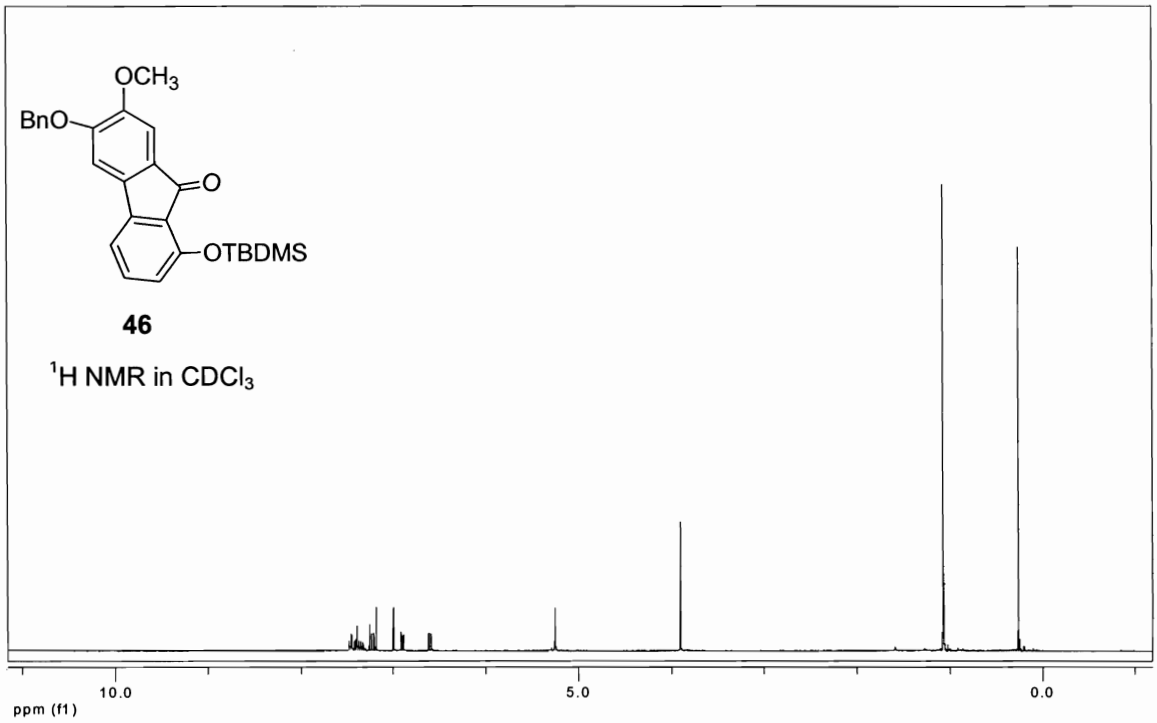
OCH3
BnO
O
OTBDMS
46
1H NMR in CDCl3
10.0
5.0
0.0
ppm (f1)

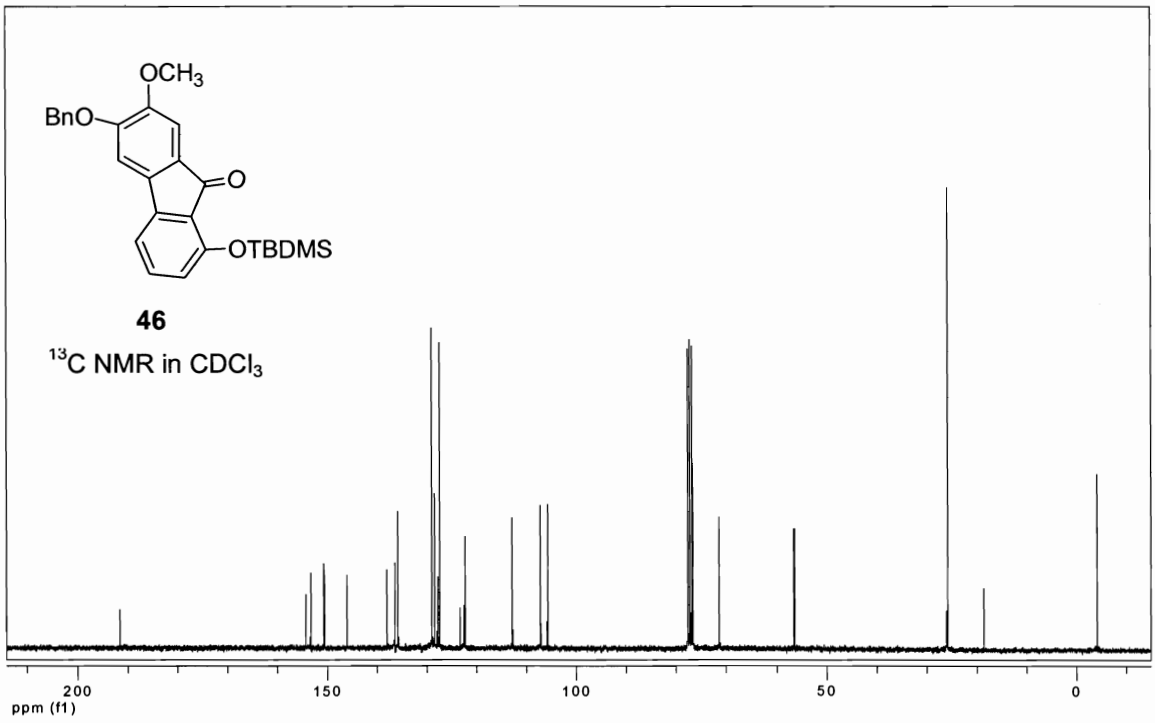
OCH3
BnO
O
OTBDMS
46
13C NMR in CDCl3
200
150
100
50
0
ppm (f1)

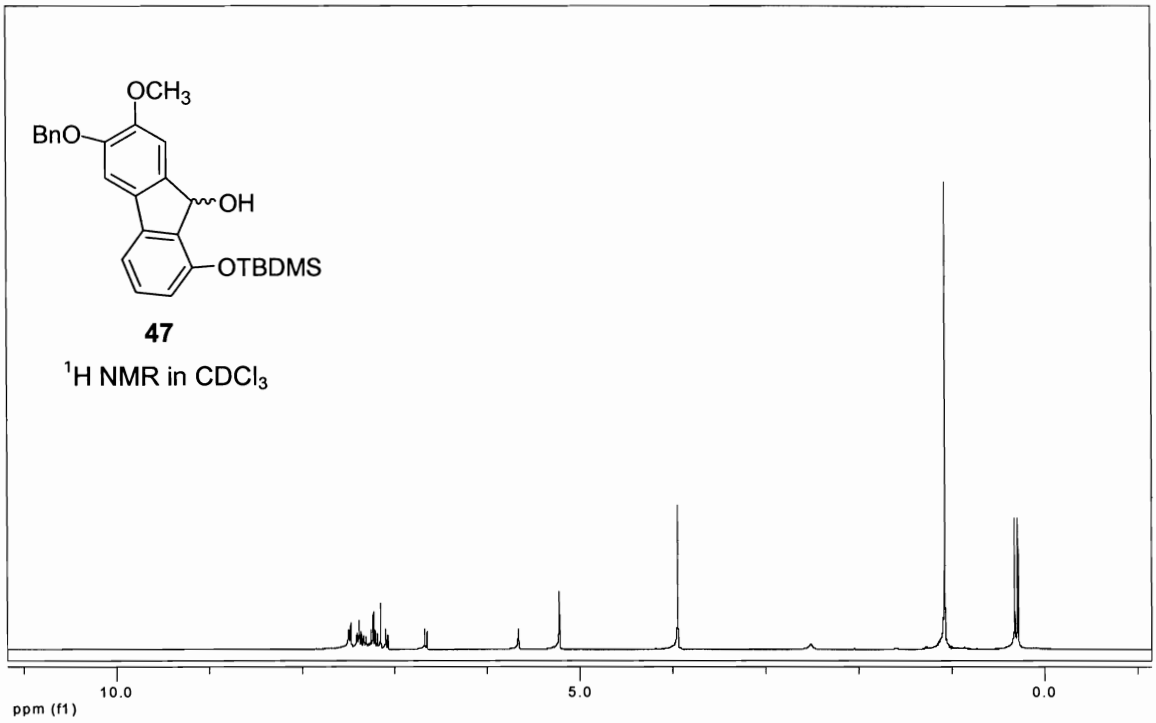
OCH3
BnO
OH
OTBDMS
47
1H NMR in CDCl3
10.0
5.0
0.0
ppm (f1)

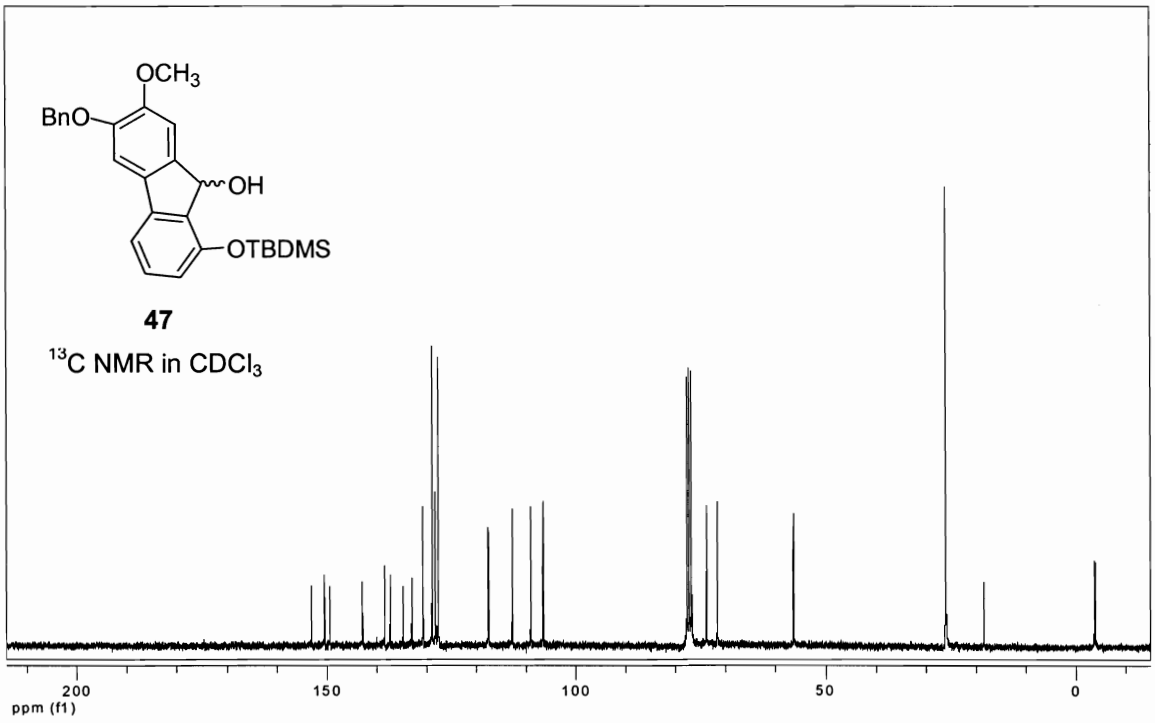
OCH3
BnO
OH
OTBDMS
47
13C NMR in CDCl3
200
150
100
50
0
ppm (f1)

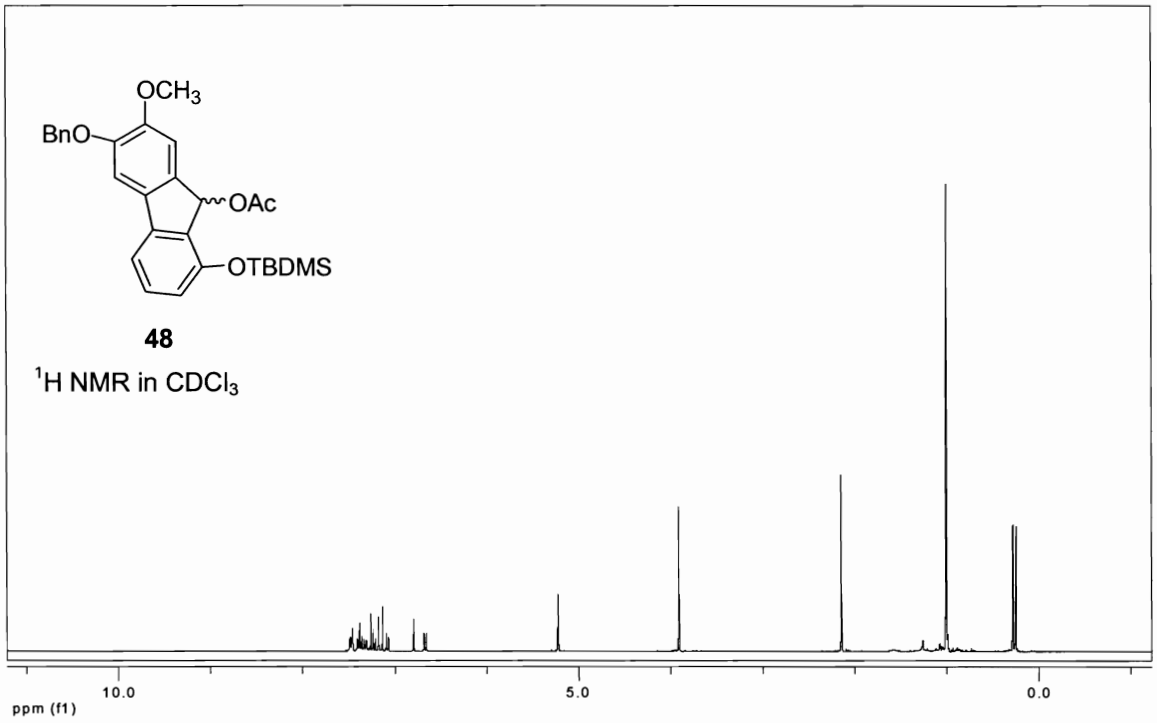
OCH3
BnO
OAc
OTBDMS
48
1H NMR in CDCl3
10.0
5.0
0.0
ppm (f1)

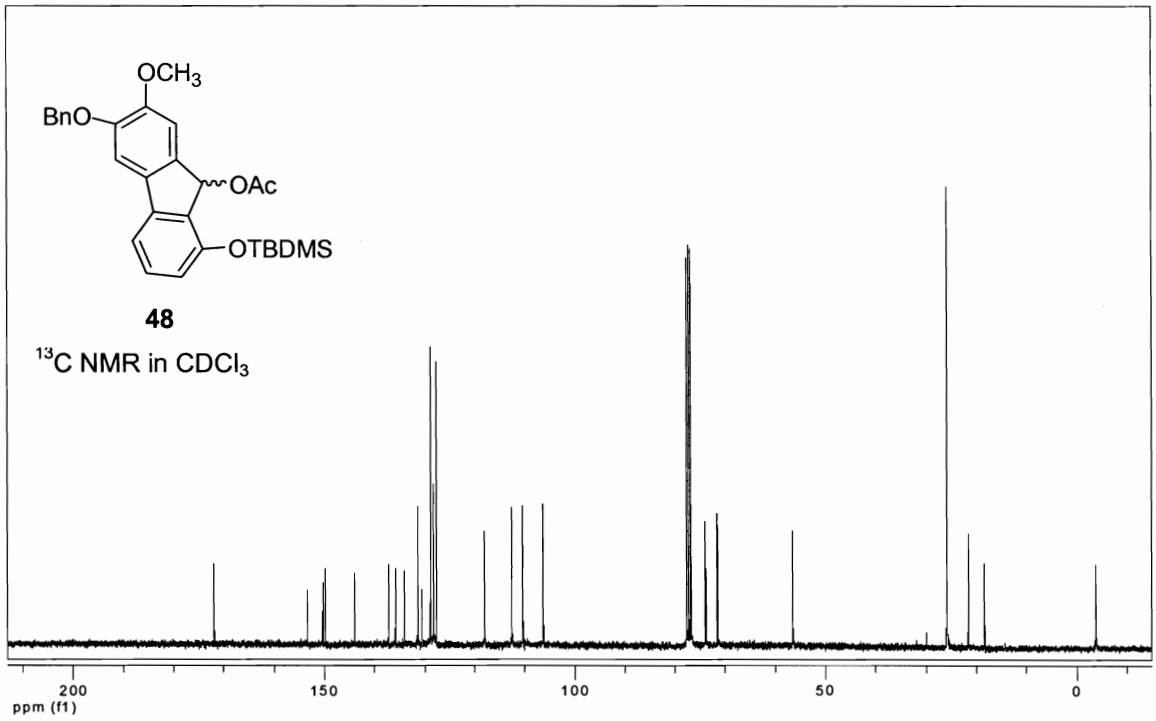
OCH3
BnO
OAc
OTBDMS
48
13C NMR in CDCl3
200
150
100
50
0
ppm (f1)

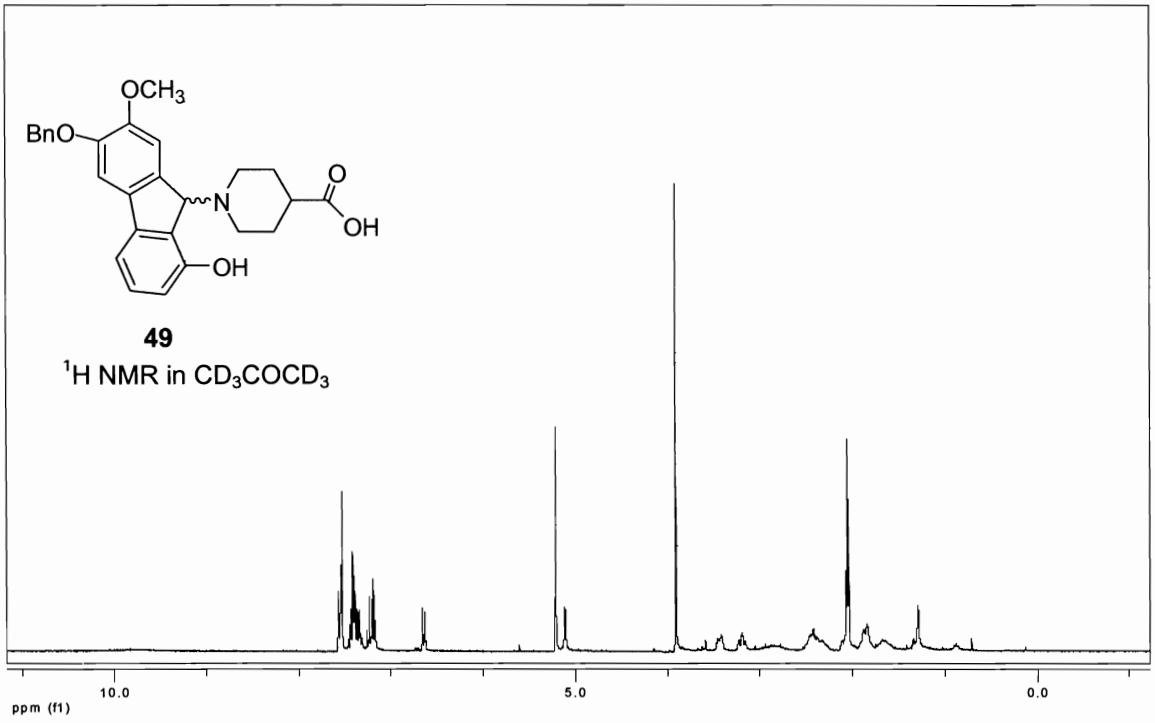

49

^{1}H NMR in CD_3COCD_3

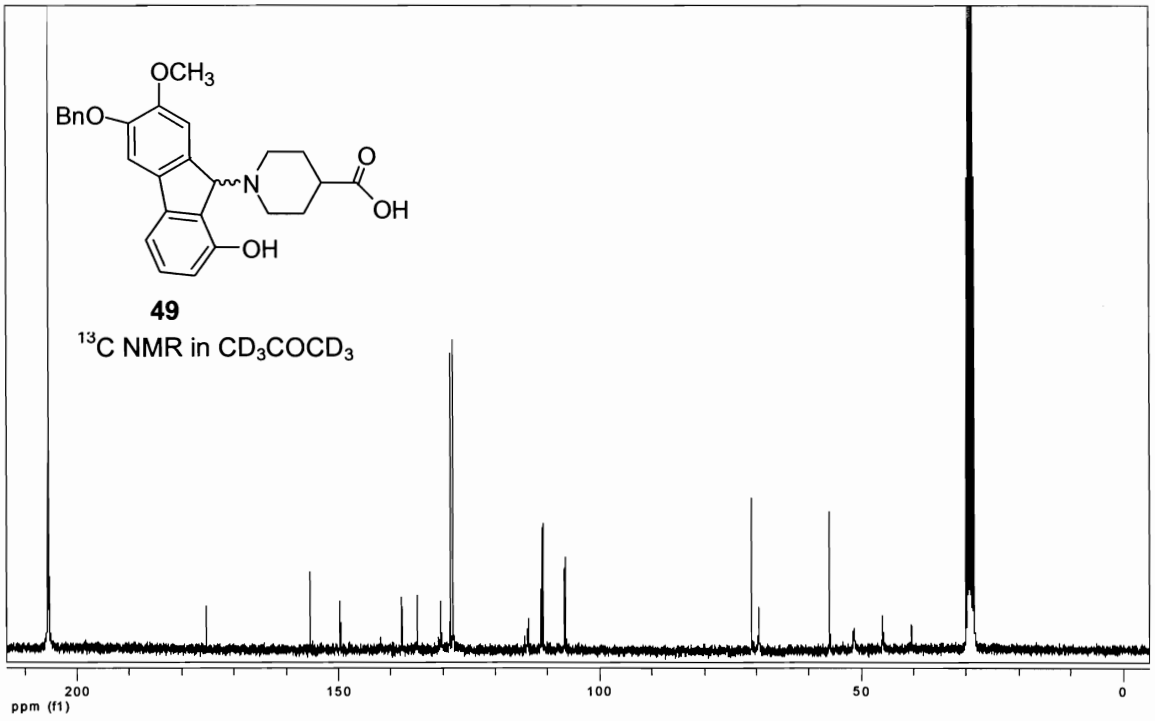

49

^{13}C NMR in CD_3COCD_3

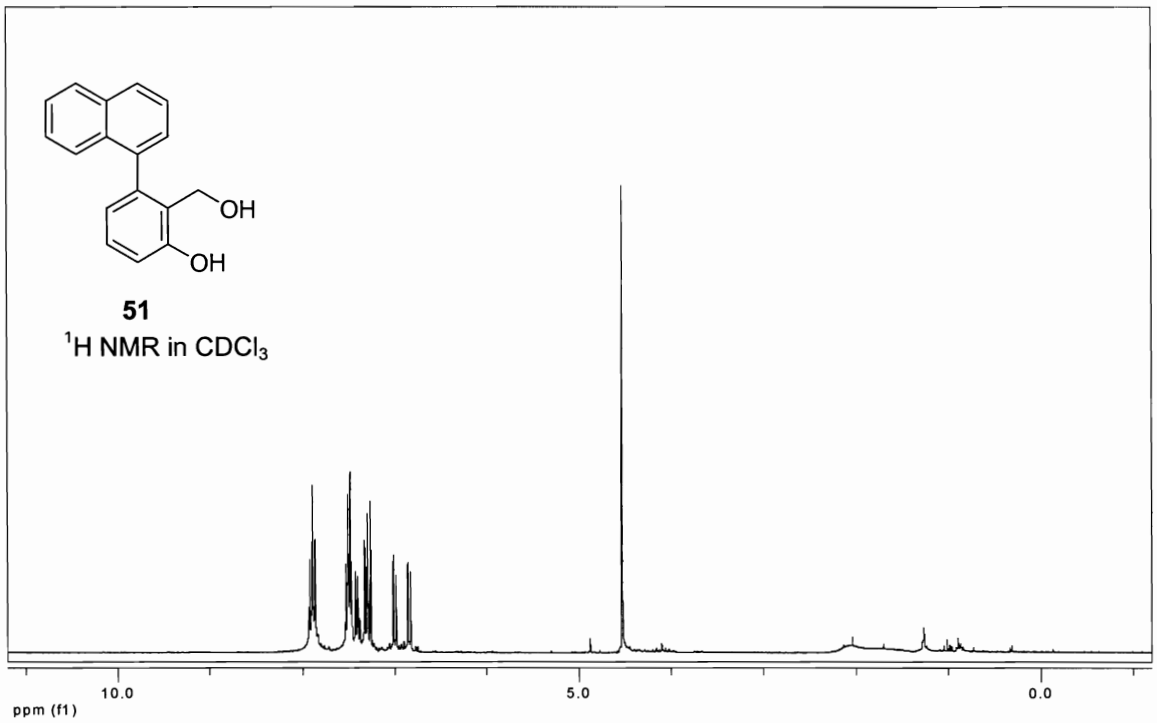

51

^{1}H NMR in $CDCl_3$

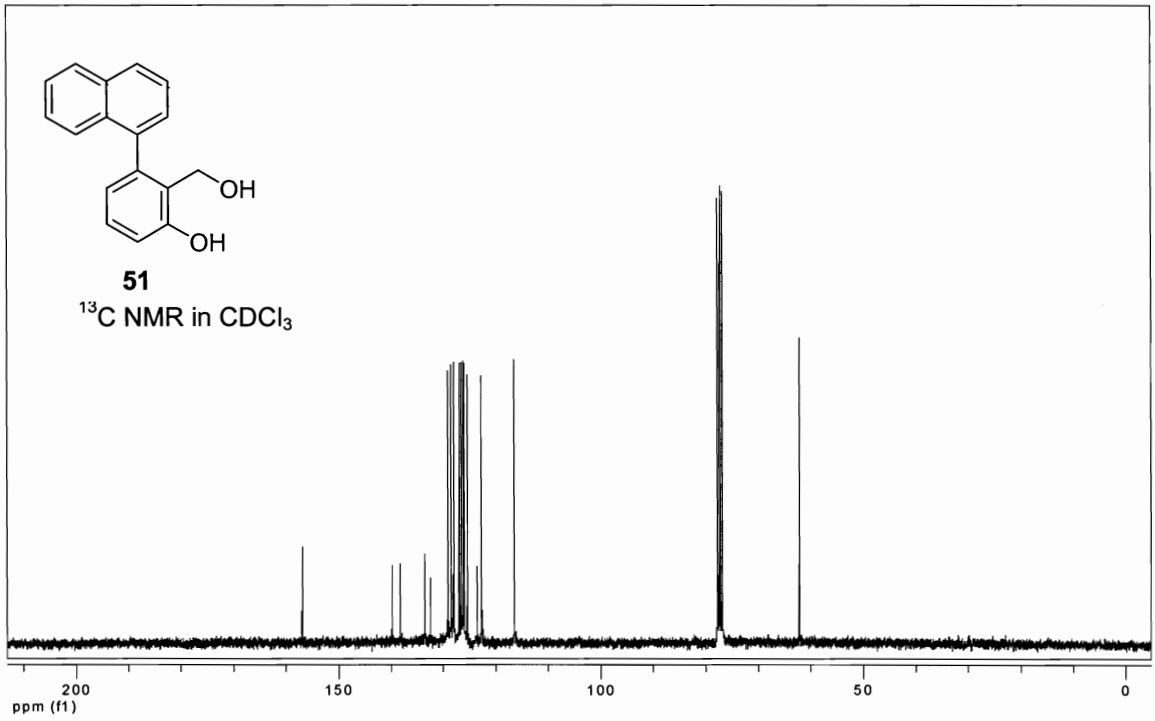

51

^{13}C NMR in $CDCl_3$

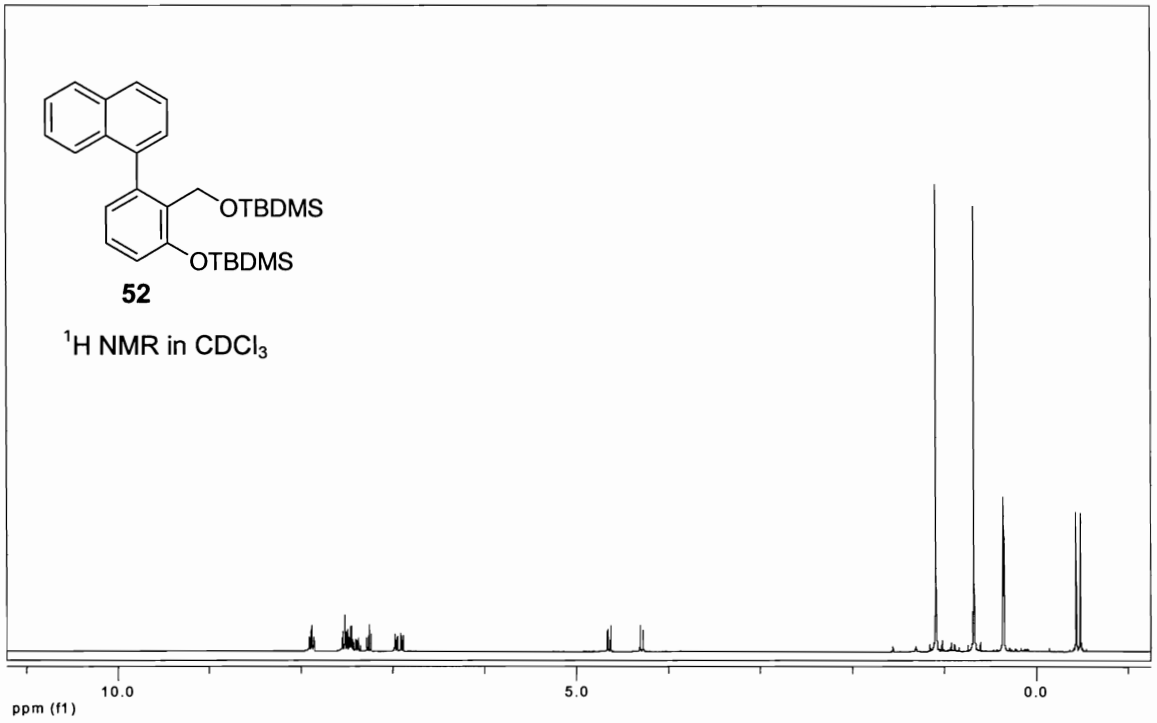
OTBDMS
OTBDMS
52
^{1}H NMR in $CDCl_3$
10.0
5.0
0.0
ppm (f1)

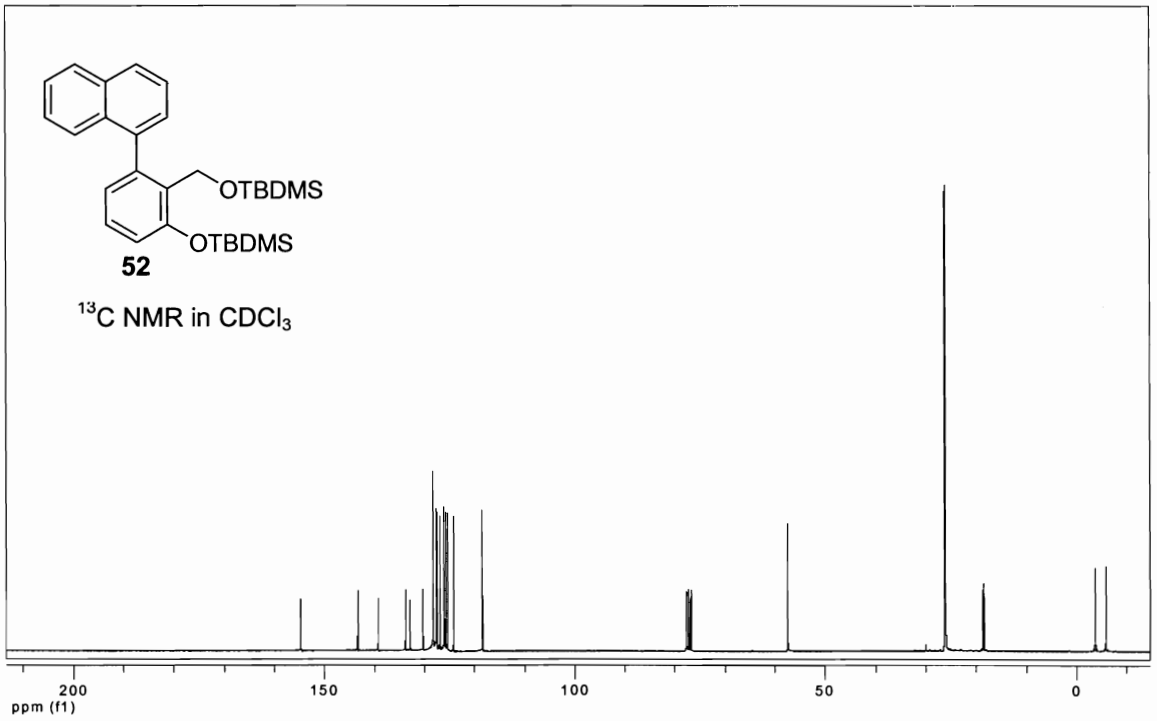
OTBDMS
OTBDMS
52
^{13}C NMR in $CDCl_3$
200
150
100
50
0
ppm (f1)

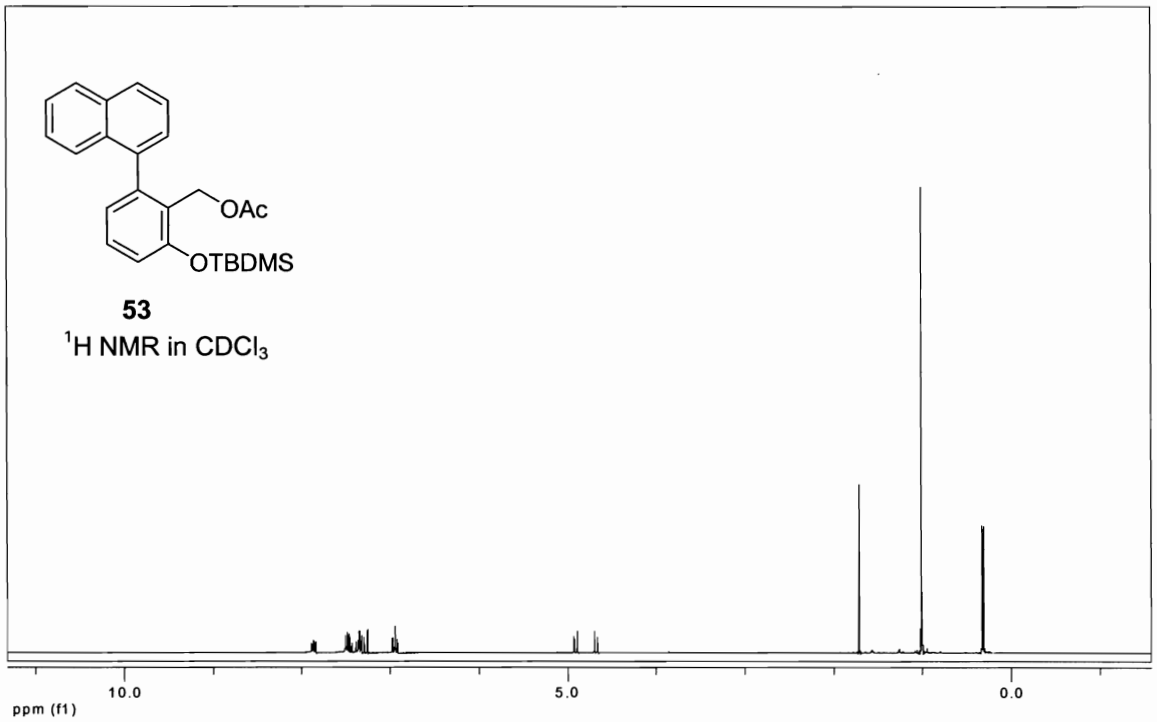

53

^{1}H NMR in $CDCl_3$

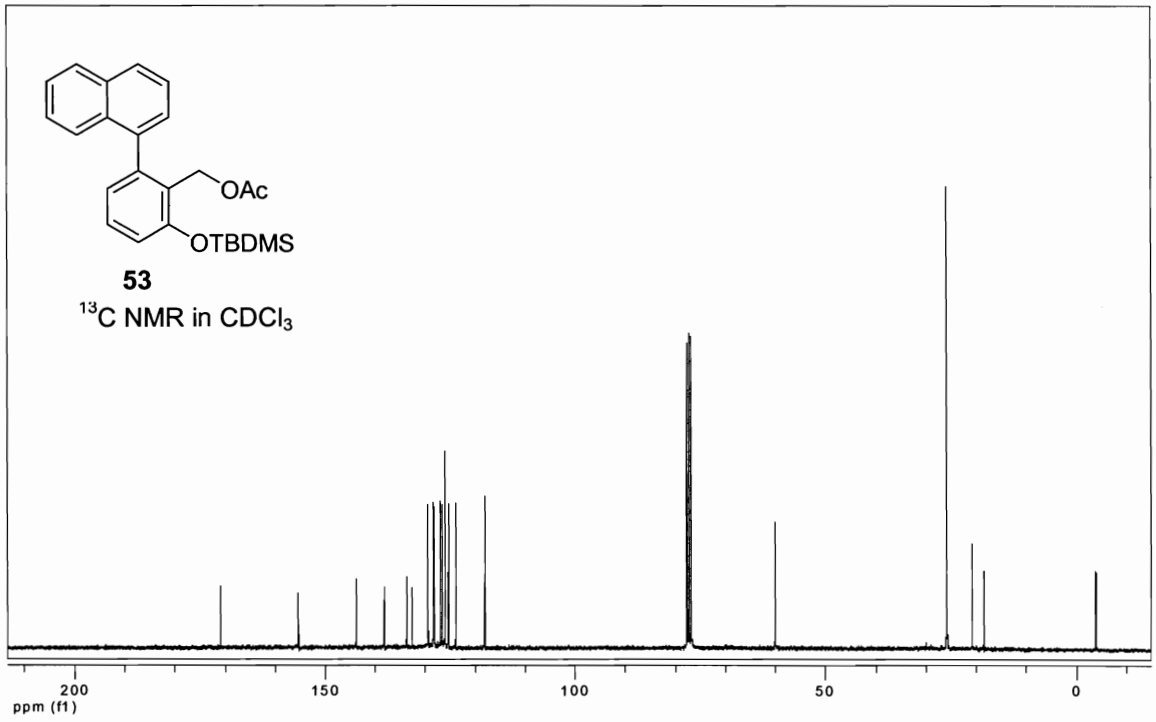

53

^{13}C NMR in $CDCl_3$

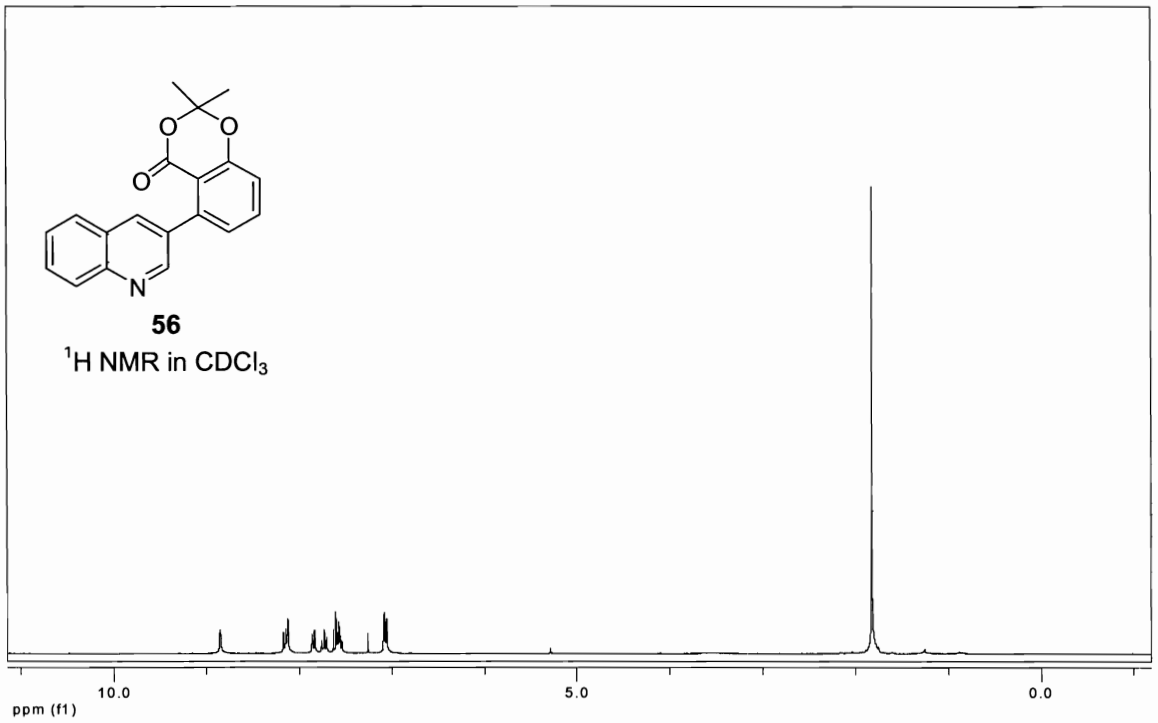

56

^{1}H NMR in $CDCl_3$

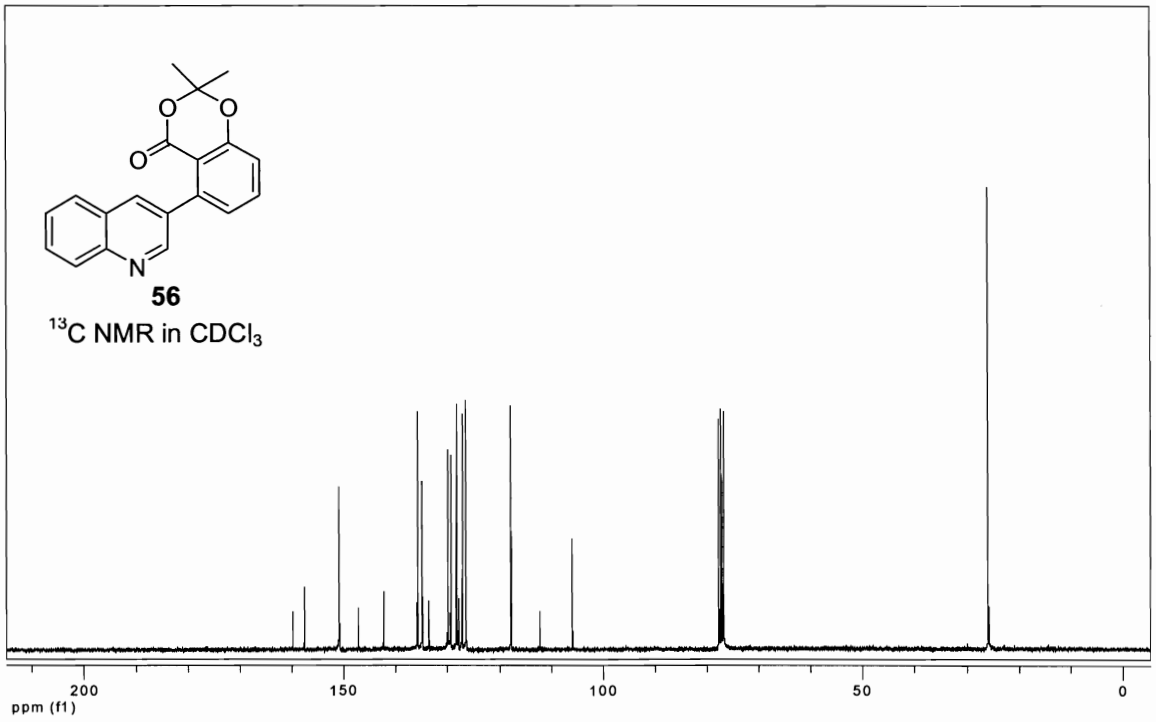

56

^{13}C NMR in $CDCl_3$

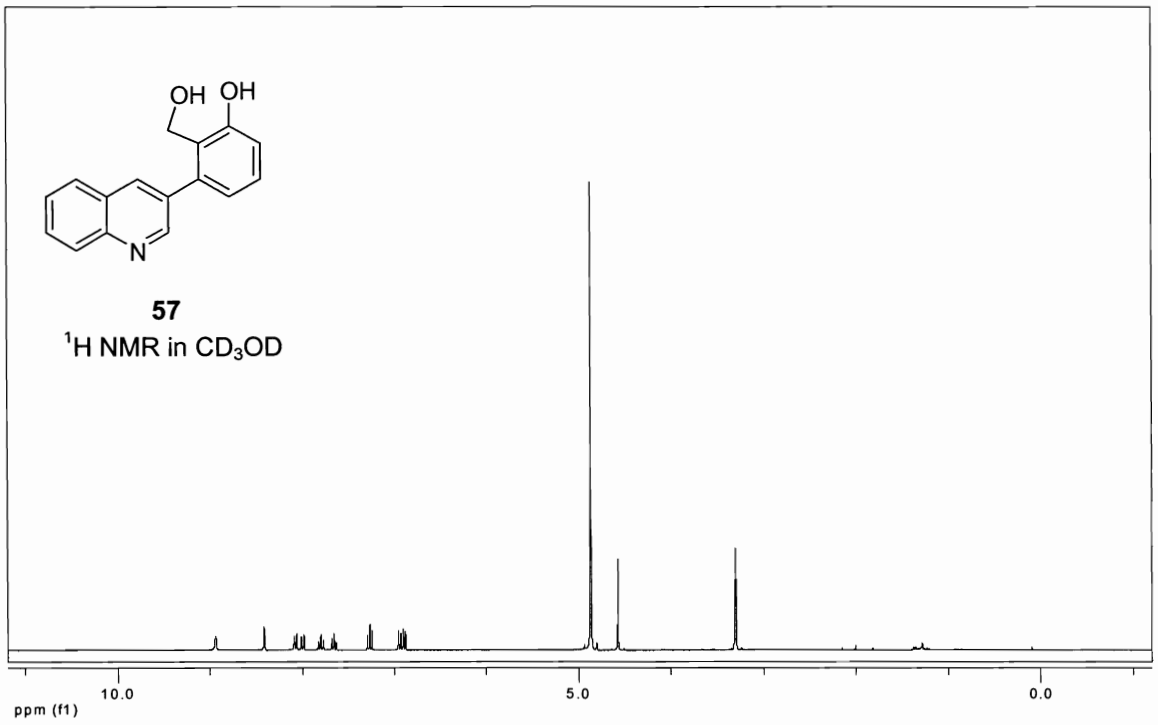

57

^{1}H NMR in CD_3OD

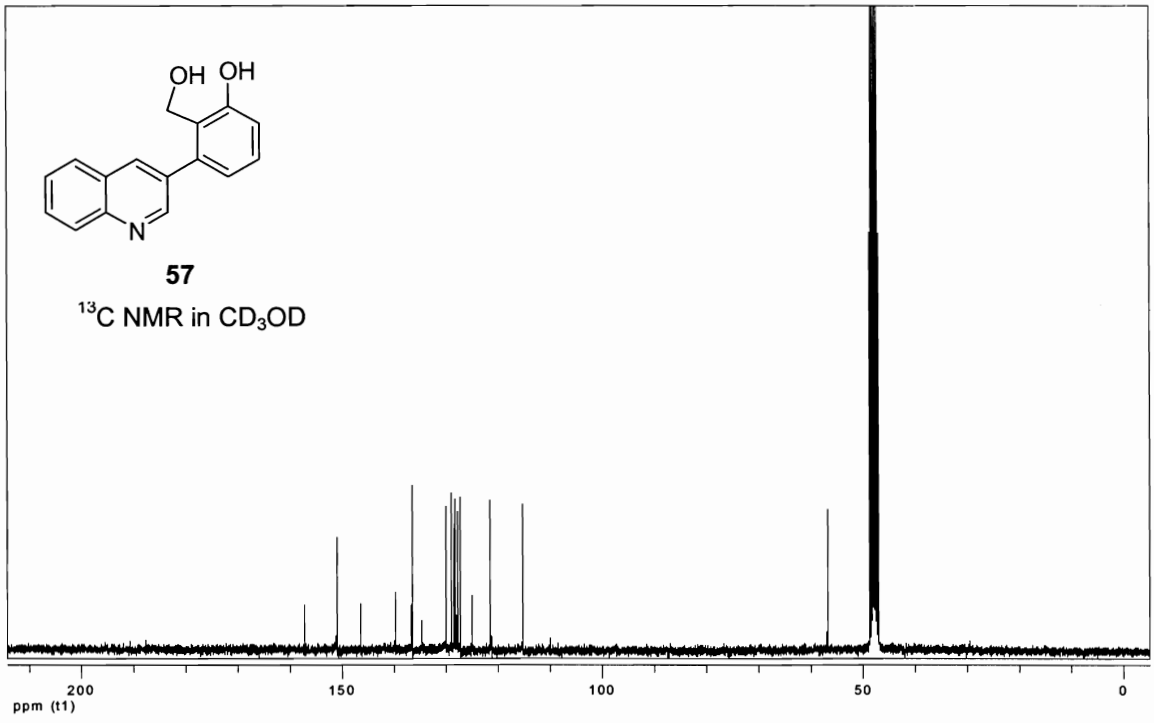

57

^{13}C NMR in CD_3OD

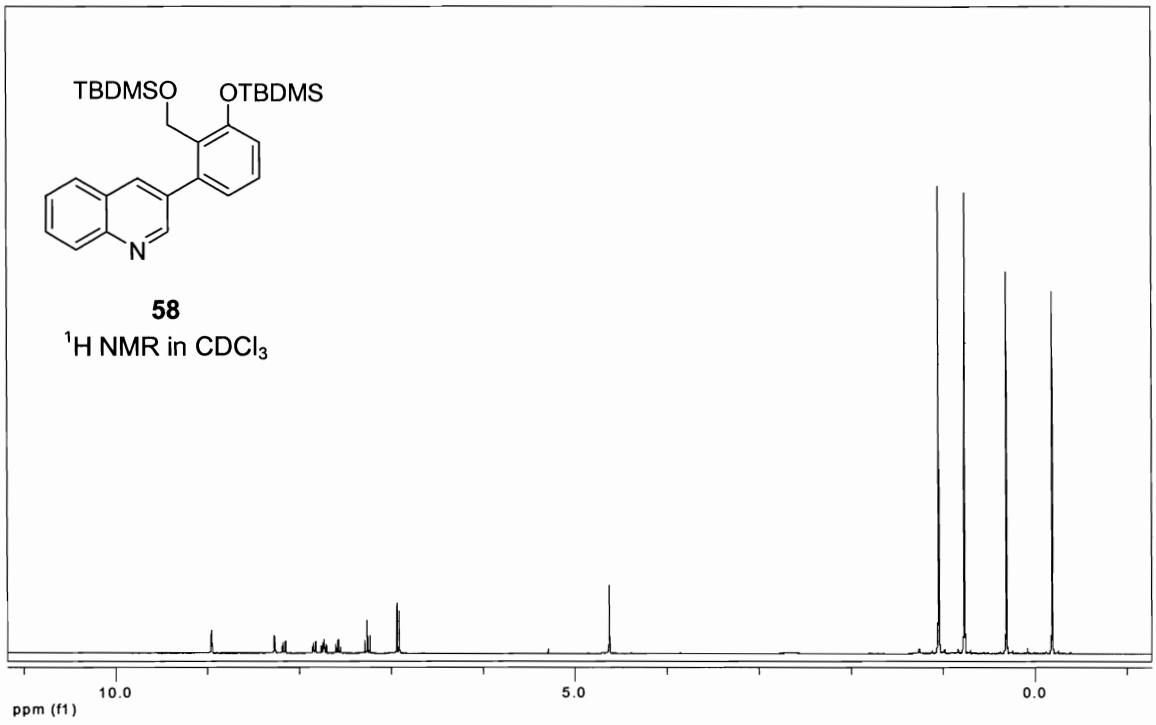

58

^{1}H NMR in $CDCl_3$

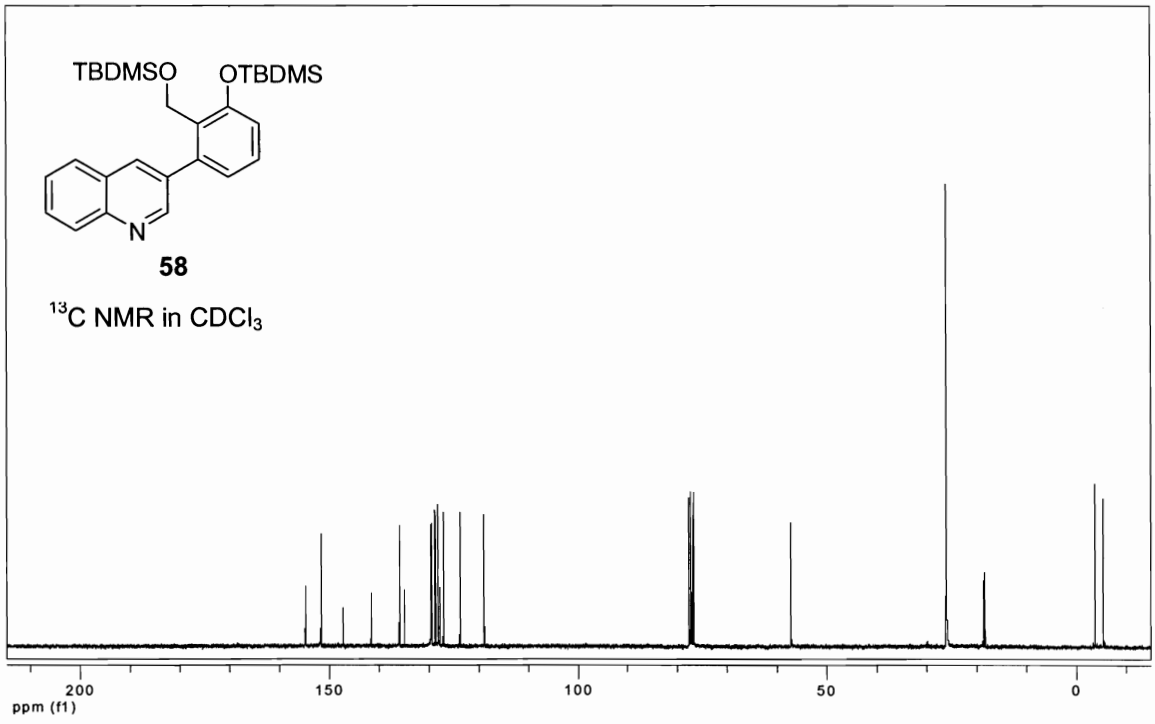

58

^{13}C NMR in $CDCl_3$

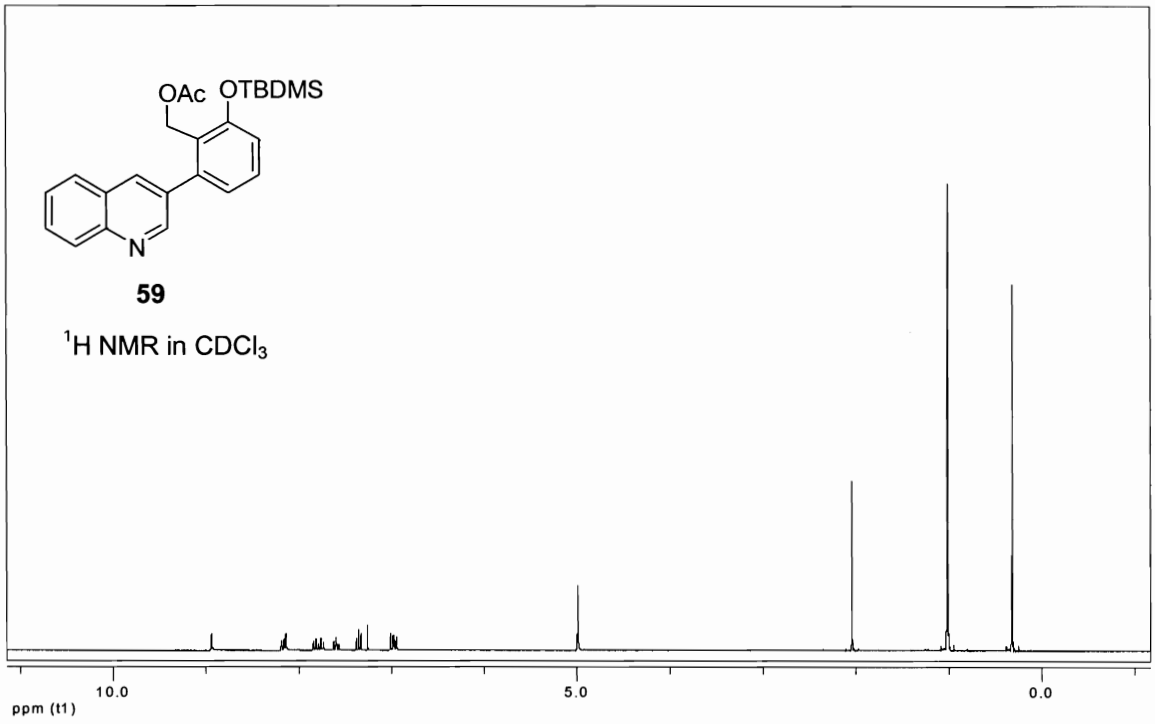
OAc OTBDMS
N
59
^{1}H NMR in $CDCl_3$
10.0
5.0
0.0
ppm (t1)

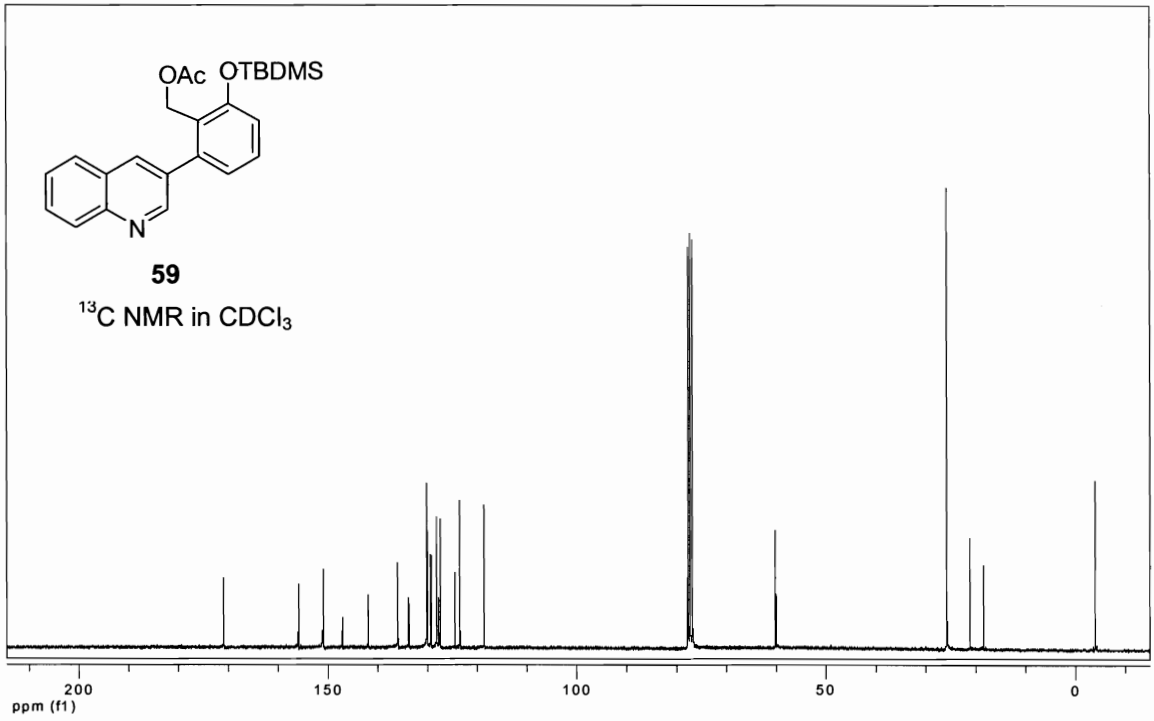
OAc OTBDMS
N
59
^{13}C NMR in $CDCl_3$
200
150
100
50
0
ppm (f1)

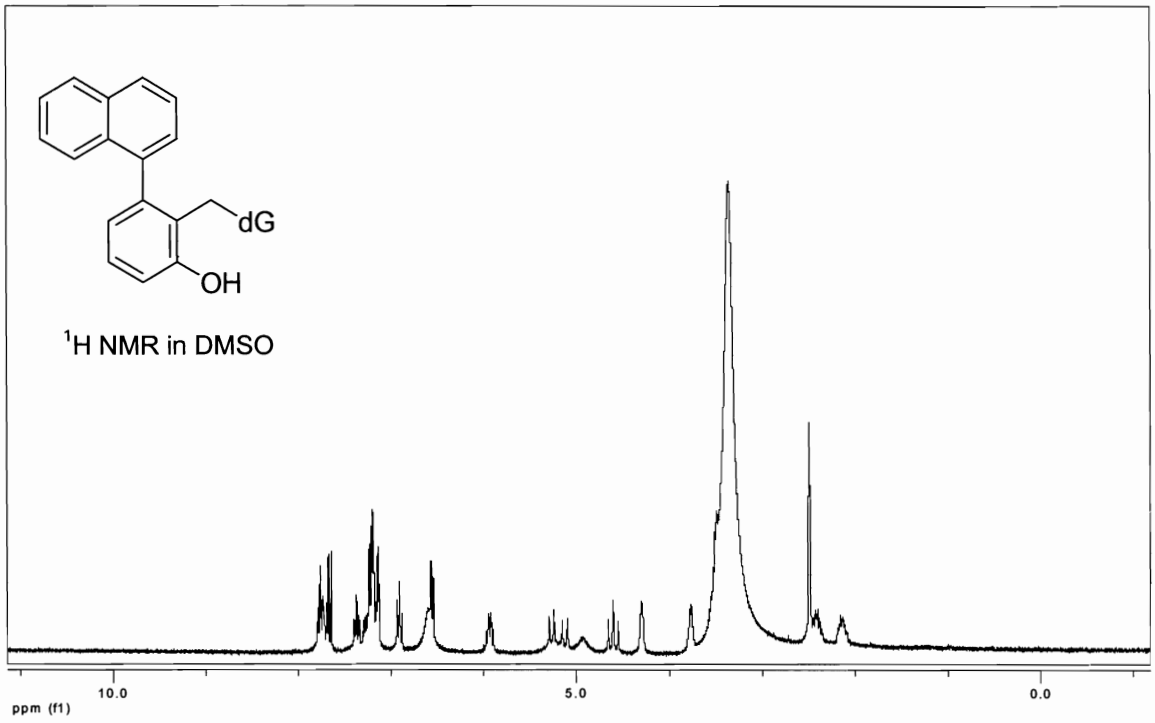
dG
OH
^{1}H NMR in DMSO
10.0
5.0
0.0
ppm (f1)

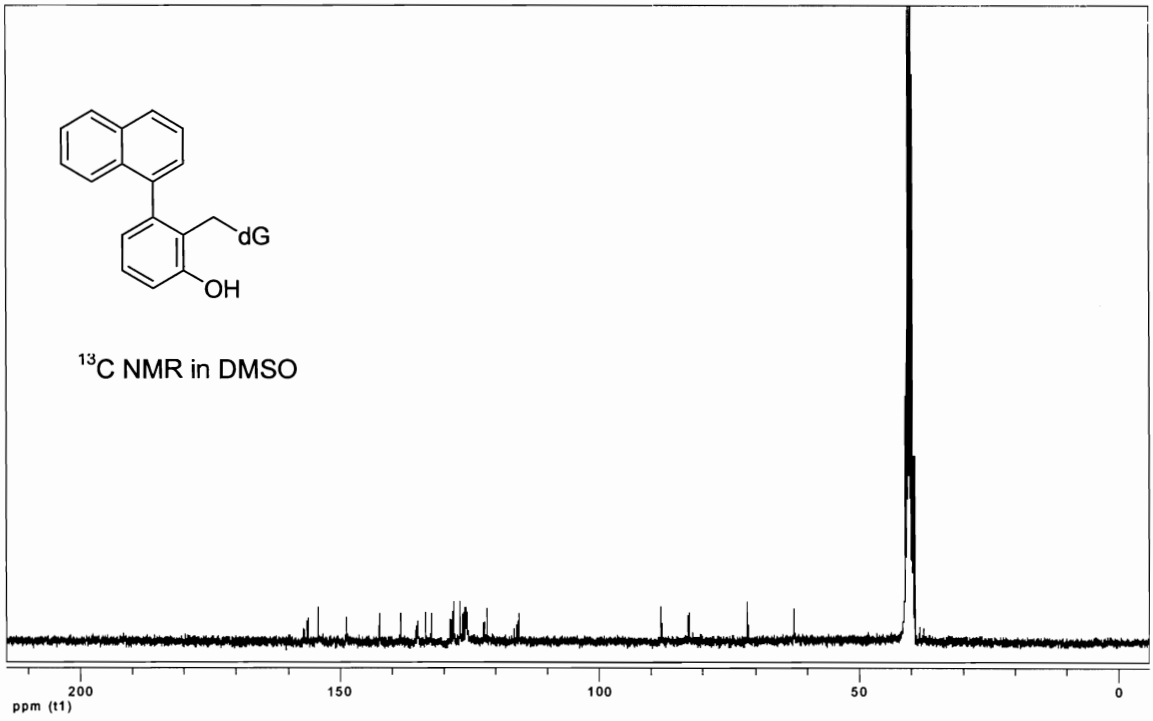
dG
OH
^{13}C NMR in DMSO
200
150
100
50
0
ppm (t1)

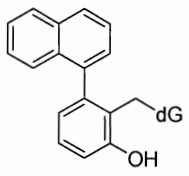

COSY in DMSO

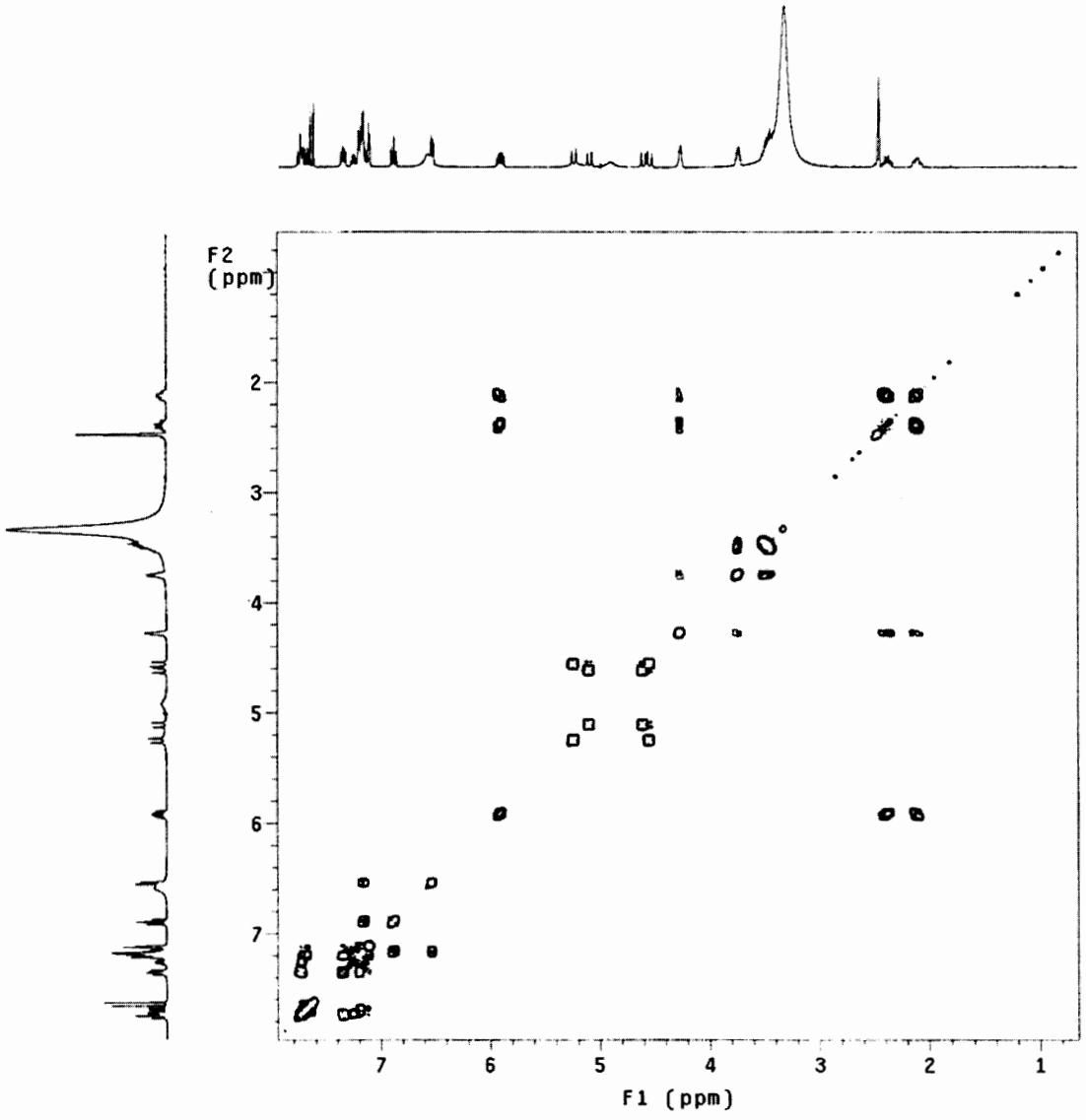

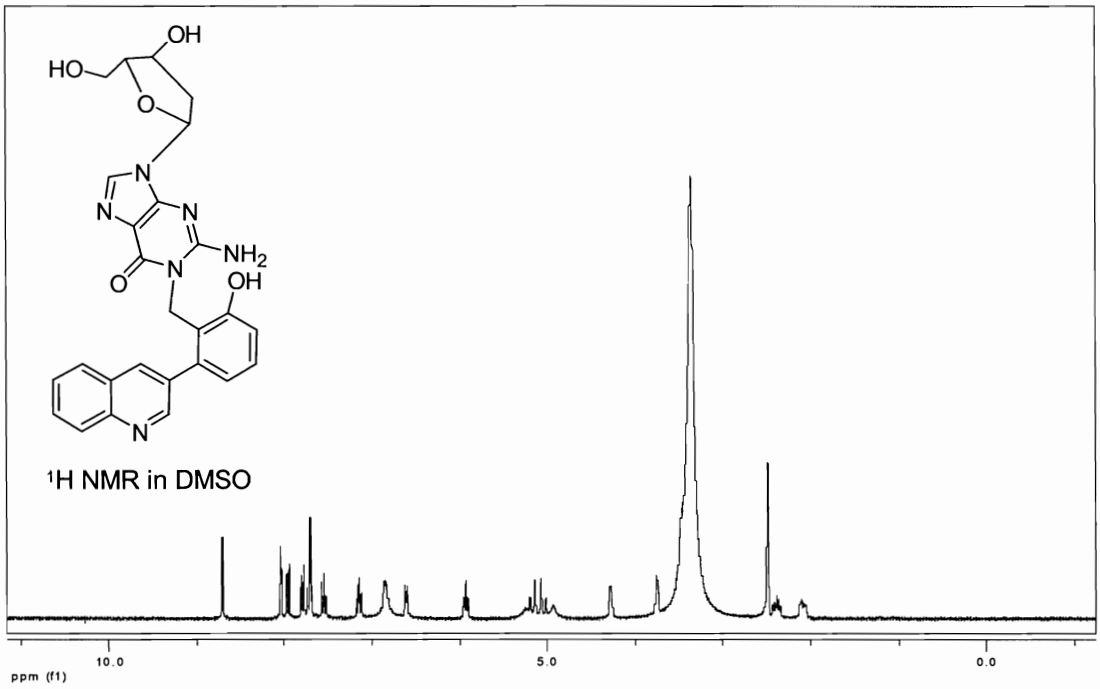
OH
HO
O
N
N
N
NH2
O
N
OH
N
1H NMR in DMSO
10.0
5.0
0.0
ppm (f1)

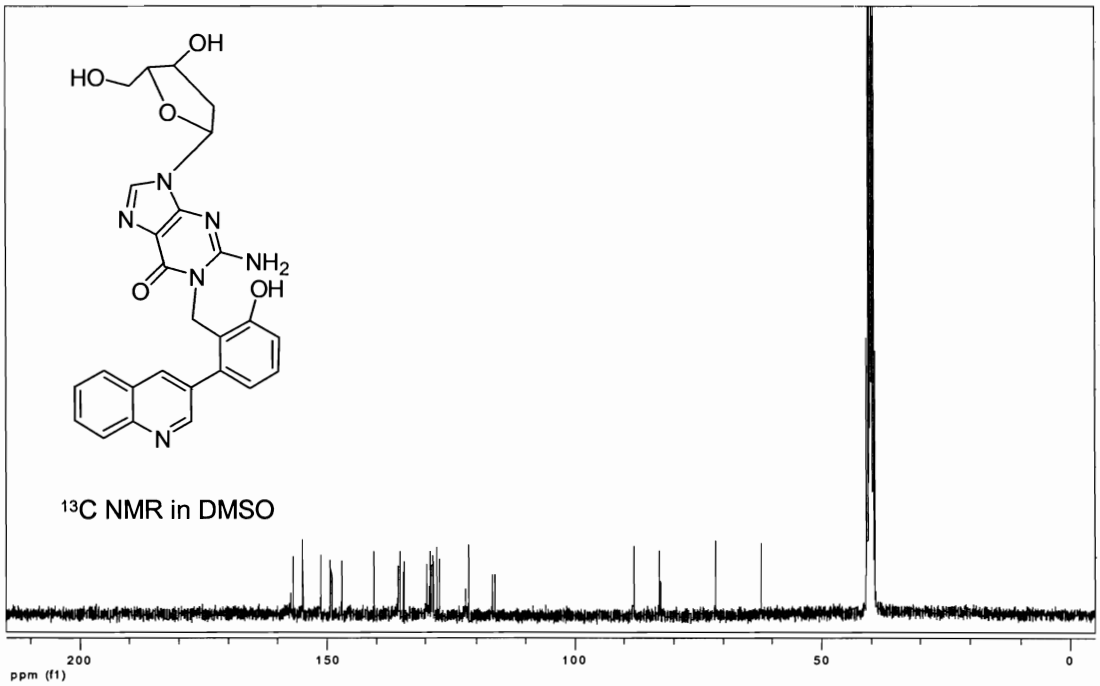
OH
HO
O
N
N
N
NH2
O
N
OH
N
13C NMR in DMSO
200
150
100
50
0
ppm (f1)

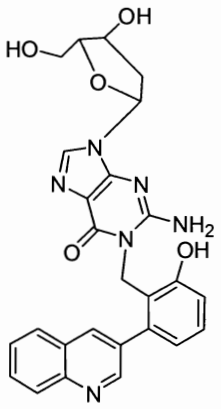

COSY in DMSO

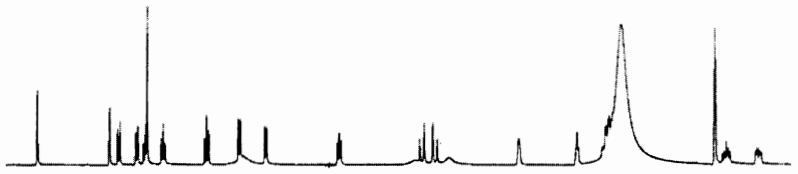

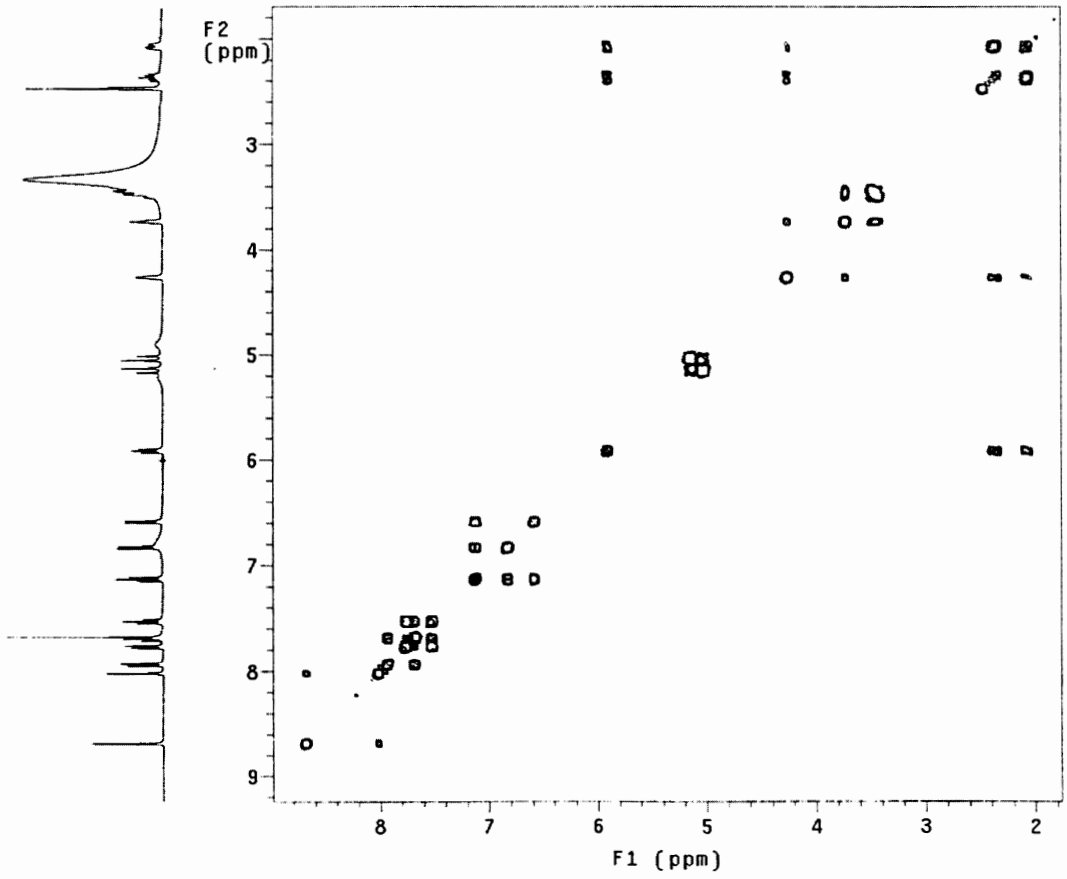

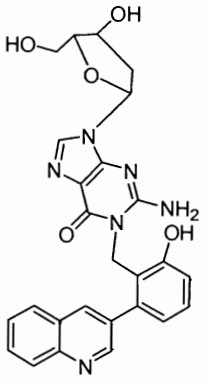
OH
HO
O
N
N
N
NH2
O
N
OH
N

HMQC in DMSO

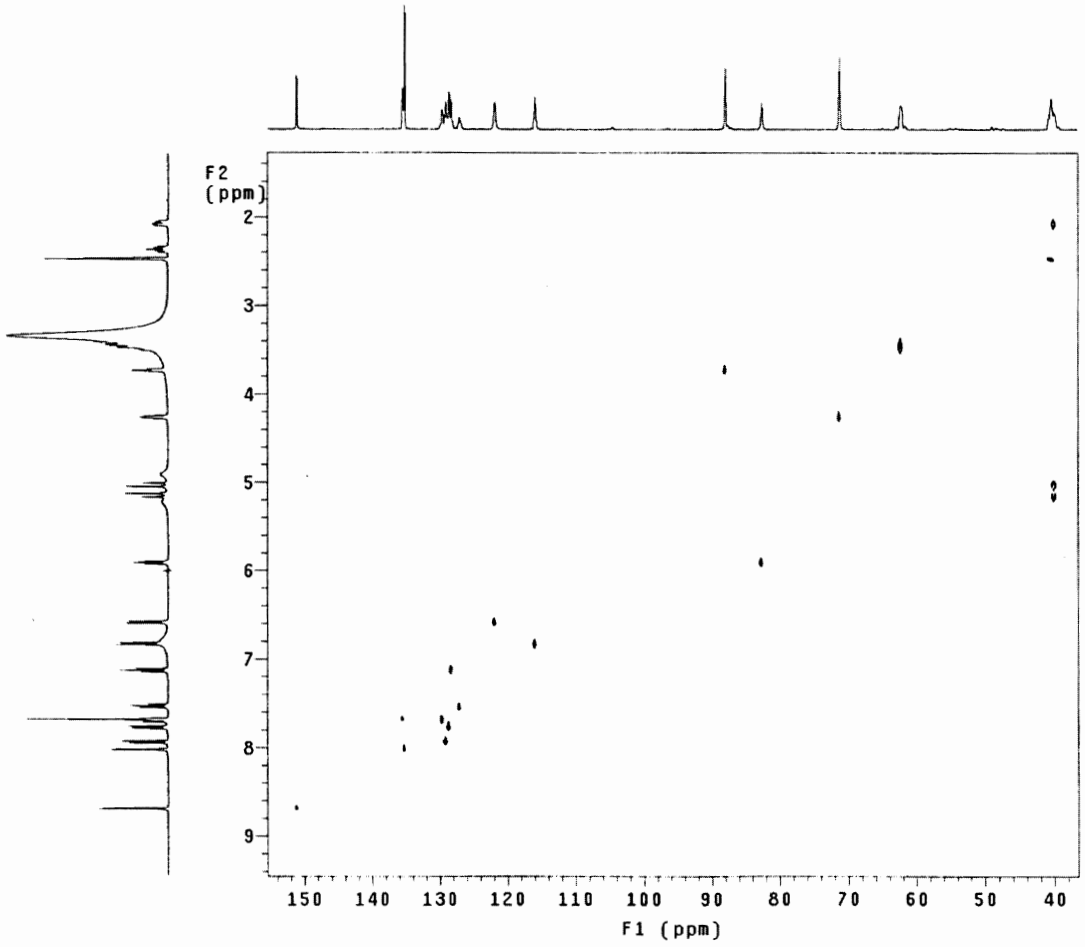
F2
(ppm)
2
3
4
5
6
7
8
9
150
140
130
120
110
100
90
80
70
60
50
40
F1 (ppm)

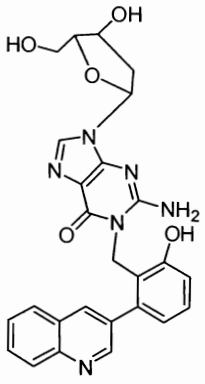
OH
HO
O
N
N
N
N
NH2
O
OH
N

HMBC in DMSO

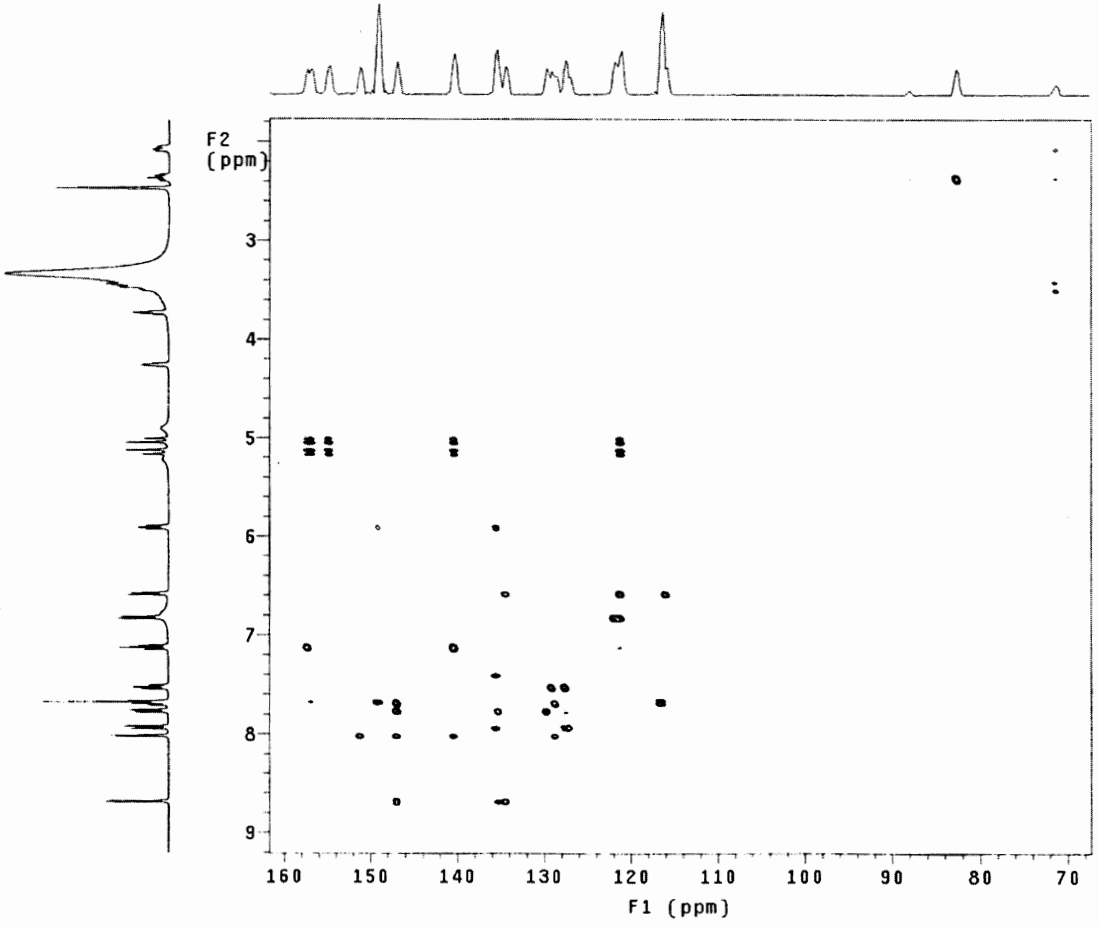
F2
(ppm)
3
4
5
6
7
8
9
160
150
140
130
120
110
100
90
80
70
F1 (ppm)

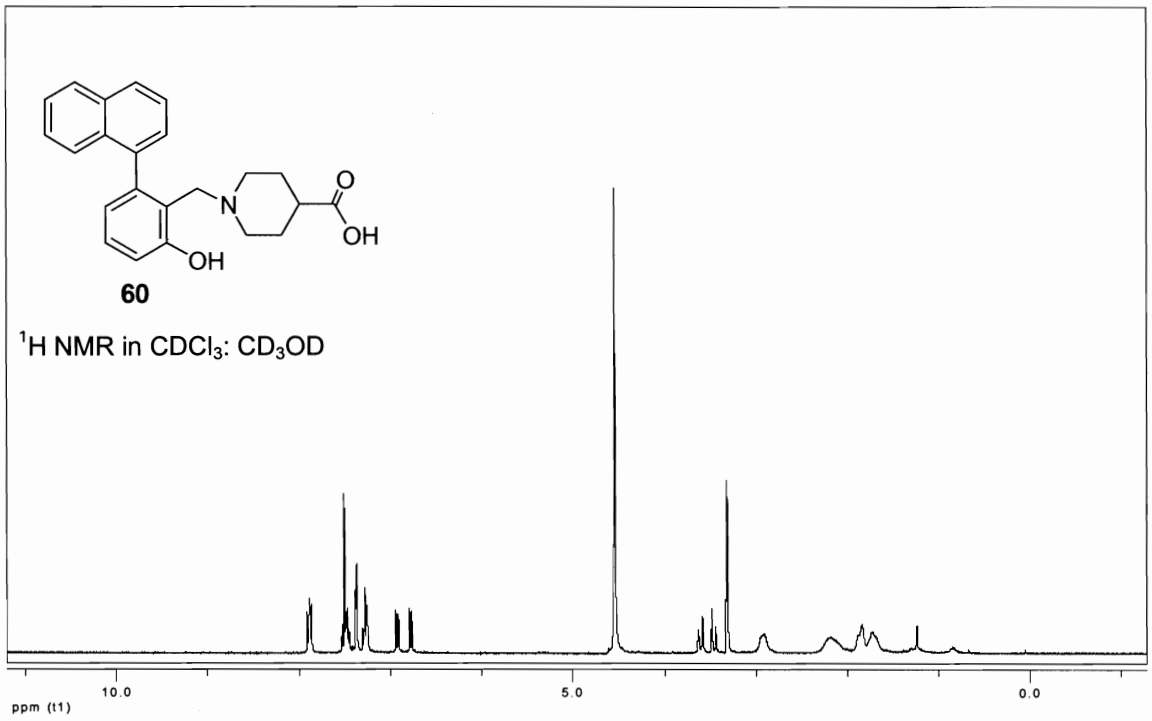

60

^{1}H NMR in $CDCl_3$: CD_3OD

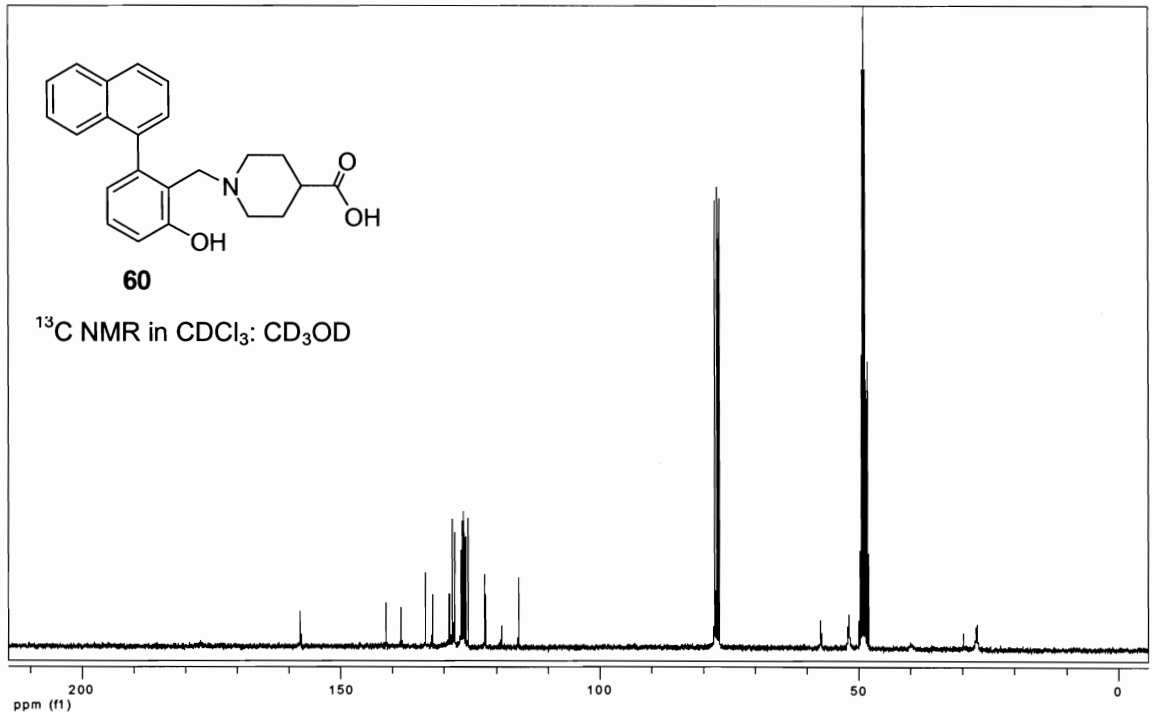

60

^{13}C NMR in $CDCl_3$: CD_3OD

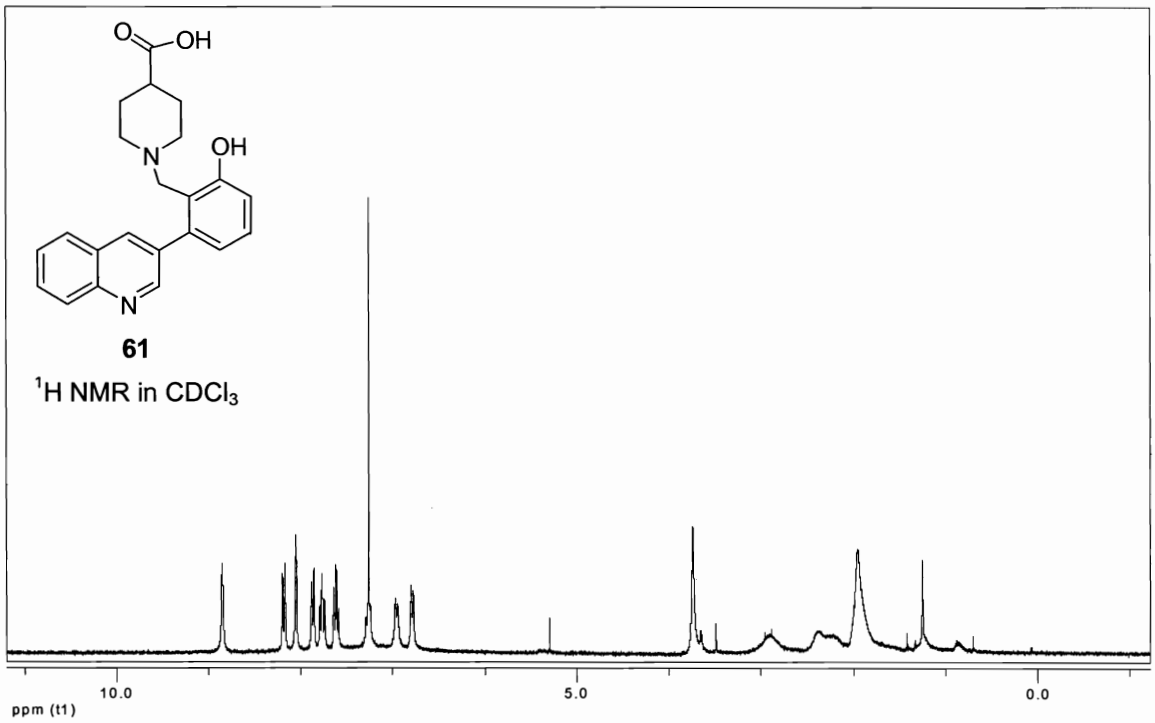

61

^{1}H NMR in $CDCl_3$

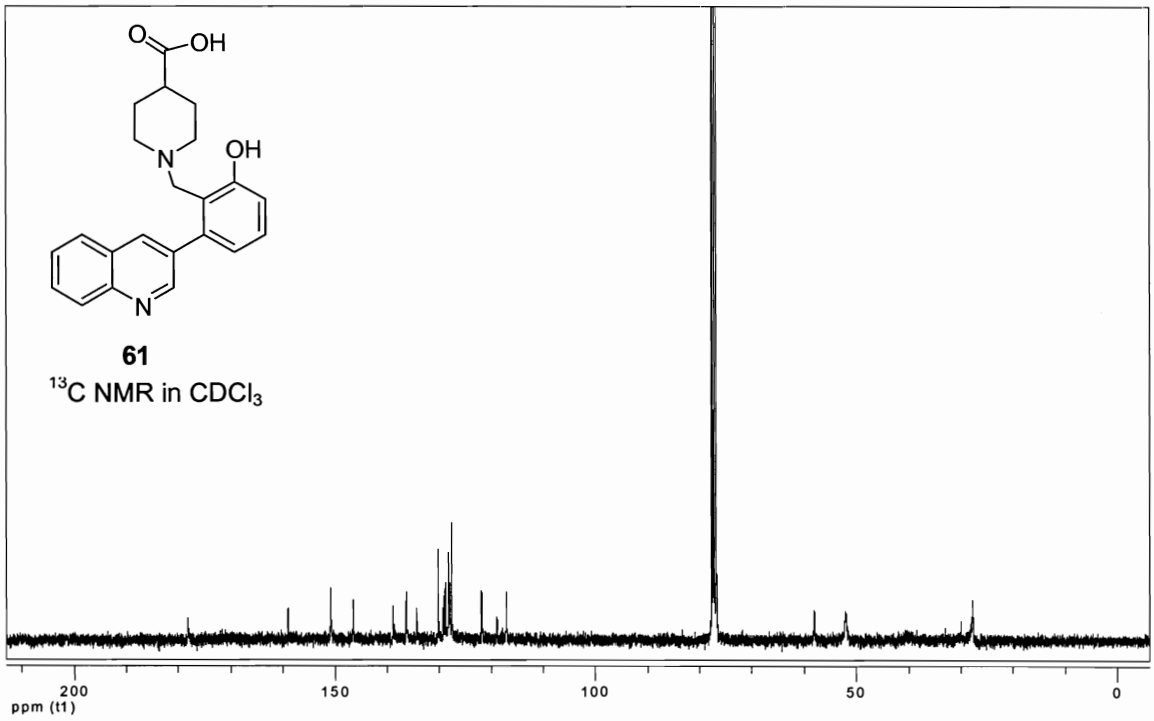

61

^{13}C NMR in $CDCl_3$

VITA

Ting Xu was born on January 19, 1977 in Chongqing, China. She received her Bachelor of Pharmaceutical Science from Shenyang Pharmaceutical University, China in July 1999. After 3-year working in pharmaceutical industry, she came to USA and was admitted into Department of Chemistry, College of Humanities and Sciences at Virginia Commonwealth University in August 2004.